The structure and function of the CGRP receptor

Michael John Woolley

A thesis submitted for the degree of

Doctor of Philosophy

University of Warwick

Warwick Medical School

May 2014

"Of course, the universe is gradually slowing down and will eventually collapse inwardly on itself, according to the laws of entropy when all its thermal and mechanical functions fail, thus rendering all human endeavors ultimately pointless. Just to put the gig in some sort of context."

Bill Bailey, Part Troll

Table of contents

List of figures

List of tables

Acknowledgements

I would like to thank my supervisor Alex for always doing way more than he needed to and for making work a pleasure to be at, most of the time!

I would like to thank my other supervisor Paul for all his advice, feedback and filling in of boring and unnecessary forms that he didn't really need to do.

I would like to thank Phil in the lab for his brain and sarcastic comments.

I would like to thank Professor Poyner at Aston University for his generosity in time and advice and his patience when it comes to deadlines!

I would like to thank my family, Mum, Dad, Pete and Clare for all their support and for pointing out how little sense science often makes.

Finally I would like to thank Holly for her patience, kindness, understanding and paying for half of the deposit even though all the mess was mine!

Declaration

This thesis is submitted to the University of Warwick in support of my application for the degree of Doctor of Philosophy. It has been composed by myself and has not been submitted in any previous application for any degree.

The work presented (including data generated and data analysis) was carried out by myself except in the cases outlined below:

1. Paragraphs in section 1.3.6 were amended from Woolley & Conner, 2013.
2. The radioligand binding experiments described in section 3.3.5 were carried out by Professor David Poyner at Aston University as part of a continued collaboration.
3. The computer modelling described in section 3.4.3 was carried out by Professor Chris Reynolds as part of a continuing collaboration.

Parts of this thesis have been published by the author:

Woolley, M. J., et al. (2013) The role of ECL2 in CGRP receptor activation: a combined modelling and experimental approach. *J R Soc Interface*, 10 (88): 20130589.

Woolley, M. J. and Conner, A. C. (2013) Comparing the molecular pharmacology of CGRP and adrenomedullin. *Curr Protein Pept Sci*, 14 (5): 358-374.

Summary

G protein-coupled receptors (GPCRs) are a superfamily of membrane proteins that bind to a diverse array of stimuli and are involved in a large number of physiological functions. The family A GPCRs are the largest and most comprehensively studied. The family B GPCRs are a small but important group of receptors (~15 members) that bind to peptide ligands and are involved in physiological processes that include vasodilation, stress, digestion and glucose homeostasis. The CGRP receptor is a unique member of this family as it is a heterodimer consisting of a GPCR subunit (calcitonin receptor-like receptor, CLR) and a single transmembrane accessory protein (receptor activity modifying protein, RAMP1).

The extracellular loop two (ECL2) domain is involved in ligand binding and activation in a number of studied GPCRs. This makes it vital both with respect to receptor function and in the design of therapeutics. The main focus of this thesis is to study the structure and function of the ECL2 domain in the CGRP receptor. This was initially done through individual alanine substitutions of each ECL2 residue and measuring the effect of this on a number of receptor processes. Residues that were identified as important for receptor function through this investigation were selected for an extensive set of mutagenesis to identify the precise molecular interactions that were involved at each position. These experiments have shown that ECL2 is the most important domain of the CGRP receptor for ligand-based activation. The N-terminal half of ECL2 contains residues predicted to have structural function and the C-terminal half is predicted to be involved in direct ligand binding. These results have been used in collaboration to refine a computer model of receptor structure and ligand binding to predict specific ligand docking sites that can be used to design therapeutics for migraine, heart attack and hypertension.

The final part of thesis produced preliminary data to support proof of concept for two techniques that can be used in the study of CGRP receptor function.

List of Abbreviations

Abbreviation	Full name
µl	Micro litre
µM	Micro molar
µm	Micro metre
α	Alpha
$A_{2A}R$	Adenosine A2A receptor
ANOVA	Analysis of variance
AM	Adrenomedullin
AMY	Amylin
AST	Active site tether
$AT_{1A}R$	Angiotensin II type 1A receptor
ATP	Adenosine triphosphate
β	Beta
β2-AR	β2-adrenergic receptor
B_{max}	Maximum number of binding sites
BSA	Bovine serum albumin
Ca^{2+}	Calcium
$CaCl_2$	Calcium chloride
cAMP	3'-5'-cyclic adenosine monophosphate
CGRP	Calcitonin gene-related peptide
$CGRP_{8-37}$	Truncated CGRP peptide antagonist
CIP	Calf Intestinal Phosphatase
CLR	Calcitonin receptor-like receptor
CNS	Central nervous system
CO_2	Carbon dioxide
COS	CV-1 (simian) in Origin and carrying the SV40 genetic material
CRH (CRF)	Corticotrophin releasing hormone (Corticotrophin releasing factor)
CRHR1	Corticotropin-releasing hormone receptor 1
CRHR2	Corticotropin-releasing hormone receptor 2
CT	Calcitonin
CTR	Calcitonin receptor
CXCR4	C-X-C chemokine receptor type 4
δ	Delta
DAG	Diacylglcerol
DMEM	Dulbecco's Modified Eagle's Medium (DMEM)
DMSO	Dimethyl sulfoxide
DNA	Deoxyribonucleic acid
Dnase	Deoxyribonuclease
dNTP	deoxynucleotide triphosphates
DTT	Dithiothreitol
EC_{50}	Half maximal effective concentration

ECD	Extracellular domain
ECE	Endothelin converting enzyme
ECL	Extracellular loop
EDTA	Ethylenediaminetetraacetic acid
ELISA	enzyme-linked immunosorbent assay
E_{max}	Maximum possible effect for the agonist
ER	Endoplasmic reticulum
ERK	Extracellular signal-regulated kinase
γ	Gamma
G protein	Guanosine nucleotide-binding proteins
GCG	Glucagon
GCGR	Glucagon receptor
GDP	Guanosine diphosphate
GEF	Guanine nucleotide exchange factor
GHRH	Growth hormone releasing hormone
GHRHR	Growth hormone releasing hormone receptor
GIP	Gastric inhibitory polypeptide
GIPR	Gastric inhibitory polypeptide receptor
GLP-1	Glucagon-like peptide 1
GLP1R	Glucagon-like peptide 1 receptor
GLP-2	Glucagon-like peptide 2
GLP2R	Glucagon-like peptide 2 receptor
GPCR	G protein-coupled receptor
GRK	G protein-coupled Receptor Kinase
GTP	Guanosine-5'-triphosphate
H_2SO_4	Sulphuric acid
HCl	Hydrochloric acid
HD	Homology domain
HEK	Human embryonic kidney
IC_{50}	Half maximal inhibitory concentration
ICL	Intracellular loop
IP_3	Inositol 1,4,5 triphosphate
KCl	Potassium Chloride
KD	Kinase domain
K_d	Ligand concentration that binds to half the receptor sites at equilibrium
LB	Ligand binding (family C)
LB	Lysogeny broth
µ	Mu
MAPK	Mitogen-activated protein kinase
$MgCl_2$	Magnesium chloride
$MgSO_4$	Magnesium sulphate
min	Minutes
ml	Milli litre
mM	Milli molar
NaCl	Sodium chloride

NC-IUPHAR	International Union of Pharmacology Committee on Receptor Nomenclature and Drug Classification
$(NH_4)SO_4$	Ammonium sulfate
nM	Nano molar
OPD	o-Phenylenediamine dihydrochloride
PAC1R	Pituitary adenylate cyclase activating polypeptide 1 receptor
PACAP	Pituitary adenylate cyclase-activating polypeptide
PAR1	Protease-activated receptor-1
PBS	Phosphate buffered saline
PCR	Polymerase chain reaction
pEC_{50}	Negative logarithm of the EC_{50}
PEI	Polyethylenimine
Pfu	Pyrococcus furiosus
PI	Phosphotidylinositol
PIP_2	Phosphatidylinositol 4,5-bisphosphate
PKA	Protein kinase A
PKC	Protein kinase C
PLC	Phospholipase C
PTH	Parathyroid hormone
PTH1R	Parathyroid hormone 1 receptor
PTH2R	Parathyroid hormone 2 receptor
RAMP	Receptor activity-modifying protein
RGS	Regulator of G protein Signalling
S1P1R	Sphingosine-1-phosphate 1 receptor
SCAM	Scanning cysteine accessibility method
SCTR	Secretin receptor
SDM	Site directed mutagenesis
SDS	Sodium dodecyl sulfate
TBE	Tris/Borate/EDTA
TM	Transmembrane
TR-FRET	Time-resolved fluorescence resonance energy transfer
TRIS	Tris(hydroxymethyl)aminomethane
TSHR	Thyroid stimulating hormone receptor
UCN	Urocortin
V1AR	Vasopressin 1A receptor
V1BR	Vasopressin 1B receptor
V2R	Vasopressin 2 receptor
VFT	Venus fly trap
VIP	Vasoactive intestinal peptide
VIPR1	Vasoactive intestinal peptide receptor 1
VIPR2	Vasoactive intestinal peptide receptor 2
WT	Wild type

1 Introduction

1.1 GPCRs

1.1.1 Introduction

G protein-coupled receptors (GPCRs) are a superfamily of membrane proteins that function to transmit an extracellular signal across the plasma membrane to the inside of a cell, resulting in a cellular response. There are over 800 different types of GPCRs in the human body (Fredriksson *et al.*, 2003) that respond to a diverse array of stimuli. These include photons, odorants, hormones, proteins, lipids, pheromones, chemokines and neurotransmitters (Bockaert & Pin, 1999). GPCRs are involved in a huge array of physiological processes, including sight, smell, taste, movement, immunity, mood, autonomic functions, homeostasis, thought and feeling. This makes GPCRs a common site of action for both medicinal and recreational drugs. Approximately 25-50% of medical pharmaceutical products target GPCRs (Salon *et al.*, 2011). The involvement of GPCRs in such a diverse array of physiological process has led to GPCR research being of considerable interest, both academically and pharmaceutically.

All GPCRs share a common molecular architecture of an N-terminal extracellular domain (ECD), seven transmembrane (7TM) spanning helices connected by 3 extracellular loops (ECLs) and three intracellular loops (ICLs) with an intracellular C-terminus (Palczewski *et al.*, 2000). However given this common three-dimensional structure, there is very little overall primary sequence homology. The standard model of ligand binding is that an extracellular ligand binds to the ECD, the ECLs or the TM bundle, stabilising a particular receptor conformation. GPCRs are coupled to an intracellular heterotrimeric G protein through their ICLs and the intracellular C-terminus (Rasmussen *et al.*, 2011b). It is through the G protein that the majority of the signalling occurs however GPCRs can also signal through G protein independent pathways (DeWire *et al.*, 2007). This phenomena has led to these receptors to be alternatively named 7TM receptors, however the GPCR terminology is more

established (Fredriksson *et al.*, 2003). All these aspects of GPCR structure and function will be discussed in more detail in this introduction.

The introduction is split into three sections. The first section discusses the whole GPCR super family, the second section focuses on the family B GPCRs and the final section looks at CGRP and its receptor in more detail. As the entire GPCR family is involved in the first section, general details of the family B GPCRs will be included however as they are being discussed in more detail in the second section, the first section will only contain a general overview.

1.1.2 Classification

The diversity of GPCRs and the lack of sequence homology that accompanies this has led to a number of different classification systems being developed. One of the original classification systems was based on primary sequence homology and separated the GPCR superfamily into six groups. These were categorized as family A (1, Rhodopsin-like), family B (2, Secretin), family C (3, Metabotropic glutamate/pheromone), family D (4, Fungal mating pheromone), family E (5, cyclic AMP) and family F (6, Frizzled/Smoothened) according to sequence homology and functional similarity (Attwood & Findlay, 1994; Kolakowski, 1994). These groups comprised GPCRs for both vertebrates and invertebrates. Human GPCRs are contained within families A-C and F. A more recent phylogenetic analysis of the human genome has organized the functional GPCRs into 5 groups. These are glutamate (G), rhodopsin (R), adhesion (A), frizzled/taste 2 (F) and secretin (S) which is commonly abbreviated as GRAFS (Fredriksson *et al.*, 2003). The phylogenetic tree of the human GPCRs is presented in Figure 1.1.

Rhodopsin is the largest family and corresponds with the family A group of receptors. The rhodopsin family is subdivided into four main groups (α, β, γ and δ) and 13 subfamilies. The α group contains the prostaglandin, amine (including the serotonin, dopamine, muscarinic, histamine and adrenergic receptors), opsin, melatonin, and MECA receptor clusters. The β group contains receptors to peptide ligands. The γ group contains the SOG (including the opioid receptors), MCH, and the chemokine receptor clusters. The δ group contains the MAS-related,

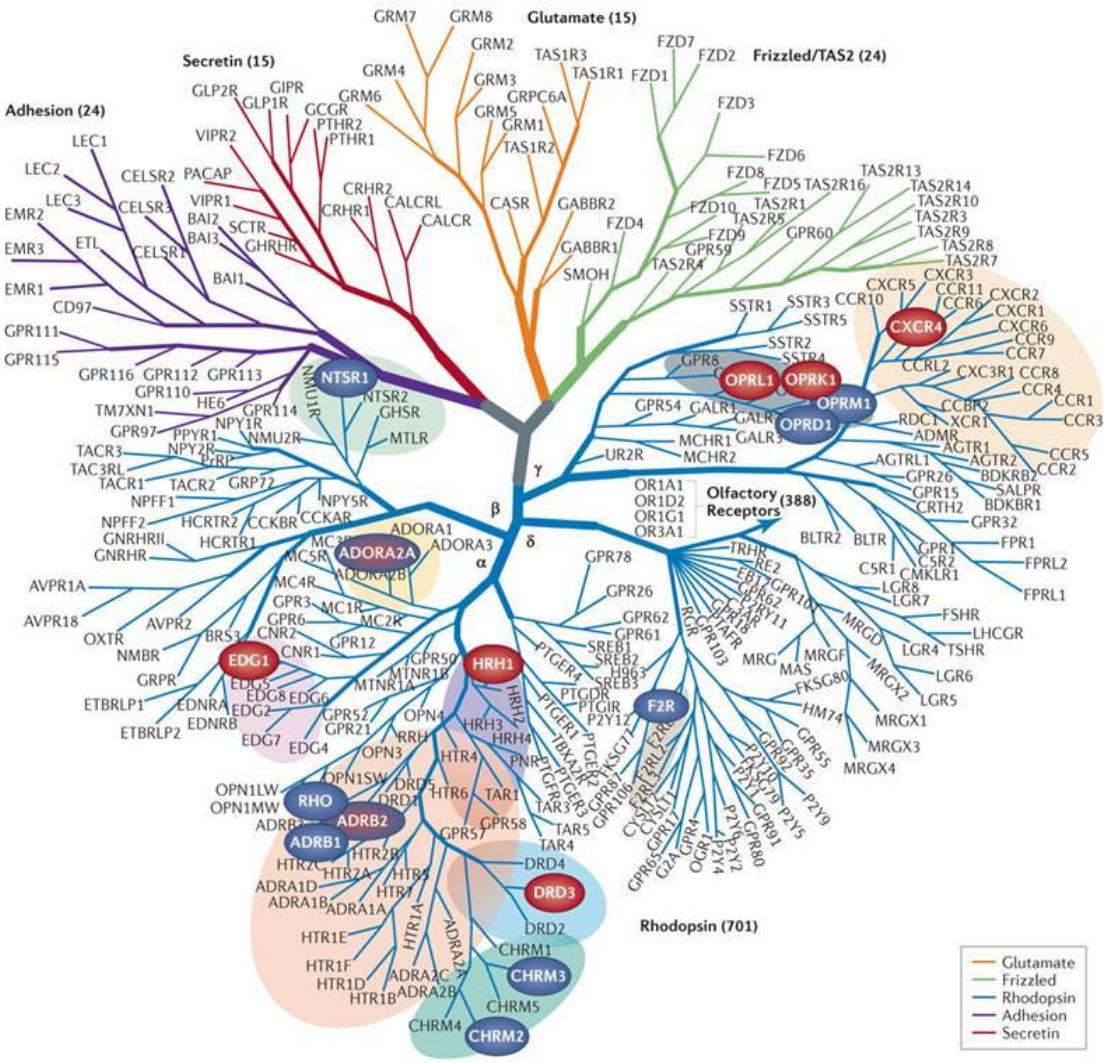

Figure 1.1. GPCR phylogenetic tree of the human GPCR superfamily classified using the GRAFS system.

The non-olfactory human GPCRs are presented following phylogenetic analysis. Classification was based on sequence similarity of the transmembrane domains. GPCRs are named based on the gene names in the Uniprot database. Families with solved structures have been highlighted. Schematic diagram was adapted from Stevens *et al.*, 2013.

glycoprotein, purine, and the olfactory receptor clusters (Fredriksson *et al.*, 2003).

The secretin and adhesion groups were combined as the family B receptors in the A-F classification system. They share structural similarities within the TM domains and a high level of N-terminal cysteine residues, however there are major differences in the N-termini of these receptor groups. The secretin family all bind to moderately large peptide ligands and are named after the first receptor in the family to be cloned. The adhesion family have large N-terminal domains which contain motifs involved in cell adhesion (Nordström *et al.*, 2011).

The glutamate family corresponds with the family C receptors. These include the metabotropic glutamate and GABA receptors found in the central nervous system, a single calcium sensing receptor and the TAS1 taste receptors. These receptors have a large N-terminus containing two "lobes" with a cavity in between. Binding of glutamate causes the lobes to close around the ligand sometimes called the "venus fly trap" mechanism. These two lobes are connected to the TM regions through a cysteine rich domain (with the exception of the $GABA_B$ receptor). Another characteristic of the glutamate family of GPCRs is constitutive dimerisation at the cell surface, either as homodimers (mGlu and CaS) or heterodimers ($GABA_B$ and T1Rs) (Kniazeff *et al.*, 2011).

The final family contains the frizzled receptors and the TAS2 taste receptors. Surprisingly these showed no sequence similarities to the TAS1 receptors in the glutamate family. Since this classification however it was found that TAS2 has greater similarity with the MCH group of the Rhodopsin family (Nordström *et al.*, 2011).

1.1.3 Nomenclature and numbering systems

The sequencing of the human genome has allowed potential human GPCR genes to be catalogued. The International Union of Pharmacology Committee on Receptor Nomenclature and Drug Classification (NC-IUPHAR) provides information on the classification, pharmacology, structure and terminology of this list through their receptor database website (www.guidetopharmacology.org) and various reports (Foord *et al.*, 2005).

The numbering of GPCR amino acids provides information into the location and order within the sequence. Often the position in the primary amino acid sequence is used. However to allow comparison between GPCRs and to provide details with respect to positioning within the structure, three different numbering systems have been proposed. The Schwartz and Baldwin numbering systems are essentially identical. The TM helix is described using I to VII and the most conserved residue within each helix is given a generic number describing the predictive relative position in a standard helix of 26 residues. However, with the exception of TM1, these two systems do not agree on the conserved residue. In the Ballesteros-Weinstein numbering system, two numbers are used. The first describes the helix that the residue is in (1-8) and the second describes the position in relation to the most conserved residue, which is given the number 50 (Gether, 2000). This numbering system has also been used to described the family B GPCRs using the same principle but using conserved residues specific to this family (Wootten *et al.*, 2013). This is referred to as the Wootten numbering system. In this work the Ballesteros-Weinstein/Wootten numbering system will be written in superscript (eg. $X^{1.50}$) and will be the Ballesteros-Weinstein system unless stated.

1.1.4 Evolution

It is thought that all the human families of GPCRs share a common ancestor. Using alignment and motif analysis of newly published sequence genomes it was found that the adhesion, frizzled and rhodopsin families descended from the cAMP family (family E) (Nordström *et al.*, 2011). The origin of these families is thought to occur at a similar point in time. Later the secretin family evolved from the adhesion family, which happened after the split of *N. vectensis* (starlet sea anemone) and before the split of *C. elegans* (nematodes) from the vertebrate lineage (Nordström *et al.*, 2009). The glutamate family was found to be one of the most ancient due to its presence in *Th. Pseudonana* (eukaryotic phytoplankton) and there are suggestions of a link in origin with the other families. cAMP receptors are the most ancient, found in alveolata, choanoflagellata, fungi and metazoan (Krishnan *et al.*, 2012). In this study, the origin of the rhodopsin family was found to have evolved from the cAMP family with the common ancestor of opisthokonts (fungi/metazoa),

~1100 million years ago. There are a number of similarities between these two families suggesting that rhodopsin expanded from the more ancient cAMP family, while this family became more redundant in more complex organisms. The melatonin subgroup had the highest identity to the cAMP and the adhesion family (Nordström *et al.*, 2011). The adhesion and frizzled families evolved from the cAMP family before the split of the unikonts (eukaryotic cells with a single flagellum or amoeba with no flagellum) ~1275 million years ago. The glutamate and the cAMP family was traced back to the common ancestor of alveolates (superphylum of protists) and unikonts, ~1400 million years ago. The secretin family evolved from the adhesion family between the split of cnidaria (aquatic animal phylum including jellyfish) and nematoda (Nordström *et al.*, 2009).

Microbial rhodopsins are 7TM proteins found in both prokaryotes and eukaryotes. These include light-sensitive proteo-, bacterio- and halorhodopsins that use light induced retinal isomerisation to create proton or chloride gradients. These are used to drive membrane bound ATPases. Sensory rhodopsins in some halobacteria are used for phototaxis (Béjà *et al.*, 2000; Fuhrman *et al.*, 2008; Oesterhelt, 1998; Spudich & Luecke, 2002). The N-terminal ECD of the family C glutamate receptors show both sequential and structural homology with bacterial periplasmic binding proteins which are involved in amino acid and nutrient transport (O'Hara *et al.*, 1993). Despite structural similarities the sequence homology with GCPRs is low and therefore phylogenetic analysis has not linked the GPCR ancestry to these proteins.

It is therefore still unknown how the 7TM bundle in eukaryotes evolved. Some of the greatest sequence similarities occur between non-homologous helices. This effect has been explained due to exon shuffling (Pardo *et al.*, 1992) or a duplication of a three helical module which results in TM1-3 and TM5-7 (Taylor & Agarwal, 1993). The search for a common ancestor is further complicated by the length of time that prokaryote and eukaryote TM proteins have been independently evolving and with lateral gene transfer observed by type 1 microrhodopsins even between prokaryotes and eukarotes (Ruiz-González & Marín, 2004; Sharma *et al.*, 2006).

The genetic expansion of GPCRs is thought to occur through gene duplication followed by independent evolution (Semyonov *et al.*, 2008). There is evidence for

two distinct genome duplication events early in the vertebrate evolution (Dehal & Boore, 2005). It was also found the GPCR genes have a greater retention rate following gene duplication compared with other gene duplicates (Semyonov *et al.*, 2008).

The plant kingdom is considerably different. Whilst there have been several proposed 7TM receptors, the homology that has been used to link these to GPCRs is weak and there is little evidence that they act as receptor GEFs (Urano & Jones, 2013).

1.1.5 GPCR Structure

All GPCRs share a common three-dimensional structure consisting of an N-terminal extracellular domain (ECD), seven transmembrane (TM) spanning helices which cluster in a barrel formation and an intracellular C-terminus. The TM helices are connected by three extracellular loops (ECLs) and three intracellular loops (ICLs) (Figure 1.2) (Palczewski *et al.*, 2000).

1.1.5.1 Techniques used to obtain GPCR structures

The first structure of a 7TM protein was that of Halobacterium halobium bacteriorhodopsin, obtained using electron microscopy (Henderson & Unwin, 1975). Using this and sequence analysis, probability maps of GPCRs were constructed (Baldwin, 1993; Baldwin *et al.*, 1997; Schertler *et al.*, 1993).

The first GPCR crystal structure was of bovine rhodopsin, published in 2000 (Palczewski *et al.*, 2000). Following this no new GPCR structures were published until that of the β2-AR in 2007 (Cherezov *et al.*, 2007; Rasmussen *et al.*, 2007). Both of these structures are presented in Figure 1.2. This delay represents the difficulty in successfully expressing, purifying and crystallising a highly dynamic eukaryotic membrane protein. Rhodopsin has proved an exception in that is has been obtained through its natural source where it is highly expressed (Palczewski *et al.*, 2000). In contrast, most GPCRs are found in small amounts.

To obtain the high yields necessary for crystallography, effective recombinant expression systems are required. Most of the crystal structures published since then

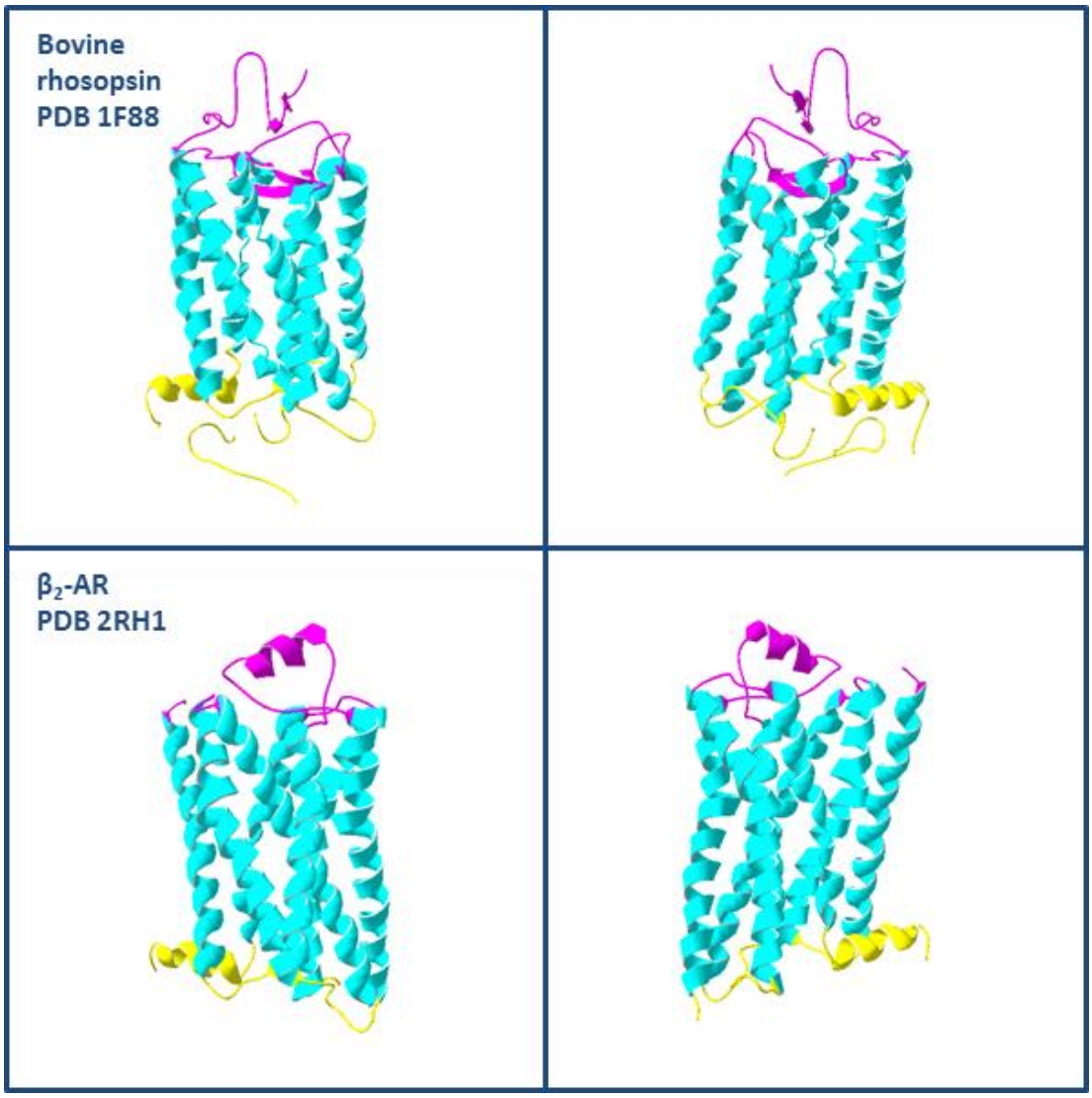

Figure 1.2. Crystal structures of bovine rhodopsin (PDB1F88) and β2-adrenergic receptor (β2-AR, PDB 2RH1).

The N-terminal extracellular domain (ECD) and extracellular loops (ECLs) are highlighted magenta, the seven transmembrane domains (7TM) are highlighted cyan and the intracellular loops (ICLs) and intracellular C-terminal domain is highlighted yellow. Each structure is presented twice, in a parallel orientation to the membrane, rotated 180°.

have used an insect expression system. This expression system is slower and more expensive than yeast and *E.coli* but is effective at expressing mammalian GPCRs. There have been exceptions for example with the human adenosine A2A receptor (A2AR) (Hino *et al.*, 2012) and the Histamine H1 receptor (Shimamura *et al.*, 2011), which have been expressed in the yeast strain *Pichia pastoris.* The yeast expression system has the benefits of a fast growth rate but also eukaryotic expression machinery. However it does differ from mammalian cells with respect to some post translational modifications and membrane lipid composition (Opekarová & Tanner, 2003). Recently the neurotensin receptor 1 has been expressed in *E.coli* (Egloff *et al.*, 2014). *E.coli* is the cheapest and most convenient system of protein expression however is not always sufficient to successfully express mammalian GPCRs. It has been a useful screening expression system. Mammalian cells have been used to successfully express and crystallise rhodopsin structures (Standfuss *et al.*, 2007).

A number of different techniques have been adopted to obtain GPCR crystal structures. These include deletions of the flexible C-terminal domain (Singh *et al.*, 2010) and in some cases the extracellular N-terminus (Tucker & Grisshammer, 1996; Warne *et al.*, 2003). The introduction of tags has also been used to enhance purification (André *et al.*, 2006). The high resolution crystal structure of β2-AR fused the T4 lysozyme in the place of the flexible ICL3 domain (Cherezov *et al.*, 2007). T4 lysozyme can crystallise but also fits between the cytoplasmic ends of TM5 and 6 with minimal disruption (Rosenbaum *et al.*, 2007). T4 lysozyme insertion into the ICL3 domain has been successfully used for the crystallisation of a number of receptors, including human A2AR, the muscarinic M2 and M3 receptors, the CXCR4 chemokine receptor, the human dopamine D3 receptor and the δ, μ, and human κ-opioid receptors (Chien *et al.*, 2010; Granier *et al.*, 2012; Haga *et al.*, 2012; Jaakola *et al.*, 2008; Kruse *et al.*, 2012; Manglik *et al.*, 2012; Wu *et al.*, 2010; Wu *et al.*, 2012). Crystal structures have also been obtained with the T4 lysozyme fused to the N-terminus (Rasmussen *et al.*, 2011b; Thompson *et al.*, 2012). A thermostabilised cytochrome b_{562} insertion in the place of ICL3 was used to successfully obtain a high resolution structure of the human A2A adenosine receptor allowing

observation of bound water and lipid molecules, providing insights into the allosteric effects of sodium ions (Liu *et al.*, 2012).

Antibody fragments and nanobodies have also been used to stabilise the receptor and facilitate crystallisation (Rasmussen *et al.*, 2007; Rasmussen *et al.*, 2011a) and thermostabilising mutagenesis has been successfully used to create receptors with increased stability. This was initially used for the turkey β1-AR (Serrano-Vega *et al.*, 2008) and has been successful in obtaining crystal structures for a number of other receptors, including that of CRHR1, the first family B GPCR crystal structure (Hollenstein *et al.*, 2013).

The use of detergents is another important factor when obtaining crystals of membrane proteins. There are two major groupings of the methods used for this. The first is the in surfo methods which utilizes detergent micelles. The other is the bilayer method which include the bicelle, vesicle and in meso methods (Caffrey & Cherezov, 2009). The in meso or lipid cubic phase (LCP) methods have proved considerably successful in obtaining crystals for GPCRs (Caffrey *et al.*, 2012).

The success in these techniques in obtaining GPCR crystals has led to receptors being crystallised in less stable conformations and in complexes with other proteins. These include the co-crystallisation of the β2-AR with its heterotrimeric G protein (Rasmussen *et al.*, 2011b), and with the G_α C-terminus which corresponds to the interaction sites between the GPCR and G protein (Scheerer *et al.*, 2008; Standfuss *et al.*, 2011).

1.1.5.2 Extracellular region

The extracellular region of GPCRs consists of the N-terminal extracellular domain (ECD) and the extracellular loops (ECL2) connecting TM2 and 3, TM4 and 5 and TM6 and 7. The extracellular region of family A GPCRs either covers the TM bundle in the case of covalently attached or hydrophobic ligands (Hanson *et al.*, 2012; Palczewski *et al.*, 2000) or leaves it open in the cases of receptors with water soluble ligands (Cherezov *et al.*, 2007; Haga *et al.*, 2012; Jaakola *et al.*, 2008).

In the case of rhopdopsin, the ligand is a covalently bound retinal chromophore within the TM bundle. The N-terminus of rhodopsin contains 34 amino acids

forming strand and β-sheet structures over the top of the TM bundle and interacting with ECL1 and 3. ECL1 and 3 run parallel with the membrane but the structure of ECL2 is a β-strand extending across the molecule forming a β-sheet structure with an anti-parallel β-strand running deeper into the pocket (Palczewski *et al.*, 2000). The N-terminus of the sphingosine-1-phosphate 1 receptor (S1P1R), which binds to a lipid ligand, is an α-helix that forms a cap over the top of the receptor. ECLs 1 and 2 of the S1P1R tightly pack over the N-terminus of the receptor forming a lid over the TM bundle (Hanson *et al.*, 2012).

GPCRs that bind water-soluble ligands have a more open extracellular region, however structures still vary. In the β2-AR, ECLs 1 and 3 are short loops. ECL2 is extended but instead of a β-sheet structure it forms a short α-helix running parallel to the top of the membrane which contains an intra-loop disulphide bond as well as the TM3-ECL2 disulphide and also a glycosylation site (Cherezov *et al.*, 2007).

The β-sheet structure of rhodopsin ECL2 is a feature common to the peptide ligand receptors of the opioid and the chemokine receptor families (Granier *et al.*, 2012; Manglik *et al.*, 2012; Wu *et al.*, 2010; Wu *et al.*, 2012). In other receptors this secondary structure element of ECL2 is absent however this domain still folds over the TM bundle and facilitates ligand entry to the binding pocket (Haga *et al.*, 2012; Kruse *et al.*, 2012).

Another feature of the extracellular regions are disulphide bonds. The TM3-ECL2 disulphide is present in most family A GPCRs and additional disulphide bonds have been observed that link the N-terminus-ECL2 (gonadotropin releasing hormone receptor), the N-terminus-ECL3/TM7 junction (CXCR4), the N-terminus-ECL3 ($AT_{1A}R$), ECL1-ECL2 ($A_{2A}R$) and an ECL3 intraloop disulphide bond ($A_{2A}R$). N-glycosylation of ECL2 is seen family A GPCRs. Sequence analysis found that 32% of the 613 family A GPCRs studied had at least one N-glycosylation consensus site and 85% of these were between the top of TM4 and the conserved cysteine of ECL2 (Wheatley *et al.*, 2012).

The family B GPCRs have a large N-terminal ECD. Currently, only two crystal structures have been solved for the family B TM domains however there are a large

number of structures of the ECD regions. These include receptors for AMY2, CGRP, CRH1, CRH2 GIP, GLP-1, Glucagon, PAC1, PTH1 and VPAC2 (Hollenstein *et al.*, 2014). These structures reveal a common N-terminal α-helix followed by two central antiparallel β-sheets connected by several loops and stabilised by three disulphide bonds. 10 out of the 11 peptide-ligand bound complexes have a similar binding orientation with the ligand adopting a α-helical conformation and binding between the two β-sheets. For the CGRP and adrenomedullin receptors, there are interactions between the N-terminal α-helix of the ECD and α-helices of transmembrane accessory (RAMP) proteins (Kusano *et al.*, 2012; ter Haar *et al.*, 2010).

The crystal structures of the CRHR1 and GCGR in 2013 showed structural similarities with both the TM domains and the ECLs (Hollenstein *et al.*, 2013; Siu *et al.*, 2013). ECL2 is the longest of the loops extending into the middle of the TM bundle. It lacks the secondary structure observed in many of the family A GPCRs. ECL3 points away from the centre in both receptors. Before these structures, identifying the TM-ECL boundaries of the family B GPCRs was attempted through various alignment strategies (Chugunov *et al.*, 2010; Donnelly, 1997; Frimurer & Bywater, 1999). Alignment of the ECLs found ECL1 to be the most variable in length, ECL2 shows the highest conservation across the family and ECL3 is relatively short. The ECLs have been implicated in ligand binding and activation (Gkountelias *et al.*, 2009; Koole *et al.*, 2012) however the specific mechanism by which this occurs is not yet understood.

The family C GPCRs have a large N-terminal ECD consisting of two regions. The N-terminal ligand-binding region is divided into an N and C-terminal domain (LB1 and 2 respectively) (Kunishima *et al.*, 2000). The ligand binds between these two domains. The cysteine rich domain is at the C-terminus of the ECD and consists of nine cysteine residues and three β-sheets. Eight of these cysteine residues are involved in four intradomain disulphide bonds stabilising the structure. The remaining cysteine forms a disulphide bond with the cysteine in LB2. It is thought the cysteine rich domain transmits the signal from the ligand binding domain to the TM bundle (Muto *et al.*, 2007). This nine cysteine domain is conserved across family

C GPCRs with the exception of the $GABA_B$ receptor (Liu *et al.*, 2004b). Another property of family C GPCRs is the constitutive dimerisation between the ECDs. This dimerisation occurs between hydrophobic patches of LB1 for mGlu1 and is stabilised by a disulphide bond between Cys140 of each monomer, located in a disordered part of the structure (Kunishima *et al.*, 2000). This interaction can still occur even when this cysteine has been mutated (Kunishima *et al.*, 2000; Ray & Hauschild, 2000; Romano *et al.*, 2001; Tsuji *et al.*, 2000). This LB1 interaction is also observed with the $GABA_2$ receptor (Liu *et al.*, 2004a; Rondard *et al.*, 2008).

1.1.5.3 TM domains

GPCRs share a similar TM architecture of seven α-helices arranged in a cylindrical bundle. This was definitively shown with the crystal structure of rhodopsin in 2000 (Palczewski *et al.*, 2000) describing the TM domain as a bundle of α-helices, stabilised by interhelical hydrogen bonding. This conformation was confirmed with the publication of the β2-AR structure (Rasmussen *et al.*, 2007) and with the continuing structures that are being obtained. The TM domain of the β2-AR is presented in Figure 1.3, with each helix highlighted a separate colour for clear identification.

Despite this structural similarity, the primary sequence homology of GPCRs is low. However there are a number of conserved residues, motifs and inter-helical contacts present between receptors. There is a conserved D/ERY motif at the cytoplasmic end of TM3, a conserved tryptophan (CWxP motif) in TM6, which is predicted to act as a toggle switch and a conserved NPxxY motif near the cytoplasmic end of TM7 (Figure 1.4).

In the D/ERY motif the arginine ($R^{3.50}$) is conserved in 96% of family A GPCRs and forms a salt bridge with the preceding $D/E^{3.49}$ in every solved inactive family A structures (Katritch *et al.*, 2013). $R^{3.50}$ also forms hydrogen bonds with a glutamate ($E^{6.30}$) at cytoplasmic end of TM6 in the rhodopsin receptor (Palczewski *et al.*, 2000). These interactions were also observed in the D3 receptor and the A2AR (Chien *et al.*, 2010; Doré *et al.*, 2011).

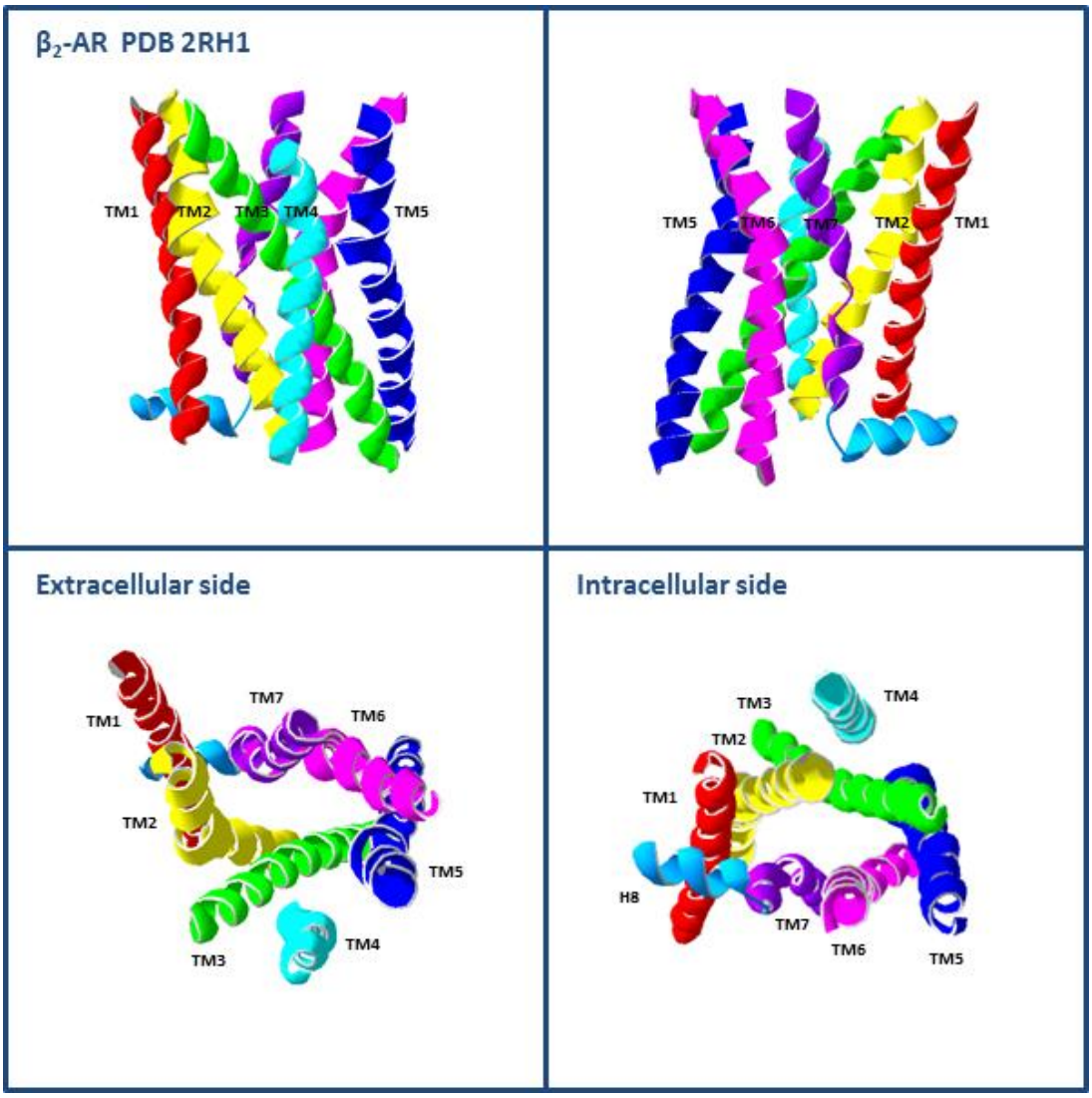

Figure 1.3. TM domain of the β2-AR (PDB 2RH1).

Each TM helix (including helix 8) has been highlighted a different colour. TM1 is red, TM2 is yellow, TM3 is green, TM4 is cyan, TM5 is blue, TM6 is magenta, TM7 is purple and H8 is light blue. The receptor is presented in four orientations. The top two are parallel to the membrane rotated 180°. The bottom two are perpendicular to the membrane from the extracellular and intracellular side.

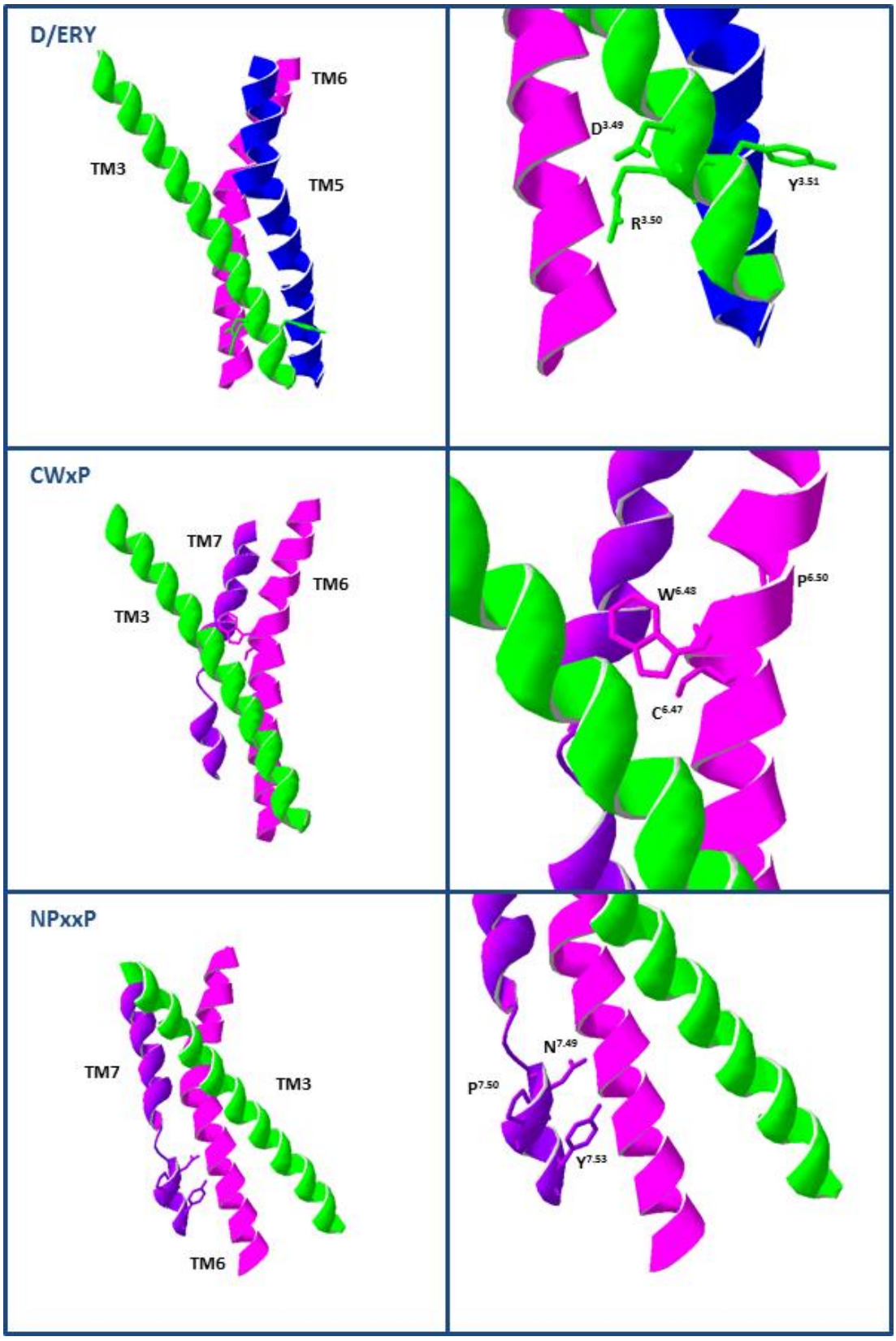

Figure 1.4. Conserved GPCR motifs highlighted using the β2-AR structure (PDB 2RH1). These are the D/ERY motif at the cytoplasmic end of TM3, the CWxP motif in TM6 and NPxxY motif in TM7.

In the β2-AR the proximity of $R^{3.50}$ to $E^{6.30}$ is not close enough for hydrogen bonding however there are hydrophobic residues at the cytoplasmic ends of TM3, 5 and 6 that are close enough to form interactions with each other and a hydrogen bond between $Y^{3.60}$ (ICL2) and $H^{6.31}$ is present (Cherezov *et al.*, 2007; Rasmussen *et al.*, 2007). In the histamine H1 receptor the ionic lock is absent however $R^{3.50}$ forms a hydrogen bond with $Q^{6.36}$ in TM6 (Shimamura *et al.*, 2011). The DRY motif also interacts with ICL2 stabilising it in a conformation that can interact with the G protein. The arginine of this motif also directly interacts with the G protein through a tyrosine residue and with the tyrosine in the NPxxY motif of TM7 (Rasmussen *et al.*, 2011b).

The CWxP motif in TM6 is highly conserved in non-olfactory family A GPCRs. $P^{6.50}$ creates a kink in the helix. $W^{6.48}$ and $F^{6.44}$ move towards $P^{5.50}$ during activation in a process named the transmission switch (originally called the rotamer toggle switch) (Deupi & Standfuss, 2011). In inactive structures $C^{6.47}$ interacts with 7.44/7.45 in TM7 which constrains TM6 and TM7 preventing the interaction that occurs between $N^{7.49}$ and $D^{2.50}$ in the active state (Olivella *et al.*, 2013).

The NPxxY motif is located near the cytoplasmic end of TM7 (Figure 1.4). The $Y^{7.53}$ residue is highly conserved (92%) and is orientated towards TM1, 2 or 8 in inactive structures. In active structures the $Y^{7.53}$ side chain changes conformation and is orientated towards the middle of the TM bundle forming interactions with TM3 and 6. In may also form a water mediated hydrogen bond with a conserved $Y^{5.58}$ reside in TM5 (Katritch *et al.*, 2013).

A common set of interactions is maintained through highly conserved ($N^{1.50}$, $D^{2.50}$, $W^{4.50}$ and $P^{7.50}$) and non-conserved residues. These interactions are orientated in the middle and cytoplasmic sides of the TM bundle between TM1-2, TM3-4, TM3-5 and TM3-6-7. Given the lack of movement of TM1 and 2 during activation it was proposed that these conserved interactions are important for correct folding, membrane insertion and receptor structure. TM3 is a structural hub. This domain is inserted into the membrane at a tilted angle, which may facilitate these multiple interactions. The consensus contacts with TM4 and 6 occur in the middle of the domain and with TM2 and 5 on the cytoplasmic side (Venkatakrishnan *et al.*, 2013).

Prolines in several of the helices caused kinking, most predominantly in TM6. Prolines are a common feature in GPCR TM domains and are predicted to enable the structural re-arrangement that occur during activation (Cherezov *et al.*, 2007).

The two crystal structures of family B GPCRs have confirmed the consistent 7TM bundle structure seen with the family A GPCRs and predicted throughout this receptor family (Hollenstein *et al.*, 2013; Siu *et al.*, 2013). Examination of these two structures in greater detail does reveal some notable differences.

The N-terminus of TM1 in the glucagon receptor (GCGR) extends much further into the extracellular space than observed in family A structures (Siu *et al.*, 2013). The reasons for this were speculated to be for glucagon binding and orientation of the ECD. The distance between the extracellular ends on TM2 and 6 and 3 and 7 is much larger than for most other GPCRs creating a wide deep cavity of the ligand-binding pocket, much larger than for family A GPCRs. This V shaped TM binding pockets was also a feature of the CRHR1 (Hollenstein *et al.*, 2013). In TM7 of both receptors, the conserved proline in the family A NP(7.50)xxY motif is absent however the glycine (7.50) that replaces it results in a helical bend. In the GCGR, this is stabilised by hydrophobic interactions with F184 in helix 2.

The TM domains of the family C GPCRs share a number of the conserved residues of family A. These include the cysteine residues of TM3 and ECL2, that form a disulphide bond, $W^{6.50}$ in TM6 and conserved basic residues at the bottom of TM3 that were proposed to function similarly to the DRY lock (Binet *et al.*, 2007).

1.1.5.4 Intracellular region

The intracellular region of GPCRs consists of three ICLs connecting TM1 and 2, TM3 and 4 and TM5 and 6. Following TM7 in some GPCRs is another α-helix (helix 8), which associates with the plasma membrane through palmitoylation sites. Following helix 8 (H8) is an intracellular C-terminal domain. ICL1 is often a short loop consisting of a helical turn. The length of ICL2 is most conserved but the secondary structure is more varied, usually consisting of a one or two turn α-helix or an unstructured stretch of amino acids. ICL3 varies considerably in length across the family A GPCRs which was proposed to relate to selectivity to different G

proteins. Crystal structures usually find ICL3 to be disordered (Moreira, 2014; Venkatakrishnan *et al.*, 2013). In the opioid receptors, ICL2 is tethered to TM3 through a salt bridge between an ICL2 arginine and $D^{3.49}$ of the DRY motif (Thompson *et al.*, 2012). A similar effect occurs with some aminergic receptors, which have an ICL2 tyrosine that forms hydrogen bonds with the DRY aspartate (Valiquette *et al.*, 1995; Warne *et al.*, 2008). In the crystal structure of the β2-AR complex with the G protein, ICL2 formed interactions with the G_{α} N-terminus (Rasmussen *et al.*, 2011b). ICL2 was also important for G protein coupling in the dopamine receptor, m5 muscarinic receptor and m3 muscarinic receptor (Blin *et al.*, 1995; Burstein *et al.*, 1998; Han *et al.*, 2009). The ICL2 domain of the TSHR had residues important for both $G_{\alpha s}$ and $G_{\alpha q}$ coupling (Kosugi *et al.*, 1994). ICL3 is also an important domain for G protein-coupling. Basic, polar and hydrophobic residues are involved in coupling to different G proteins (Burstein *et al.*, 1996; Dalman & Neubig, 1991; Wade *et al.*, 1996). The C-terminus is usually implicated in receptor phosphorylation however ICL3 can be phosphorylated in multiple receptors and in some cases ICL1 and 2 (Gurevich & Gurevich, 2006).

1.1.6 Post-translational modifications

Following expression, GPCRs can undergo a number of post-translational modifications. These include glycosylation of the N-terminal ECD and the ECLs, phosphorylation and palmitoylation of the intracellular C-terminal domain and the ICLs and interactions with cholesterol and the TM domain (Chini & Parenti, 2009; Tobin, 2008; Wheatley & Hawtin, 1999; Wheatley *et al.*, 2012).

Glycosylation can either be N-linked through the nitrogen of the asparagine side chain amide group, or O-linked glycosylation through the hydroxyl group of serine or threonine residues (Wheatley & Hawtin, 1999). N-linked glycosylation occurs at the NXS/T consensus sequence in the endoplasmic reticulum (ER) and the Golgi. O-linked glycosylation lacks a consensus motif making it harder to study (Duvernay *et al.*, 2005). N-linked glycosylation has been found in both the N-terminal ECD and the ECLs. Glycosylation can be essential for successful expression to the cell surface (Deslauriers *et al.*, 1999) and efficient folding of the receptor (Davis *et al.*, 1995), but in other cases has no effect on cell surface expression, ligand binding or

receptor signalling (Fukushima *et al.*, 1995; van Koppen & Nathanson, 1990). In the β2-AR, glycosylation of ECL2 was not required for successful cell surface expression and internalisation, however was required for the receptor to enter the degradation pathway following prolonged agonist exposure (Mialet-Perez *et al.*, 2004).

Palmitoylation is the addition of a 16 carbon saturated fatty acid (palmate), most often to cysteine residues through a thioester bond. It was first described in the transferrin receptor (Omary & Trowbridge, 1981) then in rhodopsin where it was located at the end of helix 8 and inserted into the membrane (Moench *et al.*, 1994; O'Brien & Zatz, 1984; Palczewski *et al.*, 2000). Palmitoylation was discovered in β2-AR which confirmed that in was a general feature of GPCRs and not just specific to rhodopsin (O'Dowd *et al.*, 1989). Palmitoylation appears to be important for cell surface expression of the receptor (Karnik *et al.*, 1993) and to prevent degradation (Gao *et al.*, 1999). Palmitoylation has been shown to be a transient process, with increased palmate turnover occurring in response to agonist binding. This has an influence on downstream signalling, including coupling with the G protein, phosphorylation, desensitization, internalisation and down-regulation (Qanbar & Bouvier, 2003). A bound cholesterol was discovered in the crystal structure of β2-AR between TM2 and 4 (Hanson *et al.*, 2008).

1.1.7 Ligand binding

1.1.7.1 Ligand-receptor binding sites

The binding of ligands to family A GPCRs occurs on the extracellular side of the TM bundle. Some ligands bind deeply into the pocket (doxepin at the human histamine H1 receptor) (Shimamura *et al.*, 2011) and others bind closer to the ECLs (IT1t at the CXCR4) (Wu *et al.*, 2010). In a consensus analysis of the receptor it was found that certain residues of TM3, 6 and 7 contact the ligand in nearly all receptors. Interactions with other residues occur on a more ligand-specific basis with the exception of TM1, which does not form any direct ligand binding contacts (Venkatakrishnan *et al.*, 2013).

Ligand binding of the β2-AR is similar to that of the retinal bound rhodopsin structure. The inverse agonist carazol does not bind as deeply as the retinal

chromophore however they both interact with a series of aromatic residues in TM5 and 6, which are positioned around the conserved tryptophan residue in TM6 (Cherezov *et al.*, 2007; Palczewski *et al.*, 2000). The antagonist ligand-binding pocket of the D3R was similar to β2-AR interacting with side chains of TM3, 5, 6 and 7. The lipid ligand sphingosine-1-phosphate binds to an amphipathic binding pocket in the TM bundle however the extracellular side is covered by the receptor N-terminus and ECLs 1 and 2. The entry of this ligand is through the lipid bilayer, between TM1 and 7 (Hanson *et al.*, 2012).

Ligand binding at family B GPCRs occurs predominantly at the N-terminal ECD. The peptide ligands of this family form an amphipathic α-helix at their C-terminus and form interactions with a hydrophobic ligand binding groove created by an N-terminal α-helix and two antiparallel β-sheet structures of the ECD (Hollenstein *et al.*, 2014). This allows the N-terminus of the ligand to interact with the receptor ECLs and TM bundle stabilising the active conformation through a "two-domain" model of ligand binding (Hoare, 2005). This will be discussed in greater detail in the family B GPCR section later in the review.

Ligand binding of family C GPCRs occurs at the venus fly trap (VFT) domain of the large N-terminus. It was likened to that of the bacterial periplasmic binding protein (O'Hara *et al.*, 1993). Understanding of the ligand binding mechanism was greatly enhanced with the mGlu1 receptor ECD structure in the presence and absence of glutamate (Kunishima *et al.*, 2000). These bi-lobed ECDs exist in an open and closed conformation and each receptor dimer in a resting and active state. In an open conformation, the glutamate ligand makes contacts with the LB1 domain. In the closed conformation the ligand makes contacts with both LB1 and 2 domains. In the resting orientation, the dimers interact through LB1. Binding of the ligand (in this case glutamate) causes the lobes to reorganize allowing the LB2 to interact resulting in the activation of the receptor (Tsuchiya *et al.*, 2002). The ligand binding affinity is not just based on the interactions between ligand and receptor but also the equilibrium constant between the open and closed conformations (Parmentier *et al.*, 2002).

1.1.7.2 Binding affinity and the ternary complex model

Research into the affinities of receptor agonists and antagonists in the β-adrenergic receptor system found that the affinity of antagonists remained the same in the presence of absence of guanine nucleotides. The affinity of agonists to the β-adrenergic receptor reduced in the presence of guanine nucleotides (Maguire *et al.*, 1976; Williams & Lefkowitz, 1977). This led to the ternary complex model which described the interaction of the receptor to an additional membrane component which caused the high affinity state for ligand binding (De Lean *et al.*, 1980). The effect of adding the guanine nucleotides was to de-stabilise the ternary complex causing the dissociation of both the ligand and the component protein. This component is the G protein.

1.1.8 GPCR activation

An active GPCR has adopted a conformation that allows the coupling and stabilisation of an effector molecule resulting in a downstream response (Venkatakrishnan *et al.*, 2013). It was originally thought that a receptor behaves as a molecular "switch" existing in either an on or off conformation (Schwartz *et al.*, 2006). However current understanding is that GPCRs can exist in multiple conformational states allowing binding to different effectors, facilitating a range of downstream signalling responses (Kenakin & Miller, 2010). Ligand binding stabilises a particular receptor conformation. This can result in full activation of a signalling pathway (agonist), partial activation (partial agonist), binding to the receptor with no effect on basal signalling (antagonist) and stabilising the inactive receptor conformation (inverse agonist) (Hill, 2006). Ligand affinity is also dependent on the interaction of the receptor with its G protein described as the ternary complex model (De Lean *et al.*, 1980). Ligand-specificity of a single receptor can also result in the activation of different signalling pathways with a mechanism described as biased agonism or functional selectivity (Kenakin, 2007).

Two explanations for a conformation change in proteins induced by molecule binding have been proposed. The first is the conformational induction mechanism in which the binding of a molecule contributes energy to induce a conformational

change (Koshland, 1958). In terms of GPCRs this would mean the ligand binds to the low energy inactive state and induces a conformational change to the active state. The second is the conformational selection mechanism where molecules bind to pre-existing conformations, stabilising them and shifting the equilibrium in favour of these structures (Monod *et al.*, 1965). Model simulations favored conformational selection as the mechanism for small molecule-protein interactions which include ligand-receptor interactions (Okazaki & Takada, 2008).

1.1.8.1 Crystal structures of active GPCRs

Understanding of the structural changes that occur between the inactive and active receptor were greatly enhanced with the publication of the β2-AR in complex with both an agonist and a G protein-like nanobody (Rasmussen *et al.*, 2011a) and the β2-AR in complex with an agonist and the heterotrimeric G protein (Rasmussen *et al.*, 2011b). The TM helices of these structures together with the inactive β2-AR structure are shown in Figure 1.5. The β2-AR-Nb80 structure was solved by immunizing a llama with purified agonist bound β_2-AR reconstituted at high density into phospholipid vesicles (Rasmussen *et al.*, 2011a). The differences between this active structure and the inactive structure are mainly on the cytoplasmic side, with outward movements of TM 5 and 6, inward movements of TM 3 and 7 and the formation of a two-turn α helix at ICL2. The largest conformational change was TM6 with an 11.4Å movement of the helix at Glu268$^{6.30}$. This was facilitated by a small rotation of the helix just before the conserved TM6 proline (Pro288$^{6.50}$). The β2-AR-G_s structure was solved by mixing purified GDP-Gs with purified β2-AR bound to a high affinity agonist (Rasmussen *et al.*, 2011b). The GDP released when G_s formed a complex with the β2-AR was hydrolysed to prevent the disruption of the high affinity β2-AR-G_s interaction that can occur in presence of GTP and GDP. The main differences between the inactive and active structures are a 14Å outward movement of TM6 and a smaller outward movement and extension on TM5 on the intracellular side. The β2-AR active state structure is stabilised with extensive interactions with the $G_{\alpha s}$ subunit but there are no direct interactions with $G_{\beta\gamma}$. In this crystal structure there is a 127° displacement of the $G_{\alpha s}$AH domain with relation to $G_{\alpha s}$Ras (Figure 1.6). In the Gαs-GTPγS crystal structure the nucleotide binding

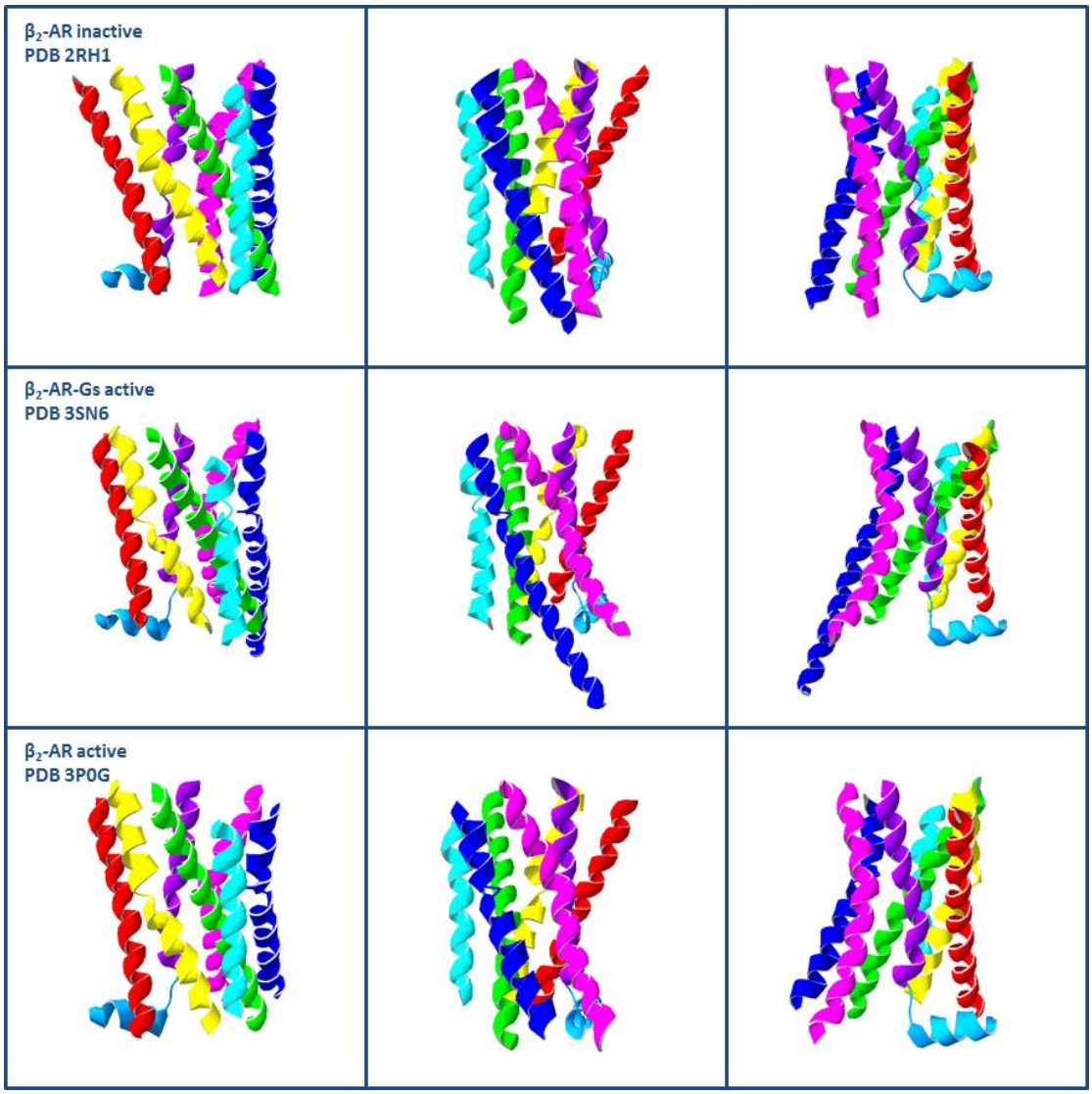

Figure 1.5. Crystal structures of the β2-AR in an inactive (PDB 2RH1) and two active conformations (G protein bound PDB 3SN6 and nanobody stabilised PDB 3P0G).
Each TM helix (including helix 8) has been highlighted a different colour. TM1 is red, TM2 is yellow, TM3 is green, TM4 is cyan, TM5 is blue, TM6 is magenta, TM7 is purple and H8 is light blue. The receptor is presented in three orientations all parallel to the plasma membrane with 120° rotations.

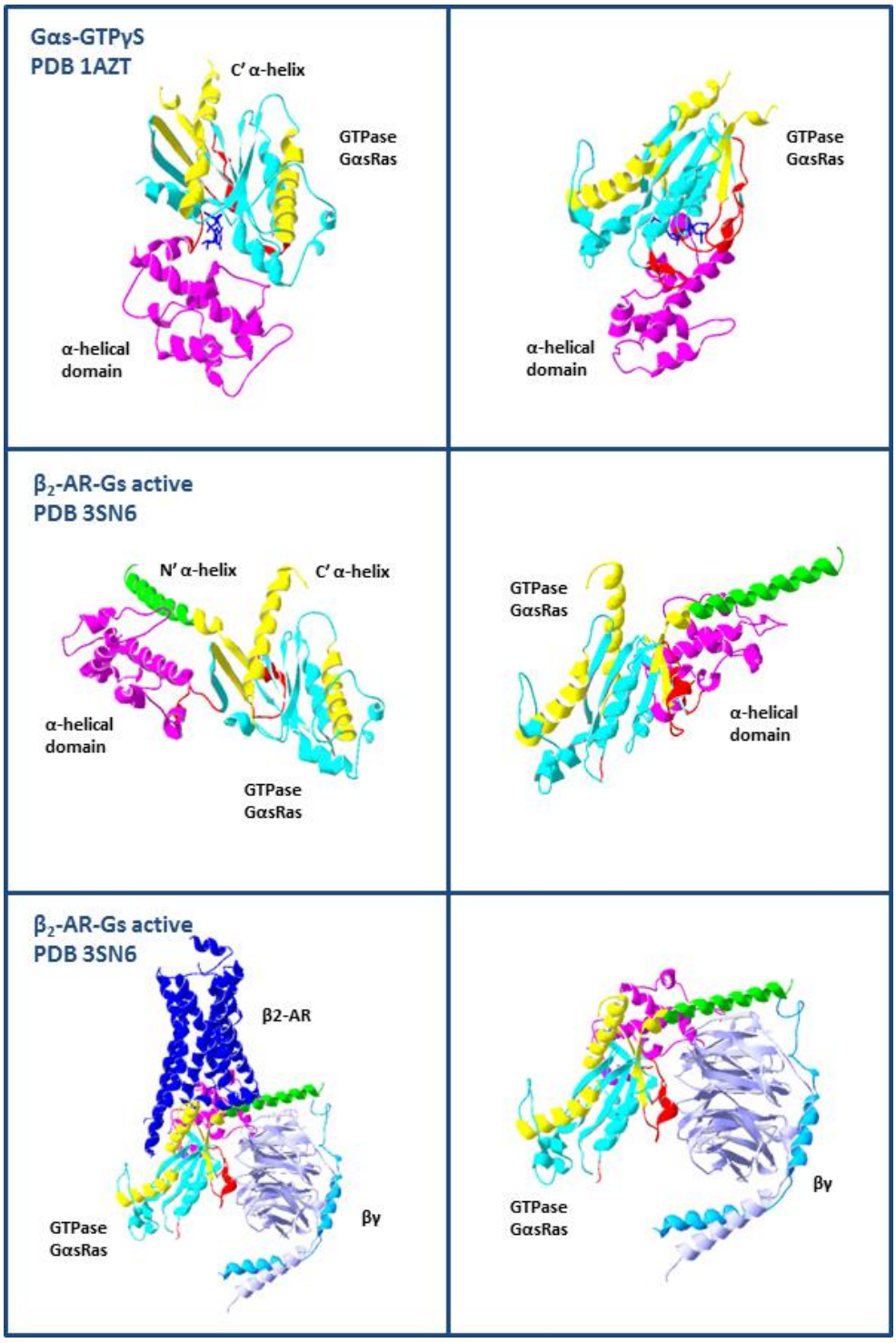

Figure 1.6. Crystal structures of the heterotrimeric G protein in different conformations.
The top row is the $G_{\alpha s}$ subunit bound to the non-hydrolysable GTPγS (PDB 1AZT) presented in two different orientations, parallel to the plasma membrane. The middle row is the $G_{\alpha s}$ subunit in the β2-AR-Gs crystal structure (PDB 3SN6). The bottom row presents all the components of the β2-AR-Gs crystal structure (PDB 3SN6). The GTPase ($G_{\alpha s}$ Ras domain) is cyan with the GPCR interactions areas (from the PDB3SN6 structure) highlighted yellow. The N-terminal α helix is green. The α-helical domain is magenta. The three switch regions are highlighted red and the bound GTPγS presented in the structure in the top row is blue.

pocket is at the interface of these two domains (Sunahara *et al.*, 1997). Guanine nucleotide binding stabilises these two domains and the crystal structures shows the flexibility of this protein.

1.1.8.2 Mechanism of activation

In the β2-AR and $A_{2A}R$, ligand-binding pulls the extracellular sides of TM3, 5 and 7 together (Lebon *et al.*, 2011; Rasmussen *et al.*, 2011b; Rosenbaum *et al.*, 2011; Xu *et al.*, 2011). This causes structural changes around $P^{5.50}$ in TM5 resulting in intracellular movement of the helix (Sansuk *et al.*, 2011). Rearrangement of the TM5-6 interface is coupled with rotation of TM6 near $F^{6.44}$. This rotation causes a large intracellular movement of this kinked helix opening the cleft required for G protein-binding (Standfuss *et al.*, 2011). TM6 is held close to TM3 in the inactive state through different mechanisms. One includes the interactions with the $R^{3.50}$ of the DRY lock motif and a glutamate in TM6 (Palczewski *et al.*, 2000). Another includes hydrophobic interactions between $L^{3.43}$ and $I^{6.40}$ occurring in the β2-AR and the M_2 mAChR (Hulme, 2013). Release of TM6 allows interactions between TM7 and TM1 and 2 to occur. This repositioning of TM7 prevents TM6 from moving back, stabilising the active receptor conformation (Scheerer *et al.*, 2008). Inactive and active conformations of the β2-AR are presented in Figure 1.5. The two active structures depict the β2-AR bound to agonist and either in complex with the $G_{\alpha s\beta\gamma}$ protein (Rasmussen *et al.*, 2011b) or stabilised by a G protein resembling a nanobody (Rasmussen *et al.*, 2011a).

In the active conformation, the cytoplasmic end of TM3 forms interactions with the heterotrimeric G protein. A key interaction is between the $R^{3.50}$ of the DRY motif and a backbone carbonyl at the C-terminus of the G protein. A consensus interface of at least 8 residues has been identified in TM3, 5 and 6 that bind to the G protein. The receptor interaction areas of the G protein are highlighted in Figure 1.6. The N-terminus of the G protein interacts with ICL2 (Choe *et al.*, 2011; Deupi *et al.*, 2012; Rasmussen *et al.*, 2011b). The side chains of $N^{7.49}$, $Y^{7.53}$, $R^{3.50}$ and $G_{\alpha s}Y391$ have a linear orientation parallel to TM3 in the activated state with $R^{3.50}$ being the upper insertion point of the G protein (Rasmussen *et al.*, 2011b). Contrastingly, $F^{3.58}$ in ICL2 has the deepest insertion into the G protein interacting with the N and C

terminal $G_{\alpha s}$ helices and residues in the β2 -β3 strand (Moro *et al.*, 1993). Similar interactions were observed between an M_3mAChR ICL2 leucine and the N-terminal helix of $G_{q\alpha}$ (Hu *et al.*, 2010). The $G_{\alpha s}$ α5 helix also forms interaction with the TM5 and 6 that have moved during activation (Rasmussen *et al.*, 2011b).

The activation of the family C GPCRs is initiated through the dramatic conformational change of the ECD dimer. Each monomer exists in an open and closed state and each dimer can exist in a resting and active conformation. Binding to the ligand stabilises the closed active conformation (although all combination have been observed) which brings the each LB2 domain into close proximity (Kunishima *et al.*, 2000; Tsuchiya *et al.*, 2002). This mechanism was confirmed with the $GABA_B$ receptor. The introduction of N-glycosylation preventing the interaction of the LB2 domains resulted in a loss of receptor activation (Rondard *et al.*, 2008). FRET analysis confirmed the movement of the TM helices of each monomer during receptor activation (Tateyama *et al.*, 2004).

In the mGlu1 receptor, binding of glutamate to one receptor monomers results in partial activation however binding of glutamate to each monomer caused a full activation (Kniazeff *et al.*, 2004). However with the $GABA_B$ receptor, the ligand only binds to just the $GABA_{B1}$ monomer, which is sufficient for receptor activation (Galvez *et al.*, 2000; Kniazeff *et al.*, 2002). Similarly the taste receptors share a T1R3 subunit with ligand specificity determined by the T1R1/2 subunit of the dimer (Chandrashekar *et al.*, 2006).

1.1.9 GPCR signalling

1.1.9.1 GPCR signalling components

1.1.9.1.1 G proteins

A G protein is a guanine nucleotide binding protein. They bind to GTP and cause the hydrolysis to GDP. The G proteins associated with GPCRs are heterotrimeric proteins consisting of an α, β and γ subunit however small monomeric GTPases also exist (McCudden *et al.*, 2005). Considering the quantity of GPCRs in the human genome, there are relatively few G proteins. There are 21 G_α subunits (16 genes), 6 $G\beta$ subunits (5 genes) and 12 $G\gamma$ subunits (Downes & Gautam, 1999). The G proteins

are divided into classes according to the G_α subunit. These are $G_{\alpha s}$, $G_{\alpha i}$, $G_{\alpha q}$ and $G_{\alpha 12/13}$ (Simon *et al.*, 1991). The class of subunit determines which signalling pathway becomes activated.

The G_α subunit consists of two domains (Figure 1.6). A GTPase (Ras) domain and an α-helical domain (Sunahara *et al.*, 1997). The GTPase domain is conserved in all G protein families including monomeric G proteins and elongation factors. This domain hydrolyses GTP and interacts with the $\beta\gamma$ subunits, the GPCR and effector proteins. This domain also contains three loops (switches) that undergo conformational changes following binding to GTP or GDP. The α-helical domain is only found in G_α and forms a lid over the nucleotide-binding pocket. Modifications at the N-terminus are involved in membrane and proteins interactions. The $G\beta$ subunit has an N-terminal α-helix followed by a seven bladed β-propeller structure. The N-terminus of $G\gamma$ interacts with the N-terminal helix of $G\beta$ and the C-terminus with blades 5 and 6 (Oldham & Hamm, 2008). This interaction is only dissociated under denaturing conditions (Schmidt *et al.*, 1992).

The best characterised contacts site of the G protein with an activated GPCR are through its C-terminal α-helix (Janz & Farrens, 2004) however interactions also occur with the N-terminal helix and contact sites within the GTPase domain (Figure 1.6). In the active structure of β2-AR, there are no direct contact sites between the GPCR and the $G\beta\gamma$ subunits however $G\beta$ does stabilise the N-terminal α-helix of G_α (Rasmussen *et al.*, 2011b).

There are two proposed models by which the G protein couples with its receptor. The first is the "collision coupling" model, which predicts that the G protein encounters an activated receptor, binds and signals (Tolkovsky & Levitzki, 1978). The other is the "pre-coupled" model which predicts that the G protein binds to its receptor before agonist activation (Galés *et al.*, 2006). The pre-coupling model explains the specificity between receptor and G protein coupling and the rapid response time in signalling however it does not account for the amplification of signalling (Hamm *et al.*, 1987). The "collision coupling" model is supported by kinetic and live cell imaging data, however co-purification and co-

immunoprecipitation experiments on inactive GPCRs and G protein and energy transfer experiments with labelled receptor and G proteins supports the "pre-coupled" model (Hein & Bünemann, 2009). Emerging evidence suggest that receptors can function through both models and it depends both on the type of receptor and G protein involved (Jakubík *et al.*, 2011).

1.1.9.1.2 Arrestins

There are four members of the arrestin family. Arrestin 1 and 4 are the visual arrestins, expressed in the rod and cone cells (Craft *et al.*, 1994; Wilden *et al.*, 1986). Arrestin 2 and 3 (alternatively named β-arrestin 1 and β-arrestin 2) interact with the non-visual GPCRs and are ubiquitously expressed (Attramadal *et al.*, 1992; Lohse *et al.*, 1990). The early view of the β-arrestins was that they bound to the activated GPCR following serine/threonine (S/T) phosphorylation of the C-terminus or ICL3, blocking G protein binding resulting in desensitization of the receptor (Shenoy & Lefkowitz, 2003a).

Arrestins share a similar structure (Figure 1.7) of an N and C-terminal domain with a central polar core, connected by a C-terminal tail (Han *et al.*, 2001). In the inactive conformation the C-terminal tail lies along the N-terminal domain of the arrestin molecule. This is displaced by the receptor through interactions with its phosphorylated residues. Upon activation there is a conformation change of arrestin, with a substantial twisting of the N and C-terminal domains in relation to each other increasing the affinity to the activated receptor (Kim *et al.*, 2013; Shukla *et al.*, 2013).

1.1.9.1.3 G protein-coupled Receptor Kinases (GRKs)

G protein-coupled Receptor Kinases (GRKs) were first identified in rhodopsin following the discovery of rhodopsin phosphorylation following activation (Bownds *et al.*, 1972; Kühn & Dreyer, 1972; Weller *et al.*, 1975). Receptor phosphorylation was subsequently observed in the β2-AR (Sibley *et al.*, 1985; Stadel *et al.*, 1983). The kinase responsible for this phosphorylation was identified as the β adrenergic receptor kinase, which later became known as GRK2. Since then a further five GRKs have been discovered. These seven GRKs are split into three subfamilies. These are

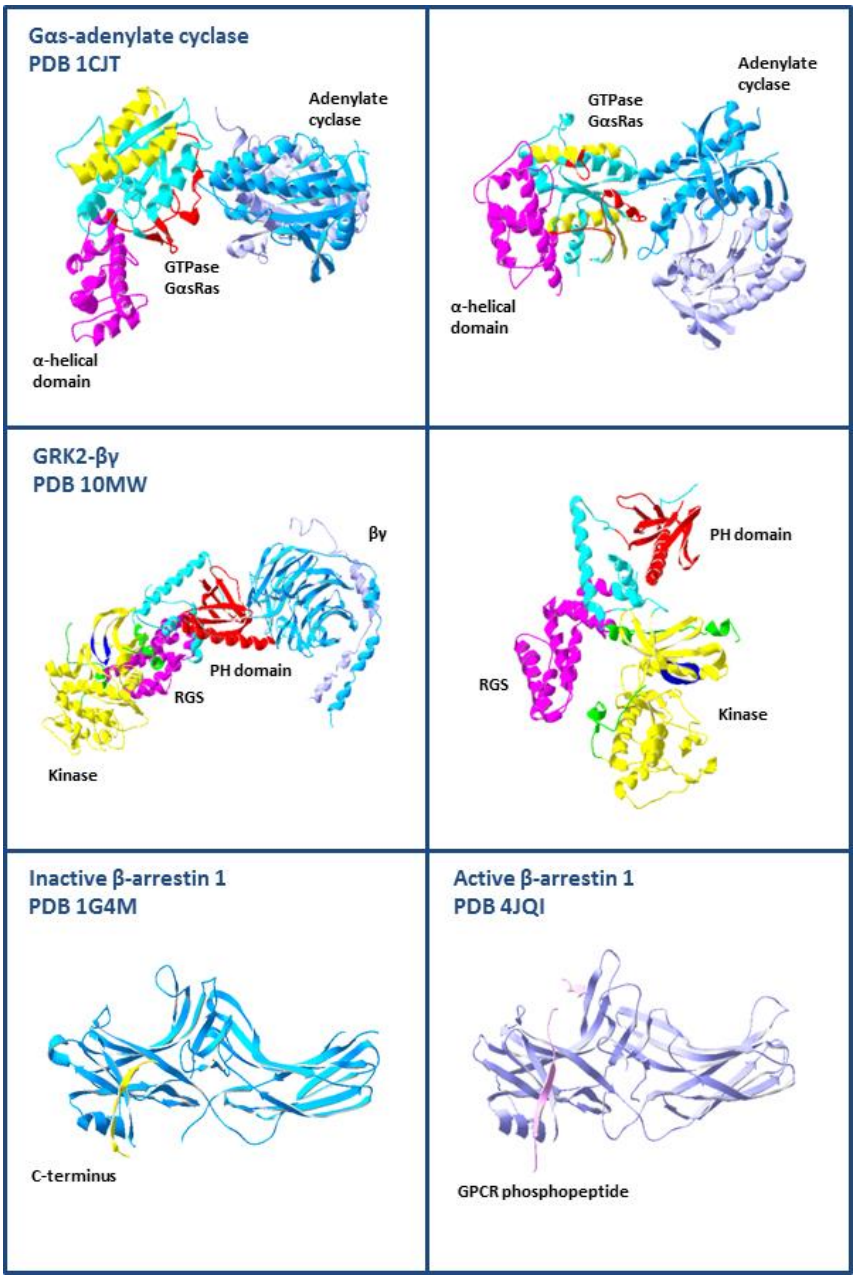

Figure 1.7. Crystal structures of key GPCR signalling components.

The top row is the $G_{\alpha s}$ subunit interacting with its effector protein, adenylate cyclase. The GTPase ($G_{\alpha s}$ Ras domain) is cyan with the GPCR interactions areas (from the PDB3SN6 structure) highlighted yellow. The three switch regions are highlighted red. The adenylate cyclase is light blue and purple. The complex is presented in two orientations, parallel to the plasma membrane and perpendicular to the plasma membrane from the intracellular side. The second row is the crystal structure of GRK2 coupled with $\beta\gamma$. GRK is cyan, with the RGS domain highlighted magenta, the kinase domain yellow, the AGC kinase C-terminus is green and the PH domain is red. The nucleotide-binding domain has been highlighted blue. The GRK2 crystal structure is in two orientations, planar to the membrane. In the second image the $\beta\gamma$ subunits are absent. The bottom row is the crystal structure of the inactive and active conformations of β-arrestin 1. In the inactive conformation the C-terminal tail lies along the N-terminal domain of the arrestin molecular. This is displaced by the receptor (GPCR phosphopeptide) in the active structure.

GRK1 and 7 (visual kinases), GRK2 (2 and 3) and GRK 4 (4, 5 and 6). GRK1 and 7 are expressed in the retinal rods and cones respectively. GRKs 2, 3 and 5 are expressed in mammalian tissues however GRK4 is limited to the cerebellum, kidney and testis (Pitcher *et al.*, 1998). GRKs consist of an N-terminal helix that binds the kinase to the active GPCRs and is important feature for the kinase activity (Lodowski *et al.*, 2006; Palczewski *et al.*, 1993), a Regulator of G protein Signalling (RGS) homology domain (HD), an S/T protein kinase domain (KD) and a C-terminus that contains different structural features that are responsible for membrane targeting (Figure 1.7). These membrane-binding domains facilitate GRK function but are not required for phosphorylation (Mushegian *et al.*, 2012). The kinase domain is inserted into a loop of the RH domain. The kinase domain consists of two lobes (small and large) with the active site in between (Lodowski *et al.*, 2006), followed by a C-tail of which a central segment called the active site tether (AST) becomes ordered once the kinase adopts a closed active conformation (Kannan *et al.*, 2007). This domain was crystallised in an open conformation in the presence of a nucleotide analogue, which is in contrast to other AGC kinases (Taylor *et al.*, 2004).

The N-terminal helix is amphipathic and contains conserved residues that do not appear to be orientated towards the kinase domains (Lodowski *et al.*, 2006). It is thought that similar to G proteins, this region is disordered until in comes in contact with the GPCR (Huang & Tesmer, 2011). The N-terminal helix interacts with the kinase domain through conserved residues (Boguth *et al.*, 2010). A hydrophobic patch at the N-terminus of the N-terminal helix is predicted to interact with the GPCR (Leitz *et al.*, 2006) and a positively charged region adjacent to this helix is correctly positioned to interact with the lipid bilayer (Pitcher *et al.*, 1996).

1.1.9.2 G protein-dependent signalling

In the inactive state, the G protein exists as a GDP bound $G_{\alpha\beta\gamma}$ heterotrimer. The active conformation of a GPCR acts as a guanine nucleotide exchange factor (GEF) catalyzing the exchange of GDP to GTP (Gilman, 1987). The nucleotide binding site is separate from the receptor contact sites, therefore GDP release must be through conformation changes of the G protein (Natochin *et al.*, 2001). These conformational chances may open up the gap between the GTPase and the helical

domains, releasing the bound GDP (Grishina & Berlot, 1998). GDP binding is stabilised through hydrophobic interactions with the C terminal helix and a β-strand (Natochin *et al.*, 2000). There is evidence showing that the opening of the nucleotide binding pocket is induced by a movement of the βγ domain, however there is no agreement as to the precise mechanism through which this occurs (Oldham & Hamm, 2008).The receptor bound, nucleotide free G_α subunit has equal affinity for both GTP and GDP (Heck & Hofmann, 2001). Binding of GTP occurs due to a higher GTP concentration in the cell (Bos *et al.*, 2007). Binding of GTP causes conformational changes in the three switch regions (Figure 1.6). This results in a hydrophobic patch that binds to the βγ subunit becoming disrupted by charged residues, leading to dissociation of the complex (Lambright *et al.*, 1996; Noel *et al.*, 1993).

The exchange of GDP for GTP causes a conformational change of the G_α subunit resulting in the dissociation of the G protein from the receptor and also the G_α unit from βγ (Oldham & Hamm, 2008). Both of the dissociated G_α and βγ subunits can activate effector proteins resulting in second messenger molecules, which initiate a cellular response. Each class of the G_α subunit activates a specific pathway. $G_{\alpha s}$ binds to adenylate cyclase (Figure 1.7) resulting in an increase in the second messenger cAMP (May *et al.*, 1985; Pfeuffer *et al.*, 1983). It has also been found to activate Ca^{2+} channels and inhibit Na^+ channels (Mattera *et al.*, 1989; Schubert *et al.*, 1989). $G_{\alpha i}$ inhibits adenylate cyclase resulting in a decrease in cAMP levels (Taussig *et al.*, 1993). The $G_{\alpha q}$ family ($G_{\alpha q}$, $G_{\alpha 11}$, $G_{\alpha 14}$, $G_{\alpha 15}$ and $G_{\alpha 16}$) activates the effector enzyme phospholipase C (PLC) which catalyses the hydrolysis of phosphatidylinositol 4,5-bisphosphate (PIP_2) creating the second messengers inositol 1,4,5 triphosphate (IP_3) and diacylglcerol (DAG) (Hepler & Gilman, 1992). IP_3 releases Ca^{2+} from intracellular stores and DAG activates protein kinase C (PKC) (Steinberg, 2008). The $G_{\alpha 12}$ subfamily consists of the $G_{\alpha 12}$ and $G_{\alpha 13}$ subunits (Strathmann & Simon, 1991). They are similar both in primary sequence and biochemical properties and ligands are able to activate both subtypes, however they do have specific physiological responses (Kozasa *et al.*, 2011). They signal through the Rho family of GTPases, a family of peripheral membrane proteins.

These cycle between an inactive GDP bound and active GTP bound state that regulate cellular process such as morphology, migration, cell cycle and gene transcription (Aittaleb *et al.*, 2010).

The βγ component was originally thought to be a regulator of the G_α subunit, stabilising the GDP bound form and anchoring the heterotrimer to the membrane. However it was found that βγ could independently signal, first in yeast (Blumer & Thorner, 1991) and then in mammalian cells, acting on both adenylate cyclase and PLC (Camps *et al.*, 1992; Tang & Gilman, 1991).

1.1.9.3 G protein independent signalling

β-arrestins were first identified as being able to initiate signalling pathways independent of the G protein through the activation of MAPK signalling and the formation of β-arrestin-src complexes (Daaka *et al.*, 1998; Luttrell *et al.*, 1999). Using agonists and mutants of the ATR1 which prevented G protein-coupling it was shown that the receptor could still activate MAPK through a β-arrestin 2 dependent pathway (Wei *et al.*, 2003). Signalling can also be temporally dependent with early ERK1/2 signalling through $G_{\alpha s}$ and $G_{\alpha i}$ and late ERK1/2 signalling through β-arrestin1 and 2 (Shenoy *et al.*, 2006) and inverse agonists have been found to activate ERK1/2 through β-arrestin, independent of cAMP production (Azzi *et al.*, 2003). β-arrestins have also been found to signal through Akt (protein kinase B) (Beaulieu *et al.*, 2005) and RhoA (Barnes *et al.*, 2005).

β-arrestins are able to scaffold MAPK signalling components to the plasma membrane preventing their translocation to the nucleus. This changes the cellular effects from transcriptional regulation to cytoskeletal reorganization and chemotaxis. They can also bind regulatory units to inhibit signalling pathways, or converge on G protein dependent pathways to act synergistically (Defea, 2008).

β-arrestin ERK activation can also depend on the GRK that is activating the GPCR. GRK5 and 6 were required for β-arrestin dependent ERK activation of the AT1AR, V2R and β2-AR. GRK2 and 3 attenuated signalling (Reiter & Lefkowitz, 2006).

1.1.9.4 GPCR phosphorylation, desensitization and internalisation

GPCR phosphorylation was first described for rhodopsin following light activation (Bownds *et al.*, 1972; Kühn & Dreyer, 1972) through an opsin kinase, which later became GRK1 (Weller *et al.*, 1975). This effect was then described with the β2-AR (Sibley *et al.*, 1985; Stadel *et al.*, 1983) through a different kinase that became GRK2 (Benovic *et al.*, 1986). Phosphorylation of rhodopsin caused the binding of another protein (arrestin), which physically prevented the binding and subsequent signalling of the G protein. The discovery of an arrestin homologue which caused desensitization of β2-AR signalling led to a two-step mechanism of GPCR deactivation (Benovic *et al.*, 1987). Rhodopsin is phosphorylated on serine and threonine residues on the intracellular C-terminus (Ohguro *et al.*, 1993), however GPCRs can be also be phosphorylated on any of the ICLs (Tobin, 2008). Given this variety in both the domain being phosphorylated and the number of receptors to which the β-arrestins bind, it has been proposed that bulk negative charge is the important factor in arrestin binding (Gurevich & Gurevich, 2006). Recruitment of arrestin to a GPCR can be both phosphorylation dependent and independent (Min *et al.*, 2002). GPCR binding to the arrestin disrupts an ionic lock in the arrestin and induces a conformational change, which creates a high affinity binding between the GPCR and arrestin. Binding of arrestin to the intracellular region of GPCRs forms a cap over the receptor preventing the coupling of the G protein resulting in receptor desensitisation (Gurevich & Gurevich, 2006). Subsequently it was found that β-arrestins can interact with cAMP phosphodiesterases enhancing their activity demonstrating a second mechanism of β-arrestin desensitisation (Perry *et al.*, 2002).

The S/T cluster of residues in the C-terminus is not present in all receptors and appears to influence β-arrestin binding affinity. Receptors have been split into two classes based on this feature (separate from the A-F/GRAFS classification systems). Class A receptors (eg. β2-AR, μ-opioid receptor, dopamine D1A receptor, and α1b-AR) do not contain this S/T rich domain. They recruit β-arrestin 2, traffic to clathrin coated pits and then dissociate, internalising without the β-arrestin and recycle rapidly. Class B receptors (eg. angiotensin II type 1A receptor, neurotensin receptor

1 and vasopressin V2 receptor) recruit both β-arrestin 1 and 2 with equal and higher affinity and internalise together forming stable endosomal vesicles (Oakley *et al.*, 2001; Oakley *et al.*, 2000).

Following desensitisation, the receptor becomes internalised. Internalisation allows the dephosphorylation and re-sensitisation of the receptor through recycling back to the cell surface, the down regulation of the receptor through the degradation pathway or the activation of intracellular signalling pathways. A common mechanism of endocytosis is through clathrin coated vesicles, however other routes such as caveolae or other uncoated vesicles have also been described (Claing *et al.*, 2002). In this process, arrestin acts as a scaffold molecule recruiting the components of the clathrin coated machinery to the GPCR. These include clathrin itself and the adapter protein AP2 (Lefkowitz & Shenoy, 2005). β-arrestin is also able to recruit ubiquitin ligase, resulting in the ubiquitination of the β-arrestin protein, essential for clathrin mediated endocytosis. This ubiquitination is transient for the class A endocytotic receptors and sustained for class B (Shenoy & Lefkowitz, 2003b; Shenoy *et al.*, 2001).

1.1.9.5 GPCR recycling and degradation

Once the GPCR becomes internalised, the receptor can follow one of two pathways. The first is a recycling of the receptor back to the cell surface; the second is degradation. There are C-terminal sequence motifs that direct the GPCR to a specific pathway. A four residue motif (DSLL) of the β2-AR was transferred into the δ-opioid receptor re-directing the post-endocytotic process from degradation to rapid recycling (Gage *et al.*, 2001). The affinity of the receptor to arrestin also determines whether the GPCR is recycled or degraded (Oakley *et al.*, 2001; Oakley *et al.*, 2000). Post-endocytotic sorting to lysosomes is mediated by C-terminal tail motifs, regulatory binding partners and covalent modifications. The tyrosine-based sequence motif YXXφ (φ = large hydrophobic residue) is involved in internalisation and may act as a lysosomal sorting motif for the protease-activated receptor-1 (PAR1) (Paing *et al.*, 2004). The same receptor was found to bind to the regulatory proteins SNX1, which functioned in lysosomal sorting and degradation (Gullapalli *et al.*, 2006; Wang *et al.*, 2002). The sorting protein GASP also associates with C-

terminal tails directing receptors to lysosomes and degradation. Manipulation of GASP re-routed the receptor to be recycled back to the cell surface (Bartlett *et al.*, 2005; Simonin *et al.*, 2004; Whistler *et al.*, 2002). Ubiquitination is also a factor in receptor degradation. GPCRs that have been mutated to prevent ubiquitination were able to internalise following prolonged exposure to agonist but were not degraded (Shenoy *et al.*, 2001). Conversely, when β-arrestin ubiquitination was blocked, internalisation was prevented with little effect on degradation.

1.1.10 Dimerisation

Early evidence for the dimerisation of GPCRs was obtained through biochemical and biophysical techniques. A common method was the co-immunoprecipitation of different epitope tagged GPCRs. This identified homodimers (Hebert *et al.*, 1996), closely related heterodimers (Jones *et al.*, 1998; Kaupmann *et al.*, 1998; White *et al.*, 1998) and more distantly related heterodimers (AbdAlla *et al.*, 2000). Different approaches have also supported receptor dimerisation. This include BRET analysis of the β2-AR (Angers *et al.*, 2000) and FRET, which was dependent on agonist stimulation (Cornea *et al.*, 2001; Horvat *et al.*, 2001). Recent structures of GPCRs have revealed a strong dimerisation interface between TM5 and 6 of each monomer and a slight interface between TM1, 2 and helix 8 (Manglik *et al.*, 2012; Wu *et al.*, 2010; Wu *et al.*, 2012).

These results provide evidence that GPCRs are able to dimerise, however do not reflect the stability or duration of this interaction. In the case of the crystal structures, the dimerisation may reflect properties of the crystal packing instead of physiological interactions. It was calculated that receptors with a K_d (dissociation constant) of 1μM had a half-life of <1s. For a dimer to be stable for the duration of time of short-lived GPCRs (2-20 hours), the monomers required an interaction with a K_d of 10-100pM which is unlikely to be achieved with hydrophobic interactions. Therefore receptors that exist as stable dimers are often covalently linked (for example class C GPCRs) (Gurevich & Gurevich, 2008).

The ratio of G protein-coupling to monomeric and dimeric receptors was investigated in both family A and C GPCRs. In receptors of both families, it was

found that GPCR complexes signal through a single G protein (Bayburt *et al.*, 2007; Margeta-Mitrovic *et al.*, 2001; Whorton *et al.*, 2007). The function of dimerisation remains unclear. The reduction in signalling efficiency of the neurotensin NTS1 receptor upon dimerisation has led to speculation of a desensitization role (White *et al.*, 2007).

1.1.11 Biased agonism

The early paradigm of a GPCR activating a single signalling pathway has changed with new evidence. There are now multiple examples of a single GPCR activating multiple signalling pathways. These include β2-AR coupling to both $G_{\alpha s}$ and $G_{\alpha i}$; the switch occurring following PKA phosphorylation (Daaka *et al.*, 1997). The protease activated receptor (PAR1) is able to signalling through $G_{\alpha i}$, $G_{\alpha q}$ and $G_{\alpha 12/13}$ depending on the ligand stimulating the receptor (McLaughlin *et al.*, 2005).

Molecular dynamic modelling has presented an alternative view of receptor dynamics, which can account for this versatility of signalling. This represents receptor conformations as wells in an energy landscape. Binding to ligands or other signalling partners creates a new thermodynamic species with an altered energy landscape with different thermodynamically stable wells. This range in receptor conformations dictated by a binding partner can account for the difference in signalling response (Kenakin, 2011; Onaran & Costa, 1997). It is therefore better to consider receptors as dynamic, moving through a range of conformations, each of which can be stabilised by ligands and initiate signalling responses (Kenakin & Miller, 2010).

The ability of a single receptor to activate different signalling pathways through the binding of specific ligands is described as biased agonism or functional selectivity (Kenakin, 2007).

1.1.12 Membrane environment

The established view of the plasma membrane as a homogenous fluid structure, as proposed in the fluid mosaic model (Singer & Nicolson, 1972), is changing to reflect the findings of discrete membrane regions that confine lipids and proteins to

specific areas. These areas have been named lipid rafts, composed of sphingolipids and cholesterol (Simons & Vaz, 2004).

Lipid rafts are important with respect to GPCRs as both the receptors and their downstream signalling components (specifically G proteins and RGS proteins) have been proposed to be targeted to them (Ostrom & Insel, 2004). This is achieved through the post-translational modifications, usually palmitoylation or other lipid additions (Barnett-Norris *et al.*, 2005).

The lipid environment surrounding the receptor can also influence its function. Both the lipid head and acyl chain composition effected rhodopsin activity (Gibson & Brown, 1993; Niu *et al.*, 2004).

1.1.13 Summary

GPCRs are one of the largest and oldest family of proteins and are found throughout the eukaryotic domain. In humans there are over 800 different receptors binding to a diverse array of ligands. However given this diversity, they share a similar three dimensional architecture of an extracellular N-terminal domain, seven transmembrane spanning alpha helices connected by three extracellular loops and three intracellular loops and an intracellular C-terminus.

Current understanding of GPCR structure and is of a complex process where the receptor exists in multiple conformations, stabilised by a variety of ligands inducing a number of signalling pathways.

1.2 Family B GPCRs

The family B (or secretin) GPCRs are a group of around 15 receptors, which bind to peptide ligands. These receptors include the calcitonin receptor (CTR), calcitonin receptor-like receptor (CLR), corticotropin-releasing hormone receptor 1 and 2 (CRHR1, CRHR2), growth hormone releasing hormone receptor (GHRH), gastric inhibitory polypeptide receptor (GIPR), glucagon receptor (GCGR), glucagon-like peptide 1 and 2 receptor (GLP1R and GLP2R), parathyroid hormone 1 and 2 receptor (PTH1R and PTH2R), pituitary adenylate cyclase activating polypeptide 1 receptor (PAC1R), secretin receptor (SCTR) and the vasoactive intestinal peptide receptor 1 and 2 (VIPR1 and VIPR2). These GPCRs are involved in a diverse range of physiological responses including vasodilation, stress, digestion and glucose homeostasis. This has made them important drug targets for a range of human diseases including diabetes, obesity, cancer, cardiovascular disease and migraine (Hollenstein *et al.*, 2014).

Family B GPCRs are characterised by their large (~100-160 residues) N-terminal extracellular domain (ECD), which is responsible for ligand binding. The TM domain consists of the seven TM-spanning α-helices common to all GPCRs. Signalling is predominantly through $G_{\alpha s}$-coupled pathways, however G_{q11}, G_i and G protein-independent signalling can occur (Hoare, 2005; Mahon *et al.*, 2002; Walker *et al.*, 2010). Some family B GPCRs have associated receptor activity-modifying proteins (RAMPs) that participate in ligand binding or have indirect conformational effects on the receptor (McLatchie *et al.*, 1998; Morfis *et al.*, 2003).

1.2.1 Evolution

Family B GCPRs are thought to have originated in a split from the adhesion family ~1000 million years ago (Nordström *et al.*, 2009; Nordström *et al.*, 2011). Genomic analysis found that protosome genes are most similar to the CT/CGRP and CRH receptor subfamilies indicating that these are likely to be the family B ancestral genes (Cardoso *et al.*, 2006). The subsequent evolution of this GPCR family is likely to be a combination of species-specific gene duplications and duplication in ancestral gene precursors.

The family B GPCRs contain multiple exons and introns in their open reading frames, which generates multiple splice variants. Primary sequence alignment comparisons shows the greatest variability in the N- and C-terminal domains (<10% of amino acids conserved in two-thirds of family B GPCRs;(Markovic & Grammatopoulos, 2009) .

1.2.2 Ligands

The endogenous peptide ligands of the family B GPCRs are hormones, neuropeptides and autocrine factors (Hoare, 2005). The peptide structure is often disordered in aqueous solution however the C-terminal portion of the ligand often becomes helical during receptor binding or under mild ambient conditions. This α-helix is stabilised through intramolecular salt bridges (Runge *et al.*, 2008) and C-terminal amidation (Pioszak & Xu, 2008). This amidation is important for ligand binding affinity. Loss of the C-terminal amidation in both CGRP and CRH caused a dramatic loss in both ligand binding affinity and cAMP signalling potency (Banerjee *et al.*, 2006; Hoare *et al.*, 2004; O'Connell *et al.*, 1993). The N-terminus of the α-helix of each peptide is stabilised through an N-terminal capping motif. This is with the exception of the calcitonin family of peptides, which stabilise the α-helix with an intramolecular disulphide bond (Neumann *et al.*, 2008). The N-terminal structure varies between ligands, with α-helical structures (PTH) and β-coil formations (PACAP) proposed (Inooka *et al.*, 2001; Monticelli *et al.*, 2002; Shimizu *et al.*, 2001).

Key residues govern ligand selectivity within receptor sub-families. CRHR2 selective ligands contain a proline at position 11. CRHR1 peptides had an arginine at position 35 and an acidic amino acid at position 39. The equivalents of these were both alanine residues in the CRHR2 specific peptides (Mazur *et al.*, 2004). In GLP-1 the N-terminal histidine residue is vital for receptor binding affinity (Gallwitz *et al.*, 1990; Hareter *et al.*, 1997) however residues in the central part of the ligand and the C-terminus are also important for ligand affinity and selectivity (Adelhorst *et al.*, 1994; Hjorth *et al.*, 1994; Mapelli *et al.*, 2009).

1.2.3 The N-terminal ECD of family B GPCRs

Until 2013 no crystal structures were solved for the TM domain of the family B GPCRs however structures for the soluble ECDs of a number of receptors have been published (both unbound and bound to ligand). Structures of the ECD of family B GPCRs unbound to a ligand have been solved for the CGRP receptor, AM receptor, CRHR1, CRHR2, GCGR, PAC1R, PTH1R and VIPR2 (Grace *et al.*, 2004; Koth *et al.*, 2012; Kumar *et al.*, 2011; Kusano *et al.*, 2012; Pioszak *et al.*, 2008; Pioszak *et al.*, 2010; ter Haar *et al.*, 2010). Structures have also been solved for the ECD bound with either agonist or antagonist ligand for the CGRP receptor, CRHR1, CRHR2, GIPR, GLP1R, PAC1R and PTH1R (Grace *et al.*, 2007; Grace *et al.*, 2010; Parthier *et al.*, 2007; Pioszak *et al.*, 2008; Pioszak & Xu, 2008; Pioszak *et al.*, 2009; Sun *et al.*, 2007; ter Haar *et al.*, 2010; Underwood *et al.*, 2010). A selection of these structures are shown in Figure 1.8.

The ECD structures suggest a common fold that may be conserved throughout the receptor family. This consists of two central antiparallel β-sheets and an N-terminal α-helix connected by loop structures and stabilised by three intramolecular disulphide bonds. This similarity is surprising as the only sequence conservation in the family includes the six cysteine residues involved in the disulphide bonding and five additional residues responsible for domain stability (Perrin *et al.*, 2007). The space between the two β-sheets acts as a ligand-binding groove that is occupied by hydrophobic residues from the amphipathic α-helix of the ligand, with the C-terminus stopped through H-bonding between side chains. These hydrophobic interactions are vital for ligand binding, which are thought to induce conformational changes within the ECD leading to receptor activation (Hollenstein *et al.*, 2014; Parthier *et al.*, 2009).

1.2.4 Extracellular loops of family B GPCRs

The ECLs are important for ligand binding and receptor activation in a number of the family B GPCRs. In CLR both ECL1 and 3 contain residues involved in CGRP-mediated receptor signalling (Barwell *et al.*, 2011).

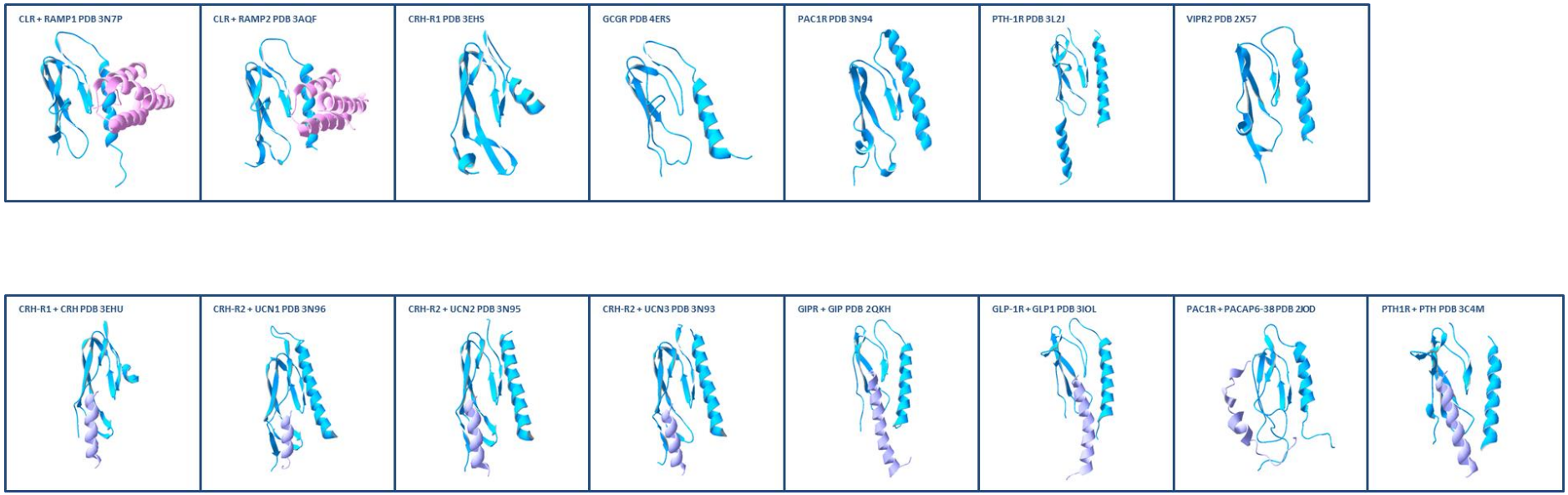

Figure 1.8. Structures of the ECDs of family B GPCRs.

The first row shows ECDs in the absence of bound ligand and the second row are ECDs in complex with a peptide ligand. The GPCR ECD is highlighted blue, accessory proteins are highlighted pink and bound ligand is lilac. The GPCR ECDs in the first row are CGRP receptor (CLR + RAMP1, PDB 3N7P), AM receptor (CLR + RAMP2, PDB 3AQF), CRHR1 (PDB 3ESH), GCGR (PDB 4ERS), PAC1R (PDB 3N94), PTH1R (PDB 3L2J) and VIPR2 (PDB 2X57). The GPCR ECDs bound to peptide ligand in the second row are PAC1R + $PACAP_{6-38}$ antagonist (PDB 2JOD), GIPR + GIP (PDB 2QKH), CRHR1 + CRH (PDB 3EHU), CRHR2 + UCN1 (PDB 3N96), CRHR2 + UCN2 (PDB 3N95), CRHR2 + UCN3 (PDB 3N93), GLP1R + GLP-1 (PDB 3IOL), PTH1R + PTH (PDB 3C4M).

Residues in each of the ECLs of the CRHR1 domain are important for agonist binding (Grammatopoulos, 2012). Specifically in ECL2 residues W259 and F260 in the centre of the loop and three residues at the ECL2-TM5 interface (V266, Y267 and T268) interact with the agonist N-terminus but not the antagonist (Gkountelias *et al.*, 2009).

In GLP1R ECL1 an aspartate was important for GLP-1 binding however this was maintained with an asparagine mutation suggesting that ligand-receptor interaction was mediated through hydrogen bonding instead of the negative charge of the WT residue (López de Maturana & Donnelly, 2002). A methionine-tyrosine pair in the centre of ECL1 were also important for interaction with the GLP-1 N-terminus (López de Maturana *et al.*, 2004).

1.2.5 TM domain of family B GPCRs

The first crystal structures of the TM domain of family B GPCRs were published in 2013 (Figure 1.9). These were for the CRHR1 (Hollenstein *et al.*, 2013) and the GCGR (Siu *et al.*, 2013). These two receptors share ~30% sequence homology and this similarity is reflected in the crystal structures. The TM domain of both receptors have a more open conformation on the extracellular side compared to the previously published family A GPCR structures. This creates a V-shaped structure as viewed parallel to the plasma membrane. One arm of the V-shape comprises TM2-5 and the other comprises TM1, 6 and 7. When comparing the two structures, there is a conserved GWGxP motif in TM4 creating a network of interactions between TM2, 3 and 4. There are also shared interactions between $S^{1.50}$ in TM1 and $S^{7.47}$, $G^{7.50}$ and $F/L^{7.51}$, stabilising the kink in TM7 (Wootten numbering system) (Hollenstein *et al.*, 2014). In the GCGR, $Y400^{7.57}$ has hydrogen bond interactions with $T351^{6.42}$ and $E245^{3.50}$ creating a conformation similar to the family A GPCRs (Siu *et al.*, 2013).

A functional equivalent to the conserved D(E)RY motif of the family A GPCRs is predicted to exist in family B. In GLP1R there is a predicted network of hydrogen bonds between $H180^{2.50}$, $E247^{3.50}$, $T353^{6.42}$ and water molecules. The proposed lock between TM3 and 6 in the inactive conformation of family A GPCRs could exist

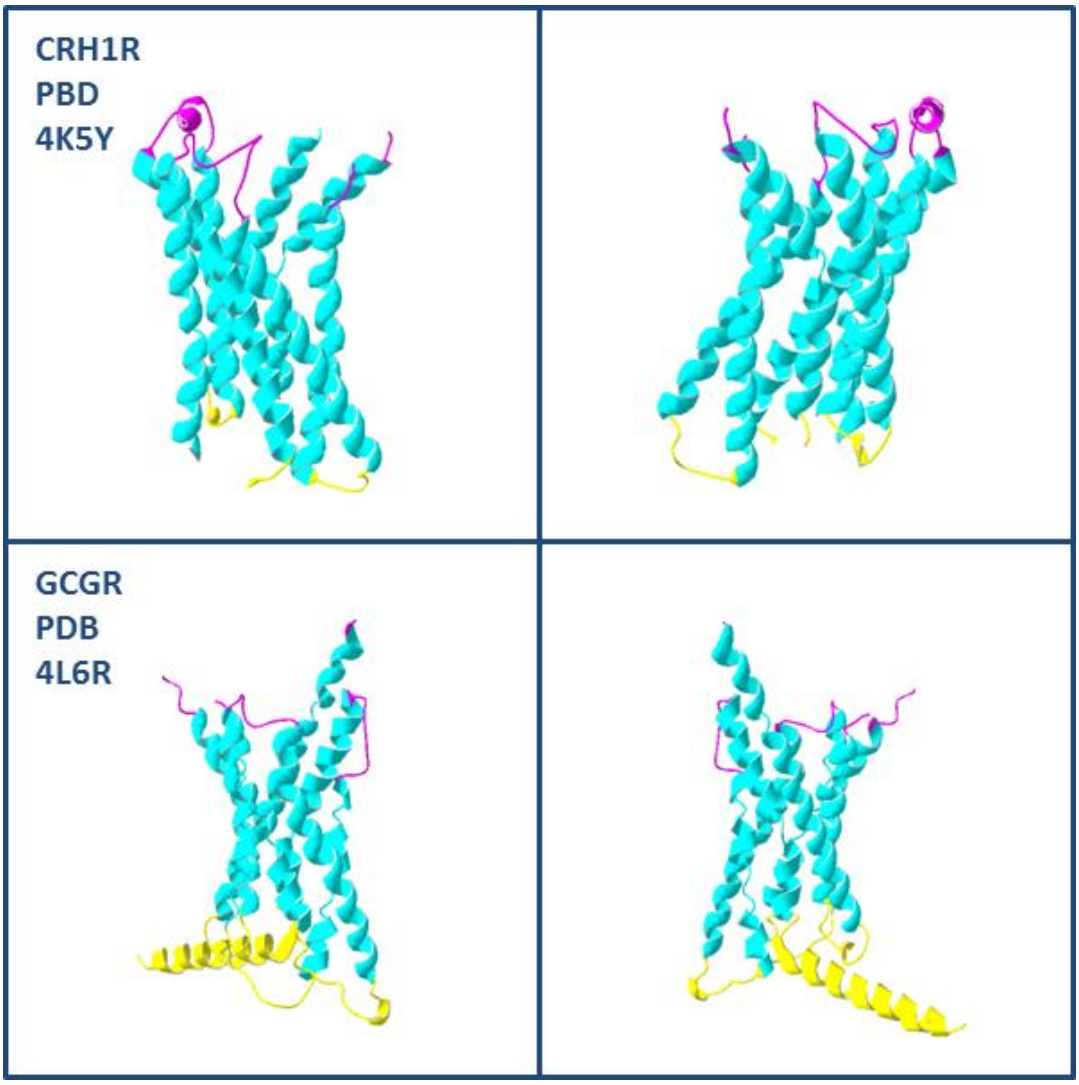

Figure 1.9. Crystal structures of the CRH1R (PDB 4K5Y) and GCGR (PDB 4L6R).
The N-terminal extracellular domain (ECD) and extracellular loops (ECLs) are highlighted magenta, the seven transmembrane helices (7TM) are highlighted cyan and the intracellular loops (ICLs) and intracellular C-terminal domain is highlighted yellow. Each structure is presented twice, in a parallel orientation to the membrane, rotated 180°.

between water-connected hydrogen bonds of E247$^{3.50}$ and T353$^{6.42}$ (Wootten *et al.*, 2013).

The tyrosine of the conserved family A NPxxY motif, which has a functional role in the activation of β2-AR (Rasmussen *et al.*, 2011b) is conserved in the family B GPCRs. In the GCGR crystal structure, Y400 is location in a similar position (Siu *et al.*, 2013) and the equivalent residue is important for receptor activation for GLP-1R and the CGRP receptor (Vohra *et al.*, 2013; Wootten *et al.*, 2013).

In the family B GPCRs, there are three conserved proline residues within TM4, 5 and 6. Alanine substitution of the TM6 proline resulted in a significant reduction in cAMP signalling compared with WT for both CTR and CLR (Bailey & Hay, 2007; Conner *et al.*, 2005).

Molecular modelling of CLR suggested that this proline produced a pronounced TM bend where the intracellular end of TM6 was positioned close to TM3 (Conner *et al.*, 2005). However some of the most compelling evidence on the requirement of the proline residue and its effect on the TM helix came with modelling predictions that the introduction of a proline, three residues above (P343A-G346P) would not result in a correctly orientated kink in the helix but the introduction of a proline four residues above (P343A-I347P) would. This was experimentally verified (Conner *et al.*, 2005).

Even though these results show the importance of these proline residues, not all data supports this. In the study of human hCTR, (Bailey & Hay, 2007) salmon calcitonin was also tested and the substitution of the proline residues for alanine did not result in a significant reduction in cAMP signalling or receptor binding.

1.2.6 Intracellular domains of the family B GPCRs

The ICLs are the main interaction points with the downstream signalling components of the GPCR signalling cascade. Each of the ICLs have a functional role however there are key conserved motifs throughout the receptor family. These include a KL motif in ICL3 involved in G protein-coupling in the secretin, GLP and VPAC receptors. There is also a basic-X-X-basic motif found at the ICL3-TM6 junction

that is conserved between both the family A and B GPCRs (Chan *et al.*, 2001; Hilairet *et al.*, 2001; Mathi *et al.*, 1997).

Research into the ICL domains of CLR identified a minor role of K167 and L169 in ICL1 in signalling through the coupled $G_{\alpha s}$ protein however mutation of R173 to either A or E dramatically reduced signalling. Mutations of Y236 and L237 in ICL2 reduced cell surface expression by 70%. The ICL3 is the largest loop region. I312 is proximal to TM5 and I312A causes a dramatic reduction in cAMP accumulation and also a decrease in CGRP affinity and internalisation. K319A and L320A did not differ from the wild type. K333 and R336 form the basic-X-X-basic motif. K333A shows no effect however R336 causes a >10 fold reduction in pEC_{50}. R336E and R336Q did not differ from the wild type, which suggests that polarity over charge is the significant factor with regards to the interactions of this residue (Conner *et al.*, 2006a).

Using synthetic peptides of GLP1R, it was shown that the N-terminus of ICL3 couples to $G_{\alpha s}$ and the C-terminus couples with $G_{i/o}$ (Hällbrink *et al.*, 2001). Basic and hydrophobic residues in ICL3 were important in a $G_{\alpha s}$-mediated cAMP response (Mathi *et al.*, 1997; Takhar *et al.*, 1996). Analysis of the other two ICLs only found one residue (R176) in ICL1 to be important for cAMP activation.

The intracellular C-terminus has been shown to be involved in G protein-coupling, cell surface localisation and agonist-driven desensitisation in family A GPCRs (Chen *et al.*, 2004; Piserchio *et al.*, 2005) with a key feature being the proposed helix 8 domain first observed in the rhodopsin crystal structure (Palczewski *et al.*, 2000). Deletion of this domain in the CGRP receptor found no significant effect on the cAMP response, however the residues of the helix proximal to the TM7 domain were required for cell surface expression of the receptor. The distal residues of the C-terminus were required for internalisation (Conner *et al.*, 2008).

1.2.7 Ligand binding at the family B GPCRs

An early study into these receptors used PTH-calcitonin ligand and receptor chimeras (Bergwitz *et al.*, 1996). A ligand peptide constructed of the C-terminal PTH and N-terminal calcitonin bound and activated a chimeric receptor containing the N-terminal extracellular domain of PTH and the TM segment of the calcitonin

receptor. Experiments using the reciprocal ligands and receptors resulted in the same outcome.

Studies using truncated versions of the ligands found that removal of the N-terminus formed competitive antagonists (Gardella & Jüppner, 2001; Gelling *et al.*, 1997; Hinke *et al.*, 2001; Nutt *et al.*, 1990; Rivier *et al.*, 1984; Thorens *et al.*, 1993). C-terminal truncations are able to activate the receptor with a significantly reduced affinity (Al-Sabah & Donnelly, 2003b; Gelling *et al.*, 1997; Hoare *et al.*, 2004; Perrin *et al.*, 2003). A chimeric receptor construct that replaced the N-terminal ECD domain of the CRHR1 with the N-terminus of the CRH peptide ligand resulted in a dramatic increase in constitutive activity (Nielsen *et al.*, 2000).

These results have led to a "two-domain" model of ligand binding. This proposes that the C-terminus of the peptide ligand binds to the GPCR N-terminal ECD. This allows the presentation of the N-terminal section of the ligand to the ECLs and the TM domain resulting in the subsequent activation of the receptor (Hoare, 2005).

The structures of the receptor ECD with bound peptide ligand shows a common binding pattern. The family B ligands generally bind through interactions between hydrophobic interactions of the amphipathic α-helix of the peptide ligand and hydrophobic binding pockets between the two β-sheets of the ECD (Figure 1.8). However comparison of the binding of CRH, PTH, GIP and exendin-4 with their cognate receptors does reveal differences. An extra residue in the β1-β2 loop of the CRHR causes a shift in peptide binding compared with the other three ligands resulting in little overlap within the binding interface (Grace *et al.*, 2007; Parthier *et al.*, 2007; Pioszak & Xu, 2008; Runge *et al.*, 2008). There is also a difference between the "anchor" point of the CRH ligand and receptor and of the other peptides. For the CRH complex, CRH is anchored by interactions of the CRH C-terminus with the β1-β2 loop, loop 3 and Y99 of the ECD. The PTH ligand is anchored by interactions of the N-terminal portion of the peptide and the N-terminal α-helix of the PTHR ECD. These differences result in a distinct interface for the binding of the ligands to their receptors, providing insights into the specificity of these receptors.

The affinity of the ligand to its receptor has also been estimated for the PTH1, PTH2, CRH1, CRH2 and GLP-1 receptors (Al-Sabah & Donnelly, 2003b; Hoare *et al.*, 2004; Hoare & Usdin, 2001; López de Maturana *et al.*, 2003; Perrin *et al.*, 2003). These studies found that the affinity of the ligand to the N-terminal ECD was between 1-100nM, however the interaction with the TM domain is ~10µM for PTH1 and CRH (Hoare *et al.*, 2004; Shimizu *et al.*, 2001). These results complement the two-domain model with the initial ligand-receptor binding between the C-terminal ligand and N-terminal receptor ECD occurring with higher affinity which enables the lower affinity N-terminal ligand/TM receptor domain interaction to occur.

Research on the secretin receptor found that modified N-terminal secretin peptides that only bound to the receptor N-terminus still activated the receptor. These peptides used acetylation of the N-terminus of photolabelled probes which removed the charge of the N-terminal amino group. These bound to the ECD of the receptor instead of TM6, however TM6 binding was recovered when a basic residue was added to the N-terminus of the ligand. All these ligands remained full agonists. Peptides corresponding to the secretin receptor's N-terminus activated the full length receptor. Further studies found that a secretin receptor epitope agonist bound near to the top of the TM6-ECL3 interface indicating that upon ligand binding, a conformational change in the N-terminal ECD causes a folding of this domain to interact with TM6 and activate its receptor (Dong *et al.*, 2006; Dong *et al.*, 2005).

Looking within the CRH family of peptides reveals factors involved in the specificity of ligand binding. Even though the sequences between CRH receptor peptides CRH and UCNI, II and III are very similar, there are distinct differences between their binding to the CRHR1 and CRHR2 receptors. CRH has a 10-40 fold higher affinity for CRHR1 than to CRHR2, and CRH and UcnI exhibit ~10 fold higher estimated affinity for the CRHR1 ECD than UcnII and III (Hauger *et al.*, 2006). Even with high sequence similarity, this substantial affinity difference has been proposed to be due to differences in two residues within the peptide. R35 is present in both CRH and UcnI, CRH contains E39 and UcnI has a similar negatively charged D39. UcnII and III have an alanine in both positions. This difference in ligand side chain properties can be

reciprocated with an E104 residue in the CRHR1 ECD and a P100 in CRHR2. This provides an explanation into the specificity of these ligands to their respective receptors (Pal *et al.*, 2010).

1.2.8 Activation of family B GPCRs by their agonists

Zn(II)-binding experiments utilise the ability of histidine to co-ordinate transition metal ions to determine proximity of different receptor regions (Sheikh *et al.*, 1996). Selected receptor residues are substituted with histidine and are activated in the presence or absence of Zn^{2+}. Experiments utilising this technique in the family A β2-AR and the family B PTHR found that even though these receptors are only 16% identical, both required the movement of TM6 in relation to TM3 for the receptor to activate the G protein (Sheikh *et al.*, 1999). This suggests that even with the differences in sequence, structure and ligand binding, receptors from these two families share a common three-dimensional structure and activation mechanism.

During the N-terminal ECD conformational changes induced by ligand binding, which may guide the ligand towards the binding pocket, the receptor N-terminus itself may interact with its TM domain to stabilise or enhance this interaction, which would explain why peptides based on receptor epitopes are able to activate receptors (Dong *et al.*, 2006; Dong *et al.*, 2005). Through ionic and hydrophobic interactions, the ligand brings the TM6 ECL domain towards that of TM3, stabilising the active conformation.

In family A GPCRs, TM6 and 7 have a proline-induced bend, shown to straighten during receptor activation (Schwartz *et al.*, 2006). There is no TM7 proline in the family B GPCRs however there is a TM6 proline that straightens during activation (Conner *et al.*, 2005). This TM bend is energetically unstable and has to be held in the inactive position through an ionic “lock” mechanism. This is a role of the DRY motif in family A and it has been proposed that residues in TM2 and 3 of family B GPCRs may act in the same way (Frimurer & Bywater, 1999).

1.2.9 Signalling pathways of family B GPCRs

The promiscuity of family B GPCR signalling has been observed in multiple receptors. The CRHRs can activate $G_{\alpha s}$, $G_{\alpha o}$, $G_{\alpha q11}$, $G_{\alpha i}$ and $G_{\alpha z}$ (Grammatopoulos *et*

al., 1999; Grammatopoulos *et al.*, 2001). Mutations of Ucn1 between residues 6-15 altered the signalling between $G_{\alpha s}$ and $G_{\alpha i}$ pathways, indicating a capability of biased signalling induced through small modifications of the peptide ligand (Beyermann *et al.*, 2007). Both ICL3 and the C-terminus of CRHR1 are important for G protein-binding (Grammatopoulos *et al.*, 1999; Papadopoulou *et al.*, 2004). In GLP1R, the N-terminus of ICL3 was responsible for $G_{\alpha s}$ coupling and the C-terminus for $G_{i/o}$ (Hällbrink *et al.*, 2001). The CGRP receptor predominantly signals through $G_{\alpha s}$ however it has also been found to signal through $G_{\alpha i}$, $G_{\alpha q11}$ and G protein-independent pathways (Walker *et al.*, 2010).

1.2.10 Desensitisation and recycling

Following activation, the family B GCPRs may undergo phosphorylation mediated desensitisation, internalisation and recycling similar to family A GPCRs.

CLR is phosphorylated by GRKs at S/T residues within the C-terminus. This recruits β-arrestin leading to subsequent desensitisation and internalisation (Conner *et al.*, 2008). In CRHR1 there are S/T clusters in both ICL3 and the last 30 amino acids of the C-terminus that can be phosphorylated by GRKs, PKA and PKC (Oakley *et al.*, 2007; Papadopoulou *et al.*, 2004; Teli *et al.*, 2005). GRK phosphorylation is required for efficient coupling to β-arrestin but recruitment can still occur without phosphorylation (Oakley *et al.*, 2007). In GLP1R, phosphorylation occurs at four serine doublets at the end of the C-terminus resulting in desensitisation and internalisation (Widmann *et al.*, 1996).

1.2.11 Summary

Family B GPCRs are a small but physiologically important class of GPCRs binding to peptide ligands. The ECD structures are best understood, with a common fold of an N-terminal α-helix following by two antiparallel β-sheet structures forming a hydrophobic ligand-binding groove that binds to an amphipathic α-helical peptide ligand. Recent crystal structures of the CRHR1 and GCGR TM domain's confirm that these receptors consist of the seven TM spanning α-helix bundle seen with the family A GPCRs. A notable difference is that the family B structures are more open on the extracellular side. Ligand binding and activation is predicted to follow a

“two-domain” mechanism. In this model the C-terminus of the peptide ligand adopts an α-helical structure binding to the receptor ECD through hydrophobic interactions. This facilitates binding of the N-terminus of the ligand to the ECLs and TM bundle of the receptor resulting in receptor activation.

1.3 CGRP and the CGRP receptor

1.3.1 Introduction

Calcitonin gene-related peptide (CGRP) is a 37 amino acid neuropeptide with potent vasodilatory effects (Poyner *et al.*, 2002). CGRP is a member of the calcitonin family of peptides (with calcitonin, adrenomedullin, amylin and AM2/intermedin). These are all ligands to several receptors constructed from two family B GPCRs, the calcitonin receptor (CTR) and the calcitonin receptor-like receptor (CLR) (Pal *et al.*, 2012). With the exception of calcitonin, the peptide receptors are a heterodimer consisting of a GPCR unit (CTR or CLR) and one of three single transmembrane accessory proteins (RAMP 1, 2 or 3) (Poyner *et al.*, 2002). The CGRP receptor is a heterodimer between CLR and RAMP1 (Walker *et al.*, 2010).

The calcitonin family of peptides are expressed throughout the body, in peripheral tissues and the central and peripheral nervous system. Other than vasodilation (CGRP and adrenomedullin), the effects of these peptides include reduced food intake (amylin) and a decrease in bone readsorption (calcitonin) (Walker *et al.*, 2010). This has led to significant pharmaceutical interest in their mechanism of action.

1.3.2 Calcitonin family of peptides

The calcitonin peptide family consists of six members. These include calcitonin (CT), amylin, (AMY), two isoforms of CGRP (α and β), adrenomedullin (AM) and adrenomedullin 2/intermedin (AM2). They have weak primary sequence homology however share secondary structure characteristics of an N-terminal loop stabilised by a disulphide bond followed by a region of amphipathic α-helix and a C-terminal amidation (Poyner *et al.*, 2002).

Calcitonin is a 32 amino acid peptide expressed predominantly in the thyroid C cells resulting in reduced blood calcium levels (Copp & Cheney, 1962; Hirsch *et al.*, 1963). This occurs through inhibition of bone resorption and enhancing calcium excretion through the kidney (Friedman & Raisz, 1965; Warshawsky *et al.*, 1980). Calcitonin is formed from the post-transcriptional splicing of exon 4 to 1-3 from the calcitonin

gene (Amara *et al.*, 1982; Rosenfeld *et al.*, 1984). There is evidence that calcitonin is also expressed in the prostate gland and the central nervous system (Davis *et al.*, 1989; Fischer *et al.*, 1983).

Amylin (or Islet Amyloid Polypeptide, IAPP) is a 37 amino acid peptide expressed in the β-cells of the pancreas (Clark *et al.*, 1987; Mosselman *et al.*, 1988). It is expressed alongside insulin through similar promoter regions that bind to the same transcription factor (German *et al.*, 1992). It has autocrine and paracrine effects on insulin and glucagon secretion, reduces appetite and the rate of gastric emptying. However it is also able to aggregate into pancreatic islet amyloid deposits, which are associated with type 2 diabetes (Westermark *et al.*, 2011).

CGRP is a 37 amino acid peptide expressed in the peripheral and central nervous system (van Rossum *et al.*, 1997) and in the cardiovascular, respiratory and gastrointestinal system (Brain & Grant, 2004). There are two isoforms of CGRP (α and β). α-CGRP is created from the post-transcriptional splicing of exons 5 and 6 to 1-3 from the calcitonin gene (Rosenfeld *et al.*, 1984). β-CGRP is transcribed from a separate gene to α-CGRP however shares sequence homology with the α-CGRP precursor mRNA (Amara *et al.*, 1985).

AM is a 52 amino acid peptide, which (like CGRP) is a potent vasodilator. AM can also inhibit oxidative stress, inflammation, apoptosis, atherosclerosis and promote angiogenesis and lymphangiogenesis (Ishimitsu *et al.*, 2006; Kitamura *et al.*, 1993; Kuwasako *et al.*, 2011). AM is predominantly expressed in endothelial and smooth muscle cells (Sugo *et al.*, 1994a; Sugo *et al.*, 1994b; Sugo *et al.*, 1995).

A second, related peptide called AM2 (also called intermedin/IMD) was independently discovered by two groups in 2004 (Roh *et al.*, 2004; Takei *et al.*, 2004). Its distribution is similar to that of AM, expressed in peripheral tissues and in the CNS, with highest levels in the kidney, hypothalamus and stomach (Hong *et al.*, 2012). It acts through both the CGRP and AM receptors, however it has highest affinity for the AM2 receptor. AM2 has vasodilatory effects on blood vessels throughout the body, however it increases sympathetic activity when administered centrally (Hong *et al.*, 2012).

1.3.3 CGRP

1.3.3.1 Peptide

CGRP exists as two isoforms. One isoform of the peptide (α-CGRP) is formed from the alternative splicing of the calcitonin gene (Amara *et al.*, 1982). A second isoform (β-CGRP) is expressed from a different gene, which differs from human α-CGRP by three amino acids. Rat α-CGRP and β-CGRP differ by one amino acid (Steenbergh *et al.*, 1985). Unless stated, CGRP will be in reference to the alpha isoform for the rest of this thesis.

The first seven residues of the CGRP peptide form an N-terminal loop stabilised by a disulphide bond between cysteine residues at positions 2 and 7. Removal of this loop forms the $CGRP_{8-37}$ antagonist. Within and adjacent to the loop, positions 1, 4, 8 and 9 influence agonist activity. Alanine at position 5 and threonine at position 6 are particularly important (Hay *et al.*, 2014). Residues 8 – 18 form an amphipathic alpha helix, which terminates in a beta turn (Boulanger *et al.*, 1995). The remainder of the peptide is thought to contain at least one further beta turn around residues 33-34 (Sagoo *et al.*, 1991). The C-terminal phenylalanine at position 37 is amidated (Poyner *et al.*, 1992).

αCGRP contains up to 88% α-helix when dissolved in 50% trifluoroethanol however removal of the N-terminal seven residues resulted in a large change in secondary structure, with a dramatic loss in α-helix (9% α-helix) and an increase in β-sheet and random coiling to compensate for this (Robinson *et al.*, 2009).

1.3.3.2 Expression

The CGRP receptor is expressed in the central nervous system (CNS) in discrete areas such as the striatum, amydala, colliculi and cerebellum, however an extensive amount of research has been in the trigeminovascular system, with CGRP immunoreactivity detected in trigeminal nerve fibres and ganglion cells, and the CLR and RAMP1 components detected in arterial blood vessels, mononuclear cells and Schwann cells in rat (Lennerz *et al.*, 2008). αCGRP is more abundant and found in areas of the central and peripheral nervous system. βCGRP is located in the gut, in

sites including those of enteric nerves (Mulderry *et al.*, 1988) and the pituitary gland (Petermann *et al.*, 1987).

1.3.3.3 Physiology

The major physiological effect of CGRP is vasodilation, caused by the release of CGRP from sensory nerve fibres, which innervate smaller arteries, passing into the vascular smooth muscle layer (Brain & Grant, 2004). Vasodilation occurs through direct action on the smooth muscle cells, via a cAMP dependent pathway, however in some vasculature, this occurs through endothelium-sensitive and NO-sensitive mechanisms (Gray & Marshall, 1992; Raddino *et al.*, 1997). Despite these physiological effects of CGRP it is not involved in the control of systemic blood pressure. The effects are instead more local, acting on the microvasculature, regulating responsiveness and protecting organs from injury (Smillie & Brain, 2011). As well as vasodilation, CGRP has been linked to inflammation and nociception and it is thought to be through these effects that migraine can occur (Durham, 2008).

CGRP is expressed in unmyelinated c nerve fibres which are present throughout the body and are associated with immune cells such as dendritic cells, mast cells and T cells. A role of CGRP as a key mediator of neuro-immune communication is emerging, with the c fibres having both sensory and local effects (Assas *et al.*, 2014).

1.3.3.4 Pathophysiology

CGRP is involved in migraines. The origin of a migraine is thought to be in the CNS, most likely the brain stem, initiated by a range of contributing factors such as stress, environmental agents, or hormones, which then activate trigeminal neurons (Goadsby *et al.*, 2002). The link with CGRP is seen with an increase in CGRP levels in the cranial circulation during migraine or cluster headache attacks (Fanciullacci *et al.*, 1995; Gallai *et al.*, 1995; Goadsby *et al.*, 1990; Juhasz *et al.*, 2003). Anti-migraine compounds stop this increase (Fanciullacci *et al.*, 1995; Goadsby & Edvinsson, 1993). CGRP antagonists are able to prevent neurogenic vasodilation that has been initiated either through the activation of trigeminal C-fibre nociceptors or agents known to trigger migraines (Goadsby *et al.*, 1988; Nicoletti *et al.*, 2008).

During myocardial ischemia, CGRP release stops the development of myocardial infarction (Franco-Cereceda & Liska, 2000). Ischemic preconditioning through a brief coronary artery occlusion releases CGRP which is cardio protective during prolonged coronary artery occlusion. This effect is repeated with exogenous CGRP and blocked with CGRP antagonists (Chai *et al.*, 2006). There is evidence that CGRP has a protective effect in hypertension (Smillie & Brain, 2011).

1.3.4 GPCR components

1.3.4.1 Calcitonin receptor (CTR)

CTR (the GPCR component of both the calcitonin and amylin receptors) was first cloned from a porcine cDNA library (Lin *et al.*, 1991). It showed high affinity for salmon calcitonin and homology to the PTH receptor. Following this, hCTR was cloned from a ovarian carcinoma cell line (Gorn *et al.*, 1992). This was 73% identical to the porcine receptor but contained a 16 amino acid insert in ICL1. A second human isoform was then cloned which did not contain the 16 amino acid insert. This isoform was found to be the most abundant, expressed at relatively constant levels in a variety of tissues including the kidney, brain, lung, stomach, placenta ovary and bone marrow. The insert positive receptor was mainly found in the ovary and placenta (Kuestner *et al.*, 1994).

A receptor for amylin was discovered when CTR was found to form dimers with RAMP1 and 3 (Christopoulos *et al.*, 1999; Muff *et al.*, 1999). A CTR-RAMP2 heterodimer consisting of the insert positive had a greater capacity for amylin that the insert negative CTR (Tilakaratne *et al.*, 2000).

1.3.4.2 Calcitonin receptor-like receptor (CLR)

CLR (the GPCR component of both the CGRP and AM receptors) was initially cloned from rat cDNA in 1993 (Njuki *et al.*, 1993) and from human soon after (Flühmann *et al.*, 1995). CGRP was not considered the ligand for this receptor until successful binding and cAMP accumulation experiments were shown in a HEK293 stable cell line, which expressed hCLR (Aiyar *et al.*, 1996). The reason for this was not discovered for another two years, when RAMP1 was identified in the HEK293 cells and was shown to be necessary for cell-surface expression and CGRP-binding of CLR

(McLatchie *et al.*, 1998). This research also found that RAMP2 (or RAMP3) could combine with CLR forming functional receptors for AM.

CLR forms a heteromeric complex with RAMPs in the endoplasmic reticulum/Golgi, and maintains this complex throughout the receptor life cycle, from cell surface trafficking to receptor activation, signalling, internalisation and the subsequent recycling to the membrane or degradation (Bomberger *et al.*, 2005; Kuwasako *et al.*, 2000; Sexton *et al.*, 2001). CLR has three N-glycosylation sites required for cell surface expression (N66, N118, N123) (Bühlmann *et al.*, 2000; Kamitani & Sakata, 2001). Historically, the labelling of the CLR residues did not include the 22 amino acid signal peptide, however in recent years this sequence has been included in the literature.

1.3.5 RAMPs

1.3.5.1 Discovery

CLR was shown to be the GPCR for CGRP through CGRP binding and cAMP production in HEK293 cells stably transfected with hCLR (Aiyar *et al.*, 1996), however CLR alone was not sufficient to be a receptor for CGRP. Through a cDNA library screen, a single cDNA was isolated called receptor activity modifying protein 1 (RAMP1) that resulted in a CGRP response. Following this discovery, analysis of sequence databases identified two similar proteins, RAMPs 2 and 3 (McLatchie *et al.*, 1998).

1.3.5.2 RAMPs with CLR and CTR

Although they share less than 30% sequence homology, all three RAMPs possess a similar secondary structure with a large extracellular N-terminus (~100 amino acids), a single TM spanning domain (22 amino acids), and a short intracellular C-terminus (~10 amino acids) (McLatchie *et al.*, 1998). Co-expression of CLR and one RAMP is essential for complete cell surface expression of the receptor (Kuwasako *et al.*, 2000; McLatchie *et al.*, 1998). RAMP1 has a bundle of three α-helices in the extracellular N-terminus (Figure 1.10) that interact predominantly with an N-terminal α-helix of CLR through electrostatic and hydrophobic interactions and hydrogen bonding (ter Haar *et al.*, 2010). A QSKRT sequence in the RAMP1 C-

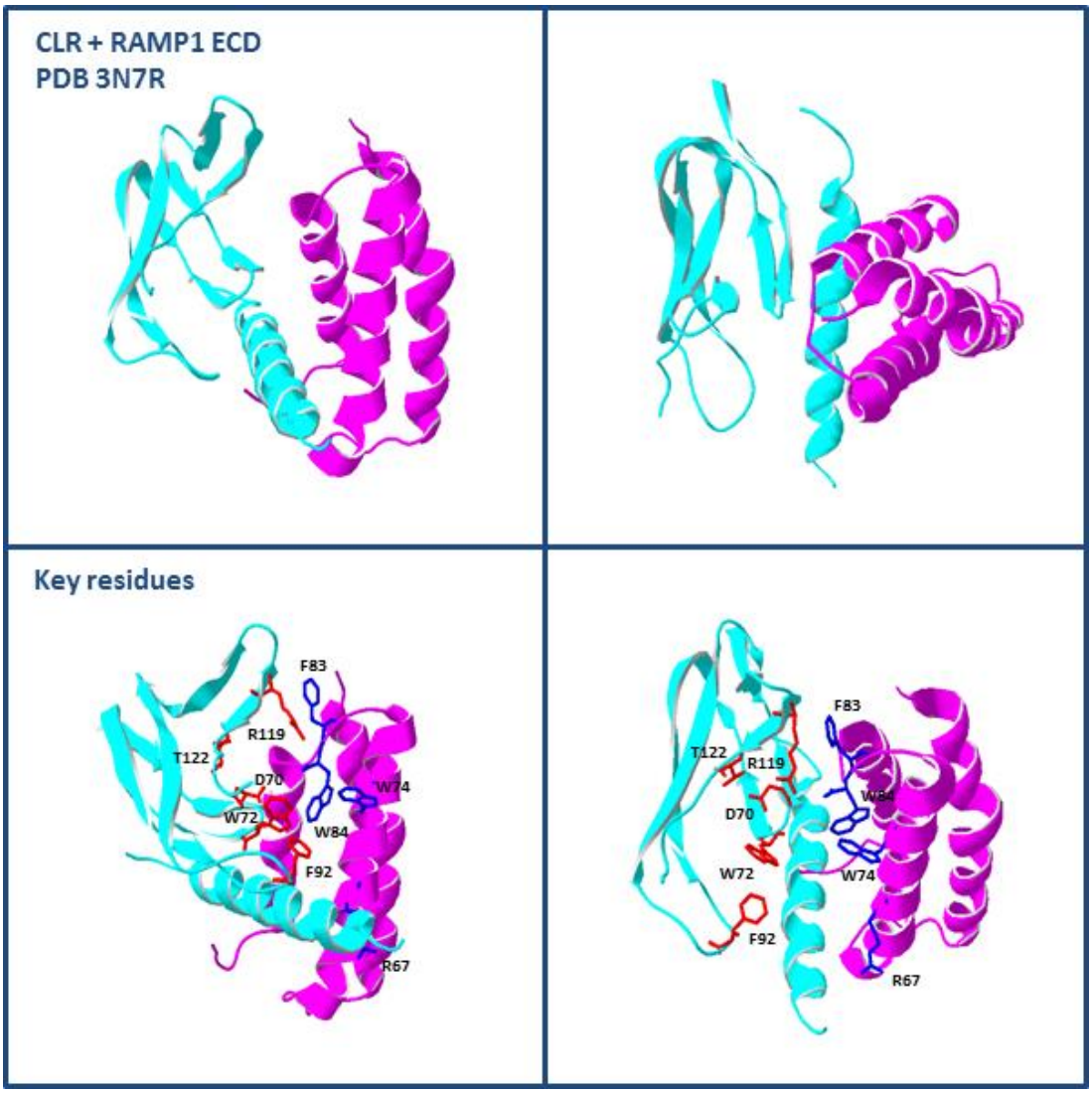

Figure 1.10. Crystal structure of the CGRP receptor ECD.

This consists of the N-terminal ECD of CLR and the N-terminus of RAMP1. CLR is cyan and RAMP1 magenta. The top row presents the receptor complex in two orientations. The exact orientation with respect to the membrane is currently unknown. The bottom row has the side chains of key structural and functional residues highlighted and labelled. The receptor complex is presented in two different orientations.

terminus appears to function as a Golgi retention motif that is sterically inhibited upon association with CLR (Steiner *et al.*, 2002). RAMP2 appears to interact with CLR in a similar way to that of RAMP1, with contacts between CLR and RAMP2 α-helices (Kusano *et al.*, 2012). However, while the overall structure is the same, the difference in amino acid residues between RAMP1 and RAMP2 produces a variation in the heterodimer interface (Kusano *et al.*, 2012). RAMP1 was not found to be glycosylated; however RAMP2 is glycosylated at N130, which facilitates trafficking to the cell surface (Aldecoa *et al.*, 2000; Flahaut *et al.*, 2002). The RAMP3 structure has yet to be solved.

1.3.5.3 RAMPs with other GPCRs

Other family B GPCRs have also been shown to interact with RAMPs. The VPAC1 receptor resulted in significant translocation of each RAMP to the cell surface, however there was no substantial difference in ligand binding affinity or receptor signalling with the RAMPs compared with wild type, except for an increase in phosphotidylinositol (PI) response with RAMP2 following stimulation with various VPAC1 agonists. Parathyroid hormone 1 (PTH1) or glucagon receptors increased cell surface expression of RAMP2 and the PTH2 receptor translocated RAMP3 (Christopoulos *et al.*, 2003). The pharmacology of the CRHR1 receptor can be altered by RAMP-association, particularly for the effects on E_{max} of its $G_{\alpha i}$ response (Wootten *et al.*, 2012).

1.3.6 CLR and RAMP1

1.3.6.1 Structure – extracellular domain

There is no available crystal structure of the full CGRP receptor or its individual components, however the structure of a complex formed between the N-terminal extracellular domains (ECDs) of CLR and RAMP1 has been solved (Figure 1.10) (ter Haar *et al.*, 2010). The N-terminal domain of CLR appears to be similar to that of other family B GPCRs (Hollenstein *et al.*, 2014). It consists of an N-terminal α-helix (αC1) followed by an unstructured region extending to a long finger-like motif with a tryptophan residue (W72) at the tip, stabilised by two disulphide bonds (C48/C74 and C65/C105). There is a third disulphide bond between C88/C127 (Kusano *et al.*,

2012; ter Haar *et al.*, 2010). After the tryptophan finger, there are two antiparallel beta sheets with the loop between them forming the base of the ligand-binding site closest to the TM domain of the receptor (Figure 1.11).

The N-terminal domain of RAMP1 has a three helix bundle (αR1 - 3) stabilised by three disulphide bonds (Figure 1.11). These disulphide bonds are located between the αR1 and αR2 helices (C40/C72), the N-terminus and the αR2 – αR3 loop (C27/C82) and connecting the αR1–αR2 loop to the C terminus (C57/C104). Alanine substitution of RAMP1 residues C40, C57, C72, or C104 significantly reduced cell surface expression of the CGRP receptor, while the deletion of C27 or the substitution of C82 by alanine did not affect the receptor function (Steiner *et al.*, 2003). There is a kink in the αR1 helix caused by L39 due to a disruptive pattern of hydrogen bonds. The interactions between the helices are mainly between hydrophobic residues, a property that is shared by intramolecular interacting sites across the three RAMP sequences (Kusano *et al.*, 2008).

In the crystal structure of the ectodomain complex of the CGRP receptor (ter Haar *et al.*, 2010), the α-helix bundle of RAMP1 was perpendicular to the α-helix of the CLR N-terminus (Figure 1.10). The essential points of structural interaction occur between the N-terminal alpha helix of CLR (αC1) and the second and third alpha helices (with some adjacent residues) of the N-terminus of RAMP1 (αR2 and αR3 respectively) (Figure 1.11). A notable non-helix interaction is the hydrophobic bond between CLR R119 and RAMP1 F83, stabilising the top of the ECD complex (ter Haar *et al.*, 2010).

1.3.6.2 CGRP model structure

Until the recent publications of the CRHR1 and GCGR crystal structures (Hollenstein *et al.*, 2013; Siu *et al.*, 2013), the absence of defined structural information for the family B GPCRs has led to difficulty in producing accurate receptor models.

The most recent technique applied to modelling CLR used a novel approach using the plant GPCR GCR1, which has sequence homology to both family A and B GPCRs, to bridge to gap between the lack of sequence homology between these two receptor families. This has allowed the CLR sequence to be fitted to family A crystal

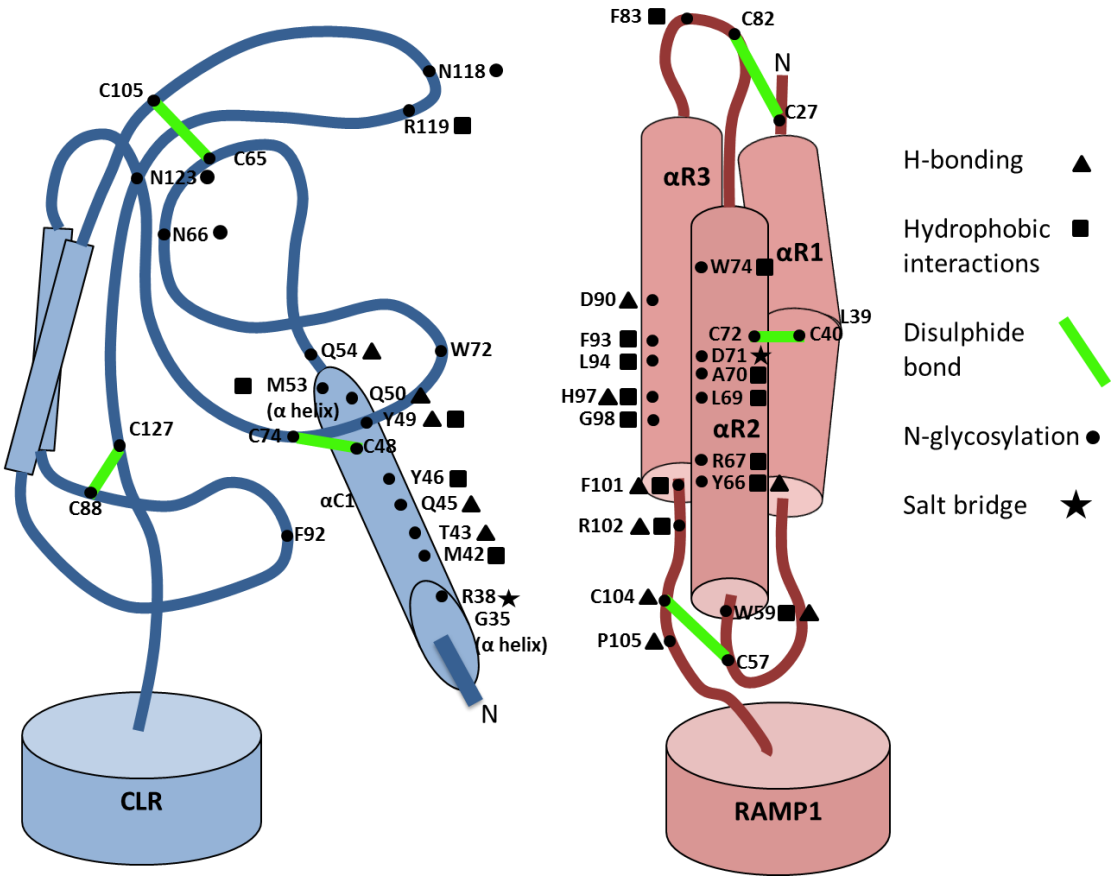

Figure 1.11. Schematic diagram showing the CLR and RAMP1 components of the CGRP receptor.

Key amino acids involved in structural interactions are displayed, together with the type of interaction involved. Figure adapted from Woolley & Conner, 2013.

structures, most notably the active β2-AR G protein complex (Vohra et al., 2013). This CLR model was further refined with the incorporation of a substantial amount of mutagenesis data, particularly within the TM domain.

In TM1 residues $K^{1.61}$ and $L^{1.63}$ comprise the $KKLH^{1.64}$ motif shared in family A and B GPCRs (Vohra *et al.*, 2013). In the CLR model $K^{1.61}$ was proposed to interact with Gβ but also with $E^{8.49}$. $L^{1.63}$ interacts with $V^{8.50}$ which stabilises $F^{7.53}$ (comprising an alternative version of the NPxxY motif) in the inactive conformation.

The TM5/ICL3 interface contains an $I/LxxL^{5.65}$ motif that is often involved in G protein-coupling (Scheerer *et al.*, 2008). A $KxxK^{6.35}$ motif in TM6 has a similar function following movement of this helix during receptor activation.

In TM3, there are a number of conserved residues. These include $E^{3.46}$ and $YLH^{3.51}$. The YLH motif forms the family B equivalent of the $DRY^{3.51}$ motif present in many family A GPCRs (Tams *et al.*, 2001). Mutagenesis of these residues has a less pronounced effect to that observed with the DRY motif, however the YLH motif forms a hydrophobic network with residues in ICL2 maintaining the inactive conformation and $E^{3.46}$ can interact with $R173^{2.39}$ and $H177^{2.43}$ in TM2 suggesting a similar functional role to that in family A GPCRs. ICL2 was also expected to make Gs contacts. $R173^{2.39}$ makes contact with $T^{6.37}$ in the inactive conformation to form a polar lock.

1.3.6.3 Ligand binding

CGRP-binding and activation of its receptor is expecting to follow the "two domain" model of ligand binding, described in the previous section (Hoare, 2005). The C-terminus of CGRP is thought to bind to the N-terminal ECD of CLR and the extracellular N-terminus of RAMP1, allowing the presentation of the N-terminal loop of CGRP to the extracellular loops and juxtamembrane regions of CLR (Conner *et al.*, 2007a; Watkins *et al.*, 2012). This stabilises the active conformation of the receptor, possibly orientated by the disulphide loop forming a similar structure to the N-cap motif found in many peptide ligands for family B GPCRs (Neumann *et al.*, 2008). This model is strengthened by the fact the $CGRP_{8-37}$ peptide is not able to

activate the receptor, however its reduction in binding affinity indicates that the interaction of the N-terminal loop residues are also important for receptor binding.

The binding affinity of CGRP varies between species, and the cell type that was being tested. CGRP binds to the CGRP receptor with nanomolar affinity. The $CGRP_{8-37}$ antagonist has a 3-10 fold reduction in binding affinity (Poyner *et al.*, 2002). The structural domains of CGRP are all important for ligand binding affinity. These include the N-terminal loop (residues 1-7), the central α-helix (residues 8-18) and the C-terminus (residues 28-37) (Poyner *et al.*, 1998; Robinson *et al.*, 2009). The C-terminal amidation of phenylalanine is also important. Loss of this amidation does not disrupt ligand structure, however it does result in a decrease in the affinity to the receptor, even if the alanine at position 36 is amidated instead (Banerjee *et al.*, 2006; O'Connell *et al.*, 1993).

A lot of information has become available with the publication of the crystal structure of the CGRP receptor ECD complex with the non-peptide antagonists Olcegepant (BIBN4096BS) and Telcagepant (MK- 0974) (ter Haar *et al.*, 2010). Both Olcegepant and Telcagepant are more effective for humans and primates than for other mammals including dogs and rodents (Hershey *et al.*, 2005; Salvatore *et al.*, 2008). Both synthetic antagonists bind to a hydrophobic binding pocket formed between the CLR ECD and the RAMP helices. Important CLR residues are R38, I41 and M42 in the αC1 helix, and W72, F92, D94, R119, T122 and Y124 in the remainder of the N-terminal domain. Important RAMP1 residues are D71, W74, F83 and W84 (Figure 1.12) (ter Haar *et al.*, 2010).

From studies prior to the crystal structure, it was observed that the CLR N-terminus contains several areas involved in CGRP binding (Figure 1.12). One particular cluster within this sequence is I32, G35 and T37. Alanine substitutions of these residues increase CGRP potency. A further cluster of I41, A44, Q45, C48 and Y49 has also been shown to be important in receptor function (Barwell *et al.*, 2010). The involvement of C48 is through disulphide bonding. CLR forms an alpha helix from G35 to M53 along which I41, Q45 and Y49 are expected to lie on the same face. Q45 and Y49 are seen in the crystal structure to interact with RAMP1. I41 of CLR is positioned too far from RAMP1 to make a significant hydrophobic interaction, and

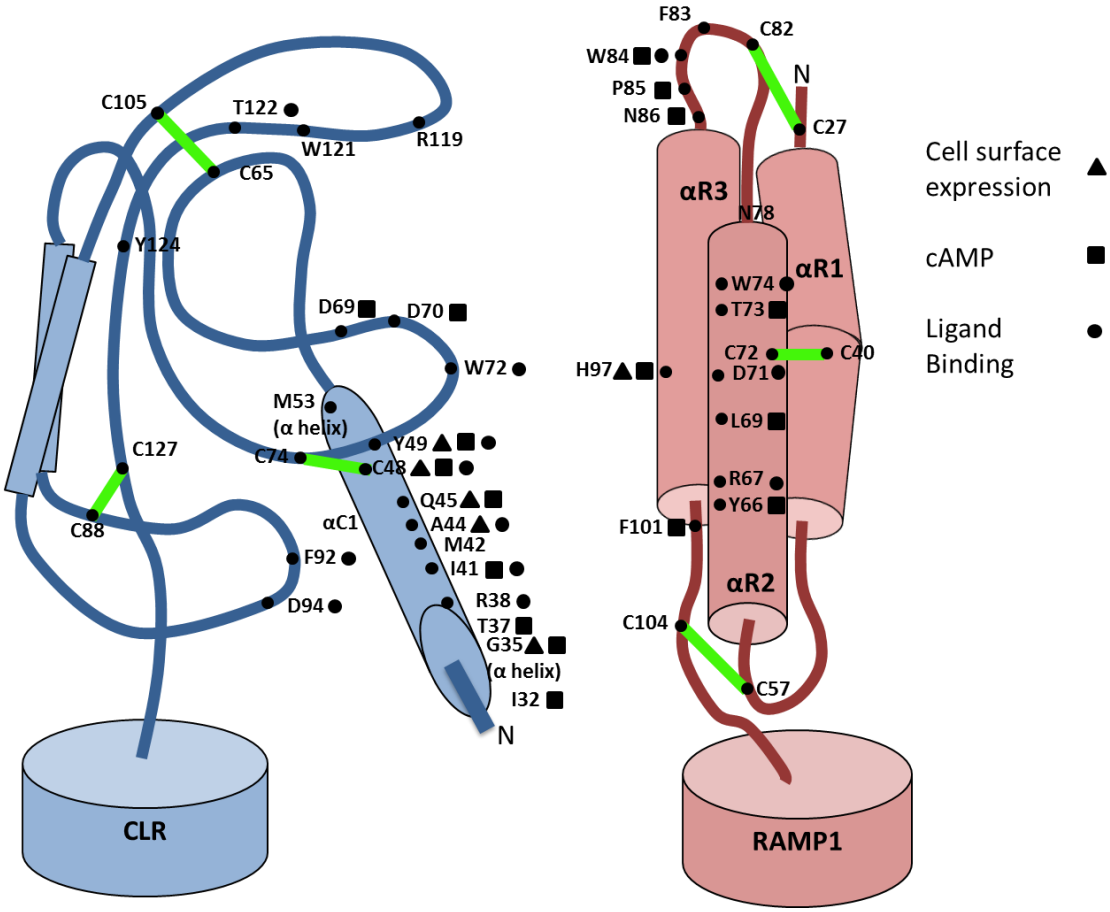

Figure 1.12. Schematic diagram showing the CLR and RAMP1 components of the CGRP receptor.

Key amino acids involved in ligand binding are displayed, together with the type of interaction involved. Figure adapted from Woolley & Conner, 2013.

A44 also faces away from RAMP1, therefore these residues may be directly involved in CGRP binding (ter Haar *et al.*, 2010).

The CLR N-terminus also contains a highly conserved aspartate residue (D70). Alanine and glutamate substitutions abolished signalling and substitution to asparagine maintained pEC_{50}, however reduced E_{max} to 24% of WT. These substitutions reduced co-immunoprecipitation with RAMP1 suggesting that this residue is involved in binding to RAMP1 (Ittner *et al.*, 2004).

In RAMP1, mutations of Y66A, L69A and T73A in helix 2, P85A, N86A in the loop from helix 2 to helix 3, and H97A and F101A in helix 3 all impaired cAMP production (Figure 1.12). The crystal structure shows that RAMP1 Y66 forms hydrogen bonds with CLR Q45 and hydrophobic binds with CLR M42 and Y46. RAMP1 H97 forms hydrogen bonds with CLR Q50 and hydrophobic bonds with CLR Y49. RAMP1 F101 forms hydrogen bonds with Q50 and hydrophobic bonds with Y46, again vital for receptor signalling. L69 is a key residue of helix 2 involved in the hydrophobic core of the RAMP1 helices (Kusano *et al.*, 2008; Simms *et al.*, 2009; ter Haar *et al.*, 2010).

Within RAMP1, it has been speculated that a cluster of residues at the C-terminal end of helix 2 (R67, D71, W74, E78 and W84) could form a CGRP binding site (Kusano *et al.*, 2008). RAMP1 R67 and D71 form structural interactions with CLR residues M42 and R38 respectively, however R67, D71, W74 and W84 all form interactions with the Olcegepant antagonist. The RAMP1 W74 and W84 residues form a hydrophobic binding pocket into which, both the Olcegepant and Telcagepant antagonists extend (ter Haar *et al.*, 2010). W74 has also been shown to be an important residue in species selectivity (Mallee *et al.*, 2002) however substitution experiments of this residue found it only affected synthetic antagonist binding but not binding or signalling with the CGRP ligand or $CGRP_{8-37}$ antagonist (Hay *et al.*, 2006; Moore *et al.*, 2010; Qi *et al.*, 2011). Alanine substitution of RAMP1 W84 resulted in a 20-30-fold reduction in CGRP potency compared with wild type, and also reduced the effect of the Telcagepant and $CGRP_{8-37}$ antagonists (Moore *et al.*, 2010).

The structure of the CLR N-terminus aligns well to the GIP and PTH receptor domains. Based on comparisons with other family B GPCR N-terminal domain

structures, it was also hypothesised that the CGRP peptide may bind with similar orientation to GIP or PTH, allowing the peptide C-terminus to come into close contact with the F83-P85 loop of RAMP1. It was proposed that these interactions could result in the specificity of the receptor to its preferred ligand (CGRP or AM) (ter Haar *et al.*, 2010).

1.3.6.4 Receptor activation

The binding of the C-terminus of CGRP to the complex formed between the N-terminus of both CLR and RAMP1 is thought to result in the presentation of the N-terminal loop formed by residues 1-7 of CGRP to the ECL domains and the TM bundle resulting in activation of the receptor. This follows the proposed "two domain" model of family B GPCR ligand binding (Hoare, 2005).

Within the N-terminal loop of CGRP, residues 5 and 6 (alanine and threonine respectively) are particularly important for receptor activation. Substitution of A5 to cysteine causes large decreases in both affinity and efficacy especially compared to the 10 fold loss in binding affinity observed with the $CGRP_{8-37}$ antagonist. Substitution of T6 to cysteine or alanine resulted in small decreases in ligand affinity but a dramatic loss in potency and efficacy. This was not recovered with the conservative serine substitution which is identical to threonine except for the absence of a methyl group on the β-carbon. This shows the specificity of the ligand binding pocket at this position, constraining both the hydroxyl and the methyl group of CGRP T6 (Hay *et al.*, 2014).

Alanine-scanning mutagenesis of ECL1 and ECL3 of CLR has revealed key residues responsible for CGRP stimulated receptor activation (Figure 1.13). In ECL1, alanine-substitution of three non-polar residues (L195A, V198A and A199L) reduced cAMP signalling (between 11- and 30-fold reductions of pEC_{50} values). These three, close residues in ECL1 are located at the top of TM2 in their model and are predicted to face into the TM bundle either binding directly with the CGRP ligand or indirectly affecting CGRP binding through disruption of the receptor structure or its interaction with its localised environment (Barwell *et al.*, 2011).

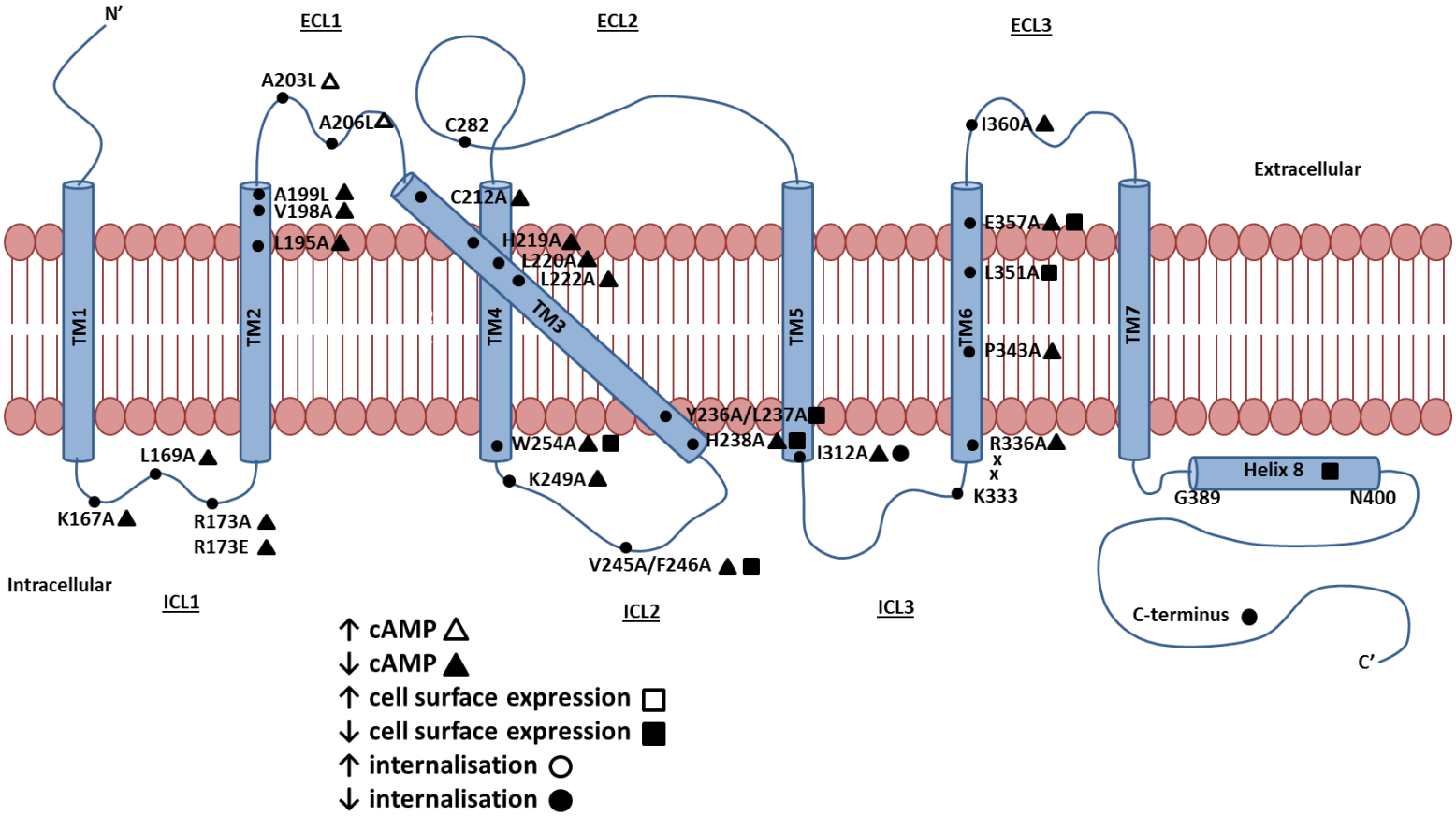

Figure 1.13. Key residues of the ECLs, ICLs and TM domain involved in CGRP mediated receptor binding and activation.
Schematic diagram showing key residues of the CLR extracellular, intracellular and TM domain. Figure adapted from Woolley & Conner, 2013.

Unusually, an increase in cAMP signalling was found in the A203L (~11 fold) and A206L (9 fold) mutants, proposed to be within the loop region of ECL1. Addition of the hydrophobic side chain of leucine promotes receptor activation, potentially by assisting CGRP docking to the receptor-binding pocket, or by stabilising the active conformation of the receptor.

Two further mutations (H219A and C212A) also reduced cAMP signalling by approximately 10-fold. The C212 residue is thought to reside at the top of TM3 and has been shown to interact with C282 of ECL2. Whilst this was proposed to be functionally important for ligand-binding in the CLR/RAMP2 AM receptor (Kuwasako *et al.*, 2003), a double mutant combining C212A and C282A was wild-type suggesting this is not functionally relevant, and rather an artefact of evolutionary redundancy (Woolley *et al.*, 2013). A similar effect occurred in the GLP1R. Substitution of the TM3 cysteine to alanine (C226A) reduced ligand potency, and the double alanine substitution (C226AC296A) restored WT signalling. However the single ECL2 cysteine alanine substitution (C296A) also restored WT signalling. Substitution of the ECL2 cysteine to leucine (C226AC296L) reduced ligand potency indicating that it is the bulky nature of the free ECL2 side chain that caused the disruption in receptor activation (Mann *et al.*, 2010). H219 is located in TM3 of the CLR model (Barwell *et al.*, 2011) alongside L220 and L222. Alanine substitutions of these residues result in a decrease in cAMP signalling (L220A ~25 fold, L222 ~6 fold). Models of CLR and the understanding of the activation mechanisms of family A and B GPCRs, has led to the prediction that TM3 could undergo subtle rotational movement upon activation, taking part in interhelical interactions, or directly interacting with CGRP itself (Barwell *et al.*, 2011; Conner *et al.*, 2005; Sheikh *et al.*, 1999).

In an experiment substituting ECL3 of CLR with that of the VPAC receptor, there was little effect on CGRP potency or efficacy. This indicates that ECL3 does not have a substantial involvement in CGRP-mediated receptor activation (Kuwasako *et al.*, 2012). However, pEC_{50} values were decreased by ~30 fold for E357A and ~10 fold for I360A (Barwell *et al.*, 2011). I360A is predicted to be located in the middle of ECL3, close to ECL2. The reduction in signalling caused by this mutation could be

due to direct CGRP binding, or due to an association with ECL2, stabilising this domain. E357 is located near the top of TM6 and along with L351A have a reduced cell surface expression (10-30% of wild type). It was found that RAMP3 dimerises with the secretin receptor at TM6 and TM7 (Harikumar *et al.*, 2009). The authors suggested that most residues that resulted in a decrease in cell surface expression were in TM6, ECL3 and TM7 with their side chains facing out towards the lipid environment. It is possible that these could be the sites of RAMP1 interaction, leading to successful cell surface expression and CGRP activation.

Proline residues found within α-helices can cause a break in the helix, with structural and functional effects. Proline residues are found within TM4, 5 and 6 throughout all family B GPCRs. Alanine substitution of the CLR TM4 and 5 prolines (P263 and P297 respectively) had no effect on receptor function, however the mutation P343A (and to a lesser extent P353A) in TM6 had a significantly decreased pEC_{50}. Modelling suggested that the kink formed in the alpha helix by P343 brought the C-terminus of TM6 closer to that of TM3. A P343A-I347P double mutation designed to reintroduce the proline kink in the same orientation of the helix restored signalling to that of wild-type (Conner *et al.*, 2005).

1.3.6.5 Receptor signalling

Basic residues in ICL1 have key roles in transducing the signalling response (Figure 1.13). K167A and R173A both reduce cAMP accumulation; with R173E having a much greater effect. Alanine substitution of the hydrophobic residue L169A also reduced cAMP accumulation (Conner *et al.*, 2006a). This indicates that both the polarity of charge and hydrophobicity are important for the interaction resulting in G protein-mediated stimulation of cAMP. However it is not yet certain whether this is through direct G protein interactions or stabilising of a G protein-binding pocket.

ICL2 also has residues important for the localisation of the receptor at the cell surface and the subsequent G protein-mediated cAMP signal transduction. H238 and K249 both cause a ~10 fold reduction in cAMP signalling. H238A also has ~90% reduction in cell surface expression, highlighting its importance for membrane localisation, however K249A retains wild type surface expression and agonist affinity indicating a direct involvement in downstream signalling. The double

mutant V245A/F246A and the single mutant W254A both had a small reduction in cAMP signalling (<5 fold) however both of these sets of mutants resulted in an approximate 50% reduction in cell surface expression, (Conner *et al.*, 2006b). The double mutant Y236A/L237A had no effect on signalling however cell surface expression was reduced by 70% (Conner *et al.*, 2006a).

Within ICL3, I312A (proximal to TM5) caused a 68% reduction in cAMP accumulation and 5-fold reduction in binding affinity and a 30% reduction in internalisation. K333 and R336 form the conserved basic-x-x-basic motif. K333A has cAMP signalling identical to WT however R336A resulted in a >10 fold reduction in pEC_{50} (Conner *et al.*, 2006a).

Unusually, the CGRP receptor has a second accessory protein required for signalling to occur. The CGRP receptor component protein (RCP) is a peripheral membrane protein that couples the CLR/RAMP1 complex to the cellular signalling pathway (Evans *et al.*, 2000). Cell culture studies with the CGRP receptor have shown that a loss of RCP expression correlates with a loss in signalling, however this is not seen with the β2-adrenergic receptor (β2AR) and the adenosine receptor, indicated that RCP is only involved with certain GPCRs (Evans *et al.*, 2000; Prado *et al.*, 2001). Yeast two hybrid assays determined that RCP interacts with the ICL2/TM3 region of CLR but not the remaining three intracellular domains (Egea & Dickerson, 2012).

1.3.6.6 Receptor recycling

The deletion of the entire C-terminus of CLR, including the predicted helix 8 domain, did not significantly change CGRP-mediated cAMP levels from that of wild type, suggesting that this region of the receptor is not involved in $G_{\alpha s}$-coupling (Figure 1.13). This deletion did limit cell surface expression to 10% of wild type, which was recovered once helix 8 was re-introduced. This indicates a possible role of helix 8 for successful cell surface expression. This could occur through interaction with RAMP1, already predicted to associate with TM6 and 7, however this is not certain. Deletion of the C-terminus up to helix 8 prevents internalisation, which is recovered by the extension of the C-terminus. This involvement in internalisation is thought to be through the phosphorylation and subsequent recruitment of β-arrestin to the C-terminus (Conner *et al.*, 2008).

Following activation, CGRP co-internalises with the receptor into early endosomes, which contain the metalloendopeptidase endothelin-converting enzyme 1 (ECE-1) that was found to degrade CGRP at endosomal pH5.5. This degradation of CGRP allows the recycling of the receptor to the cell surface. Addition of CGRP caused the recruitment of beta-arrestin 2 after two minutes followed by endocytosis into the same endosomes. Inhibition of ECE-1 or endosomal acidifications did not have an effect on receptor internalisation, but did prevent the recycling of the receptor to the membrane surface and the release of beta-arrestin 2 back to the cytosol (Padilla *et al.*, 2007).

The fate of receptor recycling depends on the duration of the CGRP-mediated activation. The receptor internalises after 10 minutes of CGRP mediated activation, and is located in early endosomes for the first hour of ligand stimulation. After this time, the trafficking of the receptor complex starts to move to lysosomes. Following a one hour stimulation with 0.1μM CGRP, the CLR RAMP1 heterodimer started to recycle back to the cell surface after 2 hours, with almost total recovery after 6 hours. This correlated with Ca^{2+} resensitisation at 80% after 6 hours, and 95% after 8 hours (compared with control), however an inhibitor of endosomal acidification abolished this (Cottrell *et al.*, 2007). Prolonged exposure to CGRP directs the receptor complex to lysosomes, however the kinetics of degradation differ between CLR and RAMP1. The CLR component shows no detectable degradation following CGRP exposure for 5 hours and degrades by 54% after 16 hours of CGRP exposure. RAMP1 degrades by 45% after just 5 hours. This degradation is independent of the ubiquitination pathway.

1.3.7 Summary

CGRP is a 37 amino acid neuropeptide with potent vasodilatory, inflammatory and nociceptive effects. The CGRP receptor is unique in that it consists of a heterodimer between the family B GPCR, CLR, and a single transmembrane accessory protein, RAMP1.

CGRP binding to the receptor is expected to follow the standard family B “two domain” model of binding, with the amphipathic α-helix of the middle and C-

terminal section of the ligand forming interactions with a hydrophobic binding groove formed between the CLR ECD and RAMP1. This is thought to present the N-terminus of the ligand to the ECLs and TM domain of the receptor. With CGRP (and the calcitonin family of peptides) this is an N-terminal loop formed by a disulphide bond between two cysteine residues. ECL1 and 3 are both involved in ligand based receptor activation however ECL2 has not yet been studied.

1.4 Aims of the study

The purpose of this research is to gain further understanding into the structure and function of the CGRP receptor using biochemical analysis. The major focus of this research is the ECL2 domain. As discussed in the GPCR section of the introduction, this is a highly variable GPCR domain with a prominent role in ligand binding and receptor activation for many receptors. However, until this point, ECL2 has not been investigated in the CGRP receptor.

The hypothesis of the ECL2 study is that this domain of the CGRP receptor has structural and functional importance for ligand binding and receptor activation. Within this loop certain residues will be vital in creating the loop structure or directly binding to the CGRP ligand and will be identified. The electrochemical properties of these residues will have functional effects and these properties can be studied.

This investigation of ECL2 used mutagenesis techniques to manipulate individual residues of this loop and used cell signalling, ligand binding and cell surface expression assays to determine the effect of this mutagenesis on receptor function. The first results chapter describes the results of alanine substitution mutagenesis on each individual residues of ECL2. The second results chapter describes a comprehensive set of further substitution mutagenesis of residues identified as functionally important in results chapter 1 to gain detailed understanding into the molecular effects at these positions. The final results chapter looks at intracellular interactions occurring during CGRP receptor signalling.

2 Materials and Methods

2.1 Materials

2.1.1 Peptides and hormone analogues.

The natural agonist human Calcitonin Gene Related Peptide-1 (hCGRP-1) was purchased from Merck (Watford, UK). The human alpha CGRP (8-37) trifluoroacetate salt antagonist was purchased from BACHEM (St Helens, UK).

2.1.2 Chemicals

All chemicals were purchased from Fisher (Loughborough, UK) at analytical grade quality unless otherwise stated.

2.1.3 Molecular biology reagents

Restriction endonucleases XbaI, EcoRI, KpnI and DpnI were obtained from New England Biolabs (NEB, Hitchin, UK). Pfu DNA polymerase and deoxynucleotide triphosphates (dNTPs) were purchased from Promega (Southampton, UK). Alkaline phosphatase (Calf intestinal phosphatase, CIP), T4 polynucleotide kinase and T4 DNA ligase enzymes were obtained from NEB (Hitchin, UK). For plasmid purification from bacterial suspensions, the Wizard SV Miniprep kit was purchased from Promega and the PowerPrep High Purity Plasmid Maxiprep System was purchased from Insight Biotechnology Ltd (Middlesex, UK). 1kb ladder was purchased from NEB (Hitchin, UK) and 100bp ladder was purchased from Promega (Southampton, UK).

2.1.4 Cell tissue culture

Dulbecco's modified Eagle's medium (DMEM), phosphate buffered saline (PBS) and 0.25% Trypsin-EDTA was purchased from Gibco (Paisley, UK). Cell culture plasticware was purchased from BD Biosciences (Oxford, UK). Polyethyleneimine solution for transfection was purchased from Sigma (Dorset, UK).

2.1.5 Plasmid vectors

The mammalian expression vector plasmid used was pcDNA3.1- (5427bp) from Invitrogen (Paisley, UK) (Figure 2.1). This plasmid features the following elements: a. CMV promoter to permit high level protein expression, b. T7 promoter/priming site for in vitro transcription in the sense orientation and sequencing through insert, c. multiple cloning site for insertion of gene, d. BGH reverse priming site, e. BGH polyadenylation sequence for efficient transcription termination and mRNA polyadenylation, f. f1 origin for rescue of single stranded DNA, g. SV40 early promoter and origin for efficient, high level expression of the neomycin resistance gene and episomal replication in cells expression SV40 large T antigen, h. neomycin resisitance gene (ORF) for selection of stable transfectants in mammalian cells, i. SV40 early polyadenylation signal for efficient transcription termination and polyadenylation of mRNA, j. pUC origin for high copy number replication and growth in *E.coli* , k. ampicillin resistance gene for selection of vector in *E.coli* , l. ORF, ribosome binding site, m. bla promoter (P3).

2.1.6 DNA constructs

The hCLR and hRAMP1 and $rG_{\alpha s}$ DNA sequences were kindly provided in the pcDNA3.1- vector by David Poyner at Aston University. The hCLR construct contained an N-terminal signal peptide and an HA tag (Figure 2.2).

2.1.7 Oligonucleotides

Oligonucleotides were synthesised in 25 µmol amounts from Invitrogen (Paisley, UK) or Sigma (Dorset, UK). Lyophilised primers were reconstituted to a 100 µM stock concentration in sterile H2O and stored at -20°C. Oligonucleotide sequences for the ECL2 alanine substitution are detailed in Table 2.1. Oligonucleotide sequences for the ECL2 further mutagenesis are detailed in Table 2.2. Oligonucleotide sequences for the ICL and C-terminus cloning are detailed in Table 2.3. Oligonucleotide sequences for the CLR-$G_{\alpha s}$ fusion construct are detailed in Table 2.4.

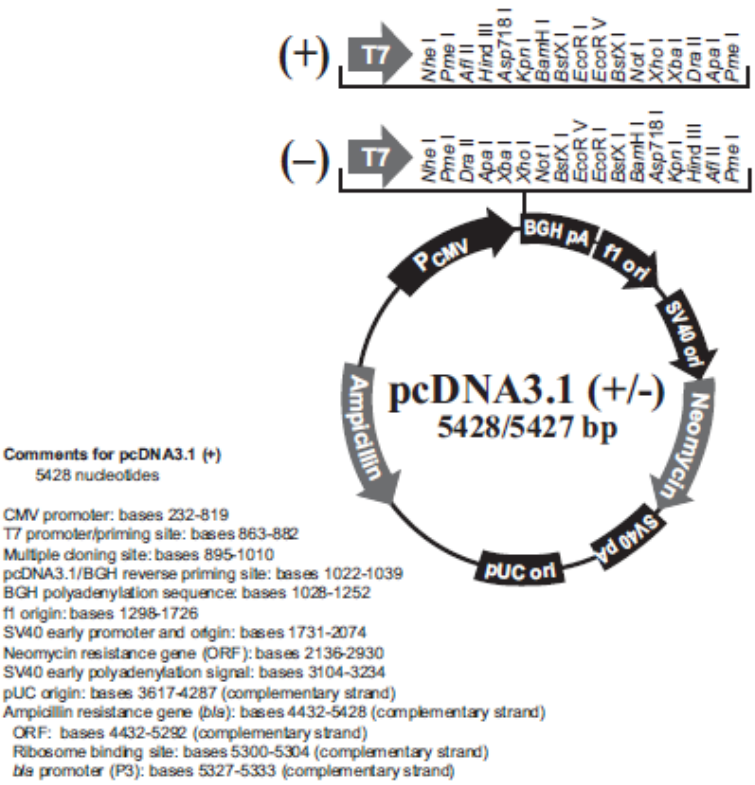

Figure 2.1. Plasmid vector map of the mammalian expression vector pcDNA3.1 (+/-).
Plasmid vector map as described from www.invitrogen.com. Key features have been annotated. The +/- plasmids contain the same features except the orientation of the multiple cloning site (MCS).

cggccgcgtcgacggaattgcgccaccatggccttaccagtgaccgccttgctcctgccg
R P R R R N C A T M A L P V T A L L L P
ctagccttgctgctccacgccgccaggccggattacgcgtcttacccgtatgacgtccca
L A L L L H A A R P D Y A S Y P Y D V P
gattacgcatcgctgggaggcccttcactcgagggatccgcagaattagaagagagtcct
D Y A S L G G P S L E G S A E L E E S P
gaggactcaattcagttgggagttactagaaataaaatcatgacagctcaatatgaatgt
E D S I Q L G V T R N K I M T A Q Y E C
taccaaaagattatgcaagaccccattcaacaagcagaaggcgtttactgcaacagaacc
Y Q K I M Q D P I Q Q A E G V Y C N R T
tgggatggatggctctgctggaacgatgttgcagcaggaactgaatcaatgcagctctgc
W D G W L C W N D V A A G T E S M Q L C
cctgattactttcaggactttgatccatcagaaaaagttacaaagatctgtgaccaagat
P D Y F Q D F D P S E K V T K I C D Q D
ggaaactggtttagacatccagcaagcaacagaacatggacaaattatacccagtgtaat
G N W F R H P A S N R T W T N Y T Q C N
gttaacacccacgagaaagtgaagactgcactaaatttgttttacctgaccataattgga
V N T H E K V K T A L N L F Y L T I I G
cacggattgtctattgcatcactgcttatctcgcttggcatattcttttatttcaagagc
H G L S I A S L L I S L G I F F Y F K S
ctaagttgccaaaggattaccttacacaaaaatctgttcttctcatttgtttgtaactct
L S C Q R I T L H K N L F F S F V C N S
gttgtaacaatcattcacctcactgcagtggccaacaaccaggccttagtagccacaaat
V V T I I H L T A V A N N Q A L V A T N
cctgttagttgcaaagtgtcccagttcattcatctttacctgatgggctgtaattacttt
P V S C K V S Q F I H L Y L M G C N Y F
tggatgctctgtgaaggcatttacctacacacactcattgtggtggccgtgtttgcagag
W M L C E G I Y L H T L I V V A V F A E
aagcaacatttaatgtggtattatttcttggctggggatttccactgattcctgcttgt
K Q H L M W Y Y F L G W G F P L I P A C
atacatgccattgctagaagcttatattacaatgacaattgctggatcagttctgatacc
I H A I A R S L Y Y N D N C W I S S D T
catctcctctacattatccatggcccaatttgtgctgctttactggtgaatctttttttc
H L L Y I I H G P I C A A L L V N L F F
ttgttaaatattgtacgcgttctcatcaccaagttaaaagttacacaccaagcggaatcc
L L N I V R V L I T K L K V T H Q A E S
aatctgtacatgaaagctgtgagagctactcttatcttggtgccattgcttggcattgaa
N L Y M K A V R A T L I L V P L L G I E
tttgtgctgattccatggcgacctgaaggaaagattgcagaggaggtatatgactacatc
F V L I P W R P E G K I A E E V Y D Y I
atgcacatccttatgcacttccagggtcttttggtctctaccattttctgcttctttaat
M H I L M H F Q G L L V S T I F C F F N
ggagaggttcaagcaattctgagaagaaactggaatcaatacaaaatccaatttggaaac
G E V Q A I L R R N W N Q Y K I Q F G N
agctttccaactcagaagctcttcgtagtgcgtcttacacagtgtcaacaatcagtgat
S F S N S E A L R S A S Y T V S T I S D
ggtccaggttatagtcatgactgtcctagtgaacacttaaatggaaaaagcatccatgat
G P G Y S H D C P S E H L N G K S I H D
attgaaaatgttctcttaaaaccagaaaatttatataattgagaattc
I E N V L L K P E N L Y N * E F

Figure 2.2. DNA and translated sequence of hCLR with an N-terminal signal peptide and HA tag.

The start codon is highlighted green, the signal peptide magenta, the HA tag is cyan and the mature hCLR sequence is yellow.

Mutant	F/R	Primer sequence 5' - 3'
A271L	F	CCTGCTTGTATACAT**CTC**ATTGCTAGAAGC
	R	GCTTCTAGCAAT**GAG**ATGTATACAAGCAGG
I272A	F	GCTTGTATACATGCC**GCT**GCTAGAAGCTTATATTAC
	R	GTAATATAAGCTTCTAGC**AGC**GGCATGTATACAAGC
A273L	F	GTATACATGCCATT**CTT**AGAAGCTTATATTAC
	R	GTAATATAAGCTTCT**AAG**AATGGCATGTATAC
S275A	F	CATGCCATTGCTAGA**GCC**TTATATTACAATGAC
	R	GTCATTGTAATATAA**GGC**TCTAGCAATGGCATG
L276A	F	GCCATTGCTAGAAGC**GCA**TATTACAATGAC
	R	GTCATTGTAATA**TGC**GCTTCTAGCAATGGC
I284A	F	GACAATTGCTGG**GCC**AGTTCTGATACCC
	R	GGGTATCAGAACT**GGC**CCAGCAATTGTC
S286A	F	CAATTGCTGGATCAGT**GCT**GATACCCATCTCCTC
	R	GAGGAGATGGGTATC**AGC**ACTGATCCAGCAATTG
D287A	F	GCTGGATCAGTTCT**GCT**ACCCATCTCCTCTAC
	R	GTAGAGGAGATGGGT**AGC**AGAACTGATCCAGC
H289A	F	CAGTTCTGATACC**GCT**CTCCTCTACATTATCC
	R	GGATAATGTAGAGGAG**AGC**GGTATCAGAACTG
L290A	F	GTTCTGATACCCAT**GCC**CTCTACATTATCC
	R	GGATAATGTAGAG**GGC**ATGGGTATCAGAAC
L291A	F	CTGATACCCATCTC**GCC**TACATTATCCATGG
	R	CCATGGATAATGTA**GGC**GAGATGGGTATCAG
Y292A	F	CCCATCTCCTC**GCC**ATTATCCATGGC
	R	GCCATGGATAAT**GGC**GAGGAGATGGG
I293A	F	CCCATCTCCTCTAC**GCT**ATCCATGGCCC
	R	GGGCCATGGAT**AGC**GTAGAGGAGATGGG
I294A	F	CTCCTCTACATT**GCC**CATGGCCCAATTTG
	R	CAAATTGGGCCATG**GGC**AATGTAGAGGAG

Table 2.1. Primer sequences for the alanine substitution site directed mutagenesis of the ECL2 domain of the CGRP receptor.

The codon being mutated is highlighted in red.

Mutant	F/R	Primer sequence 5' - 3'
A273G	F	GCTTGTATACATGCCATT**GGT**AGAAGCTTATATTACAATG
	R	CATTGTAATATAAGCTTCT**ACC**AATGGCATGTATACAAGC
R274G	F	CATGCCATTGCT**GGA**AGCTTATATTAC
	R	GTAATATAAGCT**TCC**AGCAATGGCATG
Y277F	F	GCTAGAAGCTTA**TTT**TACAATGACAATTGC
	R	GCAATTGTCATTGTA**AAA**TAAGCTTCTAGC
Y277L	F	GCCATTGCTAGAAGCTTA**TTA**TACAATGACAATTGCTGG
	R	CCAGCAATTGTCATTGTA**TAA**TAAGCTTCTAGCAATGGC
Y278F	F	GCTAGAAGCTTATAT**TTC**AATGACAATTGCTGG
	R	CCAGCAATTGTCATT**GAA**ATATAAGCTTCTAGC
Y278L	F	GCTAGAAGCTTATAT**TTA**AATGACAATTGCTGG
	R	CCAGCAATTGTCATT**TAA**ATATAAGCTTCTAGC
D280E	F	GCTTATATTACAAT**GAG**AATTGCTGGATCAG
	R	CTGATCCAGCAATT**CTC**ATTGTAATATAAGC
D280L	F	GCTTATATTACAAT**CTC**AATTGCTGGATCAG
	R	CTGATCCAGCAATT**GAG**ATTGTAATATAAGC
D280N	F	GCTTATATTACAAT**AAC**AATTGCTGGATCAG
	R	CTGATCCAGCAATT**GTT**ATTGTAATATAAGC
D280S	F	GCTTATATTACAAT**AGC**AATTGCTGGATCAG
	R	CTGATCCAGCAATT**GCT**ATTGTAATATAAGC
D280T	F	GCTTATATTACAAT**ACC**AATTGCTGGATCAG
	R	CTGATCCAGCAATT**GGT**ATTGTAATATAAGC
N281K	F	GCTTATATTACAATGAC**AAA**TGCTGGATCAGTTCTG
	R	CAGAACTGATCCAGCA**TTT**GTCATTGTAATATAAGC
W283F	F	CAATGACAATTGC**TTT**ATCAGTTCTGATACCC
	R	GGGTATCAGAACTGAT**AAA**GCAATTGTCATTG
W283H	F	TTACAATGACAATTGC**CAT**ATCAGTTCTGATACCC
	R	GGGTATCAGAACTGAT**ATG**GCAATTGTCATTGTAA
I284F	F	CAATGACAATTGCTGG**TTC**AGTTCTGATACCCATC
	R	GATGGGTATCAGAACT**GAA**CCAGCAATTGTCATTG
I284L	F	CAATGACAATTGCTGG**CTC**AGTTCTGATACCCATC
	R	GATGGGTATCAGAACT**GAG**CCAGCAATTGTCATTG
I284Q	F	CAATGACAATTGCTGG**CAG**AGTTCTGATACCCATC
	R	GATGGGTATCAGAACT**CTG**CCAGCAATTGTCATTG
S285D	F	GACAATTGCTGGATC**GAT**TCTGATACCCATCTCC
	R	GGAGATGGGTATCAGA**ATC**GATCCAGCAATTGTC
S285N	F	GACAATTGCTGGATC**AAT**TCTGATACCCATCTC
	R	GAGATGGGTATCAGA**ATT**GATCCAGCAATTGTC
S285T	F	GACAATTGCTGGATC**ACT**TCTGATACCCATCTC
	R	GAGATGGGTATCAGA**AGT**GATCCAGCAATTGTC
S285Y	F	GACAATTGCTGGATC**TAT**TCTGATACCCATCTCC
	R	GGAGATGGGTATCAGA**ATA**GATCCAGCAATTGTC

Table 2.2. Primer sequences for the further substitution site directed mutagenesis of the ECL2 domain of the CGRP receptor.

The codon being mutated is highlighted in red.

Mutant	F/R	Primer sequence 5' - 3'
D287E	F	GCTGGATCAGTTCT**GAG**ACCCATCTCCTCTAC
	R	GTAGAGGAGATGGGT**CTC**AGAACTGATCCAGC
D287L	F	GACAATTGCTGGATCAGTTCT**CTT**ACCCATCTCCTCTACATTATCC
	R	GGATAATGTAGAGGAGATGGGT**AAG**AGAACTGATCCAGCAATTGTC
D287S	F	GCTGGATCAGTTCT**TCT**ACCCATCTCCTCTAC
	R	GTAGAGGAGATGGGT**AGA**AGAACTGATCCAGC
T288D	F	GCTGGATCAGTTCTGAT**GAC**CATCTCCTCTACATTATCC
	R	GGATAATGTAGAGGAGATG**GTC**ATCAGAACTGATCCAGC
T288N	F	GCTGGATCAGTTCTGAT**AAC**CATCTCCTCTACATTATCC
	R	GGATAATGTAGAGGAGATG**GTT**ATCAGAACTGATCCAGC
T288S	F	GCTGGATCAGTTCTGAT**TCC**CATCTCCTCTACATTATCC
	R	GGATAATGTAGAGGAGATG**GGA**ATCAGAACTGATCCAGC
T288V	F	GGATCAGTTCTGAT**GTC**CATCTCCTCTAC
	R	GTAGAGGAGATG**GAC**ATCAGAACTGATCC
L290AL291A	F	CAGTTCTGATACCCAT**GCCGCC**TACATTATCCATGGCC
	R	GGCCATGGATAATGTA**GGCGGC**ATGGGTATCAGAACTG
L290AY292A	F	GATACCCAT**GCC**CTC**GCC**ATTATCCATGGCCC
	R	GGGCCATGGATAAT**GGC**GAGGGCATGGGTATC
L291AY292A	F	CTGATACCCATGCC**GCCGCC**ATTATCCATGGCCC
	R	GGGCCATGGATAAT**GGCGGC**GGCATGGGTATCAG
L291AI293A	F	CCCATCTC**GCC**TAC**GCT**ATCCATGGCCC
	R	GGGCCATGGAT**AGC**GTAGGCGAGATGGG
L290N	F	CAGTTCTGATACCCAT**AAC**CTCTACATTATCCATG
	R	CATGGATAATGTAGAG**GTT**ATGGGTATCAGAACTG
L291N	F	CTGATACCCATCTC**AAC**TACATTATCCATGG
	R	CCATGGATAATGTA**GTT**GAGATGGGTATCAG
Y292S	F	CCCATCTCCTC**TCC**ATTATCCATGGCCC
	R	GGGCCATGGATAAT**GGA**GAGGAGATGGG
I294G	F	CTCCTCTACATT**GGC**CATGGCCCAATTTG
	R	CAAATTGGGCCATG**GCC**AATGTAGAGGAG

Table 2.2 (cont). Primer sequences for the further substitution site directed mutagenesis of the ECL2 domain of the CGRP receptor.

The codon being mutated is highlighted in red.

Mutant	F/R	Primer sequence 5' - 3'
ICL1	F	CTAGA ATG AAGAGCCTAAGTTGCCAAAGG TAG G
	R	AATTC CTA CCTTTGGCAACTTAGGCTCTT CAT T
ICL2	F	TCGT TCTAGA ATG CTACACACACTCATTG
	R	TCGT GAATTC CTA CATTAAATGTTGCTTC
ICL3	F	TCGT TCTAGA ATG CGCGTTCTCATCACC
	R	TCGT GAATTC CTA TCTCACAGCTTTCATG
H8	F	CTAGA ATG GGAGAGGTTCAAGCAATTCTGAGAAGAAACTGGAAT TAG G
	R	AATTC CTA ATTCCAGTTTCTTCTCAGAATTGCTTGAACCTCTCC CAT T
C-terminus	F	TCGT TCTAGA ATG CAATACAAAATCCAATTTGG
	R	TCGT GAATTC CTA ATTATATAAATTTTCTGG

Table 2.3. Primer sequences for the cloning of the CLR ICLs, H8 and C-terminus into the pcDNA3.1- vector.

The primers have been designed with a 5' XbaI restriction site (magenta) and a 3' EcoRI site (green). A start codon (red) and a stop codon (blue) have been included in the primers.

Mutant	F/R	Primer sequence 5' - 3'
CLRSTOPA	F	GAAAATTTATATAAT**GCA**GAATTCCACCACAC
CLRSTOPA	R	GTGTGGTGGAATTC**TGC**ATTATATAAATTTTC
rGNASE	F	TGAC **GAATTC** ATGGGCTGCCTCGGC
rGNASK	R	TGAC **GGTACC** TTAGAGCAGCTCGTATTGGCG
GNASND	F	GATGAACGTGCCA**GAC**TTTGACTTCCCACC
GNASND	R	GGTGGGAAGTCAAA**GTC**TGGCACGTTCATC

Table 2.4. Primer sequences for the cloning of the $G_{\alpha s}$ gene intro the CLR construct at the 3' terminus.

The codon being mutated is highlighted in red. The $G_{\alpha s}$ amplification primers have been designed with a 5' EcoRI site restriction site (magenta) and a 3' KpnI site (green).

2.1.8 Antibodies

For the cell surface expression ELISA, the monoclonal anti-HA antibody produced in mouse and the anti-mouse IgG (whole molecule)-peroxidase antibody produced in goat were both purchased from Sigma (Dorset, UK).

2.1.9 cAMP signalling

To measure cellular cAMP levels a Perkin Elmer Lance® TR-FRET based cAMP assay and 96 well white optiplates were purchased from Perkin Elmer (Cambridge, UK).

2.1.10 ELISA

For the detection of peroxidase activity in enzyme immunoassays SIGMAFAST™ OPD (o-Phenylenediamine dihydrochloride) was purchased from Sigma (Dorset, UK).

2.2 Methods

2.2.1 Primer design for site directed mutagenesis (SDM)

Primers were designed to include the required codon change with an extended 5' and 3' sequence of 10-15 nucleotides to allow for primer annealing and extension. Where possible, primers were terminated with a cytosine or guanine nucleotide to facilitate stronger binding to the template DNA strand.

2.2.2 Primer design for PCR amplification

Primers were designed to include a flanking restriction site with appropriate restriction site and a short random base pair sequence at the terminus to facilitate restriction digest. Start and stop codons were include if required.

2.2.3 QuikChange site directed mutagenesis

100 ng of plasmid DNA was used as a template with sense and antisense nucleotides at a final concentration of 200 nM each. A final concentration of 800 µm dNTPs and a total amount of 3 units of Pfu polymerase were added to a total reaction volume of 50 µl. The final 1x reaction buffer consisted of 20 mM Tris-HCl (pH 8.8 at 25 °C), 10 mM KCl, 10 mM $(NH_4)SO_4$, 2 mM $MgSO_4$, 0.1 % Triton® X-100 and 0.1 mg/ml nuclease-free BSA. The reaction mix was denatured at 95 °C for 30 s, annealed at 55 °C for 30 s and extended at 72 °C for 16 min for 16 cycles in a Biometra T3000 thermocycler. 20 units DpnI was added to the reaction mix for 5 hours at 37 °C to digest methylated template DNA. The template DNA used was hCLR with an N terminal HA tag in the pcDNA3.1- vector.

2.2.4 PCR amplification

10 ng of plasmid DNA was used as a template with sense and antisense nucleotides at a final concentration of 200 nM each. A final concentration of 800 µm dNTPs and a total amount of 3 units of Pfu polymerase were added to a total reaction volume of 50 µl. The final 1x reaction buffer consisted of 20 mM Tris-HCl (pH 8.8 at 25 °C), 10 mM KCl, 10 mM $(NH_4)SO_4$, 2 mM $MgSO_4$, 0.1 % Triton® X-100 and 0.1 mg/ml nuclease-free BSA. The reaction mix was denatured at 95 °C for 30 s, annealed at

50 °C for 30 s and extended at 72 °C for 1 min for 30 cycles in a Biometra T3000 thermocycler.

2.2.5 Annealing and kinase treating primers

ICL1 and H8 primers (Table 2.3) were designed ready for insertion into the pcDNA3.1- vector. Sense and antisense nucleotides were added at a final concentration of 5 μM to a total volume of 50 μl. The primer mix was denatured at 95 °C for 5 min and annealed at 50 °C for 15 min. Before ligation the annealed primers were phosphorylated with T4 polynucleotide kinase. 5 μM primers were mixed with 0.5 mM ATP and 10 units T4 polynucleotide kinase in a total reaction volume of 30 μl. The final 1x reaction buffer consisted of 70 mM Tris-HCl, 10 mM $MgCl_2$ and 5 mM DTT (pH 7.6 @ 25 °C). The reaction was incubated at 37 °C for 15 min and heat inactivated at 65 °C for 10 min.

2.2.6 Restriction endonuclease digestion

~1 μg DNA was digested using 20 units restriction endonuclease in a total reaction volume of 50 μl. The final 1x reaction buffer consisted of 50 mM Potassium Acetate, 20 mM Tris-acetate, 10 mM Magnesium Acetate and 1 mM DTT (pH 7.9 @ 25 °C). The reaction mix was incubated at 37°C for 3 hours. After 2 hours 10 units of calf intestinal phosphatase (CIP) was added to the plasmid vector digest and incubated at 37 °C for 1 hour.

2.2.7 Gel electrophoresis

Agarose gels were prepared by adding 0.8-2% (w/v) agarose to 1x TBE buffer (89 mM Tris, 89 mM Boric acid, 2 mM EDTA, pH 8) and heating with regular stirring to dissolve. Ethidium bromide (0.2 μg/ml) was added and stirred to mix. The gel was poured and allowed to set. DNA samples were prepared with NEB 6x loading dye, to a final concentration of 2.5 % Ficoll-400, 11 mM EDTA, 3.3 mM Tris-HCl (pH 8.0 @ 25 °C), 0.017 % SDS and 0.015 % bromophenol blue. 0.5 μg 1kb ladder (NEB) or 0.65 μg 100bp ladder (Promega) was loaded and the gel was electrophoresed at 100-150V until sufficient separation had occurred. The gel image was captured using a GelDoc 2000 UV transilluminator with Quantity One software (Biorad, UK). To

extract DNA, fragments were excised from the gel and purified using a gel extraction kit (Qiagen).

2.2.8 Ligation

A vector:insert ratio of 1:3 (100 ng vector) was added to 400 units T4 ligase in a total reaction volume of 20 µl. The final 1x reaction buffer consisted of 50 mM Tris-HCl, 10 mM $MgCl_2$, 1 mM ATP and 10 mM DTT (pH 7.5 @ 25 °C). The reaction mix was incubated at 16 °C for 16 hours.

2.2.9 Preparation of competent cells

Top 10 cells were streaked onto an LB agar plate (no antibiotic) and grown at 37 °C, 16 hours. A single colony was used to inoculate 5ml LB medium and incubated at 37 °C, 220 rpm for 16 hours. The 5ml culture was used to inoculate 400 ml LB medium and grown at 37 °C, 220 rpm until the OD590 had reached 0.35-0.4. The culture was incubated on ice for 10 min, and cells were pelleted at 4000 x g, 4 °C for 15 min. Cells were resuspended in 80ml of ice cold 60 mM $CaCl_2$, 15 % (v/v) glycerol, 10 mM pipes pH 7 and pelleted at 4000 x g, 4 °C for 15 min. Cells were resuspended in 80 ml of ice cold 60 mM $CaCl_2$, 15 % (v/v) glycerol, 10 mM pipes pH 7, 4 °C and incubated on ice for 30 min. Cells were pelleted at 4000 x g, 4 °C for 15 min. Cells were resuspended in 16 ml 60 mM $CaCl_2$, 15 % (v/v) glycerol, 10 mM pipes pH 7, 4 °C, aliqotted into pre-cooled microcentrifuge tubes and stored at -80 °C.

2.2.10 Transformation

Competent Top10 cells were defrosted on ice and DNA was added (not exceeding 1/10 of the competent cell volume), mixed and incubated for 10 min, 4 °C. The Top10 cells and DNA mix was exposed to heat shock at 42 °C for 60 s followed by incubation on ice for 5 min. The Top10 cells were grown in 1ml LB medium for 1 hour at 37°C. Cells were pelleted at 2000 x g for 5 min and resuspended in 50-150 µl LB medium and plated onto LB agar + 100 µg/µl ampicillin and incubated at 37 °C for 16hours.

2.2.11 DNA amplification and purification

To obtain a plasmid DNA yield of ~10 µg to use for sequencing or molecular biological processes, a transformed Top10 colony was picked and grown in 3-5 ml Lbroth + 100 µg/µl ampicillin at 37 °C, 220 rpm for 16 hours. The cells were pelleted by centrifugation at 4000 x g for 5 min and DNA was purified using a Wizard® Plus SV Miniprep kit (Promega). To obtain a plasmid DNA yield of 250-1000 µg to use for mammalian cell transfections a transformed Top10 colony was picked and grown in 3-5 ml Lbroth + 100 µg/µl ampicillin at 37 °C, 220 rpm for 8 hours. This culture was used to inoculate 150 ml Lbroth + 100 µg/µl ampicillin and incubated at 37 °C, 220 rpm for 16 hours. The cells were pelleted by centrifugation at 4000 x g for 5 min and DNA was purified using a PowerPrep High Purity Plasmid Maxiprep System (Insight Biotechnology Ltd).

2.2.12 Sequencing

DNA sequencing was done by GATC biotech (Köln, Germany). Samples were prepared by adding 500 ng DNA and 5 µM sequencing primer to a final volume of 10 µl. DNA sequences were obtained using Applied Biosystems sequence scanner software and alignments were created using EMBL-EBI ClustalW2 multiple sequence alignment software.

2.2.13 Cell culture and transfection

Cos7 cells were grown in Dulbecco's Modified Eagle Medium (DMEM) supplemented with 10 % (v/v) fetal bovine serum (FBS) at 37 °C in a humidified 95 % air/5 % CO_2 atmosphere. Cos7 cells were subcultured to maintain a cellular confluence between 10 % and 80 % using 0.25 % (w/v) Trypsin - 0.53 mM EDTA solution. Cell stocks ($4x10^6$ per vial) were maintained by freezing the cells in DMEM + 10 % FBS + 5 % dimethyl sulfoxide (DMSO) and storing in liquid nitrogen. For cAMP assays, cells were seeded in 6 well plates at 5×10^{-5} cells per well and grown for 24 hours before PEI transfection. For cell surface expression ELISAs, cells were seeded in 24 well plates at $8x10^{-4}$ cell per well and grown for 24 hours before PEI transfection.

2.2.14 PEI transfection

Cells were transfected using a mixture (per 1 µg DNA) of 6 µl of 1 µg/µl polyethyleneimine PEI (pH7.4) and 50 µl DMEM (serum free) and incubating for 10 min at room temperature. 300 µl DMEM + 10 % FBS was added and the transfection mix was added to the cells. Following incubation (37 °C, 95 % air/5 % CO_2) for 3 hours, DMEM + 10 % FBS was added to an appropriate final volume. 6 well plates were treated with 2 µg DNA per well, 24 well plates were treated with 0.5 µg of DNA per well and 100 mm dishes were treated with 10 µg of DNA per dish.

2.2.15 Perkin Elmer Lance® cAMP TR-FRET signalling assay

The Perkin Elmer Lance® cAMP TR-FRET assay was used. The assay was optimised for cos7 cells transiently transfected with the CGRP receptor.

2.2.15.1 Optimisation of the Perkin Elmer Lance® cAMP assay

The cAMP assay protocol was optimised from the Perkin Elmer Lance® cAMP assay manual. The optimisation included testing the consistency of data output across a Perkin Elmer 96 well optiplate (using cAMP standards), the reproducibility of the assay over different days (using cAMP standards), the optimal cell amount per well and the optimal CGRP stimulation concentration range. The results from this optimisation are shown in Figure 2.3. The assay buffer (stimulation buffer, SB) was PBS + 0.1 % BSA + 0.5 mM IBMX. A logarithmic decrease of cAMP standards were diluted in SB over a concentration range of 10^{-6} to 10^{-12} M with SB as a basal. The cAMP standards were loaded in triplicate at two different positions on a 96 well optiplate. The top graph in Figure 2.3 describes the response. Each set of standards produced an identical output. This shows the consistency across a 96 well plate. The cAMP standards were loaded in triplicate on separate days to measure the reproducibility of the assay. The second graph describes these results. These curves are almost identical showing the reproducibility of the assay. The cAMP output of a range of cos 7 cell amounts was tested using a dose-dependent stimulation with forskolin across a concentration range of 10^{-4} to 10^{-10} M using SB as a basal. The cAMP standards across the previously described concentration range were loaded

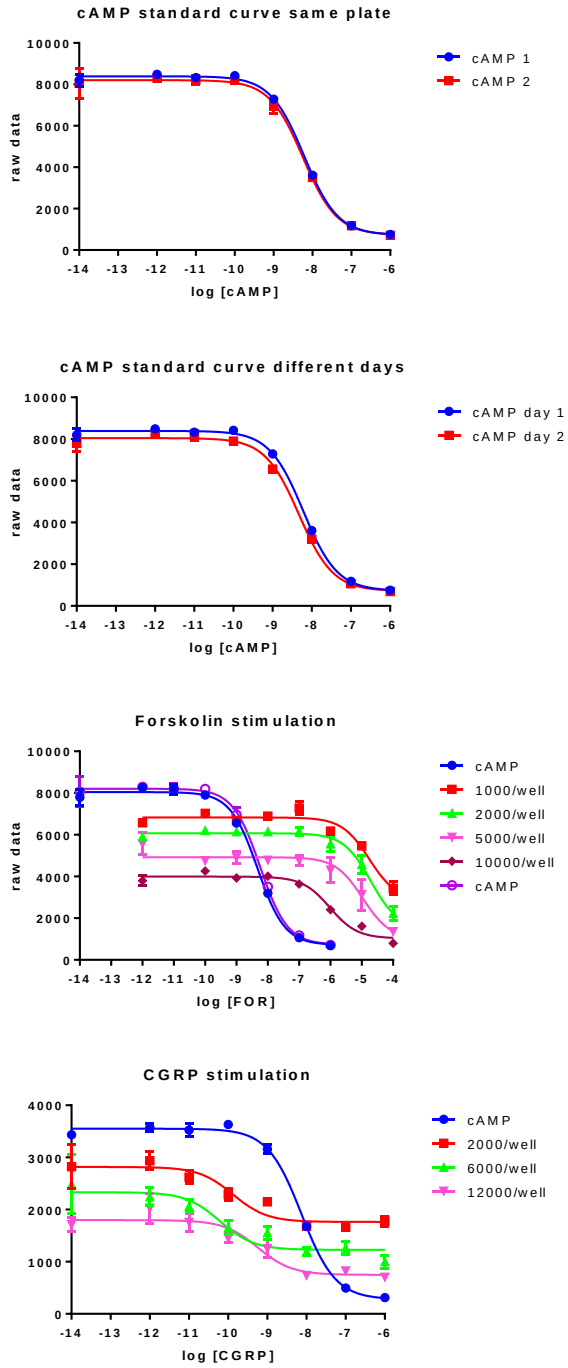

Figure 2.3. Optimisation of the Perkin Elmer Lance® cAMP TR-FRET signalling assay.
The cAMP assay protocol was optimised from the Perkin Elmer Lance® cAMP assay manual. The cAMP standard curve same plate graph loaded cAMP standards in triplicate at two different positions on a 96 well plate. The cAMP standard curve different day graph shows cAMP standards loaded in triplicate in the same plate position on separate days. The forksolin stimulation graph tested varying amounts of cos 7 cells/well (1000/well, 2000/well, 5000/well and 10,000/well) and dose dependently stimulated with forskolin. The CGRP stimulation graph tested varying amounts of cos 7 cells/well (2000/well, 6000/well and 12,000/well) and dose dependently stimulated with CGRP.

to enable the cell concentration that produced a forskolin response over the linear part of the cAMP standard curve to be chosen. These results are shown in the third graph. 1000 cells/well produced a response close to the top end of the cAMP standard curve. 10,000 cells/well produced a response close to the bottom end. 2000 cells/well and 5000 cells/well both produced a response in the linear cAMP standard range. 2000 cells/well produced a response over a slightly larger range. The cAMP output of a range of cos 7 cell amounts was tested using a dose-dependent stimulation with CGRP across a concentration range of 10^{-6} to 10^{-12} M using SB as a basal. A cAMP standard curve was loaded. These results are shown in the final graph. Again, the higher cell number (12,000 cells/well) produced a cAMP response at the bottom end of the cAMP standard curve. 2000 cells/well and 6000 cells/well both produced a response in the linear part of the cAMP standard curve with a similar window between the highest and lowest cAMP response. 2000 cells/well were chosen to use in the assay due to the slightly higher signalling window observed with the forskolin stimulation. The concentration range of CGRP (10^{-6} to 10^{-12} M with SB as a basal) was sufficient to produce a basal and E_{max} signalling response with a pEC_{50} between 9.2 and 10.2. This concentration range should be sufficient to stimulate substitutions with an increased or reduced signalling potency.

2.2.15.2 Perkin Elmer Lance® cAMP assay optimised protocol

48 hours following transfection, cells were removed from the plate with 0.25 % (w/v) Trypsin - 0.53 mM EDTA solution, washed with PBS and resuspended in assay stimulation buffer (SB, PBS + 0.1 % BSA + 0.5 mM IBMX). The cells were counted with a hemocytometer and the appropriate cell number pelleted at 500 x g, 4 min, to be resuspended in SB + 1/100 AlexaFluor® 647-anti cAMP antibody at an assay concentration of 2000 cells/10 µl. 2000 cells/well (10µl) were loaded onto a 96 well white optiplate and were dose dependently stimulated in triplicate with a logarithmic increase of CGRP diluted in SB from 10^{-6} M to 10^{-12} M with SB as a basal in a 10 µl volume at a x2 final concentration. The plate was incubated in the absence of light for 30 min before 20 µl/well of detection mix was added. The plate

was incubated in the absence of light for a further 60 minutes. FRET was recorded by excitation at 320 nm and emission at 665 nm.

2.2.16 Cell surface expression ELISA

48 hours following transfection cells were stimulated with DMEM + 10 % FBS ± 10^{-7} M CGRP for 45-60 min. The stimulation media was removed by aspiration and the cells were fixed with 3.7 % formaldehyde in PBS (250 µl/well), room temperature for 15 min. Cells were washed with PBS (500 µl/well, x3). Cells were blocked with 1 % bovine serum albumin (BSA) in PBS (500 µl/well), room temperature for 45 min, shaking. Blocking buffer was removed by aspiration and cells were incubated with mouse α-HA primary antibody (1:2000 in 1 % BSA in PBS, 200 µl/well) room temperature, 1 hour, shaking. Cells were washed with PBS (500 µl/well, x3). Cells were re-blocked with 1 % BSA in PBS (500 µl/well), room temperature for 15 min, shaking. Blocking buffer was removed by aspiration and cells were incubated with mouse α-mouse IgG peroxidase secondary antibody (1:2000 in 0.5 % BSA in PBS, 200 µl/well) room temperature, 1 hour, shaking. Cells were washed with PBS (500 µl/well, x3). SIGMAFAST™ OPD (o-Phenylenediamine dihydrochloride) substrate was prepared by adding 1 silver tablet and 1 gold tablet in 20 ml H_2O. Cover in foil until use. OPS was added to the cells (200 µl/well) and incubated in the dark for 5-30 min (until sufficient colour change has occurred). Following the incubation the plate was read immediately at 450 nm. The reaction can be stopped with the addition of 50 µl of 3 M HCl or 3 M H_2SO_4 solution per 200 µl of solution and read at 492 nm.

2.2.17 Experimental repeats

The number of experimental repeats is denoted by the N number. This refers to an experiment prepared on a separate day, using a new passage of cells and a fresh transfection. For practical reasons the cell stocks, the plasmid DNA and the transfection reagent remain consistent between experimental repeats.

2.2.18 Data analysis of cAMP FRET based signalling assay

Data from cAMP signalling were analysed by fitting a sigmoidal dose response curve to the WT CLR data. The minimum and maximum values were taken and used to

normalise the WT CLR and mutant receptor data to 0 % and 100 % respectively. A sigmoidal dose response curve was fitted to the normalised values, which produced pEC_{50} values for the WT CLR and mutant receptors and basal and E_{max} values of the mutant receptor compared to WT CLR. Experimental repeats were undertaken ($n \geq 3$) and pEC_{50}, basal and E_{max} values for each mutant were analysed using a paired t test to test for statistical significance.

2.2.19 Data analysis of the cell surface expression ELISA

Data from the cell surface expression ELISA were analysed by normalising the unactivated WT CLR and mutant receptor raw data to the basal and WT CLR maximum (minimum and maximum respectively). Experimental repeats were undertaken ($n \geq 3$) and WT CLR and mutant receptor cell surface expression values were analysed using a paired t test to test for statistical significance.

2.2.20 Data analysis of the internalisation ELISA

Data from the internalisation ELISA were analysed by normalising each WT CLR and mutant receptor data set to basal and the individual unactivated receptor maximum (minimum and maximum respectively). Experimental repeats were undertaken ($n \geq 3$) and the activated (internalised) WT CLR and mutant receptor cell surface expression values were analysed using a paired t test to test for statistical significance.

3 Alanine substitution analysis of the extracellular loop two domain of the CGRP receptor

3.1 Introduction

The extracellular loop 2 (ECL2) domain in all GPCR families is of structural and functional importance (Wheatley et al., 2012). This was first identified through chimeric receptor experiments and mutagenesis studies of this domain (Fitzpatrick & Vandlen, 1994; Olah *et al.*, 1994; Walker *et al.*, 1994). Even in receptors with known TM ligand binding pockets, the ECLs were implicated in early stage ligand binding and presentation to the TM binding site (Colson et al., 1998; Perlman et al., 1997). In other cases, effects of residues in ECL2 were speculated to be direct ligand binding due to a flexibility of the loop (Kim et al., 1996).

The unique properties of ECL2 were highlighted in the crystal structure of Rhodopsin (Figure 3.1) which discovered an antiparallel β-sheet structure formed by the loop and extended deep into the centre of the TM bundle (Palczewski et al., 2000). The role of ECL2 in this receptor was further understood using NMR spectroscopy that revealed an interaction between ECL2 and TM 5, 6 and 7 which constrained the receptor in the inactive state, until receptor activation resulted in movement of ECL2 and TM5 allowing an inward movement of TM6-ECL3-TM7 (Ahuja et al., 2009).

The high resolution structure of the human β2-adrenergic receptor (β2-AR) showed a more complex structure of ECL2 compared with the other ECLs (Figure 3.1) (Cherezov et al., 2007). In contrast with the structure of Rhodopsin, ECL2 of the β2-AR was exposed at the surface, contained an extra helical segment and an intra-loop disulphide bond as well as the familiar disulphide bond with TM3. The loop also made contacts with ECL1 and had a glycosylation site. These crystal structures highlighted the unique nature of ECL2 with respect to receptor function and show that it as an important domain to be investigated.

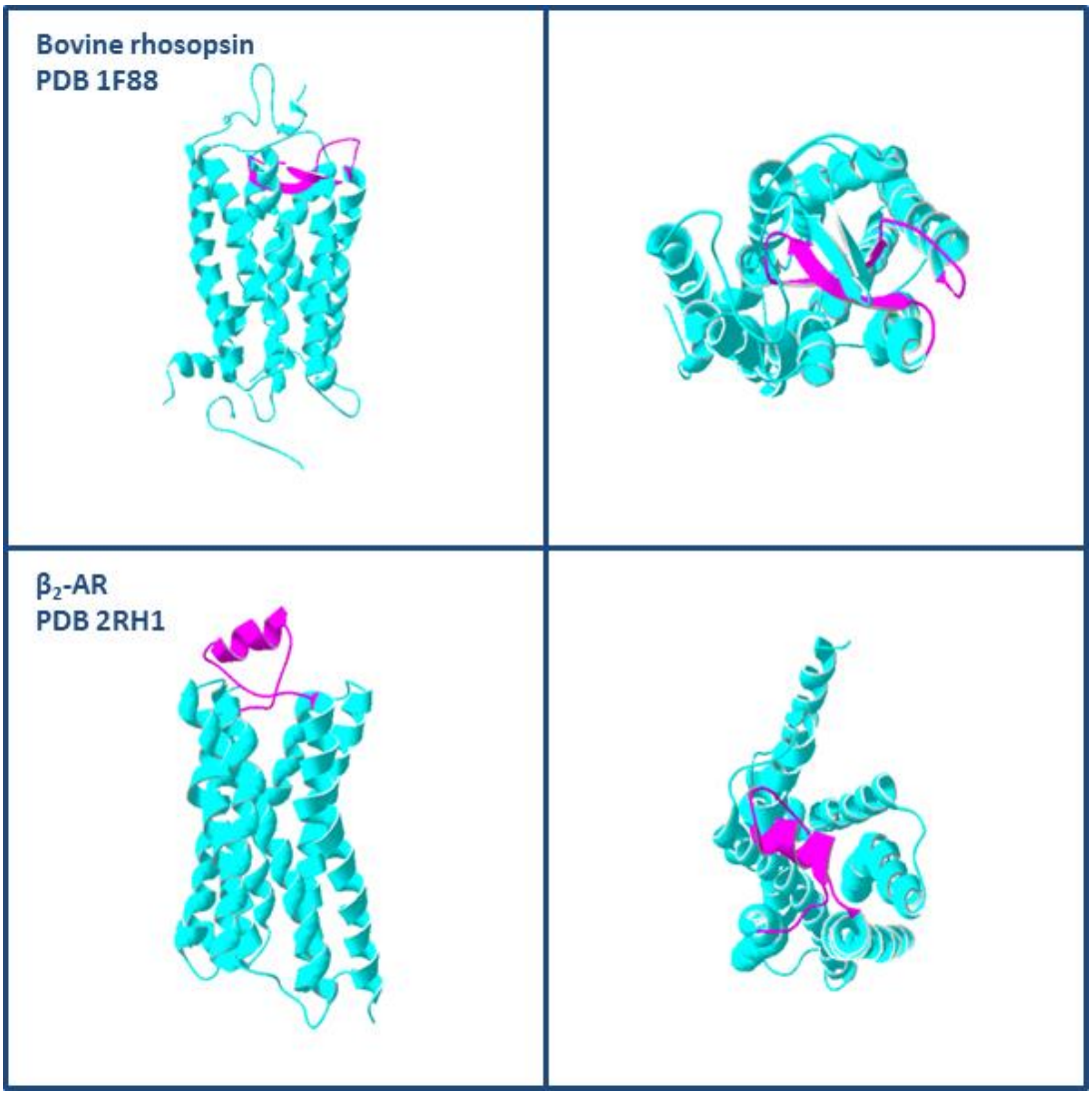

Figure 3.1. Crystal structures of the two archetypal family A GPCRs with the ECL2 domain highlighted.

Bovine rhodopsin (PDB 1F88) and the β_2-adrenergic receptor (PDB 2RH1). Each receptor is presented in two orientations. The GPCR unit is cyan, ECL2 is magenta. (Cherezov *et al.*, 2007; Palczewski *et al.*, 2000).

Following the crystal structure publication of the β2-AR, a number of other mammalian GPCR structures were published. A selection of these is presented in Figure 3.2 with the ECL2 domains highlighted. These structures reveal the high degree of variation in both the length and structure of ECL2 compared with the ECL1 and ECL3 domains which are much more restricted and uniform. However given this variation, there are features that are conserved between receptor subfamilies. The rhodopsin and sphingosine-1-phosphate 1 (S1P1) receptors both have ECL2 domains that occlude the ligand binding pocket indicating the route of entry for the hydrophobic ligands (Hanson *et al.*, 2012; Palczewski *et al.*, 2000). Water-soluble ligand GPCRs have an open ECL2 conformation however there are structural differences. Aminergic and adenosine receptors have an α-helix structure (Cherezov et al., 2007; Jaakola et al., 2008) whereas the peptide binding opioid and chemokine receptors have a β-sheet (Granier *et al.*, 2012; Manglik *et al.*, 2012; Park *et al.*, 2012; Wu *et al.*, 2010; Wu *et al.*, 2012).

In 2013, the first two family B GPCR structures were published (Hollenstein et al., 2013; Siu et al., 2013). These structures are presented in Figure 3.3 with the ECL2 domains highlighted. In comparison with the ECL2 domains of the family A GPCRs in Figure 3.1 and Figure 3.2, the structures of these loops are different again. Neither the corticotropin-releasing hormone receptor 1 (CRHR1) nor the glucagon receptor (GCGR) have the β-sheet or α-helix of Rhodopsin or β2-AR. Instead there is a loop structure for both receptors that extends from TM4 towards the middle of the TM bundle before twisting 90° to cover over the binding pocket and twisting back 90° to form TM5 which are more representative of the muscarinic and dopamine receptors (Chien et al., 2010; Haga et al., 2012; Kruse et al., 2012). Both structures are similar however the CRHR1 ECL2 domain is longer and more pronounced. Each structure confirms that the ECL2 cysteine forms a disulphide bond with the cysteine at the top of TM3, a feature conserved in most family A and family B GPCRs. In the GCGR structure, ECL2 begins at the F289, three residues to the C-terminus of the conserved basic residue at the start of ECL2. The loop is 12 residues and ends at N300. In CRHR1 ECL2 begins at Y253, three residues to the C-terminus of the conserved basic residue. ECL2 is longer than GCGR (17 residues) and ends at D269.

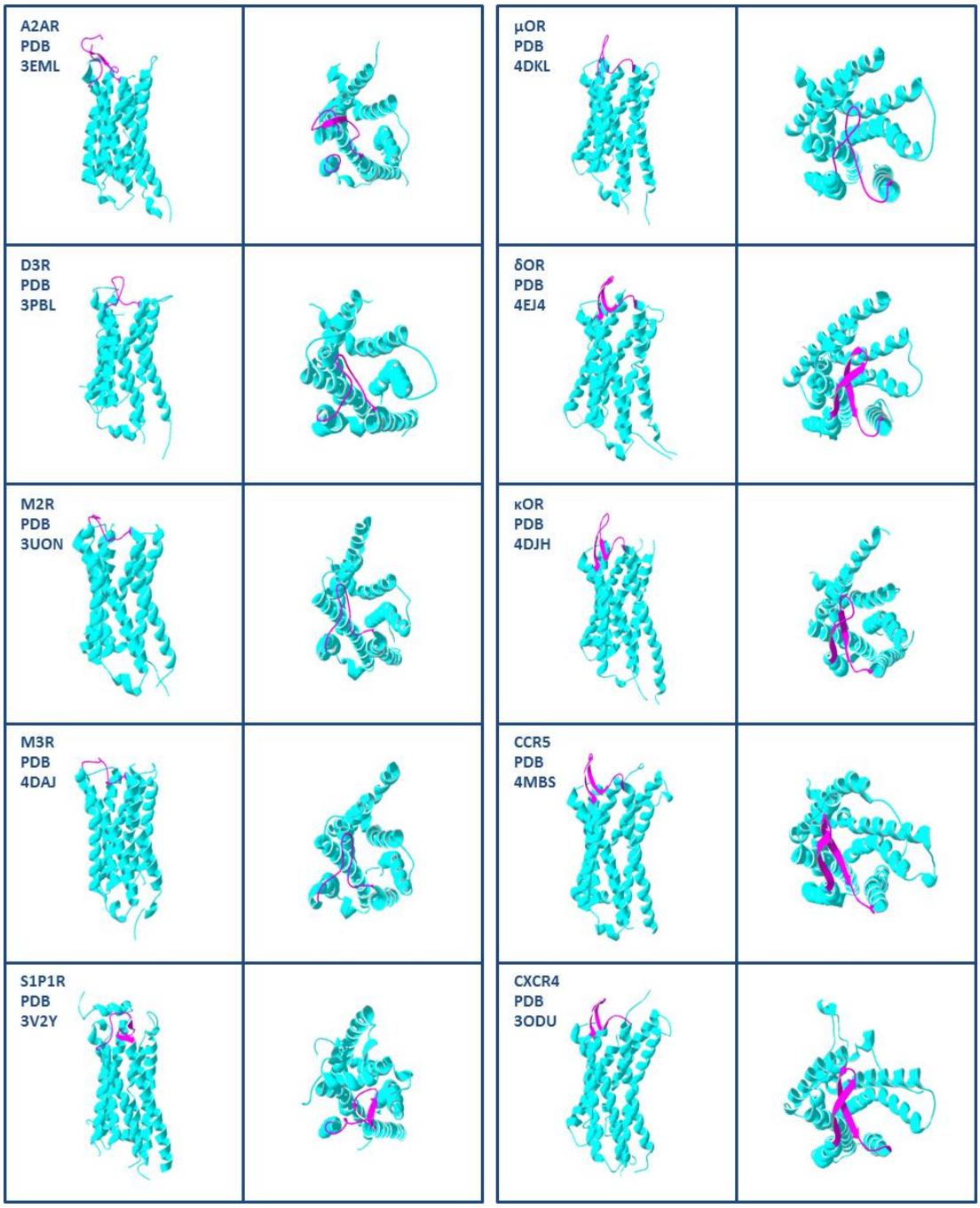

Figure 3.2. Crystal structures of selected GPCRS with the ECL2 domain highlighted.
Each receptor is presented in two different orientations. The GPCR unit is cyan, ECL2 is magenta. Human A2A Adenosine Receptor (A2AR) Bound to an antagonist, human dopamine d3 receptor (D3R) in complex with a d2/d3 selective antagonist, human M2 muscarinic acetylcholine receptor (M2R) bound to an antagonist, rat M3 muscarinic acetylcholine receptor (M3R) in complex with antagonist, human sphingosine 1-phosphate 1 receptor (S1P1R) complex with antagonist, mouse μ -opioid receptor (μ-OR) bound to a morphinan antagonist, mouse δ opioid receptor (δ-OR) bound to antagonist, human κ-opioid receptor (κOR) bound with antagonist, human CCR5 chemokine receptor bound to antagonist, human CXCR4 chemokine GPCR bound with antagonist.

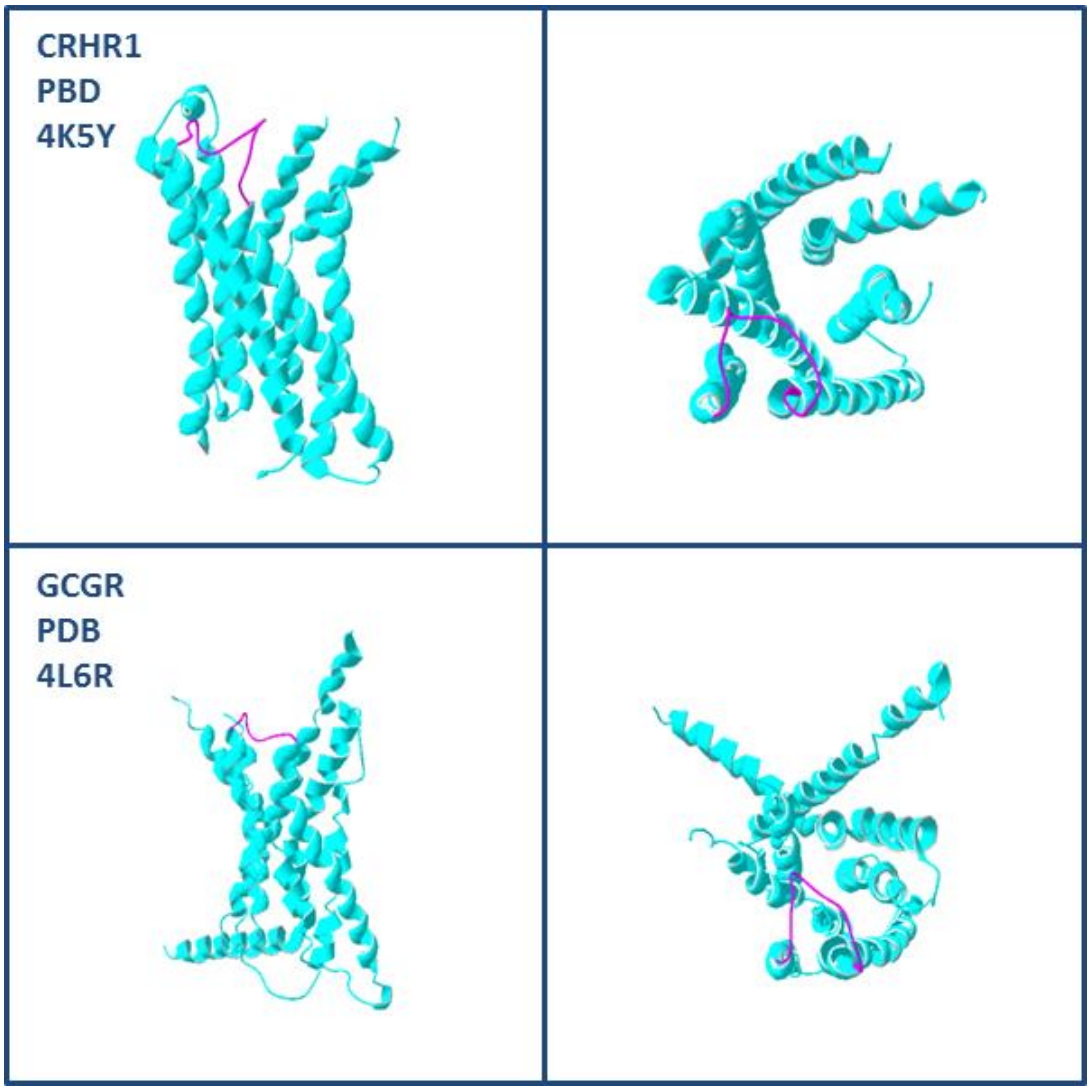

Figure 3.3. Crystal structures of the two family B GPCRs with the ECL2 domain highlighted. Corticotropin releasing hormone receptor 1 (CRH1R, PDB 4K5Y) and the Glucagon receptor (GCGR, PDB 4L6R). Each receptor is presented in two orientations. The GPCR unit is cyan, ECL2 is magenta (Hollenstein *et al.*, 2013; Siu *et al.*, 2013).

Crystal structures have been vital in gaining understanding into receptor structure and conformations, interactions with both ligands and downstream signalling partners and possible mechanisms of activation. However they are limited in that they only provide a snapshot of one particular receptor conformation at a single moment in time. GPCR signalling is a dynamic and complex process. Different ligands stabilise different receptor conformations, activating certain signalling pathways and inhibiting others. Signalling can even occur through non G protein-mediated pathways, for example using β-arrestin to activate MAPK signalling (Azzi et al., 2003). There are cases where one ligand may act as an agonist for one signalling pathway and an antagonist or inverse antagonist for another (Baker *et al.*, 2003; MacKinnon *et al.*, 2009; Rajagopal *et al.*, 2013).

This fluidity in receptor conformation and signalling means it is important to do more than just study the receptor through static observations. Biochemical and biophysical analysis together with computer modelling has been essential in complementing and refining the information from the crystal structures. Various methods have been employed to study receptor function. Site directed mutagenesis and chimeric proteins have identified key domains and residues of ECL2 that have functional importance (Bergwitz *et al.*, 1996; Conner *et al.*, 2007b; Runge *et al.*, 2003).

The scanning cysteine accessibility method (SCAM) introduces cysteine mutations into the receptor and uses their reactivity to cysteine reagents to determine their exposure to the aqueous environment (Javitch et al., 2002). Disulphide trapping experiments have been used to study ligand-receptor proximities for family B GPCRs. This technique introduces cysteine residues into the ligand and the extracellular parts of the receptor and tests the ability of these mutants to form disulphide bonds. This provides insight into those ligand-receptor residues that are in close proximity to each other (Dong et al., 2012; Monaghan et al., 2008). Zn^{2+} cross linking of endogenous and introduced histidine residues has also been used to determine the proximity of receptor domains and motifs (Elling & Schwartz, 1996). Ligand receptor contact can also be investigated using photoaffinity cross linking (Assil-Kishawi & Abou-Samra, 2002; Dong *et al.*, 2004; Kraetke *et al.*, 2005).

The first complete alanine scan of the ECL2 domain was of the family A V1A Vasopressin receptor (Conner *et al.*, 2007b). This study identified key aromatic residues located throughout the loop that were required for ligand binding and intracellular signalling. An alanine scan of the cannabinoid receptor 1 (CB1) ECL2 domain identified residues in the N-terminus of the loop important for cell surface expression (Ahn et al., 2009). Residues in the C-terminus were important for agonist binding but not inverse agonist binding.

SCAM was used to investigate the ECL2 domain of the angiotensin II type 1 receptor in different receptor states (Unal et al., 2010). In the unliganded receptor a segment either side of the conserved disulphide bond was available suggesting an open conformation. Upon binding to an agonist or inverse agonist, ECL2 acted like a lid albeit in different conformations. ECL2 was involved in slowing down the rate of dissociation of ligands but also adopted different conformations according to the functional state of the receptor. This dynamic effect of ECL2 was also observed with the M2mAChR, where a reduction of loop flexibility caused by the addition of a disulphide bond between ECL2 and TM7 reduced the ligand binding affinity (Avlani et al., 2007).

ECL2 has also been proposed as a site for allosteric enhancement of agonist signalling (Kennedy et al., 2014; Peeters et al., 2012). In the M2 crystal structure bound to the positive allosteric modulator LY2119620, the allosteric side was situated above the orthosteric binding pocket and involved interactions with the ECLs. ECL2 interactions were hydrogen bonding with E172 and stacking interactions with Y177 (Kruse et al., 2013). This domain has not just been implicated in the activation process; constitutive activity resulting from mutagenesis has led to speculation that this domain may constrain the receptor in its inactive state through interactions with the TM domain (Klco et al., 2005). In the melanocortin receptor, ECL2 is much shorter and does not interact with the TM core, leading to a higher constitutive activity (Holst & Schwartz, 2003).

The importance of ECL2 in family B GPCRs has been shown with ECL2 alanine scans of both the glucagon-like peptide-1 receptor (GLP1R) and CRHR1 (Gkountelias *et al.*, 2009; Koole *et al.*, 2012). In particular the alanine scan of the GLP1R revealed that

more than half of the 23 residues of ECL2 investigated had a significant reduction in cAMP pEC_{50} values upon stimulation with the high affinity agonist GLP-1(7-36)NH2. A large number had involvement in ligand binding affinity and the initiation of other signalling cascades. The GCGR crystal structure publication included results from mutagenesis which revealed a number of positions within the ECL2 domain that are important for receptor signalling (Siu et al., 2013).

Cross-linking experiments identified contact sites between the CRH1R and radiolabelled sauvagine (Assil-Kishawi & Abou-Samra, 2002). Disuccinimidyl suberate (DSS) was used to form cross links between ε amino groups of lysine residues that have a molecular distance of 11.4 Å. This technique revealed that K257 in the ECL2 domain is in close proximity to K16 of the ligand sauvagine.

The predicted ECL sequences of each family B GPCR have been aligned in Figure 3.4. The full protein sequence for each GPCR was aligned and the ECLs were assigned according to the predicted sequence from the Uniprot database. Identical and similar residues have been identified. With the exception of the PTH receptors, ECL1 and ECL2 are of similar length across the family (~20 amino acids) and ECL3 is shorter (~10 amino acids). There is also very little sequence homology in each ECL across the family. In ECL1 there is only the conserved cysteine found at the top of TM3. Following this cysteine is always a basic residue. At the start of ECL1 is a conserved hydrophobic residue. ECL2 has the most conserved residues with a cysteine, tryptophan (CW) motif located in the middle of the loop. There is also a conserved carboxylic acid or carboxamide amino acid positioned 3 residues before the cysteine. At the start of the loop is a conserved basic residue. There is no conservation in ECL3. What is apparent, comparing these predicted loop regions with the ECLs in the GCGR and CRHR1 crystal structure is the variability between predicted domains and observed domains.

The primary sequences of the calcitonin family of ligands have been aligned in Figure 3.5. The level of amino acid conservation between ligands that activate the same receptor is surprisingly low. The current understanding in family B activation is that the C-terminus of the peptide ligand has affinity for the extracellular N-terminus of the receptor which allows the presentation of the N-terminal domain to

ECL1

```
hCLR          HLTAVA----------------------NNQALVATNPVSCK 213
hCTR          HLVEVV----------------------PNGELVRRDPVSCK 236
hCRHR1        FVVQLT----------------------MSPEVHQSNVGWCR 218
hCRHR2        FLLQL-----------------------VDHEVHESNEVWCR 185
hGHRHR        KDAALF------------------HSDDTDHCS---FSTVLCK 203
hGIPR         RDRLLP------------RPGPYLG-DQALALWN--QALAACR 217
hGLP1R        KDAALKW-----------MYSTAAQQHQWDGLLS-YQDSLSCR 227
hGLP2R        KDVVFYN-----------SYSKRPDNENGWMSYLS-EMSTSCR 261
hGLR          IDGLLRT-----------RYSQKIGDDLSVSTWLSDGAVAGCR 225
hPACR         KDWILY------------------AEQDSNHC---FISTVECK 227
hPTH1R        KDAVLYSGATLDEAERLTEEELRAIAQAPPPPATAAAGYAGCR 282
hPTH2R        KDRVVHAHIGVKELESLIMQDD--PQNSIEATSVDKSQYIGCK 237
hSCTR         KDAVLF------------------SSDDVTYCD---AHRAGCK 216
hVIPR1        KDLALF------------------DSGESDQCS---EGSVGCK 216
hVIPR2        KDDVLY------------------SSSGTLHCPDQPSSWVGCK 203
                  .                                    *:
```

ECL2

```
hCLR          RSLYYNDNCWIS--SDTH 289
hCTR          RAVYFNDNCWLS--VETH 312
hCRHR1        KLYYDNEKCWFGKRPGVY 296
hCRHR2        KLYYENEQCWFGKEPGDL 263
hGHRHR        KLAFEDIACWDL-DDTSP 280
hGIPR         RYLYENTQCWER-NEVKA 294
hGLP1R        KYLYEDEGCWTR-NSNMN 304
hGLP2R        RAHLENTGCWTT-NGNKK 338
hGLR          KCLFENVQCWTS-NDNMG 302
hPACR         RLYFDDTGCWDM-NDSTA 304
hPTH1R        RATLANTGCWDL-SS-GN 358
hPTH2R        RATLADARCWEL-SA-GD 313
hSCTR         RHFLEDVGCWDI-NANAS 293
hVIPR1        RIHFEDYGCWDT-IN-SS 292
hVIPR2        RLYLEDTGCWDT-NDHSV 279
              :    :  **
```

ECL3

```
hCLR          RP---EGKIAEEVYD 366
hCTR          RP---SNKMLGKIYD 389
hCRHR1        NPG--EDEVSRVVFI 374
hCRHR2        NPG--EDDLSQIMFI 341
hGHRHR        L----PDNAGLGIRL 358
hGIPR         VTEEQARGALRFAKL 374
hGLP1R        VMDEHARGTLRFIKL 384
hGLP2R        ITDDQVEGFAKLIRL 418
hGLR          VTDEHAQGTLRSAKL 382
hPACR         S----PENVSKRERL 382
hPTH1R        TPYTEVSGTLWQVQM 441
hPTH2R        LPHS-FTGLGWEIRM 395
hSCTR         S----PEDA-MEIQL 370
hVIPR1        F----PDNFKPEVKM 370
hVIPR2        F----PISISSKYQI 357
```

Figure 3.4. Sequence alignment of family B ECLs as determined by the Uniprot database.
* indicates positions that have a fully conserved residue. : indicates conservation between groups of strongly similar properties. . indicates conservation between groups of weakly similar properties. The online EMBL-EBI multiple sequence analyser was used to analyse the family B sequences.

```
Calcitonin family
αCGRP             --------------ACDTATCVTHRLAGLLSRSGGVVKN-NFVPTNV-GSKAF
βCGRP             --------------ACNTATCVTHRLAGLLSRSGGMVKS-NFVPTNV-GSKAF
CT                --------------CGNLSTCMLGTYTQDFNKFH-------TFPQTAIGVGAP
Amylin            --------------KCNTATCATQRLANFLVHSSNNFGA-ILSSTNV-GSNTY
ADM               YRQSMNNFQGLRSFGCRFGTCTVQKLAHQIYQFTDKD-KDNVAPRSKISPQGY
ADM2              ------TQAQLLRVGCVLGTCQVQNLSHRLWQLMGPAGRQDSAPVDPSSPHSY
                                  .**     :  : :                .

CLR peptides
CGRP1             --------------ACDTATCVTHRLAGLLSRSGGVV-KNNFVPTNVGSK-AF
CGRP2             --------------ACNTATCVTHRLAGLLSRSGGMV-KSNFVPTNVGSK-AF
ADM               YRQSMNNFQGLRSFGCRFGTCTVQKLAHQIYQFTDKD-KDNVAPRSKISPQGY
ADM2              ------TQAQLLRVGCVLGTCQVQNLSHRLWQLMGPAGRQDSAPVDPSSPHSY
                                .*  .** .:.*:  : :      :.: .* .  *  .:


CTR peptides
CT                -CGNLSTCMLGTYTQDFNKFHTFPQTAI-------GVGAP--
Amylin            KCNT-ATCAT----QRLANFLVHSSNNFGAILSSTNVGSNTY
                   * . :**      * : :* .. .. :        **:
```

Figure 3.5. Sequence alignment of the calcitonin family peptides.

The online EMBL-EBI multiple sequence analyser was used to analyse all the family B GPCR sequences together and family B subfamilies separately. * indicate positions which have a fully conserved residue. : indicates conservation between groups of strongly similar properties. . indicates conservation between groups of weakly similar properties.

a ligand binding pocket created by the ECLs and TM bundle facilitating the activation of the receptor (Hoare, 2005). Following this mechanism, variation in the C-terminal sequence of the peptide would explain variations in affinity between the ligands and their receptors. However it would be expected that activation through a shared ligand binding pocket would require a similar set of amino acids between ligands.

The ECL1 and ECL3 domains of CLR have been studied using alanine substitution analysis (Barwell et al., 2011). This study showed that a hydrophobic cluster of residues at the top of TM2 (L195, V198 and A199) were involved in CGRP-binding and cAMP production. Within ECL1, cAMP pEC_{50} signalling was enhanced through A203L and A206L substitutions. In TM3, H219, L220 and L222 were shown to be important. Investigation of ECL3 identified a role for I260 in receptor activation with a predicted proximity to ECL2. L351 and E357 in TM6 are important for cell surface expression.

The ECL2 domain of CLR has yet to be investigated. It is likely that this domain is important as suggested by the structures obtained for both family A and B GPCRs and the key involvement in receptor function in the alanine scans of this loop in other receptors. This makes determining the role of ECL2 of CLR a priority for understanding how this receptor functions. The purpose of this chapter is to investigate the structure and function of the CLR ECL2 domain through the effect of alanine substitution mutagenesis on cellular expression and CGRP-mediated receptor signalling, internalisation and binding.

3.2 Methods

The general methods used are described in section 2. Method details that are specific to the work in this chapter will be described in this section.

3.2.1 Mutagenesis to create alanine-substitution mutants

The individual alanine substitutions of ECL2 were created using the primers described in Table 2.1 and an N-terminal HA tagged hCLR construct in the mammalian expression vector pcDNA3.1- as a template, following the QuikChange site directed mutagenesis protocol (2.2.3). Following DpnI degradation of the template DNA, the product was transformed into chemically competent Top10 *E.coli* cells (2.2.10). Colonies were picked and grown in 3-5 ml Lbroth + 100 µg/µl ampicillin at 37 °C, 220 rpm for 16 hours and the amplified plasmid DNA was purified using a Wizard® Plus SV Miniprep kit (Promega) (2.2.11). The purified DNA was electrophoresed alongside a pre-DpnI treated sample (2.2.7) to confirm successful degradation of the template DNA and was sent for sequencing (2.2.12) to confirm successful mutagenesis.

3.2.2 cAMP signalling of alanine substitutions

Cos7 cells were co-transfected with either WT CLR or the alanine-substitution CLR together with RAMP1. Transfected cells were dose dependently stimulated with CGRP across a concentration range of 10^{-12} to 10^{-6}M. Assay buffer was used as a basal stimulation. A sigmoidal dose response curve was fitted to the raw data, which were normalised to WT CLR using the minimum and maximum values obtained from the fitted curve. In deciding which values would be most appropriate to represent the WT CLR basal and E_{max} data points (allowing comparison between WT CLR and alanine-substitution CLR), the minimum and maximum values of the curve represented a consistent average of these points across experimental repeats. The alternative for the basal point was to take the individual cAMP value at the basal concentration. The alternative for E_{max} was to take either the highest cAMP data point or the cAMP produced with 10^{-6}M CGRP (the highest assay CGRP concentration). Using average values from the fitted curve minimised the error

from potentially erroneous single data points and allowed consistency with data analysis across experimental repeats. Alanine-substitution CLR data were normalised to WT CLR and a sigmoidal curve was fitted to the normalised data. Minimum, maximum and pEC_{50} values were taken from the fitted curve.

3.2.3 Radioligand binding experiments

The radioligand binding experiments described in section 3.3.5 were carried out by Professor David Poyner at Aston University as part of a continued collaboration. This was for practical reasons as the radioactivity lab at Aston University is set up for radiolabelled CGRP work.

3.3 Results

3.3.1 Identification of ECL2

The ECL2 domain of CLR was originally predicted (from SwissProt) to start from arginine at position 274 and extend to the threonine at position 288. In discussions with collaborators at Aston University, who have previously combined mutagenesis and computer modelling to study ECL1 and ECL3 of the CGRP receptor (Barwell et al., 2011), it was decided that the TM-ECL2 boundary was an important feature of ECL2 to be included in the study. The first part of this investigation was to create single alanine substitutions of all the residues of ECL2 including the predicted N- and C-terminal extensions of the loop.

Alanine was chosen as an appropriate substitution due to the relatively inert properties of its methyl side chain. This removed the properties of the wild type (WT) side chain without creating amino acid deletions of the loop. Glycine was considered as an alternative possibility however its hydrogen atom side chain can introduce flexibility to the secondary structures it comprises. This property can result in hinge-like conformations in proteins. It was therefore decided for this study that alanine would be the most suitable amino acid replacement. In the event that the WT residue was an alanine, leucine was chosen as an alternative substitution. Leucine has a short branched hydrophobic extension to the methyl side chain of alanine creating a different steric effect without the disruption being too extreme. Leucine was therefore considered an appropriate conservative mutation of alanine.

3.3.2 Selecting receptor activation assays

Upon agonist binding, the ECL2 domain of the CGRP receptor is predicted to form intermolecular interactions with the CGRP peptide and/or intramolecular interactions within the receptor stabilising the active receptor conformation and initiating the downstream signalling process through the coupled G protein. Following receptor activation the C-terminus of CLR is phosphorylated by GRKs leading to the recruitment of β-arrestin and the subsequent de-activation and

internalisation of the receptor (Conner et al., 2008; Cottrell et al., 2007; Padilla et al., 2007). Signalling assays are a reliable and accurate method of measuring receptor activation. Commercially available assays can detect second messengers (such as cAMP or Ca^{2+}) or are sensitive reporter assays that can monitor activity of response elements or target genes. The Perkin-Elmer Lance® cAMP detection kit offers high performance and robust detection of cell based cAMP and was therefore chosen to measure receptor-mediated cAMP production. To ensure that the receptor is successfully expressed at the cell surface and that any observed change in cAMP production is not because of an alteration in cell surface expression levels, an ELISA was used which detected the HA tag fused to the extracellular N-terminus of CLR. In a study manipulating extracellular domains of a receptor, any changes in cAMP levels are likely to be due to ligand-receptor interactions and a reduction in receptor signaling may correlate with a loss of ligand binding. Binding affinities of key mutants were determined using radioligand binding experiments. The final part of receptor activation is the attenuation of signaling and the subsequent internalisation, leading to the recycling of the receptor back to the cell surface or degradation. Receptor internalisation following CGRP stimulation can be quantified using the cell surface expression ELISA.

3.3.3 cAMP signalling of alanine substitutions

The effect of alanine substitution on receptor activation at each individual position of ECL2 from A271 to I294 was measured using a TR-FRET-based cAMP assay to measure levels of the second messenger cAMP signalling.

The results are summarised in Table 3.1 and a representative cAMP signalling curve for each alanine substitution is presented in Figure 3.6 to Figure 3.9. These results will be described separately according to the pEC_{50}, basal and E_{max} values to allow each component of the receptor signalling data to be clearly presented.

3.3.3.1 pEC_{50} values

The pEC_{50} values from the data set in Table 3.1 shows the pEC_{50} mean and SEM for the alanine-substitution and WT CLR and separates substitution mutants with a significant reduction compared to WT according to the level of disruption (<10 fold,

ECL2 substitution	pEC_{50} (alanine) Mean	SEM	N	pEC_{50} (WT CLR) Mean	SEM	N	pEC_{50} difference	t-test	Basal (alanine) Mean	SEM	N	t-test	E_{max} (alanine) Mean	SEM	N	t-test
A271L	-10.21	0.61	3	-10.20	0.59	3	0.01	0.8891	7.37	6.74	3	0.3885	107.80	2.19	3	0.0709
I272A	-10.21	0.58	3	-10.20	0.59	3	0.01	0.86	-1.09	5.02	3	0.85	105.30	3.39	3	0.26
A273L	-9.99	0.25	3	-10.46	0.33	3	-0.47	0.034*	4.63	2.13	3	0.16	104.10	5.66	3	0.54
R274A	-8.00	0.24	3	-10.18	0.34	3	-2.18	0.0054**	-0.15	3.96	3	0.9731	99.35	3.17	3	0.8574
S275A	-8.66	0.11	3	-8.81	0.19	3	-0.16	0.36	3.86	4.86	3	0.51	91.27	8.96	3	0.43
L276A	-8.70	0.19	3	-8.81	0.19	3	-0.12	0.05	8.06	3.25	3	0.13	106.50	7.29	3	0.46
Y277A	-8.90	0.49	4	-9.79	0.38	4	-0.89	0.0121*	-4.29	4.52	4	0.4129	96.46	7.63	4	0.6746
Y278A	-8.75	0.08	5	-9.83	0.16	5	-1.08	0.006**	-0.91	7.54	5	0.91	93.48	12.01	5	0.62
N279A	-9.65	0.27	4	-9.85	0.19	4	-0.20	0.23	-1.23	6.14	4	0.85	93.49	3.20	4	0.13
D280A	-8.01	0.13	3	-9.90	0.04	3	-1.90	0.0067**	9.73	2.58	3	0.064	103.40	5.97	3	0.062
N281A	-9.93	0.29	5	-9.84	0.26	5	0.10	0.5182	10.67	1.01	5	0.0005***	112.50	4.07	5	0.0374*
C282A	-9.58	0.06	3	-10.71	0.13	3	-1.13	0.0119*	9.64	9.26	3	0.4072	104.00	3.26	3	0.345
W283A	-8.17	0.04	3	-10.71	0.13	3	-2.54	0.0042**	6.27	7.32	3	0.4818	105.50	3.11	3	0.2189
I284A	-7.70	0.10	3	-8.81	0.18	3	-1.11	0.012*	14.92	8.28	3	0.214	114.70	9.63	3	0.267
S285A	-9.41	0.27	5	-10.11	0.19	5	-0.70	0.018*	15.20	4.55	5	0.023*	93.40	6.56	5	0.037*
S286A	-8.98	0.17	3	-8.91	0.24	3	0.07	0.63	8.42	8.74	3	0.437	104.20	9.62	3	0.702
D287A	-8.58	0.56	4	-9.30	0.42	4	-0.71	0.0475*	14.41	7.98	4	0.1689	119.00	5.43	4	0.0394*
T288A	-8.46	0.28	4	-9.85	0.35	4	-1.39	0.0021**	17.44	5.17	4	0.043*	116.10	3.86	4	0.025*
H289A	-9.82	0.10	3	-9.85	0.26	3	-0.03	0.86	8.45	12.96	3	0.58	106.90	15.86	3	0.71
L290A	-9.72	0.17	3	-10.58	0.19	3	-0.86	0.019*	5.35	7.83	3	0.57	105.10	1.75	3	0.1
L291A	-9.93	0.23	3	-10.58	0.19	3	-0.65	0.013*	12.50	5.44	3	0.15	105.90	1.76	3	0.078
Y292A	-9.60	0.48	4	-10.07	0.36	4	-0.47	0.0347*	17.04	7.50	4	0.1075	110.50	0.75	4	0.0008***
I293A	-10.34	0.22	3	-10.58	0.19	3	-0.24	0.13	10.53	8.97	3	0.36	109.10	3.85	3	0.14
I294A	-10.94	0.26	4	-10.56	0.13	4	0.38	0.0679	22.75	2.84	4	0.004**	110.80	1.83	4	0.0098**

Reduced pEC_{50}(>10 fold)/basal/E_{max} value Reduced pEC_{50}(<10 fold) Increased pEC_{50}/basal/E_{max} value

Table 3.1. Summary of the pEC_{50}, basal and E_{max} mean and SEM values for the ECL2 individual alanine substitutions and the WT receptor.

Cos7 cells transfected with WT and alanine substitution receptor were dose dependently stimulated with CGRP and levels of the cAMP second messenger were detected using a TR-FRET based cAMP assay. A sigmoidal dose response curve was fitted to the data using GraphPad Prism software. The alanine substitution data were normalised to WT, taking the maximum and minimum values obtained from the WT dose response curve. The number of experimental repeats is denoted in the N column and the significance was obtained through paired t-test. *p < 0.05, ** p < 0.01, ***p <0.001.

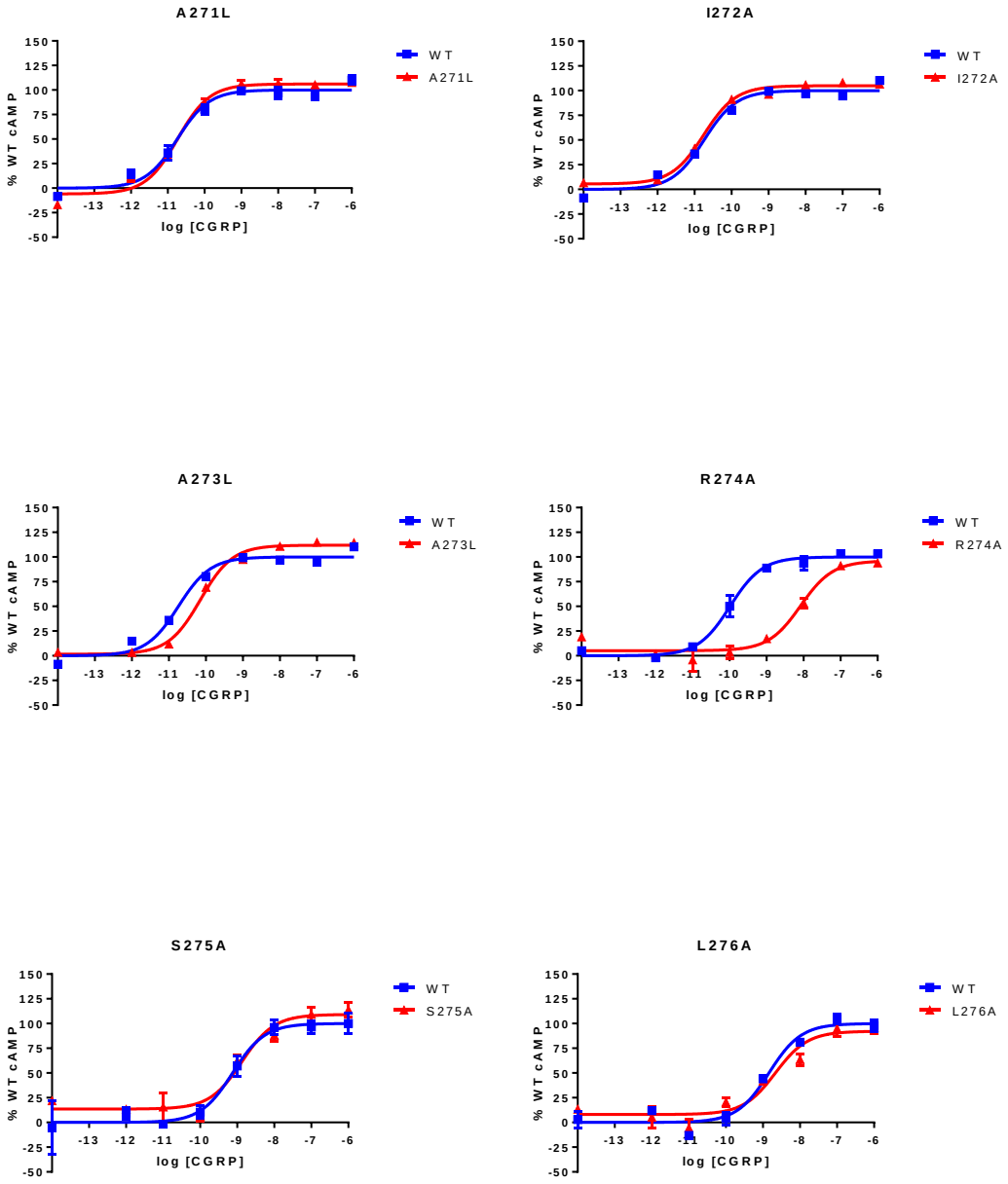

Figure 3.6. Representative cAMP signalling curves for A271L. I272A, A273L, R274A, S275A and L276A substitutions.

Cos7 cells transfected with WT and alanine substitution receptor were dose dependently stimulated with CGRP and levels of the cAMP second messenger were detected using a TR-FRET based cAMP assay. A sigmoidal dose response curve was fitted to the data using GraphPad Prism software. The alanine substitution data were normalised to WT, taking the maximum and minimum values obtained from the WT dose response curve.

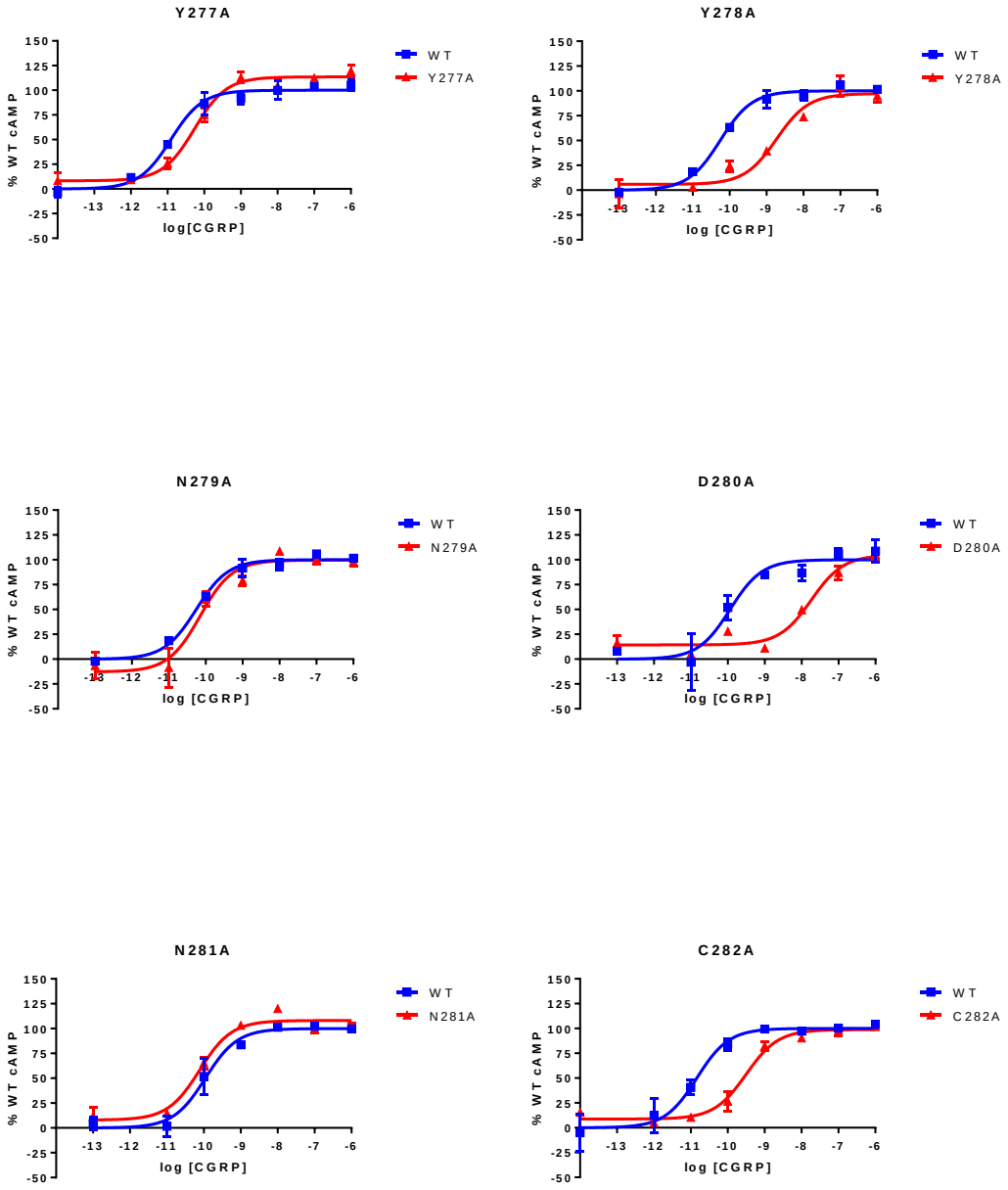

Figure 3.7. Representative cAMP signalling curves produced for Y277A, Y278A, N279A, D280A, N281 and C282A substitutions.

Cos7 cells transfected with WT and alanine substitution receptor were dose dependently stimulated with CGRP and levels of the cAMP second messenger were detected using a TR-FRET based cAMP assay. A sigmoidal dose response curve was fitted to the data using GraphPad Prism software. The alanine substitution data were normalised to WT, taking the maximum and minimum values obtained from the WT dose response curve.

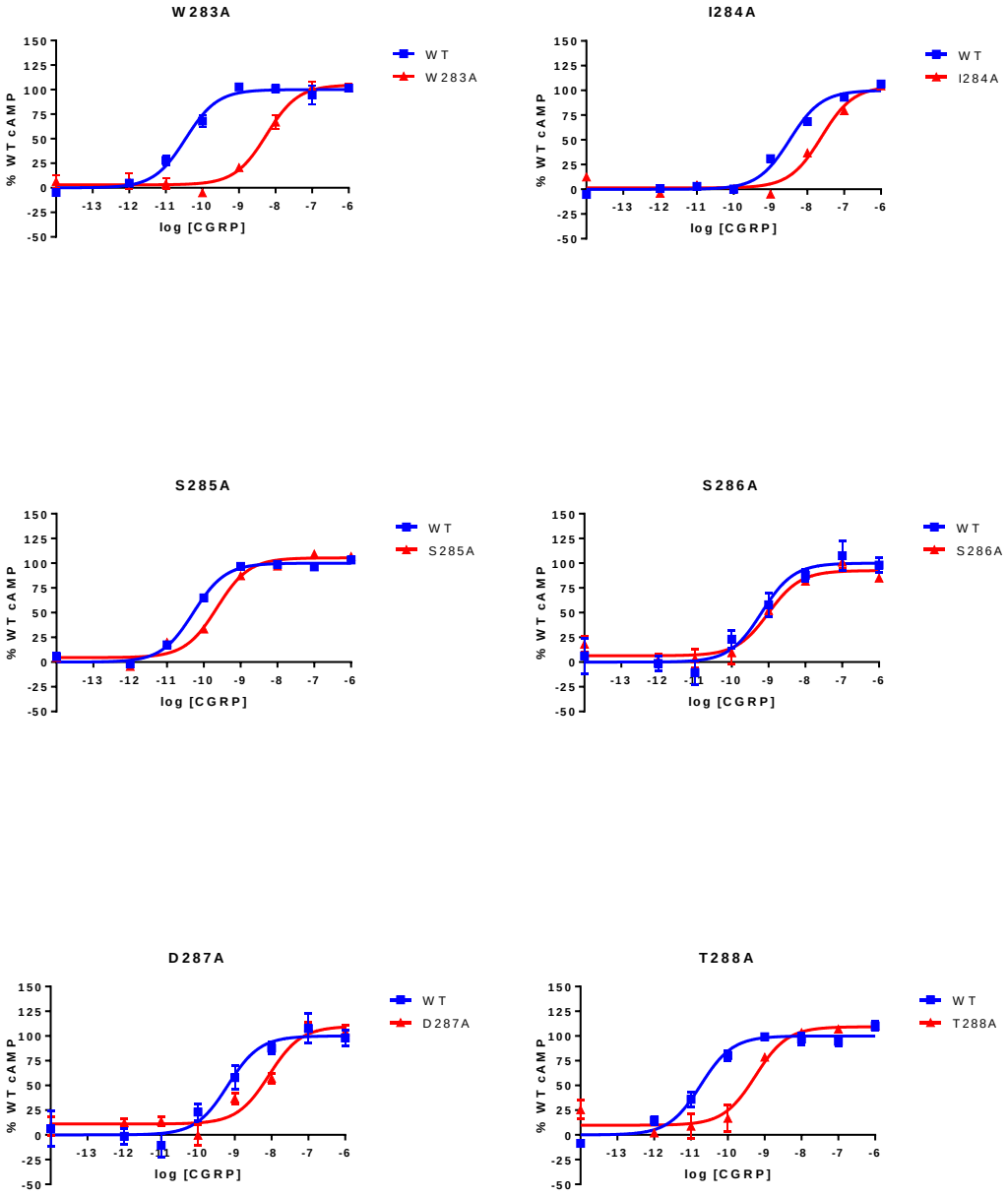

Figure 3.8. Representative cAMP signalling curves for W283A, I284A, S285A, S286A, D287A and T288A substitutions.

Cos7 cells transfected with WT and alanine substitution receptor were dose dependently stimulated with CGRP and levels of the cAMP second messenger were detected using a TR-FRET based cAMP assay. A sigmoidal dose response curve was fitted to the data using GraphPad Prism software. The alanine substitution data were normalised to WT, taking the maximum and minimum values obtained from the WT dose response curve.

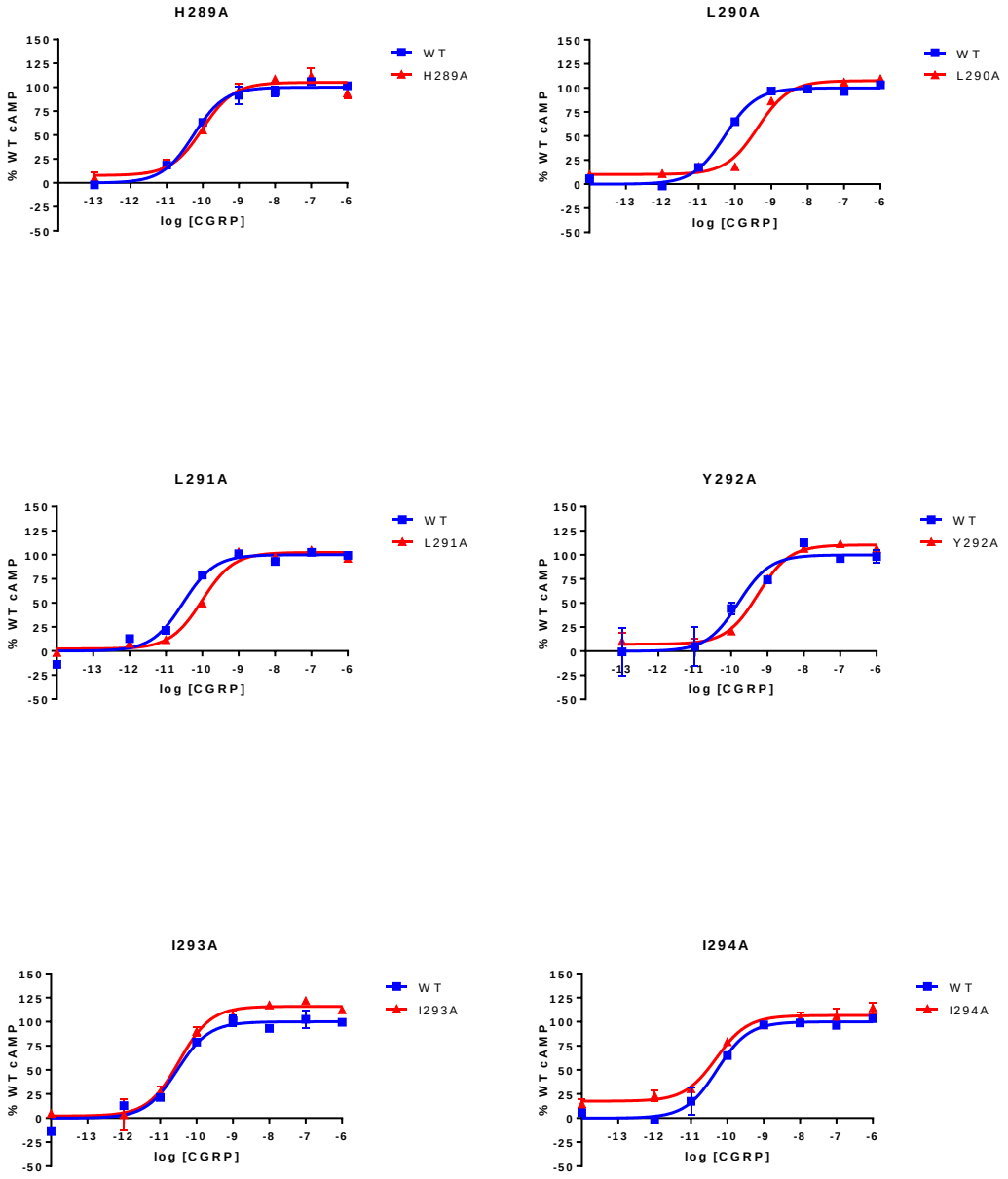

Figure 3.9. Representative cAMP signalling curves for H289A, L290A, L291A, Y292A, I293A and I294A substitutions.

Cos7 cells transfected with WT and alanine substitution receptor were dose dependently stimulated with CGRP and levels of the cAMP second messenger were detected using a TR-FRET based cAMP assay. A sigmoidal dose response curve was fitted to the data using GraphPad Prism software. The alanine substitution data were normalised to WT, taking the maximum and minimum values obtained from the WT dose response curve.

>10 fold). The mean and SEM of the log difference between the substitution mutant pEC_{50} and the WT pEC_{50} values are summarised graphically in Figure 3.10. 14 out of the 24 amino acids of ECL2 had a significant reduction in pEC_{50} value compared with WT. Of these, seven have a greater than 10 fold reduction in pEC_{50} value compared with WT (R274A, Y278A, D280A, C282A, W283A, I284A and T288A) with the remainder having a less than 10 fold reduction (A273L, Y277A, S285A, D287A, L290A, L291A, Y292A).

What is clear from the results is the extent to which the entire loop is involved in receptor activation. Between A273L and Y292A, only six out of the 20 residues (S275A, L276A, N279A, N281A, S286A and H289A) have no significant reduction in receptor signalling. However, with the exception of R274A (with ~100 fold reduction in pEC_{50}) the remaining 6 substitutions with a greater than 10 fold reduction in cAMP signalling (Y278A, D280A, C282A, W283A, I284A and T288A) are located within the middle of the loop. The greatest reductions have occurred with substitutions D280A (~100 fold) and W283A (~300 fold). T288A has a more modest reduction of ~20 fold with the remaining substitutions much closer to a 10 fold reduction in signalling. Alanine substitutions resulting in a less than 10 fold reduction in pEC_{50} are distributed throughout the loop. This includes the most N-terminal residue of ECL2 to have a significant reduction in signalling (A273L, ~3fold). Three residues are located in the middle of the loop (Y277A, S285A and D287A) with a pEC_{50} reduction of between 5-10 fold. There is a cluster of three amino acids at the C-terminus of the loop that each had a small but significant reduction in signalling (L290A, L291A and Y292A).

C282 is predicted to form a disulphide bond with C212 at the top of TM3. To further investigate the reduction in cAMP signalling observed with the ECL2 C282A substitution, the TM3 cysteine was substituted to alanine (C212A) and a double alanine substitution was made (C212A/C282A). The single alanine substitution C212A had a similar reduction in cAMP signalling to that of C282A (pEC_{50} values: WT 9.62+0.76, C212A 8.10+0.43, $n = 3$, $p < 0.05$, Student's t-test). The double alanine substitution (C212A/C282A) however had a WT response (pEC_{50} values: WT 9.49+0.11 n = 3, C212A/C282A 9.41+0.09, n = 3) (Woolley et al., 2013).

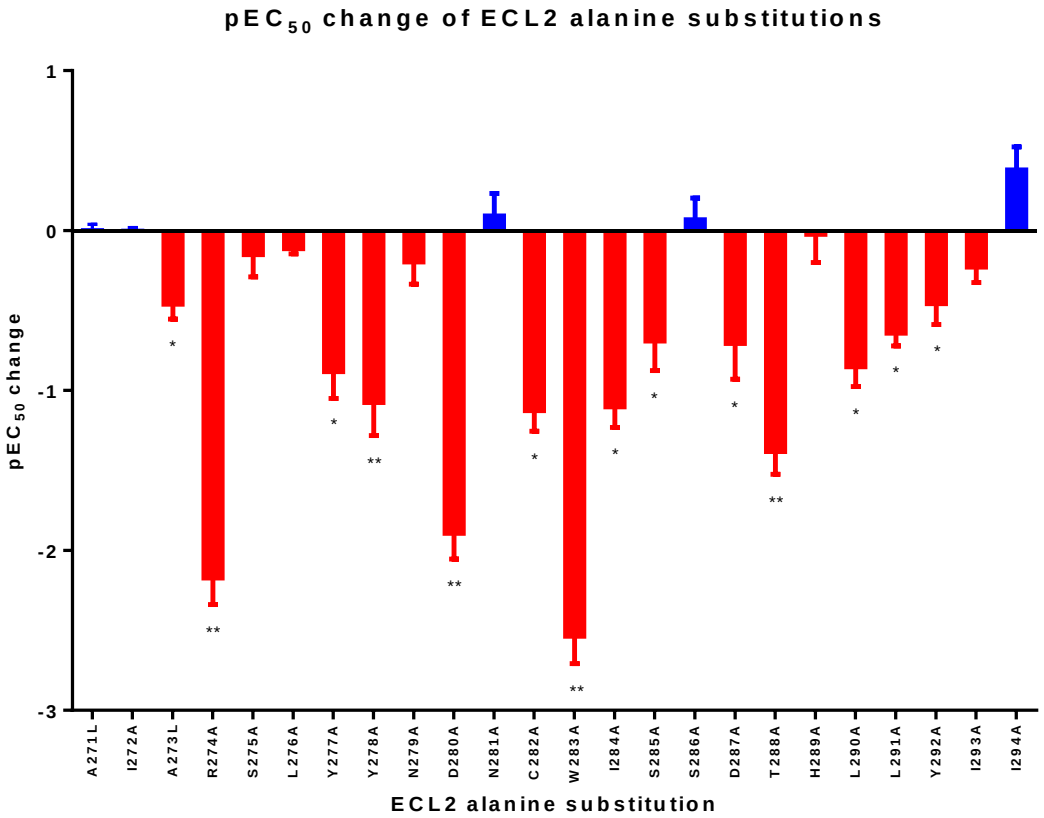

Figure 3.10. A graphical summary of the log difference in pEC_{50} values of the ECL2 alanine substitution and the WT receptor detailed in Table 3.1.

A negative change indicates a decrease in potency of the alanine substitution. Cos7 cells transfected with WT and alanine substitution receptor were dose dependently stimulated with CGRP and levels of the cAMP second messenger were detected using a TR-FRET based cAMP assay. A sigmoidal dose response curve was fitted to the data using GraphPad Prism software. The alanine substitution data were normalised to WT, taking the maximum and minimum values obtained from the WT dose response curve. Significance was obtained using a paired t-test. *p < 0.05, ** p < 0.01, ***p <0.001.

3.3.3.2 Basal signalling

The basal values of the alanine substitutions described in Table 3.1 are illustrated graphically in Figure 3.11. Four substitutions (N281A, S285A, T288A and I294A) had a significant increase in basal signalling compared with WT. The greatest increase was observed with I294A (22.75% greater than WT). The remaining substitutions had an increase of basal signalling between 10-18% of WT.

3.3.3.3 E_{max}

The data for the E_{max} signalling of the alanine substitutions normalised to the WT receptor (WT normalised to 100%) described in Table 3.1 are summarised in Figure 3.12. As Figure 3.12 clearly shows, all alanine-substituted CLR E_{max} data have broadly similar values to that of WT. However five substitutions (N281A, D287A, T288A, Y292A and I294A) showed a significant increase in E_{max}. The greatest increase was observed with D287A (119% that of WT). The other substitutions have E_{max} values between 110-116% that of WT. S285A is the only substitution to have a significantly reduced E_{max} compared with WT at 93.4%.

3.3.4 Cell surface expression of alanine substitutions

A cell surface expression ELISA was used to compare the cell surface expression of the alanine substitution mutant with WT.

The results of the cell surface expression ELISA are shown in Table 3.2 and summarised graphically in Figure 3.13. The majority (19 out of 24) of the alanine substitutions did not have a significant difference in cell surface expression compared with the WT receptor. This confirms that mutation of these residues to alanine has not resulted in a loss of receptor surface expression and trafficking. Five of the 24 substitutions (C282A, W283A, I284A, S285A and H289A) had a significant reduction in cell surface expression to that of the WT receptor. The lowest of which is S285A with receptor expression levels at 55% of WT. C282A, W283A and I284A all have receptor expression between 60-70% of WT and H289A is ~75%. It has been previously shown that cell surface expression levels below 55% WT had no deleterious effect on CGRP-mediated cAMP signalling (Bailey & Hay, 2007; Conner *et al.*, 2006a). Therefore while these mutants might be of interest when it comes to

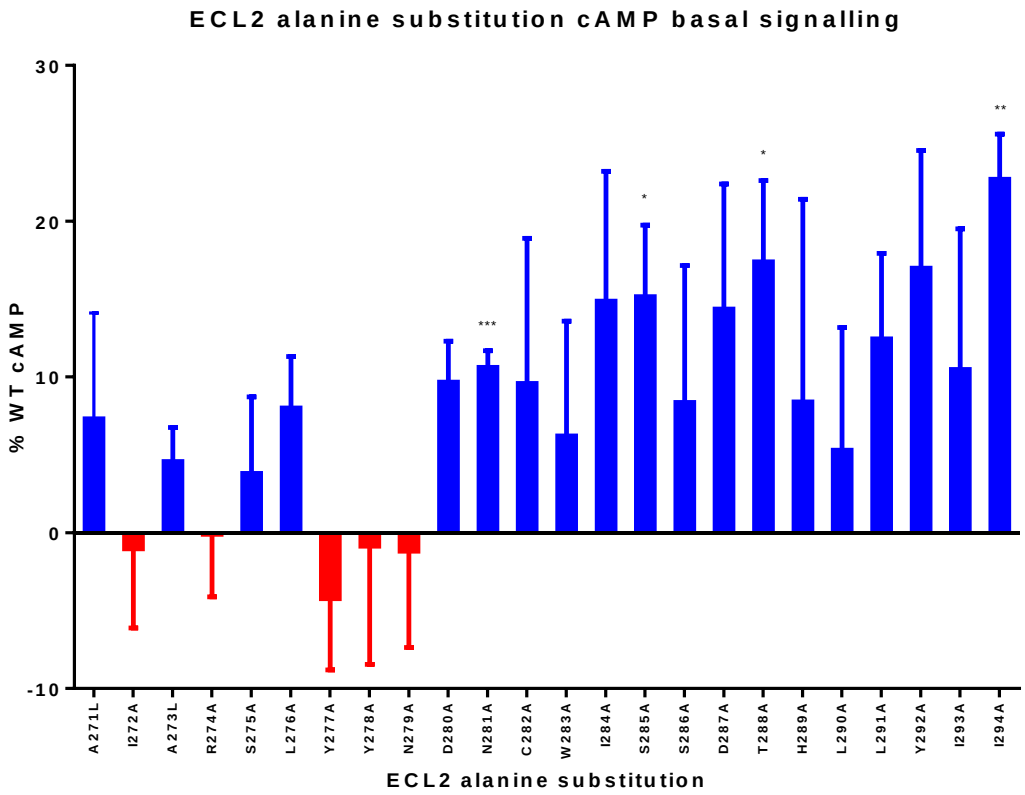

Figure 3.11. A graphical summary of the basal mean and SEM value of the ECL2 alanine substitution following normalisation to the WT receptor.

Cos7 cells transfected with WT and alanine substitution receptor were dose dependently stimulated with CGRP and levels of the cAMP second messenger were detected using a TR-FRET based cAMP assay. A sigmoidal dose response curve was fitted to the data using GraphPad Prism software. The alanine substitution data were normalised to WT, taking the maximum and minimum values obtained from the WT dose response curve. Significance was obtained using a paired t-test. *$p < 0.05$, ** $p < 0.01$, ***$p < 0.001$.

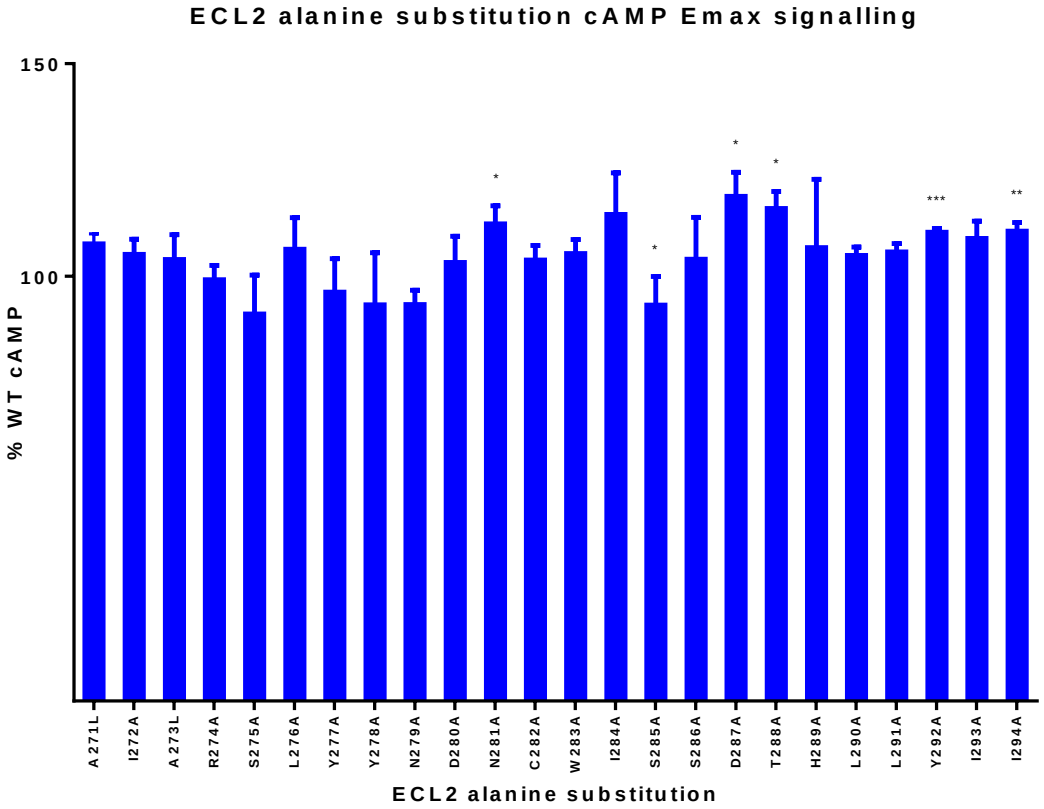

Figure 3.12. A graphical summary of the E_{max} mean and SEM value of the ECL2 alanine substitution following normalisation to the WT.

Cos7 cells transfected with WT and alanine substitution receptor were dose dependently stimulated with CGRP and levels of the cAMP second messenger were detected using a TR-FRET based cAMP assay. A sigmoidal dose response curve was fitted to the data using GraphPad Prism software. The alanine substitution data were normalised to WT, taking the maximum and minimum values obtained from the WT dose response curve. Significance was obtained using a paired t-test. *p < 0.05, ** p < 0.01, ***p <0.001.

ECL2 mutant	n	% WT cell surface expression	p value (WT and mutant + CGRP)
A271L	3	99.11±7.45	0.9165
I272A	3	134.8±12.19	0.104
A273L	3	104.20±3.95	0.3986
R274A	4	93.21±6.08	0.3458
S275A	4	78.90±14.14	0.2325
L276A	3	89.95±8.97	0.3795
Y277A	4	82.82±9.81	0.1782
Y278A	6	97.71±20.59	0.916
N279A	4	82.93±13.86	0.306
D280A	4	83.48±18.57	0.4241
N281A	4	103.30±24.79	0.9027
C282A	3	67.80±2.06	0.0041**
W283A	3	69.80±1.00	0.0011**
I284A	4	62.77±8.12	0.0195*
S285A	8	54.65±6.51	0.0002***
S286A	4	74.05±12.79	0.1355
D287A	4	95.77±10.76	0.7207
T288A	3	94.23±2.30	0.1283
H289A	3	74.83±0.13	<0.0001**
L290A	3	83.18±7.38	0.1504
L291A	3	103.70±4.07	0.4558
Y292A	3	93.90±4.54	0.3114
I293A	3	103.70±7.69	0.6798
I294A	3	100.80±9.15	0.9347

Reduced cell surface expression value

Table 3.2 Summary of the cell surface expression mean and SEM values of the ECL2 alanine substitution and the WT receptor following normalisation to the WT receptor.
Cos7 cells were transfected with WT and alanine substitution receptor and cell surface expression was measured by ELISA. Following expression, cells were fixed with formaldehyde and blocked with 1% BSA in PBS. The WT and alanine substitution receptor cell surface expression was measured using a primary α-HA antibody probing for an N-terminal HA tag on the extracellular N-terminus of the receptor. An α-mouse secondary antibody conjugated to HRP was used and the absorbance of an OPD substrate was measured at 450nm. Data were normalised to the blank mean and WT mean to produce relative minimum and maximum values respectively. Mean + SEM were taken of the normalised data and significance determined using a paired t-test. *$p < 0.05$, ** $p < 0.01$, ***$p < 0.001$.

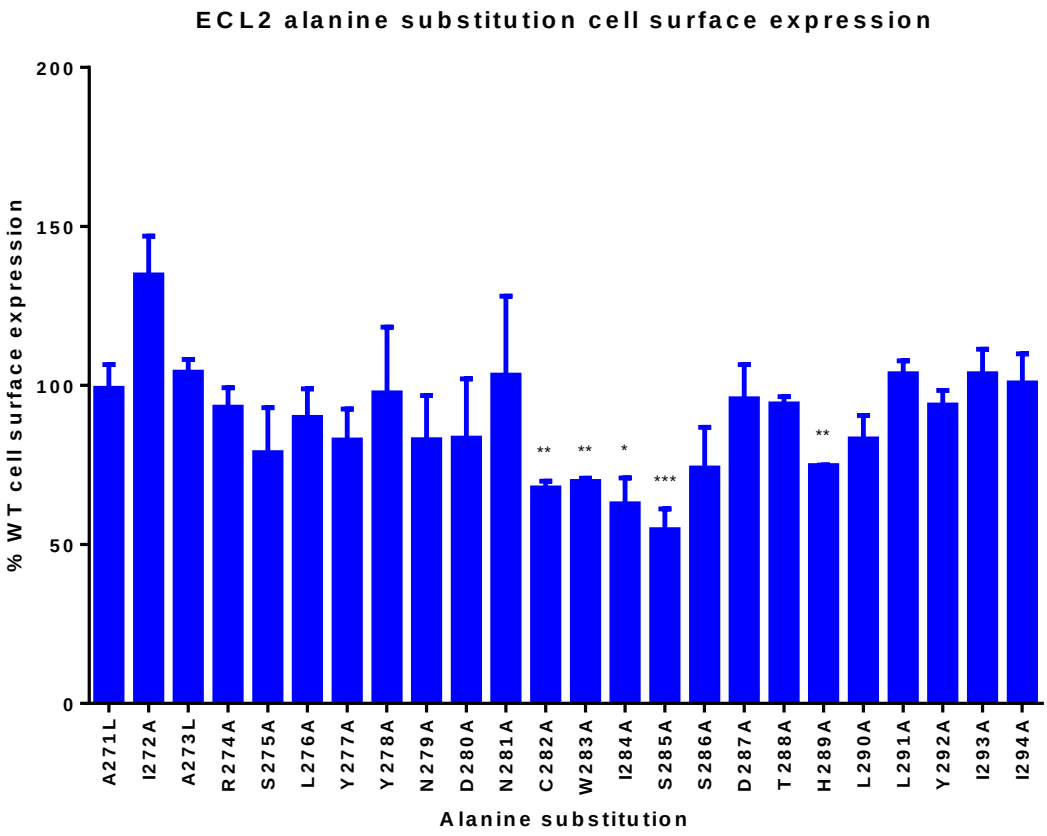

Figure 3.13. Graphical summary of the cell surface expression mean and SEM values of the ECL2 alanine substitution normalised to the WT CGRP receptor.

Cos7 cells were transfected with WT and alanine substitution receptor and cell surface expression was measured by ELISA. Following expression, cells were fixed with formaldehyde and blocked with 1% BSA in PBS. The WT and alanine substitution receptor cell surface expression was measured using a primary α-HA antibody probing for an N-terminal HA tag on the extracellular N-terminus of the receptor. An α-mouse secondary antibody conjugated to HRP was used and the absorbance of an OPD substrate was measured at 450nm. Data were normalised to the blank mean and WT mean to produce relative minimum and maximum values respectively. Mean + SEM were taken of the normalised data and significance determined using a paired t-test. *$p < 0.05$, ** $p < 0.01$, ***$p < 0.001$.

the trafficking of the receptor about the cell, the effect of this is unlikely to be sufficient to cause any observed disruption in receptor signalling.

3.3.5 Radioligand binding of alanine substitutions

Alanine substitutions in the middle of ECL2 that had the greatest reduction in cAMP signalling were subjected to radioligand binding analysis to determine the effect of the mutation on binding affinity. Following the extension of the ECL2 investigation into the TM4/ECL2 and ECL2/TM5 interface, the radioligand binding experiments of the new mutants were unsuccessful and have not been included.

The radioligand binding experiments were carried out by Professor David Poyner at Aston University as part of a continued collaboration. Cos7 cells were co-transfected with either WT CLR or alanine-mutant CLR together with RAMP1. Radioligand binding was done on the cell membranes using [^{125}I] iodohistidyl-human alpha CGRP. The results are shown in Table 3.3. pKd values were determined using the radioligand at a single concentration. Saturation binding to determine B_{max} was not done.

Six out of the eight alanine substitutions investigated had a significantly reduced binding affinity to CGRP (R274A, Y278A, D280A, C282A, W283A and T288A). The greatest effect was observed with the S285A substitution which had non-detectable levels of binding. The largest reductions in binding affinity were observed with R274A and Y278A, each having ~30 fold reduction in ligand binding affinity. W283A has ~10 fold reduction with the remainder (D280A, C282A and T288A) less than 10 fold compared with WT. Only Y277A had no significant variation in binding compared with WT.

3.3.6 Internalisation of alanine substitutions

Activation of the receptor eventually leads to the phosphorylation of the C-terminus, recruitment of β-arrestin and the internalisation of the receptor (Conner et al., 2008). To determine the effect that the alanine substitution of ECL2 has on this downstream process, the cell surface expression ELISA was used to measure internalisation levels.

Mutant	pK_d
WT	9.18±0.05
R274A	7.77±0.25 **
Y277A	8.99±0.53
Y278A	7.75±0.39**
D280A	8.39±0.64*
C282A	8.47±0.07*
W283A	8.13±0.25**
S285A	Undetectable
T288A	8.32±0.43*

Table 3.3. Radioligand binding of selected alanine substitutions with reduced pEC_{50} values.

Values are mean and SEM from three determinations. pK_d values determined from 125[I]-CGRP radioligand binding. *, ** significantly different from WT, $p < 0.05$ and $p < 0.01$, as assessed by paired Student's t-test.

The internalisation results are described in Table 3.4 and summarised graphically in Figure 3.14. The WT CLR and alanine substitutions were stimulated with 10^{-7}M CGRP to measure the effect on internalisation at ~99% WT CLR occupancy. 18 of the 24 alanine substitutions had internalisation levels similar to that of the WT receptor (~60-70% internalisation). Six residues had a significant reduction in internalisation level (R274A, Y278A, D280, C282A, W283A and T288A). Of these, two are only slightly reduced (Y278A and T288A) with ~50% of the receptor internalising. However for the remaining four substitutions (R274A, D280A, C282A and W283A), receptor internalisation has been almost completely abolished.

Two mutants have a significantly increased level of receptor internalisation (L276A and S285A), with an increase of ~10% that of WT.

ECL2 mutant	n	Cell surface expression		Internalisation difference	p value (WT and mutant + CGRP)
		WT	Mutant		
A271L	3	33.30 ± 3.07	30.46 ± 0.91	2.84	0.538
I272A	3	33.30 ± 3.07	36.65 ± 1.20	-3.35	0.3447
A273L	3	31.97 ± 3.06	34.31 ± 1.50	-2.34	0.6577
R274A	4	44.02 ± 1.29	91.02 ± 3.58	-47	0.0008***
S275A	4	42.67 ± 1.59	27.28 ± 6.99	15.39	0.1171
L276A	3	40.52 ± 1.55	31.57 ± 2.23	8.95	0.0398 *
Y277A	4	40.43 ± 1.29	38.10 ± 1.98	2.33	0.4493
Y278A	6	37.26 ± 3.80	52.70 ± 3.63	-15.44	0.0058 **
N279A	4	41.38 ± 4.33	34.71 ± 1.51	6.67	0.1258
D280A	5	40.20 ± 2.06	91.18 ± 5.68	-50.98	0.0007 ***
N281A	4	40.07 ± 2.66	36.05 ± 3.70	4.02	0.1778
C282A	3	26.62 ± 2.71	90.70 ± 3.13	-64.08	0.0066 **
W283A	3	26.62 ± 2.72	105.8 ± 3.43	-79.18	0.0056 **
I284A	4	41.07 ± 3.85	36.08 ± 4.28	4.99	0.4553
S285A	8	34.30 ± 2.71	26.76 ± 2.11	7.54	0.0355 *
S286A	4	37.99 ± 2.67	30.98 ± 7.13	7.01	0.3558
D287A	4	40.52 ± 1.55	37.23 ± 3.35	3.29	0.2268
T288A	3	30.78 ± 1.88	48.55 ± 3.44	-17.77	0.0098 **
H289A	3	37.90 ± 1.00	31.19 ± 3.25	6.71	0.0973
L290A	3	33.66 ± 2.17	35.74 ± 3.80	-2.08	0.3872
L291A	3	36.23 ± 0.96	42.35 ± 1.15	-6.12	0.0656
Y292A	3	30.96 ± 4.38	40.74 ± 0.65	-9.78	0.1222
I293A	3	30.36 ± 3.03	34.44 ± 2.25	-4.08	0.0738
I294A	3	30.36 ± 3.03	30.69 ± 1.75	-0.33	0.8276

Reduced internalisation value Increased internalisation value

Table 3.4. Summary of the internalisation mean and SEM values of the ECL2 alanine substitution and WT receptor following stimulation ± 10^{-7}M CGRP and normalisation to the non-activated receptor.

Cos7 cells were transfected with WT and alanine substitution receptor and cell surface expression was measured by ELISA. Following expression, cells were fixed with formaldehyde and blocked with 1% BSA in PBS. The WT and alanine substitution receptor cell surface expression was measured using a primary α-HA antibody probing for an N-terminal HA tag on the extracellular N-terminus of the receptor. An α-mouse secondary antibody conjugated to HRP was used and the absorbance of an OPD substrate was measured at 450nm. Data were normalised to the blank mean and WT mean to produce relative minimum and maximum values respectively. Mean + SEM were taken of the normalised data and significance determined using a paired t-test. *$p < 0.05$, ** $p < 0.01$, ***$p < 0.001$.

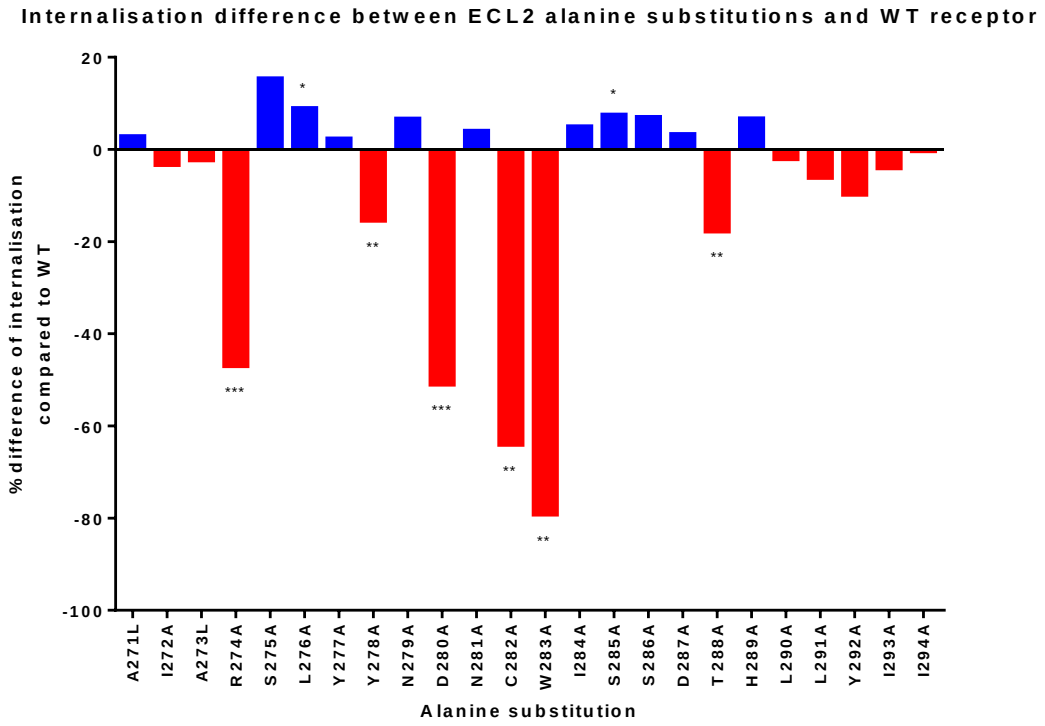

Figure 3.14. Graphical summary of the difference between the mean internalisation values of the ECL2 alanine substitution compared with the WT receptor.

A negative difference represents a reduction in ECL2 alanine substitution receptor internalisation compared to the WT receptor. Cos7 cells were transfected with WT and alanine substitution receptor and cell surface expression was measured by ELISA. Following expression, cells were fixed with formaldehyde and blocked with 1% BSA in PBS. The WT and alanine substitution receptor cell surface expression was measured using a primary α-HA antibody probing for an N-terminal HA tag on the extracellular N-terminus of the receptor. An α-mouse secondary antibody conjugated to HRP was used and the absorbance of an OPD substrate was measured at 450nm. Data were normalised to the blank mean and WT mean to produce relative minimum and maximum values respectively. Mean and SEM were taken of the normalised data and significance determined using a paired t-test. *$p < 0.05$, ** $p < 0.01$, ***$p < 0.001$.

3.4 Discussion

The results of the alanine substitution mutagenesis study of the ECL2 domain of the CGRP receptor described in this chapter provide evidence for the importance of this loop in CGRP-mediated receptor activation. 14 out of the 24 amino acids investigated had a significant reduction in CGRP-mediated cAMP signalling. These residues have been highlighted according to their side chain properties in Figure 3.15. The importance of so many residues within this loop is similar to that observed in the GLP1R ECL2 study which found that over half the residues had a significant effect on cAMP signalling (Koole et al., 2012). This compares with only six out of 30 residues investigated with the V1AR (Conner *et al.*, 2007b) and two out of 16 residues with the CRHR1 (Gkountelias et al., 2009). The involvement of ECL2 residues is therefore variable and not consistent within the receptor families.

3.4.1 ECL2 alanine substitution data integrity

3.4.1.1 cAMP signalling

The Perkin Elmer Lance® cAMP assay was optimised for cos7 cells and the CGRP receptor as described in section 2.2.15.1. The cAMP data for the ECL2 alanine substitutions are presented in Table 3.1 and Figure 3.10 to Figure 3.12.

The WT CLR pEC_{50} data for each ECL2 substitution are described in Table 3.1 and Figure 3.10. The pEC_{50} values varied from 8.81 (S275A and L276A) to 10.71 (C282A and W283A). This variation of ~100 fold in WT CLR potency is greater than expected. Using a transiently transfected cos7 system a variation in potency of ~10 fold (pEC_{50} 9.5-10.5) has been previously observed (Barwell *et al.*, 2011). The variation in WT CLR pEC_{50} values is explained through differences in coupling efficiencies between cells as the data were collected in excess of a year. This variation has been previously observed with CGRP receptors (Howitt *et al.*, 2003; Poyner *et al.*, 1998). To control for this, a paired design-test was used so that each substitution was compared in the same experiment against a corresponding WT control. The standard error at each ECL2 position varied from 0.04 (D280A) to 0.59 (A271L and I272A). This variation does not reflect the differences observed in the WT CLR pEC_{50} mean data between ECL2 substitutions supporting the explanation

that this is due to the time span the data set was accumulated over. 14 ECL2 alanine substitutions had a significant reduction in potency. Seven alanine substitutions had a greater than 10 fold reduction (R274A, Y278A, D280A, C282A, W283A, I284A and T288A). Of the remaining seven that had a less than 10 fold reduction in signalling potency, four substitutions (Y277A, S285A, D287A and L290A) had between 5-10 fold reduction in cAMP potency. The remaining three substitutions (A273L, L291A and Y292A) had a less than 5 fold reduction in cAMP signalling potency. Given the variation observed using the transient transfection system the greatest emphasis for biological effect will be placed on those residues with a greater than 10 fold reduction in potency with some interest in those residues with a 5-10 fold reduction. Substitutions with a less than 5 fold reduction in signalling potency, whilst statistically significant, are unlikely to have much biological effect.

The cAMP basal values are described in Table 3.1 and Figure 3.11. These values ranged from -4.29 % (Y277A) to 22.75 % (I294A) normalised to WT CLR basal signalling. The standard error varied from 1.01 % (N281A) to 12.96 % (H289A). Figure 3.11 clearly shows this data variation. This more likely reflects the variation observed using a transiently transfected cell based system with differing transfection efficiencies and therefore differing transfected cell numbers in the assay. It is unlikely that the statistically significant alanine substitutions (N281A, S285A, T288A and I294A) reflect a biological effect.

The cAMP E_{max} values are described in Table 3.1 and Figure 3.12. They ranged from 91.27 % (S275A) to 116.1 % (T288A) normalised to WT CLR E_{max} signalling. The standard errors of the data set ranged from 0.75 % (Y292A) to 15.86 % (H289A). As observed with the cAMP basal values, this spread of data most likely reflects the variation of a transiently transfected cell based system. The values with a statistically significant difference ranged from 93.4 % (S285A) to 116.1 % (T288A). This change is not substantial enough to reflect a strong biological effect.

3.4.1.2 Cell surface expression

The cell surface expression of the ECL2 alanine substitutions normalised to WT CLR is described in Table 3.2 and Figure 3.13. The cell surface expression of the ECL2 alanine substitutions was broadly 100 % compared with the WT CLR control. There

is a four amino acid cluster between C282A and S285A that had a significantly reduced cell surface expression (54.65 % - 39.80 %) and separately, H289A had a significantly reduced cell surface expression (74.83 %). This level of cell surface expression has been previously shown to not have a detrimental effect on the signalling ability of the receptor (Conner *et al.*, 2006a) however considering that each residue in this sequence of four had a significant reduction in cell surface expression and given the small standard error observed at these data points (1.00 % - 8.12 %), it suggests a biological importance of this cluster of residues in allowing the receptor to be successful expressed at the cell surface.

3.4.1.3 Radioligand binding

The radioligand binding data are described in Table 3.3. pKd values were determined using the radioligand at a single concentration. Saturation binding to determine B_{max} was not done. The first set of ECL2 alanine substitutions chosen to test for binding affinity were key residues in the centre of the ECL2 domain. The radioligand binding work was continued to include important residues at the TM4/ECL2 and ECL2/TM5 interface however these experiments were not successful and data were not included. Within this central section of ECL2, five out of seven residues selected for binding affinity experiments had a reduced ability to bind CGRP (Y278A, D280A, C282A, W283A and T288A). Binding for S285A could not be detected. Only Y277A retained WT binding affinity. The greatest reductions were observed with R274A and Y278A (~30 fold reduction). This confirms that the reduced signalling observed in this section of the loop is due to disrupted ligand binding. What these data does not confirm is whether this is because of direct ligand-receptor interactions or a structural change in the ligand binding pocket.

3.4.1.4 Internalisation

The WT CLR and alanine substitutions were stimulated with 10^{-7}M CGRP to measure the effect on internalisation at ~99 % WT CLR occupancy. The substitutions that had a significant reduction were R274A, Y278A, D280A, C282A, W283A and T288A. These substitutions had a reduction in signalling of 10-300 fold. In the internalisation assay, the receptor was stimulated with 10^{-7}M CGRP, a concentration 100 fold higher than that of the receptor K_d (~10^{-9}M). Given the

reduction in signalling caused by the alanine substitution, stimulation with CGRP at this concentration would fail to activate a large proportion of receptors, corresponding with reduced downstream internalisation. This showed that receptor internalisation required the activation of the receptor. However this experimental set up does not show if the alanine substitutions have an effect on receptor internalisation separate to activation. To investigate this, the ECL2 alanine substitution could be stimulated by a CGRP concentration at a consistently increased concentration to the pEC_{50} (e.g. 100 fold). Due to time constraints and the continuation of the study, this was not done.

3.4.2 ECL2 alanine substitution analysis

ECL2 was originally proposed to extend from R274 through to H289. In this study, the alanine scan was extended to A271 through to I294 to investigate the TM/ECL2 interfaces, which were hypothesised to be extensions of the loop domain. The 14 amino acids which resulted in a significant reduction in cAMP signalling after alanine substitution can be split into three different regions within ECL2 (see Figure 3.15). The first is at the TM4/ECL2 interface (A273A and R274A). The majority of the alanine substitutions with reduced signalling are located in the middle of the loop (Y277, Y278, D280, C282, W283, I284, S285, D287 and T288) and there are three residues at the ECL2/TM5 interface where alanine-substitution had an effect on signalling (L290, L291 and Y292).

3.4.2.1 TM4/ECL2 interface

Mutation of A271L and I272A did not affect any aspect of receptor function that was investigated. A273L however did have a small, significant reduction in cAMP signalling (~3 fold) with no change in cell surface expression. Adjacent to A273L, R274A had a large reduction in pEC_{50} (~100 fold) together with an almost complete abolition of internalisation (~10%). These two residues form an interesting doublet at the N-terminus of the loop, which were not expected to be involved directly in the ligand binding pocket. The properties of each side chain, a short hydrophobic methyl group (alanine) and a positively charged terminus of a hydrocarbon chain (arginine) suggest that these residues maybe important in creating a structural

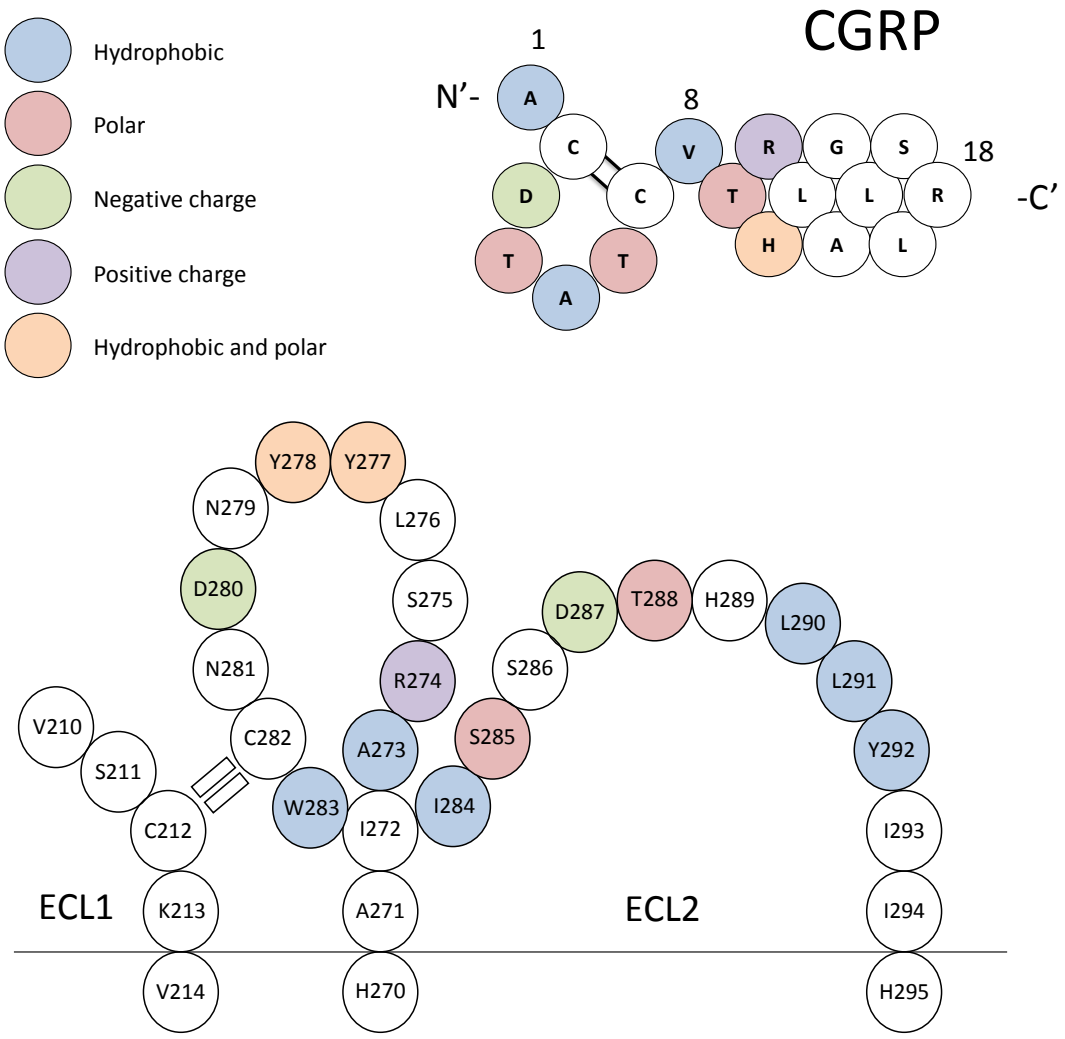

Figure 3.15. A schematic of the N-terminal 18 residues of the CGRP peptide and the ECL2 domain of CLR with key residues of the alanine substitution analysis highlighted.
CGRP residues 1-11 and each ECL2 residue that had a significant reduction in cAMP pEC_{50} after substitution with alanine have been highlighted to describe the property of the side chain.

scaffold with the hydrophobic membrane and the polar environment of the phospholipid bilayer, conferring structural stability to the loop. Polar resides (such as lysine, arginine, tryptophan and tyrosine) in TM helices can extend their side chains perpendicular to the membrane to orientate them away from the hydrophobic membrane core towards the polar interface in an effect known as snorkelling (Chamberlain et al., 2004). The conserved basic residue at the TM4-ECL2 interface could be positioned within the membrane helix and follow this behaviour. This positioning at the top of TM4 is observed in the two family B crystal structures (Hollenstein et al., 2013; Siu et al., 2013). The equivalent basic residue in the GCGR is a lysine (K286) and substitution of this residue to a leucine residue attenuates binding (Siu et al., 2013). In the author's model, this effect was predicted to be due to a salt bridge formed with E290. The GLP-1R alanine scan also identified the importance of a basic residue at the TM4-ECL2 interface (Koole et al., 2012). K288 appears to function similarly to R274 of CLR and K286 of GCGR. Like GCGR, four residues into the loop from K288 is a glutamate (E292) which has reduced binding and pEC_{50} when substituted with alanine. It is not unreasonable to predict that a similar structural bridging could be occurring in the GLP-1R ECL2 domain as observed with the GCGR. The equivalent interaction could occur in CLR between R274 and D280 or a similar interaction could occur between R274 and either Y277 or Y278. The sequence alignment of the family B GPCR ECL2 domains in Figure 3.4 shows a conserved basic residue in each receptor at the equivalent R274 position. This conservation, together with its positioning away from the middle of the TM bundle suggests that this residue does not have a direct ligand binding effect but that the reduction in receptor signalling observed through the alanine substitution is due to indirect, possible structural interactions of this residue. This will be discussed further in the modelling section. The large reduction of CGRP-mediated internalisation with the R274A substitution mutant reflects the dramatic loss of receptor signalling ability.

3.4.2.2 ECL2 domain

The ligand-receptor binding sites of ECL2 are expected to occur in the middle of the loop, which is itself predicted to extend into the middle of the transmembrane

bundle. The results of this study support this prediction with 9 out of the 14 residues between position S275 and T288 having a significant reduction in cAMP signalling. Of these, six had a reduction greater than 10 fold (Y278A, D280A, C282A, W283A, I284A and T288A) which illustrates how important these residues are in receptor signalling. Only one other substitution in the rest of the loop had a greater than 10 fold reduction in pEC_{50} (R274A).

The greatest reductions were observed with substitutions D280A (~100 fold) and W283A (~300 fold). T288A has a more modest reduction of ~20 fold. Interestingly, each side chain of these residues has a different property. Aspartate has a negatively charged carboxyl group at the terminus of a hydrocarbon chain, tryptophan has a large imidazole-benzene double ring structure and threonine has a polar hydroxyl group at the terminus of a hydrocarbon chain. The negative charge of the D280 side chain and the hydroxyl group polarity or methyl group of the T288 side chain provide potential contact sites with the CGRP ligand. W283 could either be forming direct hydrophobic or electrostatic interactions with CGRP or by creating structural integrity in the centre of the loop.

The importance of a negatively charged residue in ECL2 in a position similar to that of D280 in CLR was observed in the study of the GLP-1R ECL2 domain (Koole et al., 2012). In this receptor there is a cluster of two adjacent acidic residues (E292 and D293) just to the N-terminus of the disulphide bonded cysteine which had reduced signalling after mutation to alanine. In the GCGR there is an EN motif just before the conserved cysteine, which also reduces ligand binding upon substitution (E290A, N291A and N291D). According to the author's model, the glutamate residue is not thought to make direct interactions with the glucagon ligand but indirectly facilitates ligand binding through a salt bridge with K286 (Siu et al., 2013). An identical interaction could exist between R274 and D280 of CLR. The importance of acidic residues in ECL2 has not just been observed in the family B GPCRs but is also a feature in family A GPCRs with mutation of these residues having a detrimental effect on ligand binding and receptor activation (Kim *et al.*, 1996; Moro *et al.*, 1999; Walker *et al.*, 1994).

The other residues in the middle of ECL2 with reduced signalling (Y278A, C282A and I284A) have a smaller reduction in CGRP-mediated cAMP stimulation (~10 fold). Tyrosine is interesting as the side chain is a phenol, comprising a benzene ring and a hydroxyl group. This leads to a variety of potential interactions that could occur, from hydrophobic interactions with the carbon ring, pi-cation or stacking interactions with the delocalised electrons in a planar orientation above and below the ring or polar interactions with the hydroxyl group. From these data it is not possible to establish what these functional interactions are. Isoleucine at position 284 has a branched hydrocarbon chain forming hydrophobic interactions. Again, similar to the tryptophan adjacent to this residue (W283), the nature of the hydrophobic properties could be due to direct interactions with CGRP or structural effects within the loop.

Apart from C282, W283 is the only other conserved residue in the family B GPCR ECL2 domains. Both the cysteine and tryptophan were important in the GLP-1R (Koole et al., 2012). Mutation of these residues to alanine resulted in a loss of ligand binding, cell surface expression and receptor signalling. This importance is also in the family A V1AR (Conner *et al.*, 2007b). The function of this tryptophan is not just of significance for CLR, but for family B GPCRs as a whole and potentially family A GPCRs as well.

The cysteine at position 282 is conserved across GPCR families and forms a disulphide bond with a cysteine at the top of TM3 (Wheatley et al., 2012). In the case of CLR, this is C212. The disulphide bond confers structural integrity to the loop in other GPCRS (Conner *et al.*, 2007b) therefore its effect was investigated further for the CGRP receptor. The single alanine substitution (C212A) had a similar reduction in cAMP signalling to that of C282A however the double alanine substitution (C212A/C282A) had a WT response (Woolley et al., 2013). This experiment shows that the disulphide bond for the CGRP receptor is not essential for receptor integrity and that reduction in signalling caused by the single alanine substitution is more likely due to the disruption from the free sulfhydryl group from the remaining cysteine. This result has also been observed in the GLP-1R (Mann et al., 2010). Mutation of the TM3 cysteine to alanine (C226A) reduced GLP7-36

potency. This was recovered with the double TM3-ECL2 cysteine to alanine substation (C226A/C296A). Interestingly the single ECL2 cysteine to alanine substitution (C296A) had WT potency indicating that the disruption in signalling is due to the free sulfhydryl in ECL2. This recovery with the double alanine substitution is not always observed. With the C5aR, the double alanine substitution did not produce a signalling response upon ligand stimulation however constitutively active substitutions remained active (Klco et al., 2005). In this case the disulphide bond was required for ligand based activation of the receptor but is not required for the receptor to achieve an active conformation.

The remaining three substitutions in the middle of the loop (between S275 and T288) with a significant reduction in cAMP signalling are Y277A, S285A and D287A. Mutation to alanine at each of these positions resulted in a 5-10 fold reduction in signalling. As with Y278, the effect at position 277 could be due to potential hydrophobic, pi-cation, stacking or polar interactions of the phenol side chain. Similar to threonine, serine has a polar hydroxyl group at the terminus of a hydrocarbon chain allowing potential hydrogen bond interactions. The negatively charged carboxylic acid group of D287 allows for potential salt bridge interactions (electrostatic or hydrogen bonding). The Y277A mutation did not cause a significant change in basal or E_{max} signalling, however S285A had a significant increase in basal (~15%) and decrease in E_{max} (93.2%). D287A had WT basal signalling but a significantly increased E_{max} (119%). After the CW motif on GLP-1R, there is a sequence of polar and basic residues important for binding affinity and signalling (Koole et al., 2012). This is similar to the S/T sequence in CLR, except CLR has an acidic D287 residue instead of R299.

The cluster of residues between C282 and S285 all have a reduction in cell surface expression (60-70% of WT). This level of cell surface expression has been previously shown to not have a detrimental effect on the signalling ability of the receptor (Conner *et al.*, 2006a) however considering that each residue in this sequence of four has a significant reduction in cell surface expression, it suggests an importance of these residues in allowing the expression of the receptor to the cell surface. There is a similar motif in the GLP-1R of (C296, W297 and R299) of which alanine

substitution results in a decrease in cell surface expression (Koole et al., 2012). However the threonine adjacent to W297 results in an increased expression upon mutation to alanine. Cell surface expression requires successful completion of multiple stages. The receptor needs to be correctly folded across the membrane, post translational modifications including oligomerisation need to occur and successful translocation from the ER through the Golgi network to the cell surface is required (Achour *et al.*, 2008; Drake *et al.*, 2006; Tan *et al.*, 2004). The reduced cell surface expression observed with the C282 to S285 alanine substitutions does not reveal the mechanism for the loss of cell surface expression. However it does suggest this motif may have structural or conformational integrity.

Within this central section of ECL2, five out of seven residues selected for binding affinity experiments had a reduced ability to bind CGRP (Y278A, D280A, C282A, W283A and T288A). This confirms that the reduced signalling observed in this section of the loop is due to disrupted ligand binding. What these data does not confirm is whether this is because of direct ligand-receptor interactions or a structural change in the ligand binding pocket.

Considering the reduction in binding affinity and receptor signalling of these key substitutions, it is not surprising that these also resulted in a reduced internalisation. The substitutions that had a significant reduction were R274A, Y278A, D280A, C282A, W283A and T288A. These substitutions had a reduction in signalling of 10-300 fold. In the internalisation assay, the receptor was stimulated with 10^{-7}M CGRP, a concentration 100 fold higher than that of the receptor K_d (~10^{-9}M). Given the reduction in signalling caused by the alanine substitution, stimulation with CGRP at this concentration would fail to activate a large proportion of receptors, corresponding with reduced downstream internalisation.

3.4.2.3 ECL2/TM5

The C-terminal extension of the alanine screen also produced some interesting data. The extreme C-terminus of ECL2 (I293 and I294) did not result in any change in cAMP signalling. This contradicts published data, which found I294A to show constitutive activity (Woolley et al., 2013). Further experimental repeats changed the significance of these results, however with a p value close to 0.05 in all

experiments, there is no certainty in either finding. This substitution had a significantly increased basal (~23% increase of WT) and E_{max} (110% of WT). Isoleucine has a branched hydrophobic side chain. It is possible that this stabilises the inactive conformation of the receptor through interaction with the hydrophobic chains of the phospholipid bilayer. Removal of the side chain could allow for greater flexibility of the receptor for the active conformation.

Individual alanine substitution of three adjacent residues (L290A, L291 and Y292A) all had small reductions in receptor pEC_{50} values (3-10 fold). This hydrophobic cluster forms an interesting motif. It is possible that they form intermolecular interactions with the phospholipid bilayer, or form intramolecular interactions with either each other or adjacent residues from other domains. Either set of interactions is likely to confer structural integrity to the loop, facilitating ligand binding, which is diminished with the alanine substitution. The alanine substitution had no significant effect on basal or E_{max} signalling, with the exception of a slight increase in E_{max} for Y292A (110% of WT). Cell surface expression and internalisation were unaffected. The end of ECL2 for GLP-1R contains important hydrophobic residues in Y305 and W306, similar to the LLY motif of CLR (Koole et al., 2012). The tyrosine residue at the ECL2-TM5 interface has been previously shown to be important in family A GPCR ligand binding and receptor signalling (Conner *et al.*, 2007b). There appears to be a conserved functional effect of hydrophobic residues at the top of TM5 across GPCR families.

3.4.3 CGRP receptor modelling

At this moment, the only structural information on the CGRP receptor is a crystal structure of the RAMP1 ECD and the heterodimeric CLR-RAMP1 ECD in complex with synthetic antagonists (Kusano *et al.*, 2008; ter Haar *et al.*, 2010). This has provided excellent information into both the structure of the ECD of the CGRP receptor and also in identifying key residues involved in the interaction of the CLR-RAMP1 interface and contact sites with particular ligands. However at this moment, no structure has been obtained for the complete receptor. Instead, a high degree of computer modelling has been done, using molecular dynamics to predict thermodynamically stable receptor conformations. This data has been used

iteratively with experimental data to refine and adjust the model as more data is produced. The publication of family A GPCR structures, first with bovine rhodopsin (Palczewski et al., 2000) followed by β2-AR (Rasmussen et al., 2007) and a number of more recent structures, can be used as a framework for the modelling of other GCPRs. However a particular difficulty with family B GCPRs until very recently was the lack of a crystal structure of any receptor in this family and a lack of sequence homology with family A GCPRs to facilitate computer modelling based on those structures. A novel approach was used with the CGRP receptor (Vohra et al., 2013), which used a plant GPCR (GCR1) that has sequence similarity to both family A and family B mammalian GPCRs. β2-AR-GCR1 and GCR1-CLR homology was used to produce a computer model of CLR based on the β2-AR-Gs crystal structure (pdb code 3SN6).

The results from the alanine scan described in this results chapter were used by collaborators to refine the CLR model (Vohra et al., 2013) and to predict a potential CGRP docking site (Woolley et al., 2013). Molecular dynamics generated a number of different ECL2 structures and potential CGRP docking orientations. Results from the alanine scan were used to predict the most likely conformations. A number of loops adopted similar conformations which satisfied many of the requirements from the mutagenesis studies. These included CGRP T6 interacting with CLR ECL2 D280, D287 and T288, CGRP not directly interacting with CLR ECL2 R274 and W283 (of CLR ECL2) positioned vertically allowing interaction with T191 (TM2) and H219 (TM3), which have been identified as important residues during previous alanine substitution investigations (Barwell et al., 2011; Vohra et al., 2013).

3.4.3.1 Predicted ECL2 structure

Six high scoring conformations of the published model have been edited using the Swiss-PdbViewer 4.1.0 software to isolate the ECL2 domain. Figure 3.16 shows these six conformations of ECL2 with selected residues of ECL2 identified as important through the alanine substitution work highlighted to show the orientation compared with the loop. The highest scoring model is shown in Figure 3.17 with residues that result in a greater than 10 fold reduction and a less than 10 fold reduction in pEC_{50} signalling values highlighted both separately and together.

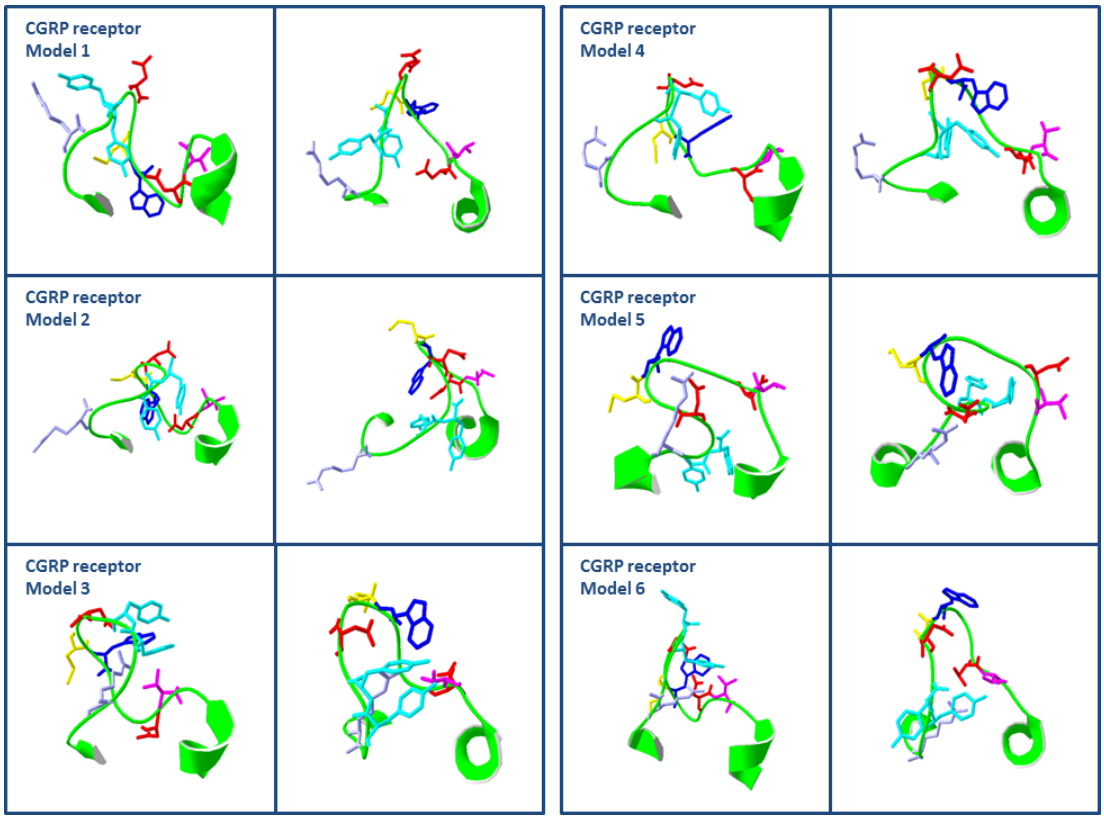

Figure 3.16. Six high scoring models of the ECL2 domain of CLR as proposed in Woolley et al., 2013 and edited using Swiss-PdbViewer 4.1.0.

Selected key residues have been highlighted to show their position and orientation with respect to the loop. R274 is violet, Y277 and Y278 are cyan, D280 and D287 are red, C282 is yellow, W283 in blue, T288 is magenta.

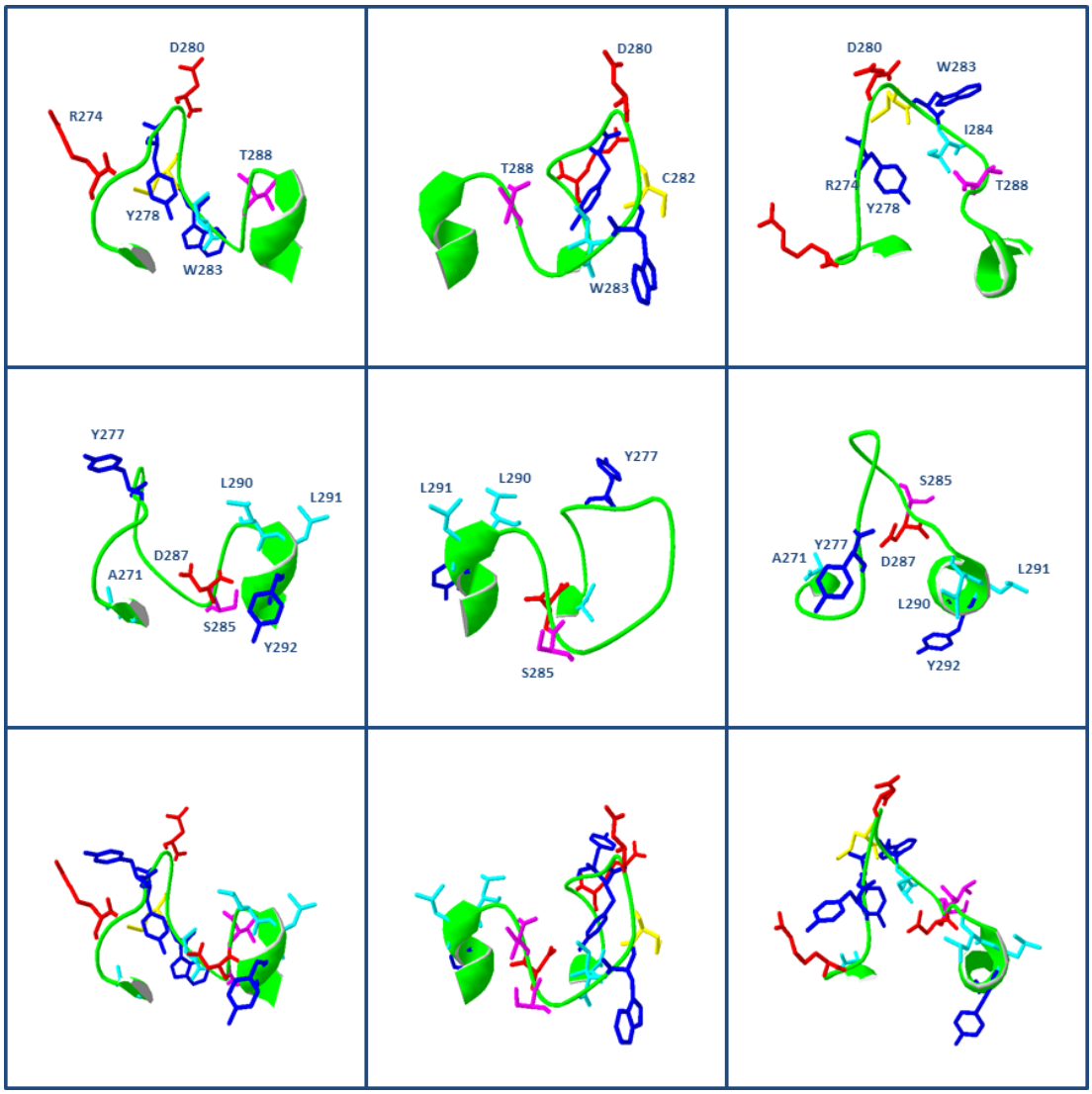

Figure 3.17. A high scoring model of the ECL2 domain of CLR as proposed in Woolley et al., 2013 and edited using Swiss-PdbViewer 4.1.0.

The first row presents the loop in three orientations with the seven amino acids side chains of residues with a greater than 10 fold reduction in cAMP signalling during the alanine highlighted. The second row presents the loop in three orientations with the seven amino acids side chains of residues with a less than 10 fold reduction in cAMP signalling during the alanine highlighted. The third row presents the loop in three orientations with all the residues highlighted. Charged side chains are red, polar are purple, hydrophobic are cyan, hydrophobic and polar are blue and the cysteine is yellow.

These ECL2 conformations show both similarities and differences in loop structure. All the models have the domain as a loop that covers the TM bundle but without any defined secondary structure. With the exception of model 5, the N-terminal half of ECL2 extends to the middle of the TM bundle with the C-terminal half forming a groove as it loops back to TM5.

The predicted length of the loop in each of the models is fairly consistent. In models one to four, ECL2 begins at I272 and extends to L290. In model 5 ECL2 begins at R274 and extends to L291. In model 6 it begins at A273 and extends to L290. This is slightly different to the TM4-ECL2 and ECL2-TM5 interfaces of the crystal structures. In the GCGR structure, ECL2 begins at the F289, three residues to the C-terminus of the conserved basic residue at the start of ECL2 (Siu et al., 2013). The loop is shorter than expected (12 residues) and ends at N300. In CRHR1 ECL2 begins at Y253, three residues to the C-terminus of the conserved basic residue. ECL2 is longer than GCGR (17 residues) and ends at D269 (Hollenstein et al., 2013).

The overall position of the loop between conformations in Figure 3.16 is broadly similar with most of the variation occurring between side chain orientations. A good example of this is R274 which is either projecting away from the TM bundle (model 1 and 4) towards the plasma membrane (model 2) or pointing towards the TM bundle (model 3, 5 and 6). The CLR models propose that possible bridging can occur between R274 and either Y277 or D280. This is an effect seen with the modelling of the GCGR between K286 and E290 (Siu et al., 2013). The side chains of Y278, D280, I284 and T288 are all positioned within the loop forming potential structural interactions or direct ligand-receptor interactions. W283 adopted a number of different combinations during the modelling process but the version that satisfied the results for the experimental data was the vertical positioning of the side chain. This positions the side chain away from likely CGRP contact sites. This broadly agrees with the orientation of the tryptophan residue in the CRHR1 ECL2 CW motif, in which the tryptophan side chain points back towards TM3 and TM4, away from the centre of the bundle (Hollenstein et al., 2013). The orientation of the CW tryptophan residue in the GCGR crystal structure is orientated in the opposite direction, towards the middle of the TM bundle (Siu et al., 2013). What is evident

from this model, is how concentrated to the centre of the loop these side chains are. It shows that this area of the receptor is of fundamental importance for ligand based activation. The separation of residues that have a greater than 10 fold and a less than 10 fold reduction in signalling in Figure 3.17 reveals that the residues with the biggest reduction in signalling are often located in the middle of the loop. The majority of the residues with a small reduction in cAMP signalling are on the terminals of the loop (A271, L291 and Y292) or are positioned away from the middle of the domain (Y277 and S285). Only D287 and potentially L290 are positioned towards the middle.

Comparing the highest scoring structure of CLR ECL2 proposed in the model in Figure 3.17 with that of the published family B structures (Figure 3.3), it can been seen that all three share a similar loop structure, extending into the middle of the bundle forming a slight lid over the TM pocket (Hollenstein et al., 2013; Siu et al., 2013). However, compared with both the CRHR1 and GCGR structures, the loop of ECL2 proposed in the model of CLR has a more prominent groove occurring between D280 and T288 (Figure 3.17). This may be due to the differences in ligand binding discussed in the next section. The equivalent groove in the CRHR1 starts with an acidic side chain (E256) however at the end of the groove are the basic residues K262 and R263. GCGR has a valine (V292) in place of the CLR aspartate (D280), however the end of the groove has a similar sequence of amino acids to CLR (D287 and T288), with an aspartate (D299) followed by an asparagine (N300).

What is also evident is that in computer modelling which has restrained TM4 and TM5 to that of the β2-AR-Gs and restricted the position of the centre of the loop through the disulphide bond between TM3 and ECL2 (C212-C282), there is still a reasonable amount of variation in the number of energetically favourable conformations of the loop. This may reflect limitations in the computer modelling process, reinforcing the importance of the experimental data. It also may suggest that ECL2 is able to adopt these variable and energetically favourable conformations. This might be an explanation into the multiple signalling and physiological effects being observed with GCPRs.

3.4.3.2 Potential CGRP-ECL2 docking sites

Figure 3.18 illustrates potential docking sites between CGRP and six CLR models (Woolley et al., 2013). CGRP is shown together with the ECL1, ECL2 and ECL3 domains of CLR. As discussed, these CGRP-CLR interaction sites all occur in the central part of ECL2. D280 interacts much further towards the C-terminus of CGRP than previously thought, forming contacts with H10 and R11 of CGRP. I284, S285 and D287 of CLR form a shelf at the bottom of the bind pocket, holding A5 CGRP at the bottom of the CGRP N-terminal loop in position. The T6 CGRP residue interacts with T288 of CLR. The hydrophobic side chain of CLR L290 positioned towards the centre of the domain makes interactions with L12 on CGRP.

ECL2-CLR intramolecular bonds are also very interesting. W283, orientated down into the TM region is able to form interactions with residues in other TM helices (TM2 and TM3). R274 in its orientation away from the binding pocket, forms contacts with Y277, suggesting a structural role. It was also predicted that R274 could bridge with D280 facilitating the interaction between D280 of CLR and R11 of CGRP. L291, which again angles away from the ligand binding pocket, might be exerting its effect through interactions with TM7 or interestingly, RAMP1.

As discussed in section 3.4.3.1, the predicted ligand binding groove formed between D280 and T288 of CLR is much more pronounced than in the CRHR1 and GCGR crystal structures. These structures did not incorporate the peptide ligand, therefore binding had to be assumed. In each case however, the binding pocket was proposed to extend into the TM bundle (Hollenstein et al., 2013; Siu et al., 2013). This is different to the ligand binding proposed in the CGRP model in which CGRP docked to the extracellular side of the ECLs. The N-terminus of the CRHR1 and GCG ligands are alpha helices that form a stick-like structure able to penetrate into the TM core. It is possible that the N-terminal loop of CGRP formed by the disulphide bond between residues C2 and C7 forms a ball-like structure that sterically holds the ligand at the membrane surface. The greater resulting interaction with the ECL domains may result in the more pronounced ligand binding groove of CLR.

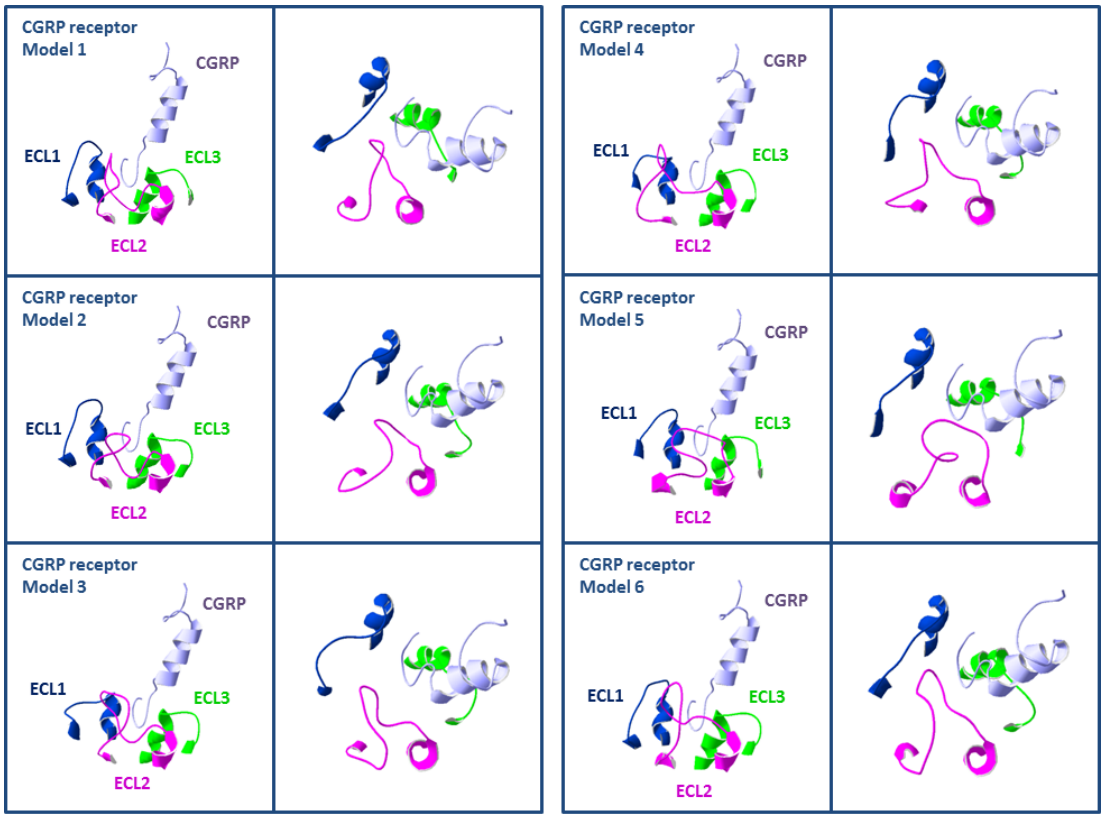

Figure 3.18. Proposed CGRP and ECL docking taken from the six highest scoring models described in Woolley et al., 2013.

Each model has been presented in two orientations. ECL1 is coloured blue, ECL2 is magenta, ECL3 is green, and CGRP is coloured violet.

3.4.4 Conclusions

This study has established for the first time that the ECL2 domain of the CGRP receptor has a substantial involvement in CGRP-based receptor activation. Each region of the loop has apparent functional roles. The TM4-ECL2 interface is likely to be of structural importance, particularly the R274 residue possibly forming interactions with the lipid bilayer and the centre of the loop. In the middle of ECL2, D280, W283, D287 and T288 are the most important residues, probably forming direct CGRP contacts and stabilising intramolecular interactions. The ECL2-TM5 interface is again of structural importance with a hydrophobic cluster of L290, L291 and Y292 essential for CGRP-mediated cAMP signalling.

Computer modelling has created a number of high scoring loop conformations. There is variation between structures but they broadly agree on the fundamental loop conformation. This exists as a loop structure acting as a lid over the TM bundle, similar to that of the family B crystal structures of CRHR1 and glucagon (Hollenstein *et al.*, 2013; Siu *et al.*, 2013). The modelling proposes contact sites between D280, D287 and T288 with the CGRP ligand. The effects of residues at the TM interfaces are likely to be structural.

Having identified ECL2 residues of functional importance, establishing the precise effect of these residues and the exact contact sites with CGRP would be the focus for the next aspect of the ECL2 research.

4 Non-alanine substitution analysis of the extracellular loop two domain of the CGRP receptor

4.1 Introduction

The ECL2 domain of GPCRs has a diverse structural and functional role. The recent influx of crystal structures together with the original rhodopsin and β2-AR structures have shown how varied ECL2 can be, especially with relation to ECLs 1 and 3 (Cherezov *et al.*, 2007; Chien *et al.*, 2010; Palczewski *et al.*, 2000; Park *et al.*, 2012; Shimamura *et al.*, 2011). Mutagenesis and chimeric receptor studies have implicated this domain in direct ligand binding (Conner *et al.*, 2007b; Koole *et al.*, 2012; Olah *et al.*, 1994), presentation of the ligand to the TM ligand binding domain (Colson et al., 1998; Perlman et al., 1997), facilitating the conformational change of the receptor to an active conformation (Ahuja et al., 2009) or retaining the receptor in its inactive conformation (Klco et al., 2005).

Analysis of the individual alanine substitution mutagenesis of the CLR ECL2 domain described in chapter 3 provided evidence for the first time that this loop has a direct involvement in CGRP-mediated receptor activation. 14 residues of the CGRP receptor ECL2 domain had a significant reduction in CGRP-mediated cAMP signalling. Seven of these alanine substitutions had a greater than 10 fold reduction in pEC_{50} signalling, highlighting the importance of this loop in ligand mediated activation. The remaining seven mutants had a less than 10 fold reduction in cAMP pEC_{50} signalling. In comparison, only nine residues of ECL1 had a significant change in cAMP signalling (five alanine substitutions resulted in a decreased potency and four had an increase). In ECL3 only two substitutions had a significant change in signalling (both reduced potency) (Barwell et al., 2011). All of the ECLs of CLR have now been investigated with alanine substitution mutagenesis and the residues of ECL2 have been identified as being particularly important with respect to CGRP-mediated receptor activation.

Alanine substitution analysis identifies residues that have an effect on receptor activation through the interactions of their side chains. Common alternatives to alanine for substitution mutagenesis include cysteine or histidine substitutions. These were discussed in the introduction to chapter 3. These types of mutations utilise the properties of the side chains to provide information on their proximity to other residues within the receptor or to other interacting molecules (Elling & Schwartz, 1996; Javitch *et al.*, 2002). Another type of mutagenesis analysis uses random mutagenesis and screening. This was done for the M3 muscarinic receptor, which was screened in genetically modified yeast organisms to recover activity of previously studied point mutations (Li et al., 2005; Schmidt et al., 2003). This method identified functional motifs within this receptor.

The effects of specific residues have been analysed further by using point mutations to investigate particular properties such as charge or polarity. This methodology discovered that R314 in the CLR ICL3 domain could be mutated to either glutamate (R314E) or glutamine (R314Q) and still retains wild type signalling. This showed that polarity is the important functional property at this position for signalling, not specifically the positive charge of the WT arginine residue (Conner *et al.*, 2006a). Properties of amino acids have also been mimicked. For example, using aspartate or glutamate substitutions to confer a similar effect to that of phosphorylation to the protein being studied (Prado et al., 1998). Single site saturation mutagenesis is a technique that mutates a single amino acid to each of the remaining 20. This was used with GCGR to create an allosteric inhibitory antibody (Mukund et al., 2013).

In the publication of the GCGR crystal structure, a number of substitution mutations were created throughout the receptor and the ligand binding affinity was measured (Siu et al., 2013). A variety of substitutions were chosen, including alanine, which introduced particular properties to the receptor that could be investigated. This type of mutagenesis started to open up new possibilities with respect to the information that can be obtained. Not only can substitution analysis identify important residues but also the particular effect of those residues can be analysed.

The aim of the study in this chapter is to provide a detailed understanding of the precise molecular interactions that are occurring between CGRP and the ECL2

domain of its receptor, which result in CGRP-mediated cAMP stimulation. The majority of this investigation will be conducted through a comprehensive set of amino acid substitutions of the residues identified in chapter 3 as important for ligand-mediated receptor activation. These substitutions will attempt to mimic potential interactions through which the WT side chain may exert its effect. This information will provide a more comprehensive understanding into the mechanism through which CGRP binds and activates its receptor.

14 residues of ECL2 were identified as being important for CGRP-mediated cAMP signalling in chapter 3. This included C282 which probably forms a disulphide bond with C212 at the top of TM3. The effects of the C212A mutation were recovered with the double cysteine-alanine substitution (C212A/C282A). Therefore it appears that the function role of this disulphide bond is to prevent the disruptive properties of the remaining non-bonded cysteine side chain. This leaves 13 residues of CLR ECL2 that have an important function in ligand-mediated receptor activation, through unknown mechanisms. Two additional alanine-substitutions were previously identified as possible CAMs (Woolley et al., 2013) however further experimental repeats during the investigation in chapter 3 resulted in a loss of significance. To ensure the extended investigation into this domain was a comprehensive study, these residues were also included in the design of further mutants.

The final aspect of this continued investigation into the ECL2 domain is to examine the effect of $CGRP_{8-37}$ antagonist competition binding on the cAMP signalling for the WT receptor and selected alanine substitution mutants. The classic use of antagonist competition studies is to determine antagonist activity (Arunlakshana & Schild, 1959). This experiment has been simplified to use the competition effect of a single concentration of the $CGRP_{8-37}$ peptide with selected ECL2 alanine substitution mutants, to establish whether these substituted ECL2 residues have a change in affinity to the $CGRP_{8-37}$ ligand. This would show if the ECL2 position binds to the CGRP ligand at positions 1-7 or 8-37. The experimental design is illustrated in Figure 4.1. Using the TR-FRET cAMP signalling assay, the CGRP receptor transfected

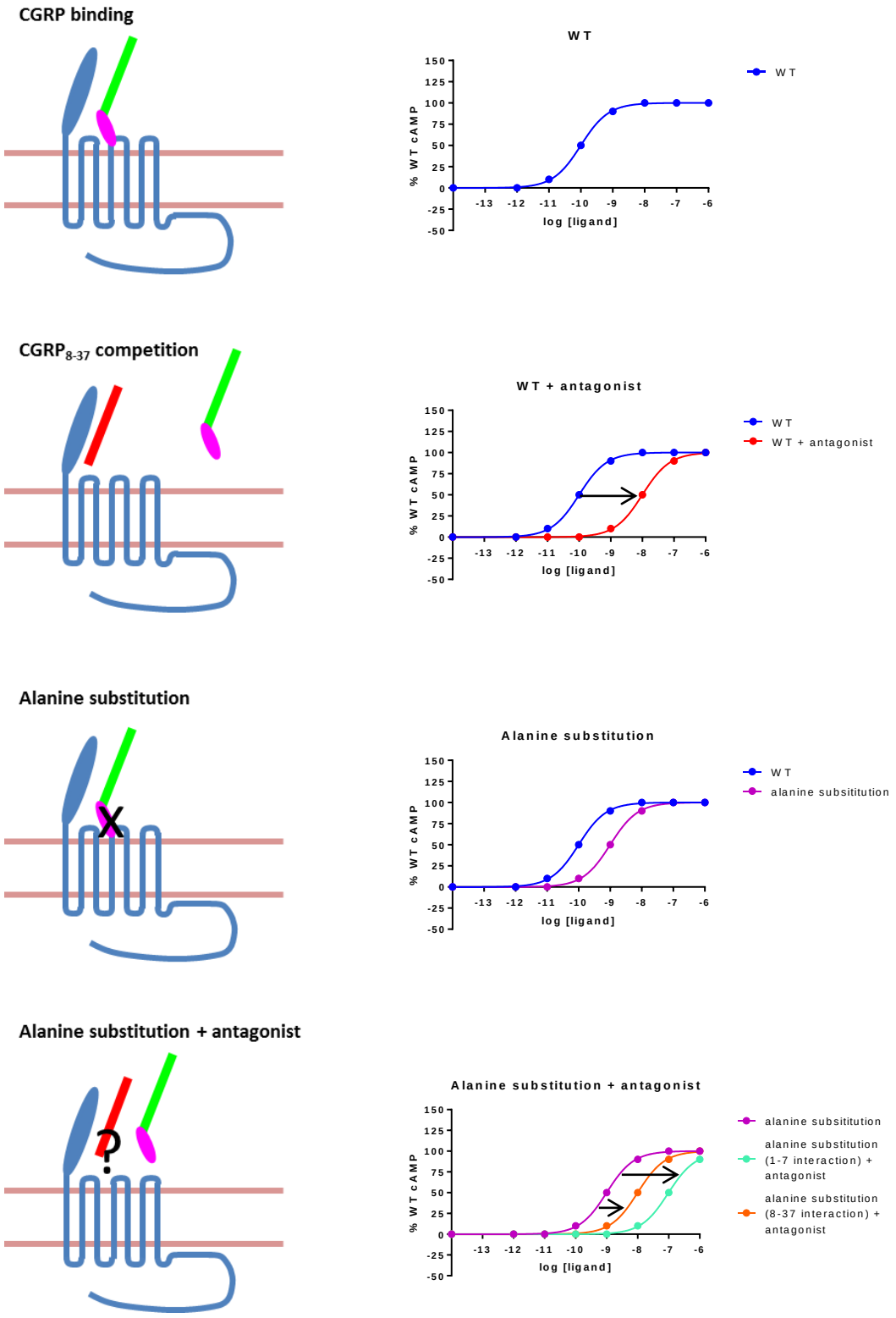

Figure 4.1. Schematic illustration of the interactions that occur between the CGRP agonist or the $CGRP_{8-37}$ antagonist with both the WT and the alanine substitution receptor.
The predicted effect of the various binding variations on the cAMP signalling response is presented with example dose response curves.

Cos7 cells were incubated with $CGRP_{8-37}$ antagonist before dose dependent stimulation with CGRP led to a competition between the agonist and the antagonist, resulting in an increased pEC_{50} at equilibrium. If the WT side chain of the residue that had been substituted with alanine would normally bind to the first 7 residues of CGRP ($CGRP_{1-7}$), then affinity to the $CGRP_{8-37}$ antagonist is not likely to be affected and the same shift in pEC_{50} observed with WT receptor was expected to be seen with the alanine substitution. If however the WT side chain of the position that had been substituted normally binds to $CGRP_{8-37}$, then the affinity for the $CGRP_{8-37}$ antagonist was expected to be reduced and therefore be displaced more easily with the full length CGRP ligand. This should result in a reduced shift in pEC_{50}.

This experiment is a simplified alternative to a full Schild plot analysis. The simplified version was chosen as an initial screen to determine the success of this method using the alanine substitutions. It was decided that a full Schild plot analysis would not be cost and time effective as an initial screen. This approach was chosen instead of binding analysis as the Perkin Elmer Lance® cAMP signalling assay protocol is established in the laboratory. Radioligand binding has been done by collaborators and has not always been successful.

The substitution mutagenesis and the antagonist competition experiments have been designed to study this loop to a level that has not been done before in any GPCR. This should greatly enhance the understanding of binding and activation of CGRP-CLR specifically and for all GPCRs.

4.2 Methods

The methods used are as described in chapters 2 and 3. Methods that are specific to this chapter are described in this section.

4.2.1 Mutagenesis to create ECL2 substitutions

The individual substitutions of ECL2 and the double substitutions L290A/L291A, L290A/Y292A and L291A/I293A were created using the primers described in Table 2.2 and an N-terminal HA tagged hCLR construct in the mammalian expression vector pcDNA3.1- as a template, following the QuikChange site directed mutagenesis protocol (2.2.3). The triple substitution L290A/L291A/Y292A was created using the L291A/Y292A primers described in Table 2.2 with the L290A alanine- substitution as a template. The S285Y/Y292S double substitution was created using the Y292S primers described in Table 2.2 and the S285Y further substitution as a template.

Following DpnI degradation of the template DNA, the PCR product was transformed into chemically competent Top10 *E.coli* cells (2.2.10) and plasmid DNA was amplified and purified (2.2.11). The purified DNA was electrophoresed alongside a pre-DpnI treated sample (2.2.7) to confirm successful degradation of the template DNA. Purified DNA was sent for sequencing (2.2.12) to confirm successful mutagenesis.

4.2.2 cAMP TR-FRET signalling assay with $CGRP_{8-37}$ competition

48 hours following transfection, cells were removed from the plate with 0.25% (w/v) Trypsin - 0.53 mM EDTA solution, washed with PBS and resuspended in assay stimulation buffer (SB, PBS + 0.1% BSA + 0.5mM IBMX). The cells were counted with a haemocytometer and the appropriate cell number pelleted at 500g for 4 min, to be resuspended in SB + 1/100 AlexaFluor® 647-anti cAMP antibody at an assay concentration of 2000 cells/10µl. 2000 cells/well (10µl) were loaded onto a 96 well white Optiplate. The cells were incubated in triplicate with 5µl SB ± $4x10^{-6}$M $CGRP_{8-37}$ (x4 final concentration) and were dose dependently stimulated in triplicate with a logarithmic increase of CGRP diluted in SB from 10^{-6}M to 10^{-12}M with SB as a basal

in a 5µl volume at a x4 final concentration. The plate was incubated in the absence of light for 30 min before 20µl/well of detection mix was added. The plate was incubated in the absence of light for a further 60 minutes. TR-FRET was recorded by excitation at 320mm and emission at 665nm.

4.3 Results

4.3.1 Amino acid substitution mutagenesis of ECL2

4.3.1.1 Criteria for deciding on the ECL2 substitutions

All residues shown to have a significant reduction in CGRP-mediated cAMP pEC_{50} signalling in the alanine substitution mutagenesis described in chapter 3 were targeted for further investigation, with the exception of C282. Signalling of this mutant was recovered with the double alanine substitution C212A/C282A. Two additional residues of this loop were included for further investigation. These were N281 and I294, previously identified as CAMs (Woolley et al., 2013). The aim of this study was to mutate these residues to amino acids different to that of wild type, whilst retaining particular properties to that of the wild type, in order to deduce the particular molecular interactions that are involved in CGRP-mediated receptor interaction. The positions of ECL2 being studied, the amino acids chosen as a substitution and the rational for that choice is summarised in Table 4.1. This rational will be described in more detail in this section.

A273: The A273L substitution resulted in an ~3 fold decrease in cAMP signalling potency. To investigate whether the extended hydrophobic side chain caused a loss of structural integrity of the loop or impeded CGRP binding, glycine (A273G) was chosen as a substitution mutation to determine if the reduction of side chain length improved signalling compared to WT CLR.

R274: The R274A substitution resulted in ~100 fold reduction in cAMP signalling potency. To establish if it is just a positive charge that is required in this area of the loop, or if the particular position of the charge is vital, a conservative substitution of a lysine residue (R274K) was selected.

Y277 and Y278: Both alanine substitutions resulted in ~10 fold reduction in cAMP signalling potency. To establish if the effect of the tyrosine side chain is due to the OH group, the benzene ring or just the presence of hydrophobicity in this area of the loop, mutation to phenylalanine (Y277F and Y278F) and to leucine (Y277L and Y278L) was chosen.

Alanine	ECL2 substitutions	Reason
A273L	A273G	L reduced pEC_{50}, will G increase pEC_{50}
R274A	R274K	Amine group in different position
Y277A	Y277F	Benzene ring
	Y277L	Hydrophobic side chain
Y278A	Y278F	Benzene ring
	Y278L	Hydrophobic side chain
D280A	D280E	Carboxyl group in different position
	D280L	Hydrophobic side chain, similar shape
	D280N	Steric effect with similar polar side chain
	D280S	Polar side chain
	D280T	Extended polar side chain
N281A	N281K	Inactivation lock with positive charge
W283A	W283F	Benzene ring
	W283H	Imidazole ring
I284A	I284F	Hydrophobic side chain different shape
	I284L	Hydrophobic side chain different shape
	I284Q	Polar side chain with similar shape
S285A	S285D	Negative charge similar position
	S285N	Polar effect
	S285T	OH group in different position
	S285Y	Control for the S285YY292S reciprocal
	S285Y/Y292S	Reciprocal substitution testing for recovery
D287A	D287E	Carboxyl group in different position
	D287L	Hydrophobic side chain, similar shape
T288A	T288D	Negative charge similar position
	T288N	Polar effect similar position
	T288S	OH group in different position
	T288V	Hydrophobic side chain, similar shape
L290A-Y292A	L290A/L291A/Y292A	Combined effect of triple mutant
	L290A/L291A	Combined effect of double mutant
	L290A/Y292A	Combined effect of double mutant
	L291A/I293A	Combined effect of double mutant
	L290N	Polar side chain with similar shape
	L291N	Polar side chain with similar shape
	Y292S	Control for the S285YY292S reciprocal
I294A	I294G	Increased CAM effect

Table 4.1. Summary of the new substitutions selected for further investigation of key residues identified through alanine substitution analysis.
The amino acids chosen for substitution at each position and the hypothesis for the effect being tested with the new substitution is described.

D280: The D280A substitution resulted in a ~100 fold reduction in cAMP signalling potency. The computer modelling of ECL2 (Woolley et al., 2013) positioned D280 in the middle of the loop projecting towards the centre of the TM bundle. This suggests that D280 may be important in CGRP binding and subsequent receptor activation. A number of substitutions were therefore chosen at this position to establish the role of the aspartate residue at position 280. These were a conservative glutamate substitution (D280E) to see if just the presence of a negative charge is required. Leucine (D280L) was chosen as its side chain closely resembles the steric properties of the aspartate side chain however with all the charged properties removed. To determine if polarity at a position close to the negative charge of the aspartate side chain is sufficient to recover signalling, asparagine, serine and threonine were also selected (D280N, D280S and D280T respectively).

N281: The N281A substitution previously resulted in a CAM (Woolley et al., 2013). It was speculated that the polarity of the asparagine side chain could act as a lock, retaining the receptor in the inactive conformation. Lysine (N281K) was selected for substitution in an attempt to increase the effects of this potential locking effect through the positive charge of the side chain.

W283: The W283A substitution resulted in ~300 fold reduction in cAMP signalling potency. The tryptophan side chain consists of an imidazole ring and a benzene ring. To establish which component of the side chain is important, mutation to histidine and phenylalanine was chosen (W283H and W283F respectively).

I284: The I284A substitution had ~10 fold reduction in CGRP-mediated cAMP signalling potency. To determine if this position requires hydrophobicity, substitutions to both phenylalanine (I284F) and leucine (I284L) were selected. Phenylalanine has a large hydrophobic side chain. The side chain of leucine has a similar steric effect to isoleucine and is therefore a conservative substitution to attempt to recover signalling. The polar side chain of glutamine was used to see if the function of this position is due to the shape of the side chain as opposed to the hydrophobicity.

S285: The S285A substitution had ~5 fold reduction in cAMP signalling potency. To establish whether there was flexibility in the size and position of the hydroxyl group in the side chain, a conservative threonine substitution (S285T) was used. Asparagine (S285N) was chosen to determine if the role of S285 is due to a requirement for general polarity of the side chain, and aspartate (S285D) was chosen to see if the effects of the wild type side chain are due to the negative polarity within serine hydroxyl group. Earlier models of the ECL2 domain (Pers. Comms.) also suggested that the side chain of S285 could form interactions with Y292. To test this prediction, a reciprocal double substitution was made (S285Y/Y292S) in an attempt to recover signalling, together with the single mutants (S285Y and Y292S) as controls.

D287: The D287A substitution had ~5 fold reduction in cAMP signalling potency. A conservative glutamate substitution (D287E) was used to establish if just a negative charge is required in this position. A leucine mutation (D287L) was also chosen to determine if the effects at this position are due to the shape of the side chain rather than the charge.

T288: The T288A substitution had ~20 fold reduction in cAMP signalling potency. A conservative serine substitution (T288S) was used to establish if there is flexibility in the positioning of the hydroxyl group to recover signalling. To establish if the negative polarity of the wild type hydroxyl group is utilised, an aspartate substitution (T288D) was chosen. To determine if the functional effect of the wild type is through general polarity in this position, an asparagine substitution was used (T288N).

L290, L291 and Y292: The effects of the alanine substitutions for L290A, L291A and Y292A were ~6 fold, ~4 fold and ~2 fold reduction in cAMP signalling potency respectively. These reductions are small, however the fact that each residue of this triplet of amino acids at the extreme C-terminus of ECL2 has an effect indicates the possibility of an important functional motif. To investigate this further, the effect of the combined double alanine substitution L290A/L291A L290A/Y292A and L291A/I293A and the triple substitution L290A, L291A and Y292A (L290A/L291A/Y292A) was tested. Finally, to gain a more detailed understanding

into the effect of the two leucine residues at positions 290 and 291, each were mutated to asparagine (L290N and L291N), which has a similar shaped side chain, however with a polar property instead of a hydrophobic property.

4.3.1.2 Selecting receptor activation assays

The criteria for selecting receptor activation assays have been previously described in section 3.3.2. The rationale for undertaking the substitution mutagenesis analysis is to identify the key molecular interactions of ECL2 that are responsible for the ligand mediated activation of the receptor, by observing the effect on cAMP signalling. To quantify this effect, the Perkin-Elmer Lance® cAMP detection kit will be used. As previously described it is important to ascertain whether any effect on signalling is shown by a receptor that is successfully expressed at the cell surface. To account for this the cell surface expression ELISA will be used.

It was decided that cAMP signalling and cell surface expression analysis would be sufficient for the investigation of the substitution mutations. The Lance® TR-FRET cAMP signalling assay used in chapter 3 provided a sensitive and accurate means to measure ligand-induced receptor activation. Any effect on ligand binding was detected through this assay. It was therefore decided that the signalling assay would be a sufficient means to test for receptor activation. Receptor internalisation occurs in response to receptor activation. Like the binding assays, receptor internalisation levels in the alanine scan were in direct relation to signalling. It was decided that results from the internalisation assay would not provide any further useful information.

4.3.1.3 cAMP signalling of ECL2 substitutions

The effect of the substitutions of the ECL2 domain of CLR on receptor activation was tested by measuring the effect on CGRP-mediated cAMP signalling using a TR-FRET based cAMP assay.

Cos7 cells were transfected with WT or mutated CLR (together with a RAMP1 construct) and the TR-FRET cAMP assay and analysis were carried out as previously described (2.2.15 and 2.2.18).

A comprehensive summary of the pEC_{50}, basal and E_{max} results is presented in Table 4.2. Significantly reduced cAMP pEC_{50} values have been separately highlighted to show a <10 fold decrease (orange), a 10-100 fold decrease (purple) and a >100 fold decrease (red) compared with WT receptor. Significantly increased pEC_{50}, basal and E_{max} values have also been highlighted (blue). A representative cAMP signalling curve for each substitution is shown in Figure 4.2 to Figure 4.7.

36 new CLR ECL2 substitutions were constructed and analysed as described. These are shown in Table 4.2. These results will be separated into pEC_{50}, basal and E_{max} sections to allow each component of the receptor signalling data to be clearly described.

4.3.1.3.1 pEC_{50} values

The pEC_{50} values are shown in full in Table 4.2. In this table the pEC_{50} mean and SEM values are detailed for both the substituted receptor and the WT experimental control. The substitutions have been highlighted to describe the level of reduction observed compared with WT.

Seven ECL2 substitutions (A273G, Y277F, Y277L, Y278F, W283H, D287E and I294G) have pEC_{50} values statistically similar to that of the WT receptor showing a complete recovery in cAMP signalling compared with the alanine substitution. 10 substitutions had a modest reduction (<10 fold) in cAMP pEC_{50} signalling (N281K, I284L, S285D, S285N, S285T, D287L, T288S, L290N, L291N and Y292S). 16 substitutions had a 10-100 fold reduction in cAMP pEC_{50} signalling (R274K, Y278L, D280E, D280L, D280N, D280S, D280T, W283F, I284F, I284Q, S285Y, S285Y/Y292S, T288N, T288V, L290A/Y292A and L291A/I293A). Three substitutions had a >100 fold reduction in cAMP pEC_{50} signalling (T288D, L290A/L291A/Y292A and L290A/L291A). It is useful to compare how the cAMP pEC_{50} signalling with the substitution mutations compares with that of the original alanine substitution analysis from chapter 3. This was determined by comparing the difference in pEC_{50} values between the substituted receptor with its WT experimental control and the alanine substitution with its experimental WT control.

ECL2 substitution	pEC_{50} (ECL2 substitution)			pEC_{50} (WT CLR)			pEC_{50}		Basal (ECL2 substitution)				E_{max} (ECL2 substitution)			
	Mean	SEM	N	Mean	SEM	N	difference	t-test	Mean	SEM	N	t-test	Mean	SEM	N	t-test
A273G	-10.74	0.09	3	-10.85	0.12	3	-0.11	0.4798	13.37	4.94	3	0.1136	104.30	2.11	3	0.1804
R274K	-8.62	0.52	3	-10.03	0.52	3	-1.41	0.0007***	-0.33	3.03	3	0.9236	99.30	6.86	3	0.928
Y277F	-9.87	0.53	4	-10.02	0.45	4	-0.15	0.2103	13.56	6.13	4	0.1137	100.40	6.30	4	0.9481
Y277L	-9.57	0.44	4	-9.88	0.42	4	-0.31	0.1308	16.64	6.40	4	0.0805	109.30	4.88	4	0.1513
Y278F	-9.81	0.41	4	-9.92	0.49	4	-0.10	0.4251	16.71	8.22	4	0.1349	110.50	4.42	4	0.0983
Y278L	-8.98	0.46	3	-10.11	0.54	3	-1.13	0.0085**	9.58	5.09	3	0.2003	99.79	5.68	3	0.9743
D280E	-8.78	0.46	4	-10.03	0.42	4	-1.25	0.0231*	2.58	7.54	4	0.7545	112.90	9.48	4	0.2673
D280L	-8.44	0.23	4	-10.41	0.29	4	-1.97	0.0157*	11.14	10.11	4	0.3508	99.15	3.44	4	0.8206
D280N	-8.71	0.23	4	-10.44	0.30	4	-1.73	0.0335*	20.95	6.21	4	0.0432*	107.40	5.52	4	0.2728
D280S	-8.66	0.39	4	-10.06	0.44	4	-1.40	0.0005***	4.18	8.97	4	0.6733	97.86	9.32	4	0.8334
D280T	-8.89	0.35	4	-10.20	0.43	4	-1.31	0.0038**	14.54	6.92	4	0.1265	94.66	2.78	4	0.1503
N281K	-9.19	0.31	6	-10.04	0.30	6	-0.85	0.0141*	15.42	7.27	6	0.0874	102.20	8.63	6	0.8114
W283F	-9.07	0.33	5	-10.13	0.20	5	-1.06	0.0111*	7.57	8.10	5	0.4031	103.30	5.14	5	0.5609
W283H	-10.81	0.09	4	-10.86	0.09	4	-0.05	0.7674	16.37	5.72	4	0.0645	104.60	6.02	4	0.4964
I284F	-9.76	0.20	3	-10.89	0.22	3	-1.13	0.0048**	13.66	3.16	3	0.0494*	113.10	3.45	3	0.0629
I284L	-10.24	0.10	3	-10.73	0.13	3	-0.49	0.0059**	6.24	4.05	3	0.2633	108.60	5.56	3	0.2619
I284Q	-9.45	0.05	3	-11.15	0.11	3	-1.70	0.0024**	14.45	3.76	3	0.0617	104.00	0.19	3	0.0021**
S285D	-9.26	0.39	4	-10.00	0.40	4	-0.74	0.0057**	5.43	2.90	4	0.1579	99.25	5.37	4	0.8974
S285N	-9.83	0.30	6	-10.35	0.28	6	-0.52	0.011*	5.78	4.70	6	0.273	98.55	4.13	6	0.7401
S285T	-9.96	0.36	5	-10.30	0.35	5	-0.34	0.0004***	13.51	5.89	5	0.0833	95.48	4.74	5	0.3943
S285Y	-9.12	0.29	3	-10.48	0.22	3	-1.36	0.0051**	8.19	2.08	3	0.0591	91.01	9.77	3	0.4544
S285YY292S	-8.32	0.51	3	-9.89	0.45	3	-1.57	0.0058**	11.45	3.43	3	0.0792	116.30	14.54	3	0.3782
D287E	-10.70	0.18	3	-10.90	0.25	3	-0.20	0.2112	15.03	4.23	3	0.0709	106.50	2.43	3	0.115
D287L	-10.53	0.13	4	-10.94	0.14	4	-0.41	0.0196*	17.17	6.16	4	0.0686	103.80	4.46	4	0.4554
T288D	-7.35	0.30	3	-9.66	0.35	3	-2.31	0.0047**	5.03	6.71	3	0.5317	97.91	16.69	3	0.9119
T288N	-8.54	0.48	3	-10.15	0.55	3	-1.61	0.0025**	7.64	4.62	3	0.2399	93.93	8.48	3	0.5487
T288S	-9.56	0.41	4	-9.90	0.49	4	-0.35	0.0079**	12.76	2.38	4	0.0127*	104.20	4.74	4	0.4376
T288V	-8.52	0.45	3	-10.36	0.26	3	-1.84	0.0247*	8.12	6.19	3	0.3195	102.30	4.91	3	0.6865
LLYAAA	-6.46	0.74	3	-10.38	0.43	3	-3.92	0.0065**	10.27	1.99	3	0.0355*	104.60	2.90	2	0.3581
L290AL291A	-7.93	0.13	3	-10.58	0.12	3	-2.65	0.0084**	16.39	7.15	3	0.1489	110.40	3.95	3	0.1199
L290AY292A	-7.84	0.31	4	-9.47	0.42	4	-1.63	0.0007***	0.16	5.41	4	0.9789	114.40	10.75	4	0.2727
L291AI293A	-8.01	0.07	4	-9.09	0.10	4	-1.08	0.0006***	10.80	3.08	4	0.0393*	118.90	12.49	4	0.2274
L290N	-10.18	0.03	4	-10.87	0.05	4	-0.69	0.0009***	10.58	6.99	4	0.2274	97.65	2.16	4	0.3571
L291N	-10.60	0.10	5	-10.88	0.04	5	-0.28	0.0386*	17.50	2.91	5	0.0038**	110.10	5.25	5	0.1267
Y292S	-9.27	0.44	3	-9.97	0.50	3	-0.71	0.0059**	15.63	7.93	3	0.1876	112.60	14.05	3	0.4647
I294G	-10.48	0.38	4	-10.31	0.40	4	0.17	0.4323	10.16	9.51	4	0.3634	109.30	7.72	4	0.3138

Decrease < 10 fold | Decrease 10-100 fold | Decrease > 100 fold | Increase

Table 4.2. Summary of the pEC_{50}, basal and E_{max} mean and SEM values for the ECL2 substitution and the WT receptor.

Cos7 cells transfected with WT and substituted receptor were dose dependently stimulated with CGRP and levels of the cAMP second messenger were detected using a TR-FRET based cAMP assay. A sigmoidal dose response curve was fitted to the data using GraphPad Prism software. The substituted receptor data were normalised to WT, taking the maximum and minimum values obtained from the WT dose response curve. The number of experimental repeats is denoted in the N column and the significance was obtained through paired t-test. *$p < 0.05$, ** $p < 0.01$, ***$p < 0.001$.

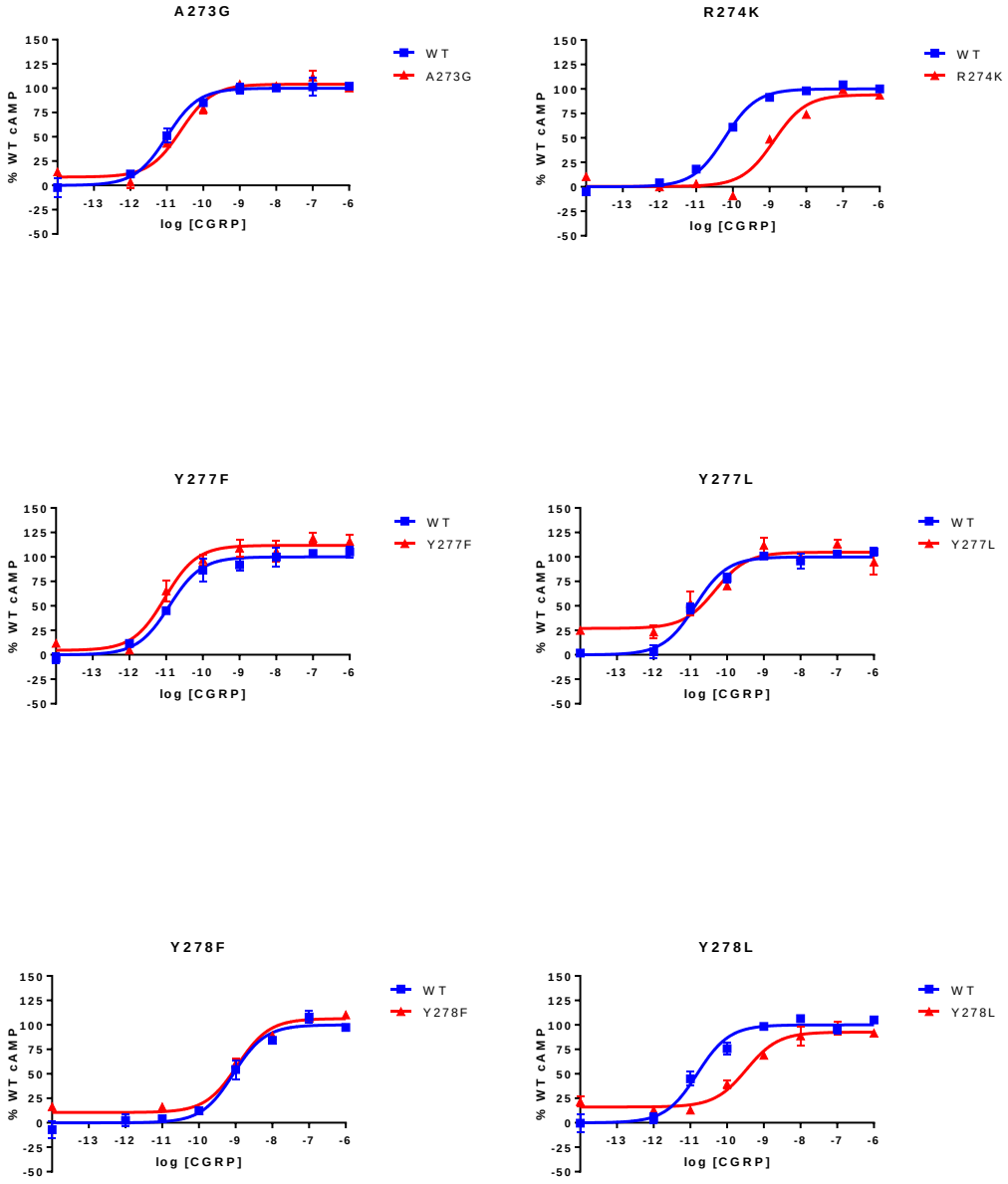

Figure 4.2. Representative cAMP signalling curves for A273G, R274K, Y277F, Y277L, Y278F and Y278L substitutions.

Cos7 cells transfected with WT and mutated receptor were stimulated with CGRP in a dose-dependent manner. Levels of the cAMP second messenger were detected using a TR-FRET based cAMP assay. A sigmoidal dose response curve was fitted to the data using GraphPad Prism software. The substituted receptor data were normalised to WT, taking the maximum and minimum values obtained from the WT dose response curve.

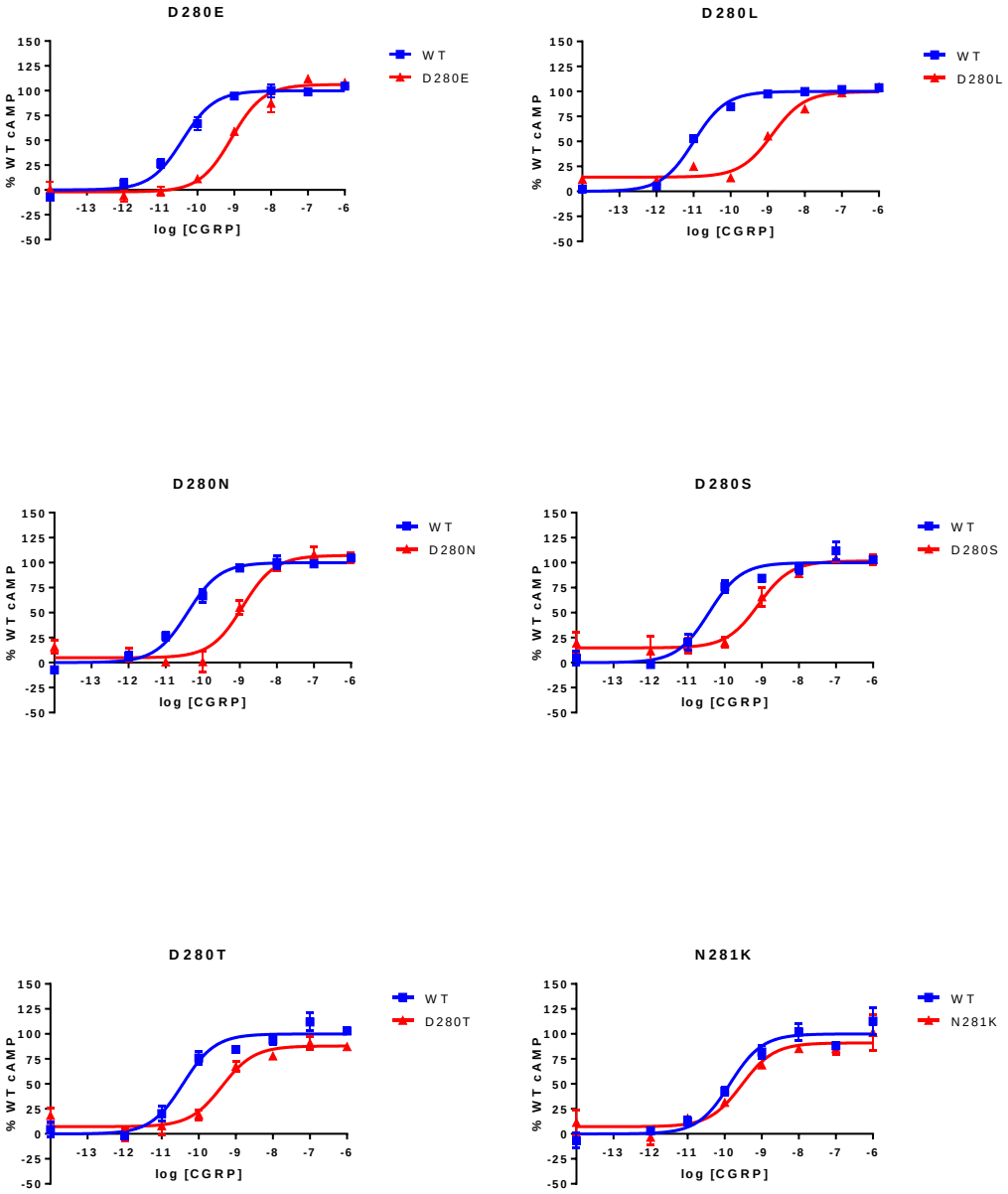

Figure 4.3. Representative cAMP signalling curves for D280E, D280L, D280N, D280S, D280T and N281K substitutions.

Cos7 cells transfected with WT and substituted receptor were stimulated with CGRP in a dose-dependent manner. Levels of the cAMP second messenger were detected using a TR-FRET based cAMP assay. A sigmoidal dose response curve was fitted to the data using GraphPad Prism software. The substituted receptor data were normalised to WT, taking the maximum and minimum values obtained from the WT dose response curve.

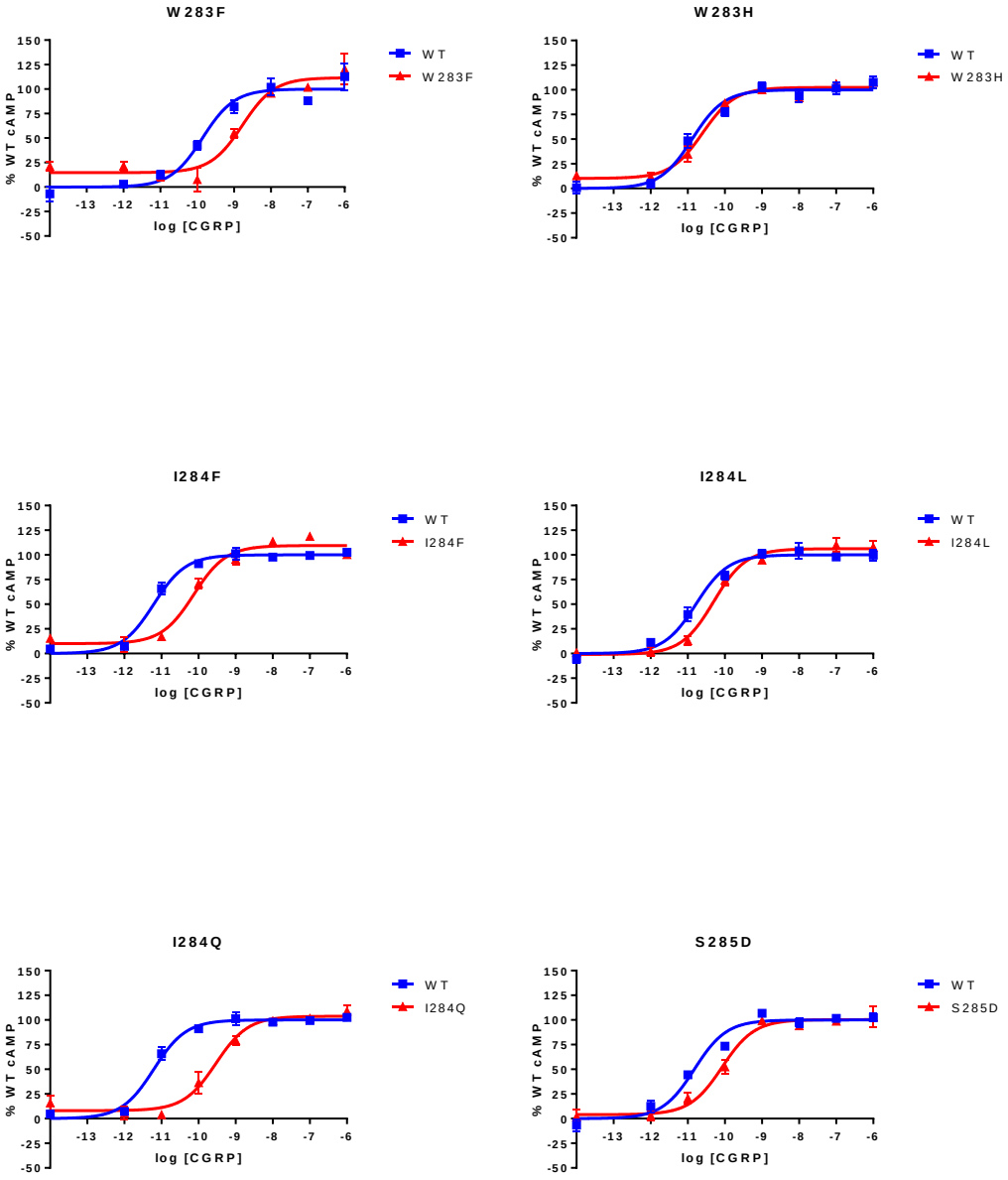

Figure 4.4. Representative cAMP signalling curves for W283F, W283H, I284F, I284L, I284Q and S285D substitutions.

Cos7 cells transfected with WT and substituted receptor were stimulated with CGRP in a dose-dependent manner. Levels of the cAMP second messenger were detected using a TR-FRET based cAMP assay. A sigmoidal dose response curve was fitted to the data using GraphPad Prism software. The substituted receptor data were normalised to WT, taking the maximum and minimum values obtained from the WT dose response curve.

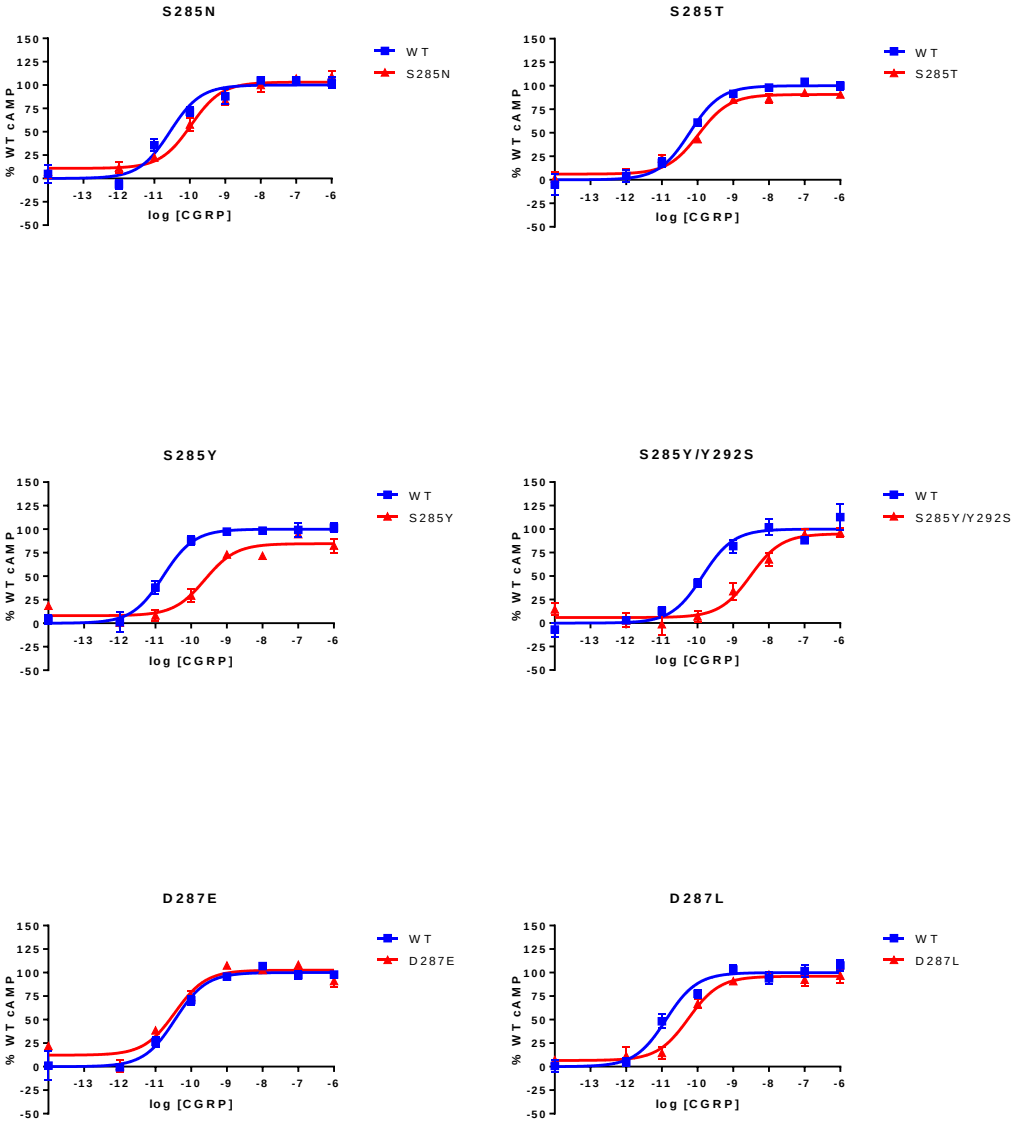

Figure 4.5 Representative cAMP signalling curves for S285N, S285T, S285Y, S285Y/Y292S, D287E and D287L substitutions.

Cos7 cells transfected with WT and substituted receptor were stimulated with CGRP in a dose-dependent manner. Levels of the cAMP second messenger were detected using a TR-FRET based cAMP assay. A sigmoidal dose response curve was fitted to the data using GraphPad Prism software. The substituted receptor data were normalised to WT, taking the maximum and minimum values obtained from the WT dose response curve.

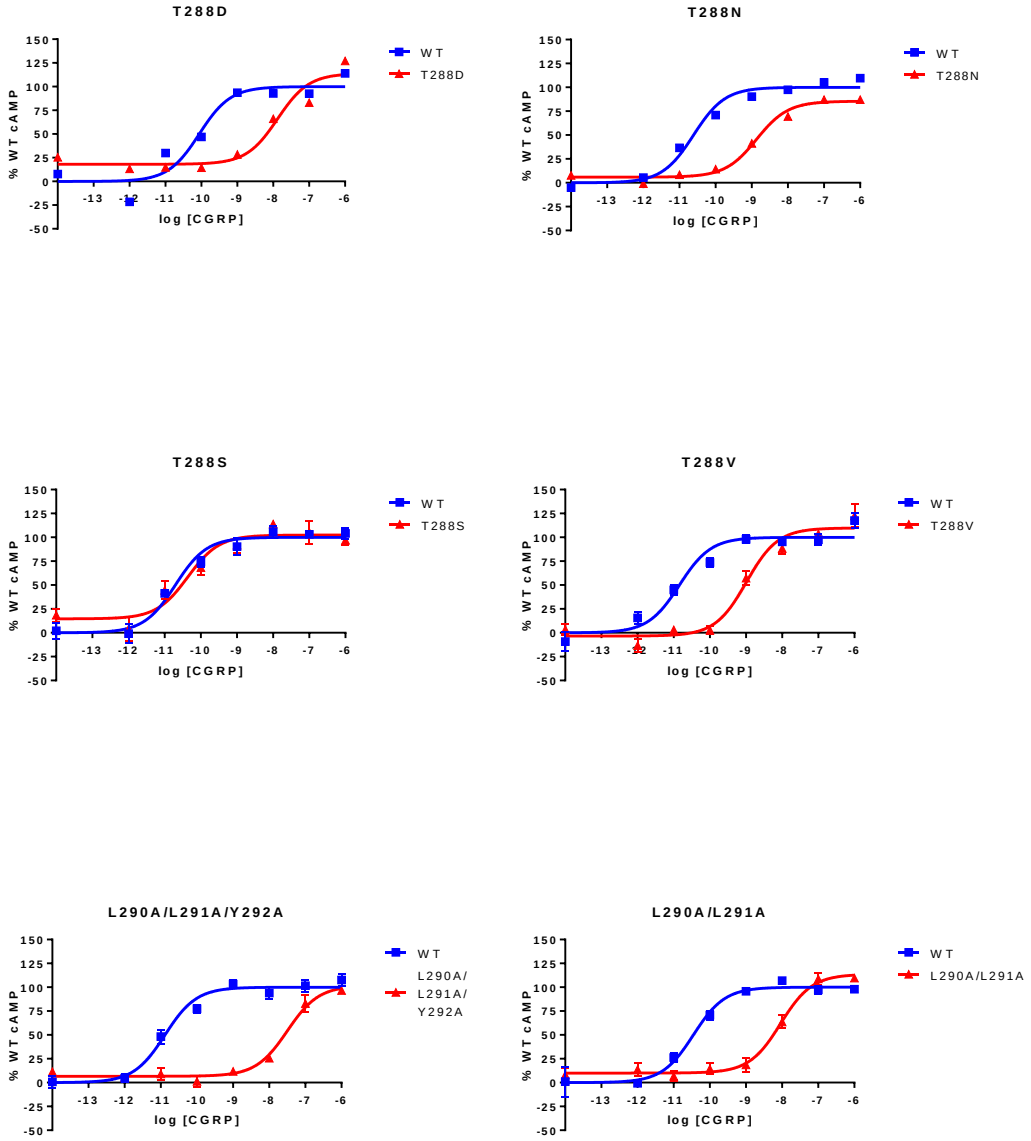

Figure 4.6. Representative cAMP signalling curves for T288D, T288N, T288S, T288V, L290A/L291A/Y292A and L290A/L291A substitutions.

Cos7 cells transfected with WT and substituted receptor were stimulated with CGRP in a dose-dependent manner. Levels of the cAMP second messenger were detected using a TR-FRET based cAMP assay. A sigmoidal dose response curve was fitted to the data using GraphPad Prism software. The substituted receptor data were normalised to WT, taking the maximum and minimum values obtained from the WT dose response curve.

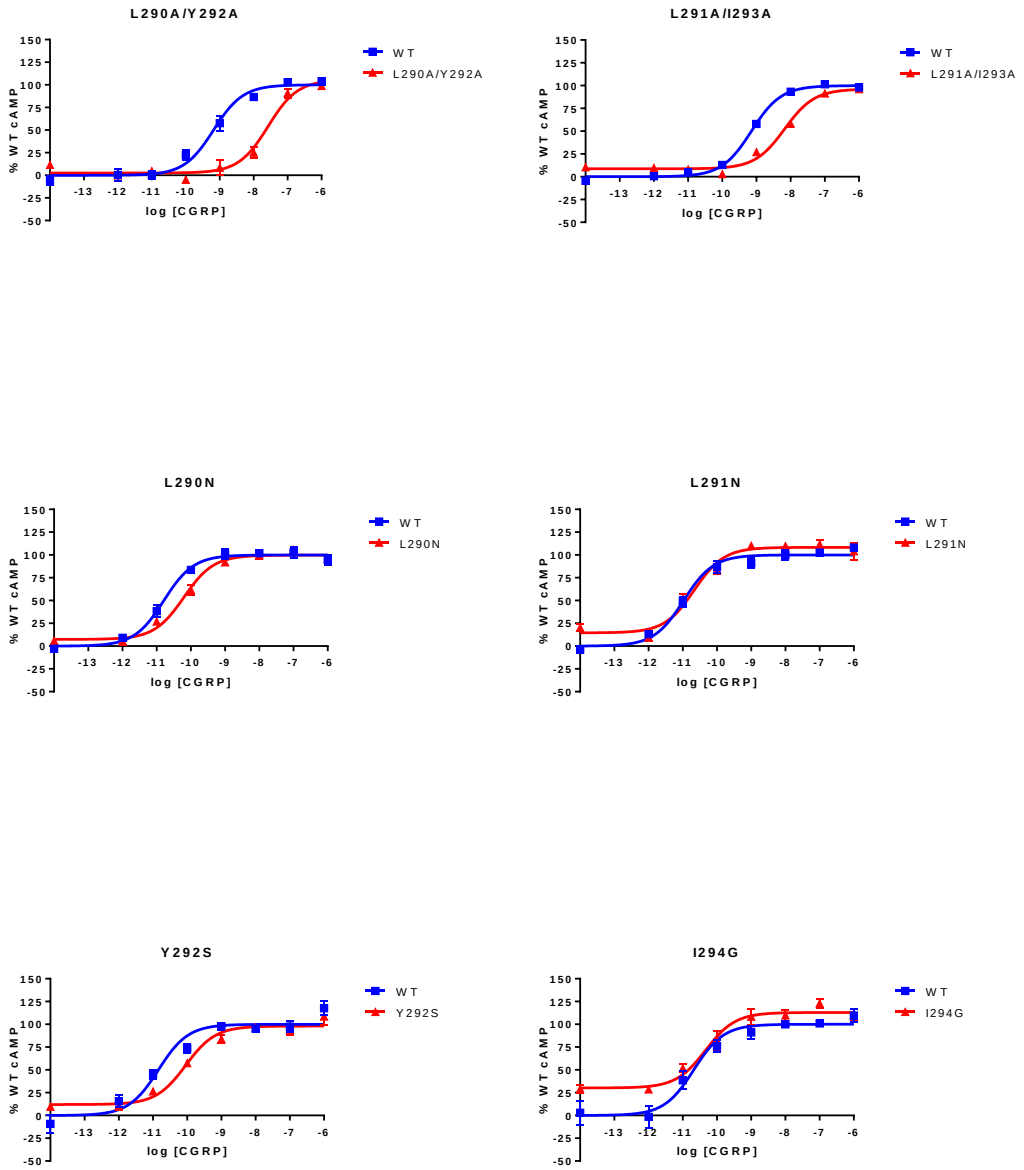

Figure 4.7 Representative cAMP signalling curves for L290A/Y292A, L291A/I293A, L290N, L291N, Y292S and I294G.

Cos7 cells transfected with WT and substituted receptor were stimulated with CGRP in a dose-dependent manner. Levels of the cAMP second messenger were detected using a TR-FRET based cAMP assay. A sigmoidal dose response curve was fitted to the data using GraphPad Prism software. The substituted receptor data were normalised to WT, taking the maximum and minimum values obtained from the WT dose response curve.

The results from this analysis are presented in Table 4.3 and illustrated graphically in Figure 4.8. In Table 4.3 the first set of columns detail the pEC_{50} difference of the alanine substitutions with the WT control for the residues, which were chosen for further investigation. The second set of columns detail the pEC_{50} difference of the substituted receptor with the WT control. The final column shows the results of the unpaired t-test comparing the differences of the substituted receptor with that of their respective alanine substitutions. In this column, values are highlighted to distinguish between substitutions that:

1. Recover signalling (no significant different between substituted receptor and WT pEC_{50}).

2. Partially recover signalling (significant difference between substituted receptor with WT pEC_{50} and substituted receptor with alanine substitution pEC_{50} difference).

3. Substitutions with no recovery (significant difference between substituted receptor with WT pEC_{50} but no difference between substituted receptor with alanine substitution pEC_{50} log difference).

4. Those that further reduced the pEC_{50} values compared with the alanine substitution (significant difference between substituted receptor with WT pEC_{50} and substituted receptor with alanine substitution pEC_{50} difference).

Figure 4.8 is a graphical representation of the difference between the substituted receptor and WT pEC_{50} values for both the alanine substitution and the substituted receptor analysis. The results of the statistical comparison between these two set of values is also shown.

The results of this analysis show the effect of the substitutions compared with the original alanine substitution analysis. Six substitutions (A273G, Y277F, Y277L, Y278F, W283H and I294G) had a complete recovery of cAMP signalling. Six substitutions (R274K, D280S, W283F, I284L, T288S and L291N) had a partial recovery of cAMP signalling compared with the respective alanine substitution. 14 substitutions (Y278L, D280E, D280L, D280N, D280T, I284F, S285D, S285N, S285T, D287L, T288N, T288V, L290N and Y292S) show no recovery of cAMP signalling. Five substitutions (N281K, I284Q, S285Y, S285Y/Y292S and T288D) resulted in a significant reduction

pEC_{50} difference alanine vs wt					pEC_{50} difference non-alanine vs wt					alanine vs
Alanine	Mean	SEM	N	t test (WT)	Non-alanine	Mean	SEM	N	t test (WT)	non-alanine t test
A271L	0.01	0.03	3	0.8891						
I272A	0.00	0.01	3	0.86						
A273L	-0.47	0.09	3	0.034*	A273G	-0.12	0.14	3	0.4798	0.0964
R274A	-2.18	0.16	3	0.0054**	R274K	-1.42	0.04	3	0.0007***	0.0098**
S275A	-0.16	0.13	3	0.36						
L276A	-0.12	0.03	3	0.05						
Y277A	-0.89	0.16	4	0.0121*	Y277F	-0.16	0.10	4	0.2103	0.0087**
					Y277L	-0.31	0.15	4	0.1308	0.0402*
Y278A	-1.08	0.20	5	0.006**	Y278F	-0.10	0.11	4	0.4251	0.0057**
					Y278L	-1.13	0.11	3	0.0085**	0.8561
N279A	-0.20	0.13	4	0.23						
D280A	-1.90	0.16	3	0.0067**	D280E	-1.26	0.29	4	0.0231*	0.1431
					D280L	-1.97	0.40	4	0.0157*	0.8861
					D280N	-1.73	0.46	4	0.0335*	0.7781
					D280S	-1.40	0.09	4	0.0005***	0.0302*
					D280T	-1.31	0.16	4	0.0038**	0.0509
N281A	0.10	0.14	5	0.5182	N281K	-0.85	0.23	6	0.0141*	0.0085**
C282A	-1.13	0.12	3	0.0119*						
W283A	-2.54	0.17	3	0.0042**	W283F	-1.06	0.24	5	0.0111*	0.0046**
					W283H	-0.05	0.15	4	0.7674	< 0.0001****
I284A	-1.11	0.12	3	0.012*	I284F	-1.13	0.08	3	0.0048**	0.8695
					I284L	-0.50	0.04	3	0.0059**	0.0091**
					I284Q	-1.70	0.08	3	0.0024**	0.0165*
S285A	-0.70	0.18	5	0.018*	S285D	-0.75	0.11	4	0.0057**	0.831
					S285N	-0.52	0.13	6	0.011*	0.4477
					S285T	-0.34	0.03	5	0.0004***	0.083
					S285Y	-1.36	0.10	3	0.0051**	0.0375*
					S285YY292S	-1.57	0.12	3	0.0058**	0.0141*
S286A	0.07	0.13	3	0.63						
D287A	-0.71	0.22	4	0.0475*	D287E	-0.19	0.11	3	0.2112	0.1172
					D287L	-0.41	0.09	4	0.0196*	0.2427
T288A	-1.39	0.14	4	0.0021**	T288D	-2.31	0.16	3	0.0047**	0.0071**
					T288N	-1.61	0.08	3	0.0025**	0.2576
					T288S	-0.35	0.12	4	0.0079**	0.0012**
					T288V	-1.83	0.29	3	0.0247*	0.1902
H289A	-0.03	0.17	3	0.86						
L290A	-0.86	0.12	3	0.019*	LLYAAA	-3.92	0.32	3	0.0065**	
L291A	-0.65	0.07	3	0.013*	L290AL291A	-2.65	0.25	3	0.0084**	
					L290AY292A	-1.63	0.11	4	0.0007***	
					L291AI293A	-1.08	0.07	4	0.0006***	
					L290N	-0.69	0.05	4	0.0009***	0.2078
					L291N	-0.28	0.09	5	0.0386*	0.0318*
Y292A	-0.46	0.13	4	0.0347*	Y292S	-0.71	0.05	3	0.0059**	0.1771
I293A	-0.23	0.09	3	0.13						
I294A	0.39	0.14	4	0.0679	I294G	0.17	0.19	4	0.4323	0.3858

Decreased EC50 | Full recovery | Partial recovery | No recovery | Reduced signalling

Table 4.3 Summary of the mean and SEM values of the difference between the substitution and WT pEC_{50} values for both the alanine substitution and the substituted receptor investigations.

The difference between the substitution and WT pEC_{50} values for each experimental repeat were obtained and mean and SEM values calculated. A paired t-test was used to determine significance between substitution and WT values. To calculate significance between the alanine and the substituted receptor an unpaired t-test was used on the values calculated from the difference between alanine substitution vs WT and substituted receptor vs WT.

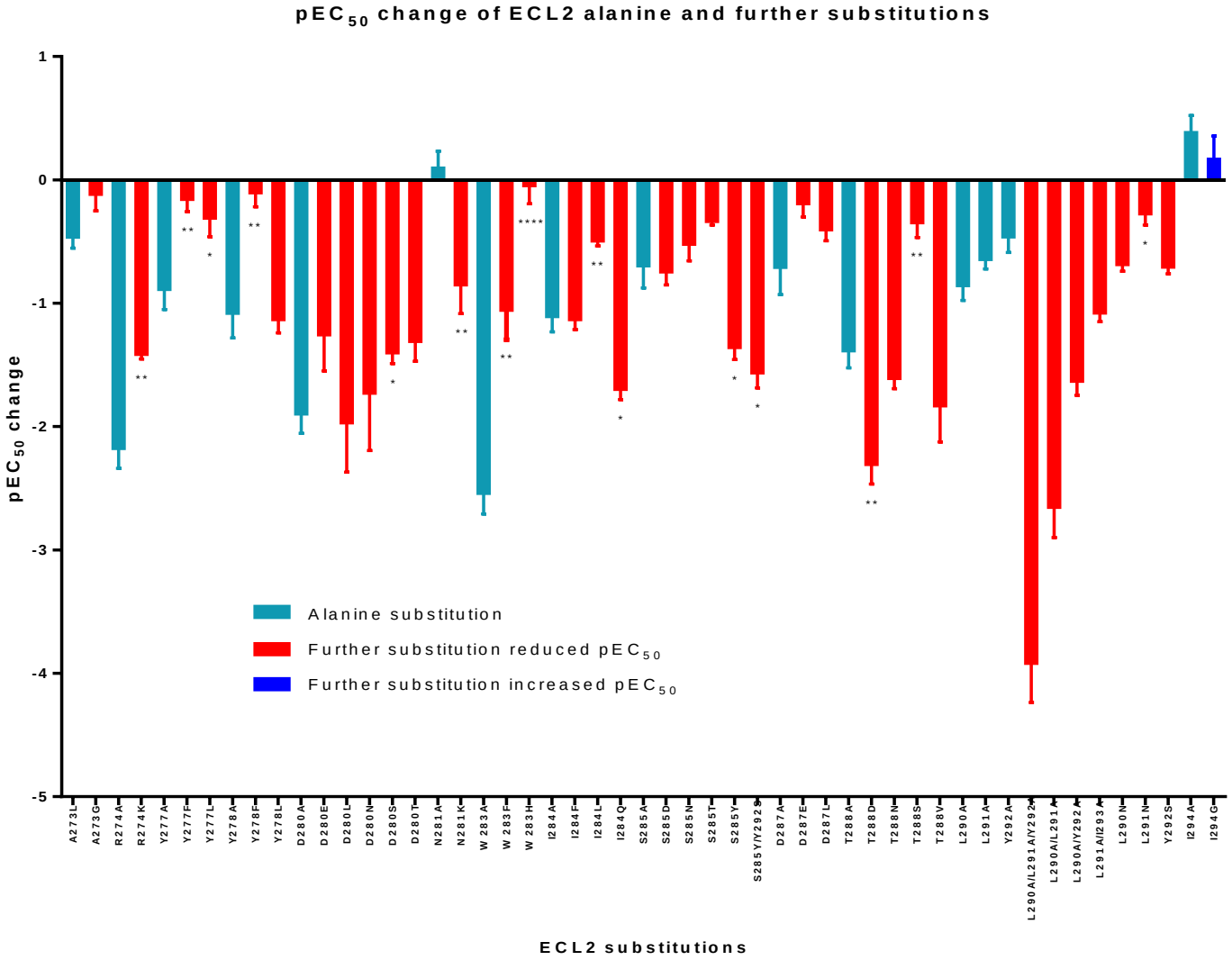
pEC50 change of ECL2 alanine and further substitutions
pEC50 change
1
0
-1
-2
-3
-4
-5
Alanine substitution
Further substitution reduced pEC50
Further substitution increased pEC50
A273L
A273G
R274A
R274K
Y277A
Y277F
Y277L
Y278A
Y278F
Y278L
D280A
D280E
D280L
D280N
D280S
D280T
N281A
N281K
W 283A
W 283F
W 283H
I284A
I284F
I284L
I284Q
S285A
S285D
S285N
S285T
S285Y
S285Y/Y292A
D287A
D287E
D287L
T288A
T288D
T288N
T288S
T288V
L290A
L291A
Y292A
L290A/L291A/Y292A
L290A/L291A
L290A/Y292A
L291A/I293A
L290N
L291N
Y292S
I294A
I294G
ECL2 substitutions

Figure 4.8. A graphical summary of the difference between the pEC_{50} values of both the ECL2 alanine substitution and substituted CGRP receptors compared with the pEC_{50} values of the WT receptor detailed in Table 4.2.

A negative change indicates a decrease in potency of the CLR substitution. The statistical significance between the substituted receptor pEC_{50} difference and the alanine substitution pEC_{50} log difference is also shown. Cos7 cells transfected with WT and substituted receptor were dose dependently stimulated with CGRP and levels of the cAMP second messenger were detected using a TR-FRET based cAMP assay. The difference in pEC_{50} values between the WT and substituted receptor for each experimental repeat were used to calculate mean and SEM values. To compare the difference observed with the alanine substitution and the substituted receptor, an unpaired t-test was used. The results of the t-test are displayed on the graph. *$p < 0.05$, ** $p < 0.01$, ***$p < 0.001$, ****$p < 0.0001$.

in cAMP signalling compared with their respective alanine substitution. D287E had no significant difference with both the WT and the alanine substitution in the analysis.

In this investigation four multiple amino acid substitutions were tested (L290A/L291A/Y292A, L290A/L291A, L290A/Y292A and L291A/I293A). For these substitutions, there was not an appropriate individual alanine substitution mutant to use for a statistical comparison. If the effects of the two alanine substitutions are not related, one might expect a multiplier effect. If they are affecting exactly the same process, one might expect the same pEC_{50} shift as the alanine-subs and if they are acting at a similar effect but in different ways, one might expect an effect in excess of the multiplication of the two alanine subs. This is interesting and hints to an effect but requires more analysis for a full explanation. Multiplying the individual pEC_{50} difference of the L290A, L291A and Y292A substitutions results in ~100 fold reduction in cAMP signalling. However the triple alanine substitution L290A/L291A/Y292A results in an almost 10,000 fold reduction in signalling. Multiplying L290A and L291A results in ~30 fold reduction in signalling. The double substitution L290A/L291A results in ~450 fold reduction in cAMP signalling. Multiplying L290A and Y292A results in ~20 fold reduction. The double substitution L290A/Y292A is much less severe with ~40 fold reduction. Finally the multiplied L291A and I293A values result in ~5 fold decrease, with the L291A/I293A double substitution resulting in an ~12 reduction.

4.3.1.3.2 Basal signalling

The basal values for the ECL2 substitutions are shown in Table 4.2 and the difference between the wild type and the substituted receptor basal values are illustrated graphically in Figure 4.9.

Six of the 36 substitutions investigated had a significant increase in basal cAMP signalling compared with that of WT (D280N, I284F, T288S, L290A/L291A/Y292A, L291A/I293A and L291N). The greatest increase was that of D280N with a 20.95 % increase on WT. L291N had an increase of 17.5% that of WT. The remaining substitutions had an increase of between 10-15% of WT basal signalling. These positions are different to the alanine substitutions which resulted in a significantly

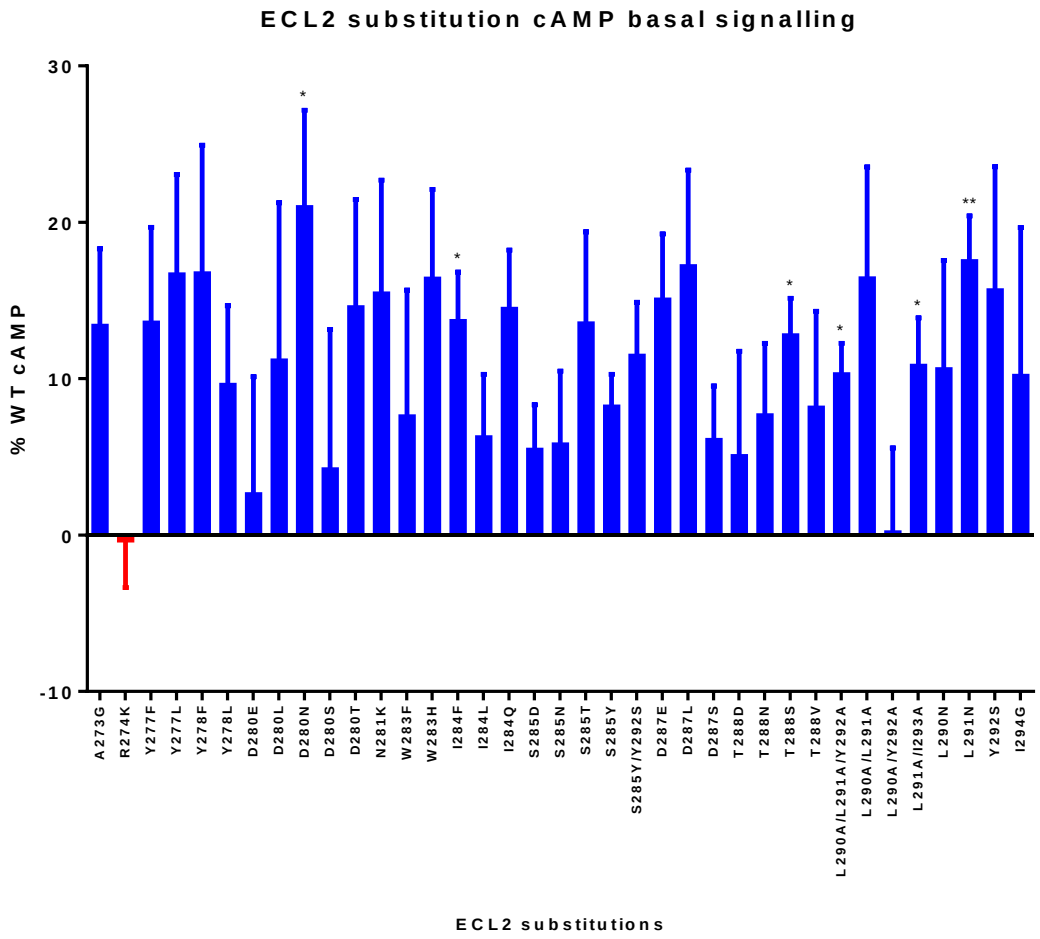

Figure 4.9. A graphical summary of the basal mean + SEM value of the ECL2 substitution following normalisation to the WT receptor.

Cos7 cells transfected with WT and substituted receptor were dose dependently stimulated with CGRP and levels of the cAMP second messenger were detected using a TR-FRET based cAMP assay. A sigmoidal dose response curve was fitted to the data using GraphPad Prism software. The substituted receptor data were normalised to WT, taking the maximum and minimum values obtained from the WT dose response curve. Significance was obtained using a paired t-test. *p < 0.05, ** p < 0.01, ***p <0.001.

increased basal signalling (N281A, S285A, and I294A) with the exception of T288 (T288A).

None of the substitutions resulted in a significant decrease in basal signalling compared with WT. This is comparable with the alanine substitutions.

4.3.1.3.3 E_{max}

The data for the E_{max} cAMP signalling of the substituted receptor normalised to WT (WT normalised to 100%) are described in Table 4.2. The results are presented graphically in Figure 4.10.

Only one substitution has a significantly altered E_{max} compared with WT. I284Q has a significant increase at 104% of WT however this is a very small effect. This is different to the results of the alanine substitutions which had a significantly increased E_{max} at five positions (N281A, D287A, T288A, Y292A and I294A) and a significantly reduced E_{max} at one position (S285A).

4.3.1.4 Cell surface expression of ECL2 substitutions

To measure the levels of expression of the substituted receptor at the plasma membrane, a cell surface expression ELISA was used. Cos7 cells were transfected with WT or substituted CLR and RAMP1. The cell surface expression ELISA and analysis were carried out as previously described (2.2.16 and 2.2.19).

The results of the cell surface expression ELISA are shown in Table 4.4 and represented graphically in Figure 4.11. Six mutations have a significantly reduced cell surface expression compared with WT (Y278L, D280L, D280T, L291A/I293A, L290N and I294G). The greatest reduction is observed with D280T, with cell surface expression levels at 37.33% that of WT. The remainder (Y278L, D280L, L291A/I293A and L290N) have cell surface expression levels ~80% of WT with the exception of I294G, which is higher at 86%.

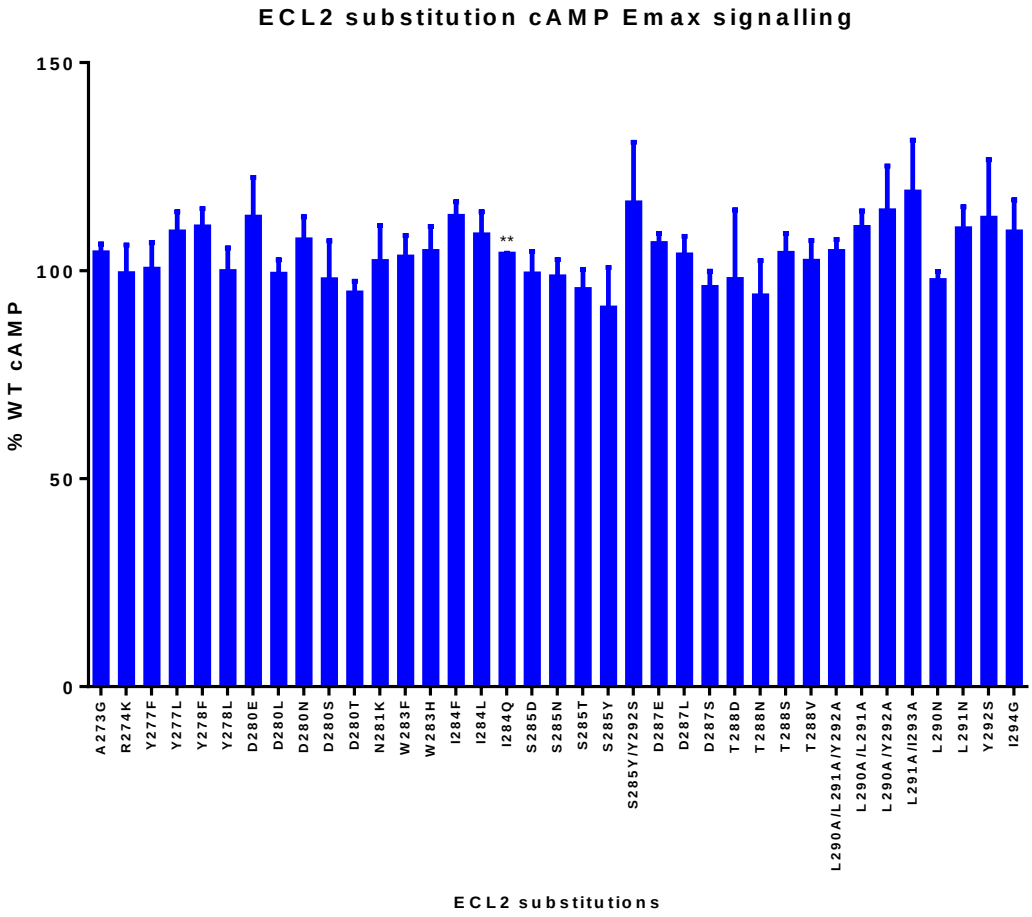

Figure 4.10. A graphical summary of the E_{max} mean and SEM value of the ECL2 substituted CGRP receptor normalised to the WT receptor.

Cos7 cells transfected with WT and substituted receptor were dose dependently stimulated with CGRP and levels of the cAMP second messenger were detected using a TR-FRET based cAMP assay. A sigmoidal dose response curve was fitted to the data using GraphPad Prism software. The substituted receptor data were normalised to WT, taking the maximum and minimum values obtained from the WT dose response curve. Significance was obtained using a paired t-test. *$p < 0.05$, ** $p < 0.01$, ***$p < 0.001$.

Substitution	n	Cell surface expression	P value
A273G	3	98.05±1.60	0.346
R274K	4	94.44±3.07	0.1681
Y277F	3	97.96±10.54	0.8641
Y277L	3	99.12±1.83	0.6777
Y278F	3	104.5±4.41	0.4134
Y278L	4	77.65±5.65	0.0289*
D280E	3	94.62±5.99	0.4643
D280L	4	78.11±2.54	0.0033**
D280N	3	91.74±4.33	0.1972
D280S	3	88.87±8.05	0.3006
D280T	3	37.33±2.07	0.0011**
N281K	3	101.9±3.22	0.6144
W283F	3	100.4±1.68	0.8166
W283H	4	94.37±1.92	0.0609
I284F	3	101.8±3.97	0.698
I284L	4	109.9±3.92	0.0862
I284Q	3	103.2±3.44	0.4535
S285D	3	106±2.22	0.1122
S285T	3	94.26±5.78	0.4258
S285V	3	106±1.94	0.0907
S285Y	3	95.57±4.38	0.4184
S285Y/Y292S	3	95.92±1.32	0.0905
D287E	3	104.6±2.55	0.2095
D287L	3	94.12±2.72	0.1639
T288D	3	94.14±2.87	0.1793
T288N	3	97.42±0.93	0.1108
T288S	3	97.04±1.11	0.1162
T288V	3	97.37±1.61	0.155
L290A/L291A/Y292A	3	85.72±4.38	0.0825
L290A/L291A	3	91.80±3.69	0.1561
L290A/Y292A	3	80.39±5.59	0.0725
L291A/I293A	3	82.87±3.38	0.0368*
L290N	4	83.68±2.82	0.0103*
L291N	3	99.96±2.64	0.9902
Y292S	3	96.77±4.78	0.5687
I294G	3	86.11±2.10	0.0070**

Decreased cell surface expression value

Table 4.4. Summary of the cell surface expression mean and SEM values of the ECL2 substitution normalised to the WT receptor.

Cos7 cells were transfected with WT and substituted receptor and the cell surface expression was measured by ELISA. Following expression, cells were fixed with formaldehyde and blocked with 1% BSA in PBS. The WT and substituted receptor cell surface expression was measured using a primary α-HA antibody probing for an N-terminal HA tag on the extracellular N-terminus of the receptor. An α-mouse secondary antibody conjugated to HRP was used and the absorbance of an OPD substrate was measured at 450nm. Data were normalised to the blank mean and WT mean to produce relative minimum and maximum values respectively. Mean and SEM were taken of the normalised data and significance determined using a paired t-test. *$p < 0.05$, ** $p < 0.01$, ***$p < 0.001$.

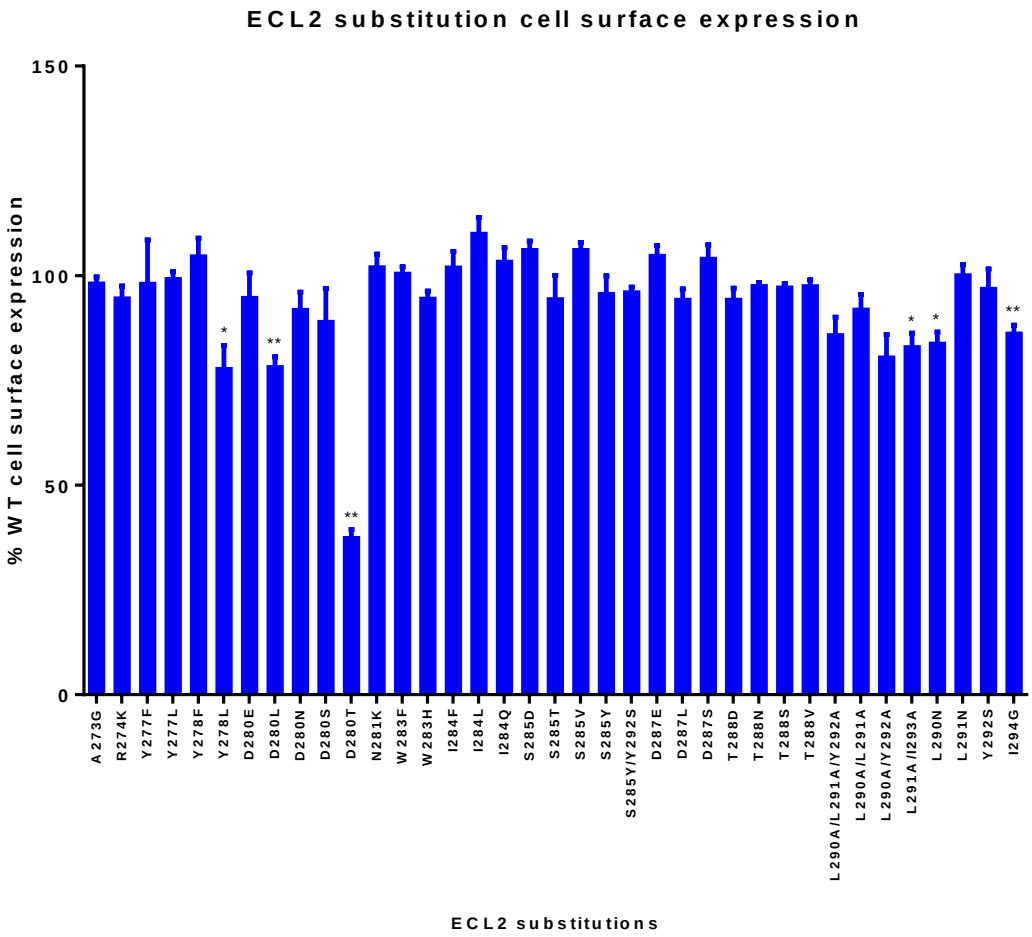

Figure 4.11. Graphical summary of the cell surface expression mean and SEM values of the ECL2 substitution normalised to the WT receptor.

Cos7 cells were transfected with WT and substituted receptor and the cell surface expression was measured by ELISA. Following expression, cells were fixed with formaldehyde and blocked with 1% BSA in PBS. The WT and substituted receptor cell surface expression was measured using a primary α-HA antibody probing for an N-terminal HA tag on the extracellular N-terminus of the receptor. An α-mouse secondary antibody conjugated to HRP was used and the absorbance of an OPD substrate was measured at 450nm. Data were normalised to the blank mean and WT mean to produce relative minimum and maximum values respectively. Mean and SEM were taken of the normalised data and significance determined using a paired t-test. *$p < 0.05$, ** $p < 0.01$, ***$p < 0.001$.

4.3.2 Antagonist competition study

A modification to the TR-FRET cAMP assay was devised to investigate the interaction points between the CGRP ligand and the ECL2 domain. This was described in the introduction and Figure 4.1.

Four ECL2 residues were selected as part of this study (R274, D280, D287 and T288). This was due to their distribution throughout the loop, the significant reduction in cAMP signalling observed with their respective alanine substitutions and having being identified as potentially interacting with CGRP in the collaborative computer modelling in chapter 3. Following this prediction this work was done to see if the interaction was with the 1-7 or 8-37 region of CGRP. Ligand competition was optimised to use an antagonist concentration of 10^{-6}M which resulted in ~50-100 fold reduction of pEC_{50} value for the WT receptor.

The results are summarised in Table 4.5 with representative curves of the results in Figure 4.12. None of the alanine substitutions investigated resulted in a significant variation in the change in pEC_{50} values with and without antagonist competition compared to the WT receptor. As only two or three experimental repeats were done for each substitution, more N numbers are required.

ECL2 substitution	WT pEC_{50} difference Mean	SEM	Alanine pEC_{50} difference Mean	SEM	N	t-test (paired)
R274A	1.67	0.20	1.76	0.26	2	0.3743
D280A	1.83	0.19	1.68	0.10	2	0.3536
D287A	1.77	0.04	1.45	0.13	3	0.1425
T288A	1.84	0.08	2.28	0.02	2	0.0843

Table 4.5. Summary of the mean and SEM of the difference in pEC_{50} values for WT CLR ± $CGRP_{8-37}$ and alanine substituted CLR ± $CGRP_{8-37}$.

Cos7 cells transfected with WT and alanine substituted receptor were incubated ± 10^{-6}M $CGRP_{8-37}$ and dose dependently stimulated with CGRP. Levels of the cAMP second messenger were detected using a TR-FRET based cAMP assay. A sigmoidal dose response curve was fitted to the data using GraphPad Prism software. The data were normalised to WT, taking the maximum and minimum values obtained from the WT dose response curve. The mean and SEM difference in pEC_{50} values for the WT and mutant receptor ± $CGRP_{8-37}$ competition were calculated. The number of experimental repeats is denoted in the N column and the significance was obtained through paired t-test. *p < 0.05, ** p < 0.01, ***p <0.001.

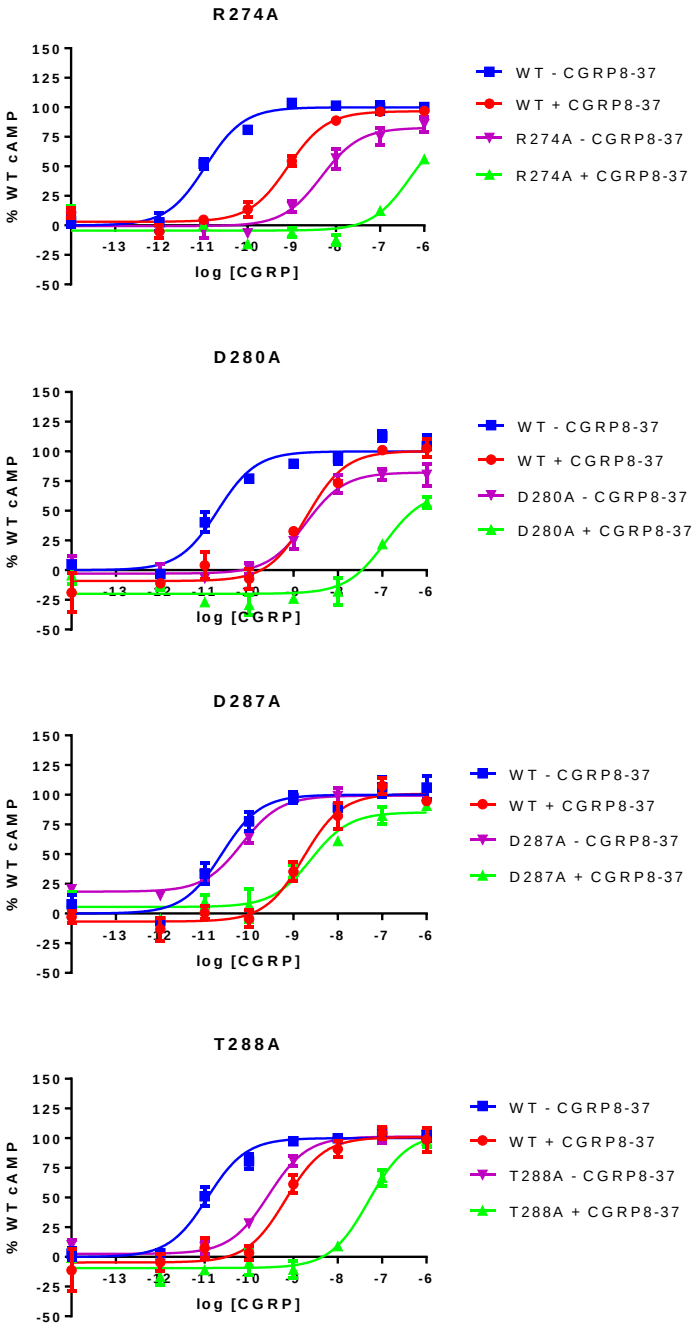

Figure 4.12. Representative cAMP signalling curves for alanine substitution and WT receptor incubated ± $CGRP_{8-37}$ and stimulated in a dose dependent manner with CGRP.
Cos7 cells transfected with WT and alanine substituted receptor were incubated ± 10^{-6}M $CGRP_{8-37}$ and dose dependently stimulated with CGRP. Levels of the cAMP second messenger were detected using a TR-FRET based cAMP assay. A sigmoidal dose response curve was fitted to the data using GraphPad Prism software. The data were normalised to WT, taking the maximum and minimum values obtained from the WT dose response curve.

4.4 Discussion

36 substitutions were created to investigate 15 ECL2 residues. Seven ECL2 substitutions (A273G, Y277F, Y277L, Y278F, W283H, D287E and I294G) had pEC_{50} values that were not statistically different to WT CLR showing a complete recovery in cAMP signalling compared with the alanine substitution. 10 substitutions had a modest reduction (<10 fold) in cAMP pEC_{50} signalling (N281K, I284L, S285D, S285N, S285T, D287L, T288S, L290N, L291N and Y292S). 16 substitutions had a 10-100 fold reduction in cAMP pEC_{50} signalling (R274K, Y278L, D280E, D280L, D280N, D280S, D280T, W283F, I284F, I284Q, S285Y, S285Y/Y292S, T288N, T288V, L290A/Y292A and L291A/I293A). Three substitutions had a >100 fold reduction in cAMP pEC_{50} signalling (T288D, L290A/L291A/Y292A and L290A/L291A).

The current data set for the antagonist study investigating potential contact sites between residues R274, D280, D287 and T288 show that these residues bind to the 1-7 region of the ligand. However the number of experimental repeats is low (two or three) therefore more are required to be confident in these results.

4.4.1 ECL2 extended substitution investigation data integrity

4.4.1.1 cAMP signalling

The cAMP data for the signalling extended substitution investigation of ECL2 are presented in Table 4.2 and Figure 4.2 to Figure 4.7.

4.4.1.1.1 pEC_{50} values

The pEC_{50} values described in Table 4.2 are graphically illustrated in Figure 4.8. The WT CLR pEC_{50} values varied from 9.09 (L291A/I293A) and 11.15 (I284Q). This variation of ~100 fold in pEC_{50} values was also observed during the alanine substitution investigation in chapter 3 and was explained as reflecting differences in coupling efficiencies between cells due to the time period that the data was collected over. This data set was collected over a similar time period (over a year) and this observed difference is not unexpected. To control for this, a paired design-test was used so that each mutant was compared in the same experiment against a corresponding WT control. The standard error for the WT CLR controls varied from

0.09 (W283H) to 0.55 (T288N). This range is similar to the SEM variation observed during the alanine substitution analysis.

4.4.1.1.2 Basal signalling

The basal signalling of the ECL2 substitutions is described in Table 4.2 and Figure 4.9. Basal signalling was normalised to WT CLR (0 %) and ranged from -0.33 % WT CLR (R274K) to 20.95 % (D280N). The standard error ranged from 1.99 % (L290A/L291A/Y292A) to 10.11 % (D280L). Six substitutions had a statistical significant difference from WT CLR basal signalling. These are D280N, I284F, T288S, L290A/L291A/Y292A, L291A/I293A and L291N. However as Figure 4.9 illustrates quite clearly, the differences observed in these basal values are very similar to the differences in basal values for the majority of the substitutions. It is unlikely that this statistical significant has any biological impact.

4.4.1.1.3 Emax signalling

The E_{max} signalling of the ECL2 substitutions is described in Table 4.2 and Figure 4.10. The E_{max} signalling was normalised to WT CLR (100 %) and ranged from 91.01 % (S285Y) to 118.9 % (L291A/I293A). The standard error ranged from 0.19 % (I284Q) to 16.69 % (T288D). Figure 4.10 clearly illustrates how all the data points are broadly 100 % of WT CLR E_{max} signalling. One ECL2 substitution E_{max} (I284Q) had a statistically significant increase to WT CLR. However the Emax was 104 % WT CLR. This difference is unlikely to have any biological effect.

4.4.1.2 Cell surface expression

The cell surface expression data are described in Table 4.4 and Figure 4.11. Levels of cell surface expression for the ECL2 substitutions varied from 37.33 % WT CLR (D280T) to 109.9 % (I284L). The standard error ranged from 0.93 % (T288N) to 10.54 % (Y277F). Six ECL2 substitutions had a statistically significant reduction in cell surface expression compared with WT CLR. The greatest difference observed was with D280T (37.33 %). This was unexpected as this level of cell surface expression is substantially lower that all the other substitutions, including other substitutions of D280. If a substitution of this residue prevents successful cell surface expression of the receptor, it would be expected that other substitutions would have a similar

effect, especially the conservative D280S substitution. This substitution was not significantly different to WT CLR. The D280T plasmid DNA was sequenced to see if the effect was due to an issue with the DNA however the sequencing was returned successfully. The reduction in D280T signalling might be a result of the low expression however this level has been previously observed to retain WT signalling (Conner *et al.*, 2006a). Y278L and D280L both had a similar significant reduction in WT CLR cell surface expression (~78 %). This should not be enough to effect cAMP signalling however it might be biologically relevant. The remaining three ECL2 substitutions to result in a significant reduction in cell surface expression were L291A/I293A, L290N and I294G (~85 % WT CLR). As illustrated in Figure 4.11 these values are lower than the majority of the ECL2 substitutions but not substantially. Again the effect of these substitutions is unlikely to be biologically important.

4.4.1.3 Antagonist competition study

The data for the antagonist competition study are shown in Table 4.5 and Figure 4.12. The representative curves that most accurately illustrated the differences observed in pEC_{50} values for both the WT CLR control and the alanine substitution +/- $CGRP_{8-37}$ were selected. However this may not always accurately reflect the specific differences in signalling. The difference in pEC_{50} values +/- $CGRP_{8-37}$ antagonist for the WT CLR control ranged from 1.67 to 1.84. The standard errors ranged from 0.04 to 0.2. The difference observed for each WT CLR control value is broadly comparable. The difference in pEC_{50} values +/- $CGRP_{8-37}$ antagonist for the alanine substitutions was greater, ranging from 1.45 (D287A) to 2.28 (T288A). No substitution had a statistically significant difference from WT CLR.

4.4.2 Analysis of ECL2 substitutions

The purpose of this study was to investigate the residues of the ECL2 domain that had been identified as important for CGRP-mediated receptor activation during the alanine substitution study in chapter 3. This involved a targeted selection of substitutions of these key residues to amino acids with a particular side chain property comparable to WT. This was to test through which particular interactions the WT residue had its effect. This approach has been previously used to study

particular functional motifs within a receptor (Conner *et al.*, 2006a) and expanded to study a greater range of residues in ligand binding of the GCGR (Siu et al., 2013). This is the first time this method has been used to comprehensively investigate the molecular interactions of a functional domain.

In total, 36 new substitution mutations were created to investigate 15 functionally important residues of ECL2 identified through the alanine substitution study. These mutations had a range of cAMP signalling responses compared with the original alanine substitutions, from complete recovery to more disrupted signalling. This information has provided a deeper understanding into the mechanism by which CGRP binds and activates its receptor.

The results of this chapter will be initially discussed with respect to each individual residue of ECL2 that was studied in order to understand the information gained through each set of amino acid substitutions. The results of this will be brought together in an overall conclusion.

4.4.2.1 Key findings

The ECL2 substitution analysis has revealed some very interesting properties of this loop. The N-terminus of ECL2 in all family B GPCRs contains a conserved basic residue (R274 in CLR). This positive charge may be required to "anchor" the loop to the membrane, however two family B GPCR models have predicted this side chain to form a bridge with a central ECL2 acidic residue orientating this for ligand binding (Siu et al., 2013; Woolley et al., 2013). This acidic residue is located four amino acids away from the basic residue in the GCGR (Siu et al., 2013) similar to a functionally important acidic residue in the GLP-1R (Koole et al., 2012). In CLR the equivalent residue is Y278 however R274 is predicted to form interactions with Y277 in a greater number of CLR models. Given that Y277L retains WT signalling it makes it unlikely that an R274-Y277 interaction is occurring. Therefore R274 is more likely to interact with either Y278 or D280. Given that the R274A and D280A alanine substitutions cause a similar reduction in cAMP signalling (~100 fold) an R274-D280 interaction remains a strong possibility. The fact that a conservative lysine substitution (R274K) has ~25 fold reduction in signalling highlights the importance of the size of this side chain. This might account for the lack of recovery observed

with the D280 substitutions, particularly the conservative D280E mutation. W283 is an important residue in a complex part of the receptor that appears to be exerting its effects through a number of different interactions. Recovery with both histidine and phenylalanine (W283H and W283F) was unexpected and strengthens the hypothesis that the W283 side chain forms interactions with TM2 and 3, however there are still a variety of interactions through which this could happen. There is an electrostatic shelf created by residues S285 and D287 that requires the hydroxyl group and negative charge respectively that is likely to form the base of the ligand binding pocket. T288 requires hydroxyl group however there is flexibility in the positioning. The CLR models predict that the C-terminal half of ECL2 forms multiple interactions with the CGRP ligand. The recovery in signalling observed with a greater number of substitutions in this half of the domain may reflect a level of flexibility of this part of the loop that may have functional effects with respect to the activation mechanism.

4.4.2.2 Detailed discussion of the substitutions at each ECL2 position

A273: The leucine substitution (A273L) at this position resulted in ~3 fold reduction in cAMP signalling potency. Given that the extension to the WT alanine methyl group reduced signalling ability, the glycine substitution was used to see the effect of reducing the side chain length. The A273G substitution recovered signalling to that of WT. A space or interaction is required in this position which is produced by both the alanine and the glycine. The slight reduction in cAMP signalling observed with the initial leucine substitution in chapter 3 is more likely to be due to a disruption caused by the extension of the leucine side chain, rather than a function of the WT residue. In the six high scoring models of CLR described in chapter 3, the start of ECL2 was I272 (four models), A273 (one model) and R274 (one model). A273 is therefore likely to be at the TM4/ECL2 junction. Both the alanine and glycine residues could provide a structural flexibility at this interface that the leucine restricts.

R274: The alanine substitution (R274A) resulted in ~100 fold reduction in cAMP signalling potency. Mutation to lysine (R274K) partially recovered signalling to ~25 fold reduction compared to WT. This shows that just having a positive charge in this

region of the loop is not sufficient for wild type signalling; the precise position is important. A positively charged residue at the start of ECL2 is a conserved feature of the family B GPCRs and its importance has been shown with the disruption in binding affinity and signalling in mutagenesis experiments for the GCGR and GLP1-R (Koole *et al.*, 2012; Siu *et al.*, 2013). However both signalling and binding affinity was recovered in the GLP1-R with an K288R substitution (Al-Sabah & Donnelly, 2003a). In the published CLR model (Woolley et al., 2013), R274 may be forming a bridge with Y277 or D280, which is an effect similar to those proposed in other family B GPCRs between the equivalent residues (Siu et al., 2013). If this is the function of R274 then the precise positioning of its positive charge could be vital in forming the bridge with either Y277 or D280.

Y277: The alanine substitution (Y277A) reduced cAMP signalling potency by ~10 fold. Substitution to both phenylalanine and leucine (Y277F and Y277L) recovered pEC_{50} signalling to WT. The phenylalanine recovery shows that the hydroxyl group is not a necessary part of ligand binding. However this similarity between side chains does not guarantee recovery. A study of the Thyrotropin-Releasing Hormone Receptor (TRHR) found that a Y181F (ECL2) substitution resulted in no ligand binding at the concentrations investigated (Perlman et al., 1997). However given the similarity between tyrosine and phenylalanine side chains, there is likely to be shared interactions between these amino acids. The recovery with leucine is more surprising. This side chain has hydrophobic properties like phenylalanine but lacks the ring structure and delocalised electrons. This suggests that the key effect in this position is through hydrophobicity. The shared functional effects of phenylalanine and leucine have been observed in the A2BR (Peeters et al., 2011). An F71L substitution in ECL1 resulted in an increase in agonist potency. There was a slight reduction in potency with a F71Y mutation. A number of the CLR models in Woolley et al., 2013 had Y277 interacting with R274. The WT signalling of Y277L makes the models that proposed electrostatic interactions between these residues much less likely. If interactions between R274 and Y277 occur then they are hydrophobic, or Y277L induces a conformational change that maintains WT signalling. This is unlikely.

Y278: As with Y277A, the Y278A alanine substitution resulted in an ~10 fold reduction in cAMP signalling potency. Again, signalling was recovered to WT with the phenylalanine substitution (Y278A) however unlike Y277 the leucine substitution (Y278L) showed no significant recovery. This confirms the importance of the aromatic ring of both the phenylanine and the WT tyrosine residue and the redundancy of the hydroxyl group. However there are properties of the aromatic ring that are vital for signalling. This could be either through hydrophobicity or the delocalized pi electrons. This maintains the possibility that electrostatic interactions could be occurring through R274 and Y278 however this is not favoured by the high scoring CLR conformations.

D280: The alanine substitution (D280A) resulted in ~80 fold reduction in cAMP signalling potency. This large disruption in signalling together with the positioning of the residue in the middle of the loop suggested that D280 is a key residue in the binding to CGRP and activation of the receptor. A number of substitutions were used to investigate this residue (D280E, D280L, D280N, D280S and D280T). None of these substitutions significantly recovered signalling to that of WT. This shows that both the positioning and the charge in this position is specifically required for signalling. The leucine and asparagine substitutions (D280L and D280N) both had large reductions similar to that of alanine (~100 fold and 50 fold respectively). Substitution for glutamate, serine and threonine (D280E, D280S and D280T) all resulted in between 15-25 fold reduction in signalling however only D280S was significant different to the alanine substitution. This is due to the high standard error with the other substitutions. The reduction in D280T signalling might be a result of the low expression (~37% WT) however this level of expression has been previously observed to retain WT signalling (Conner *et al.*, 2006a). These data show the importance of the WT aspartate at this position to maintain receptor integrity. Even the conservative glutamate substitution was unable to have the same functional effect as the WT aspartate. A similar effect was also observed in the ECL2 domain of the human A2AR. Reduction in ligand binding caused by an E151A mutation was not recovered with a conserved E151D mutation (Kim et al., 1996). The effect of the carboxylic acid side chain can vary even within the same receptor

domain. Investigation of ECL2 of the P2Y1 receptor showed disruption in signalling using an alanine substitution at position D204, which was exacerbated with further asparagine and glutamate substitutions. However abolished signalling caused by an alanine substitution at position E209 was recovered by aspartate, glutamine and arginine mutations (Hoffmann et al., 1999). In another case, an aspartate in the ECL1 domain of the adenosine A2BR was substituted for a diverse range of amino acids without any detrimental effect on ligand binding. These included glutamine, serine and tyrosine as well as the more conserved glutamate (Peeters et al., 2011). D280 was predicted to interact with R274 in some of the CLR models. Alanine substitutions at both of these residues (R274A and D280A) resulted in a similar reduction in cAMP potency (~100 fold) and signalling could not be recovered to WT even with conservative mutations (R274K and D280E). This could be explained through interactions between these residues side chains however the current data are not sufficient to confirm this.

N281: The alanine substitution (N281A) resulted in a CAM in Woolley et al., 2013. Further experimental repeats in chapter 3 resulted in a loss of statistical significance. As part of the comprehensive study of this chapter this residue was still chosen for further substitution analysis. The hypothesis in creating a lysine substitution (N281K) was that the CAM effect of the alanine substitution could be due to a locking effect through hydrogen bonding in the asparagine side chain. The lysine mutation was an attempt to increase the effect of this lock if this was due to hydrogen bonding through the δ^+ H atoms. Substitution with an acidic residue to investigate the same speculated hydrogen bonding effect with the δ^- N or O atoms of the side chain was not investigated. CGRP mediated cAMP signalling was indeed dramatically impeded, with a reduction of ~10 fold from WT. This effect could be due to locking effects, holding the receptor in the inactive state. It is also possible that the introduction of a positive charge disrupts signalling or receptor integrity and signalling is reduced through this effect. The evidence as it stands is not sufficient to clarify this discrepancy.

W283: The alanine substitution (W283A) resulted in ~300 fold reduction in cAMP signalling potency. This was substantially improved with a phenylalanine

substitution (W283F) which resulted in ~10 fold reduction in signalling compared to WT. However mutation to histidine (W283H) resulted in a complete recovery of signalling. The imidazole ring of histidine is in a similar position to the imidazole ring of tryptophan. Therefore the recovery is likely to be due to shared interactions. In the CLR models with the vertically orientated W283 residue, the imidazole group was predicted to form a hydrogen bond with H219 in TM3. This can also be formed with the W283H residue. The effect of W283F is more surprising, as the benzene ring is much closer to the backbone than with tryptophan where the benzene ring is extended further out. This cross over could be explained if the hydrogen bonding with H219 (TM3) is with the delocalised electron ring of the imidazole group, an effect that would be similar for the phenylalanine benzene ring. It is also possible that a novel set of interactions is occurring compensating for the change in amino acid in this position. In the GCGR, alanine substitution of the equivalent CW tryptophan residue in ECL2 resulted in abolition of ligand binding. This binding was recovered with leucine and phenylalanine, however substitution with histidine resulted in no binding similar to the alanine substitution (Siu et al., 2013). This difference in recovery could be due to the variations in orientation of the tryptophan residues proposed to point toward the middle of the transmembrane bundle in the glucagon receptor crystal structure (Siu et al., 2013) and in a more vertical position in the CGRP receptor model (Woolley et al., 2013) more similar to that of the CRHR1 (Hollenstein et al., 2013).

I284: Alanine substitution caused an ~10 fold reduction in cAMP signalling potency. The conserved leucine mutation (I284L) partially recovered signalling (~3 fold reduction). A phenylalanine substitution (I284F) did not recover signalling and glutamine (I284Q) had a more detrimental effect than the alanine substitution. These effects are not surprising. Leucine is a conservative mutation exerting similar effects to the WT isoleucine but showing that the steric effect of the side chain branching is important at this position. Phenylalanine has a different side chain arrangement, which causes more disruption in signalling. Glutamine was used to introduce polarity instead of hydrophobicity. This has the most pronounced reduction in signalling showing that a linear hydrophobic chain is important in this

position. The CLR model in Woolley et al., 2013 proposed that I284 together with W283 could interact with residues at the top of TM2 and 3. I284 was also predicted to interact with CGRP A5. This interaction would explain why the substitutions of phenylalanine and glutamine were more detrimental to signalling.

S285: The alanine substitution (S285A) resulted in ~5 fold reduction in cAMP signalling potency. This signalling was not recovered with any of the substitutions. This included the conserved threonine mutation (S285T; ~2 fold reduction) which almost reached significance (P 0.083), the negative charge of aspartate (S285D; ~5 fold) and the similarly polar asparagine (S285N; ~3 fold). This shows the importance of the hydroxyl group and its positioning. The S285Y/Y292S reciprocal mutation resulted in an increased reduction in signalling making it unlikely that these two residues form a sole interaction with each other.

D287: The alanine substitution (D287A) had ~5 fold reduction in cAMP signalling potency. The D287E substitution had ~1.6 fold reduction in cAMP signalling potency. This value was not significantly different to either the WT or the alanine substitution. More experimental repeats are required to determine the effect of this substitution. The sterically similar but hydrophobic leucine substitution (D287L) did not recover signalling compared with the alanine substitution. This shows that a negative charge is required in the side chain of this residue however more experimental repeats are required to establish if there is flexibility as to the precise position of this charge.

T288: The alanine substitution (T288A) resulted in ~25 fold reduction in cAMP signalling potency. The conservative serine mutation (T288S) almost completely recovered signalling (~2 fold reduction) but was significantly reduced compared with WT. Signalling was not recovered with the polar asparagine residue (T288N) or the leucine substitution (T288L). The aspartate substitution (T288D) had significantly reduced signalling compared with the alanine substitution (T288A). In the CLR models (Woolley et al., 2013), T288 was the most likely residue to interact with the functionally important T6 residue of CGRP. In the GCGR model (Siu et al., 2013), N298 at the C-terminus of ECL2 was predicted to interact with the glucagon ligand. Substitution to alanine or aspartate resulted in a 4-10 fold reduction in

ligand binding and the conserved glutamine substitution caused a >10 fold reduction. These two models of family B GPCRs predict ligand-receptor interactions between an ECL2 C-terminal polar residue and the peptide ligand.

L290, L291 and Y292: This motif resulted in small significant signalling reductions during the alanine substitution analysis (~7, 4 and 3 fold respectively). The double and triple mutants in these positions had dramatic reductions in cAMP signalling (L290A/L291A/Y292A ~10,000 fold reduction, L290A/L291A ~450 fold, L290A/Y292A ~45 fold, L291A/I293A ~10 fold).) The prediction from the model in chapter 3 was that L290 could form interactions with CGRP (residues L12 and L291) with TM7 of CLR and also potentially with RAMP1. This could help explain the significant effects seen through these double and triple mutations. It may also explain the unexpected and different results observed with the substitution of both L290 and L291 to asparagine (L290N and L291N). L290N did not recover signalling compared with the alanine substitution however L291N partially recovered signalling to ~2 fold reduction. This suggests that the ligand receptor interactions between CGRP and L290 are hydrophobic, however the effects of L291 are either different or there is some compensatory effect occurring. According to the high scoring CLR models, ECL2 is predicted to extend to either L290 or L291. If L291 is at the membrane interface then it could potential be forming hydrophobic interactions with the membrane core or the L291N substitution could form polar interactions with the hydrophilic head group.

I294: The alanine substitution (I294A) created a CAM in Woolley *et al.*, 2013 however further experimental repeats in chapter 3 made this result not significant. As part of the comprehensive study of this chapter this residue was chosen for further substitution. It was speculated that the CAM effect was due to a “locking” action of the hydrophobic WT isoleucine residue, potentially with the plasma membrane. If the alanine substitution “freed” this position from the locked conformation then further substitution to glycine may increase the CAM effect. I294G had WT signalling. It is unlikely that this residue is having an important functional effect.ECL2 substitution further work

4.4.2.3 ECL2 substitution further work

The current hypothesis to be emerging from these results with respect to CGRP-mediated receptor activation is that the N-terminal half of ECL2 has a structural role providing structural integrity to the remainder of the loop which directly binds to the CGRP ligand.

R274 appears to be a key residue forming potential interactions with either Y277, Y278 or D280. An important next step would be to investigate this further. If R274 is interacting with either of the tyrosine resides, it is likely to be through pi-cation interactions with the delocalised electrons of the aromatic ring. To test this substitutions of each tyrosine reside to glutamate could test for recovery through electrostatic interactions between the basic and acid side chains. Reciprocal mutagenesis of each pairing (R274-Y277 and R274-Y278) can also be used to test for these interactions. Two combinations are either direct reciprocals (R274Y/Y277R and R274Y/Y278R) or reciprocals of the previously mentioned substitution (R274E/Y277R and R274E/Y278R). An alternative interaction possibility is between R274 and D280 which was proposed to form a bond with CGRP R11 (Woolley et al., 2013). Reciprocal mutagenesis would be useful in testing this possibility including using a CGRP R11E analogue. Combinations of mutagenesis would include R274E/D280N(H)/CGRPR11, R274/D280N(H)/CGRPR11E and R274E/D280H(R/K)/R11E.

The next residue of particular interest is W283. The W283H substitution resulted in WT signalling suggesting that the functional effect of the tryptophan residue is through the imidazole ring. A W283Y substitution could test for the possibility of hydrogen bonding at this positon and a W283E substitution would test for interactions through the aromatic imidazole ring. Potential interaction partners of W283 include Y278 in ECL2 and H219 in TM3. To test the Y278-W283 interaction, the reciprocal Y278W/W283Y mutant could be used. To test for hydrogen bonding to histidine residues, Zn^{2+} binding experiments are a suitable option.

4.4.3 $CGRP_{8-37}$ antagonist competition

This study was designed to determine the residues of ECL2 that interact with the $CGRP_{1-7}$ loop domain and the remaining $CGRP_{8-37}$ part of the ligand. An antagonist competition assay was used to measure the change in pEC_{50} values observed using the $CGRP_{8-37}$ antagonist between the WT receptor and four selected alanine substitutions. R274A, D280A, D287A and T288A were chosen because of their significantly reduced cAMP signalling, their distribution throughout ECL2 and the prediction in the CGRP receptor modelling described in chapter 3 that they interact with CGRP.

No alanine substitution resulted in a significant difference in the change in pEC_{50} value compared with WT CLR +/- $CGRP_{8-37}$. These data show that if these ECL2 residues are interacting with CGRP, it is with the 1-7 loop. However given the small differences observed when comparing pEC_{50} values and the low number of experimental repeats, more N numbers are required to be confident in this conclusion.

4.4.3.1 $CGRP_{8-37}$ antagonist competition further work

In the current state, these results show that any interaction between CGRP and ECL2 residues R274, D280, D287 and T288 are through the 1-7 region of the ligand. However this may change following further experimental repeats. Following this then other ECL substitutions can be tested in this way.

4.4.4 Overall conclusion

The ECL2 substitution analysis has revealed several key features of this domain and provided evidence to an emerging hypothesis on a function mechanism for the loop. The N-terminal half of ECL2 is proposed to function as a scaffold providing structural integrity to the remainder of the loop facilitating CGRP binding to the C-terminal half. R274 is expected to be a key residue potentially forming interactions with either Y277, Y278 or D280. W283 is another important residue forming interactions through the imidazole ring of the side chain potentially with Y278 (ECL2) or H219 (TM3). The remainder of the loop is expected to form interactions with CGRP, most notably the T288 residue.

5 CGRP receptor signalling

5.1 Introduction

Agonist-induced GPCR activation causes a structural rearrangement of the intracellular domains consisting of the intracellular loops (ICLs), helix 8 (H8) and the C-terminus. This is induced by the rearrangement of the TM helices, specifically a movement of TM5 coupled with a rotation of TM6 that results in an intracellular outward movement of the helix (Sansuk et al., 2011; Standfuss et al., 2011). This conformational change creates a G protein-binding pocket that facilitates the exchange of GDP for GTP in the G protein and leads to subsequent activation of downstream signalling pathways. In the active structure of the β2-AR, the G protein can bind through interactions with residues in TM3, 5 and 6 and ICL2 (Rasmussen *et al.*, 2011b).

The effect of individual GPCR domains on GPCR signalling was first investigated through the co-expression of the ICL3 domain of the α1B-adrenergic receptor (α1B-AR) with α1B-AR. This resulted in a reduced E_{max} of ligand induced IP_3 signalling (Luttrell et al., 1993). Following this, ICL2, ICL3 and the C-terminal domains of the α1B-AR were co-transfected with α1B-AR. Both the α1B-AR ICL3 and C-terminal domains significantly reduced IP_3 maximal accumulation with the α1B-AR and the M1AChR. Only the α1B-AR ICL3 and C-terminus reduced cAMP maximal signalling for the D1A dopamine receptor (D1ADR) (Hawes et al., 1994). The δ-OR ICL3 domain was transfected into cells stably expressing μ-OR, δ-OR, β2-AR and the α2AR. The expressed peptide was able to inhibit G protein GTP binding and downstream signalling not only for the δ-OR but in other receptors signalling through the same G protein (Morou & Georgoussi, 2005).

In the CGRP receptor, residues in each of the ICLs have been shown to be involved in cAMP signalling and residues in ICL2 and 3 are involved in both cAMP signalling and cell surface expression (Conner et al., 2006a; Conner et al., 2006b). The H8 domain is important for cell surface expression of the receptor and the remainder of the C-terminus is involved in receptor internalisation (Conner et al., 2008).

The role of the ICL and C-terminal domains in cell surface expression, cAMP signalling and internalisation makes them possible candidates for pharmaceutical targeting. To determine the effect of these individual domains in the functioning of the CGRP receptor, the DNA encoding each domain was separately amplified using PCR and cloned into the mammalian expression vector pcDNA3.1-. Each domain was co-transfected with the CGRP receptor and the functional effect was measured through the effect on cAMP production.

In GPCR signalling research, there are multiple variables that need to be taken into account. These include the coupling of the GPCR with different G proteins, differences in membrane localisation of signalling components and signalling through G protein independent pathways. In an attempt to minimise this variability a GPCR-$G_{\alpha s}$ fusion protein was created through the cloning of the $G_{\alpha s}$ DNA to the 3' terminus of the β2-AR (Bertin et al., 1994). The β2-AR-$G_{\alpha s}$ fusion construct was expressed in S49 cyc- cells that lack endogenous $G_{\alpha s}$ and was able to recover cAMP signalling.

$G_{\alpha s}$ fusion to the GPCR allows for consistency in the 1:1 stoichiometry between receptor and G protein, the close proximity of these signalling components and the membrane localisation of the G protein required for analysis of this signalling process. This approach has been successfully applied to a number of different GPCRs and G proteins and used to calculate expression levels, rates of GTP turnover and hydrolysis and efficacies of partial agonists and inverse agonists (Seifert et al., 1999).

This approach to GPCR signalling analysis was applied to the CGRP receptor. The DNA encoding the $rG_{\alpha s}$ gene was kindly provided by David Poyner at Aston University and was cloned into the CLR C-terminus following mutation of the CLR stop codon. A single amino acid substitution of $rG_{\alpha s}$ created the $hG_{\alpha s}$ sequence. Two CLR fusion constructs will therefore be created for functional analysis, CLR-$hG_{\alpha s}$ and CLR-$rG_{\alpha s}$.

The purpose of this chapter is to provide a proof of concept for the intracellular loop competition study and the CLR-$G_{\alpha s}$ fusion construct technique described in this section. If successful these techniques could be useful new tools in studying the

structure and function of the CGRP receptor and could also provide a target for new pharmaceuticals.

5.2 Methods

5.2.1 Selecting ICL1/ICL2/ICL3/H8/C-terminal domain DNA sequences

The ICL1, ICL2, ICL3, H8 and C-terminal DNA sequences were selected based on the sequences identified in Conner *et al.*, 2006a and Conner *et al.*, 2008.

5.2.2 ICL1/ICL2/ICL3/H8/C-terminal domains into pcDNA3.1- mammalian expression vector

ICL1 and H8 double stranded DNA ligation inserts with overhanging restriction site ends were created directly by annealing the primers described in Table 2.3 following protocol 2.2.5.

ICL2, ICL3 and C-terminal DNA sequences were amplified using the polymerase chain reaction (PCR, section 2.2.4) with the primers described in Table 2.3 and the N-terminal HA tagged hCLR construct as a template, described in Figure 2.2. Following PCR amplification, the PCR products were digested using restriction enzymes XbaI and EcoR1 as described in section 2.2.6.

The pcDNA3.1- vector was digested using restriction enzymes XbaI and EcoR1 and the 5' phosphate groups were removed using calf intestinal phosphatase following protocol 2.2.6 to prevent self-ligation. The restriction digest products were separated using agarose gel electrophoresis following protocol 2.2.7. The required DNA band was excised and purified using a Qiagen gel extraction kit.

The intracellular domain fragments were ligated into the pcDNA3.1- vector following protocol 2.2.8. The ligation reaction was transformed into chemically competent Top10 *E.coli* cells (2.2.10) and plasmid DNA was amplified and purified (2.2.11). The purified DNA was sequenced (2.2.12) to confirm successful mutagenesis.

5.2.3 Generating the CLR-$G_{\alpha s}$ fusion constructs

The molecular biology approach used to create the CLR-$G_{\alpha s}$ fusion proteins is described in Figure 5.1. The CLR stop codon of the N-terminal HA tagged hCLR

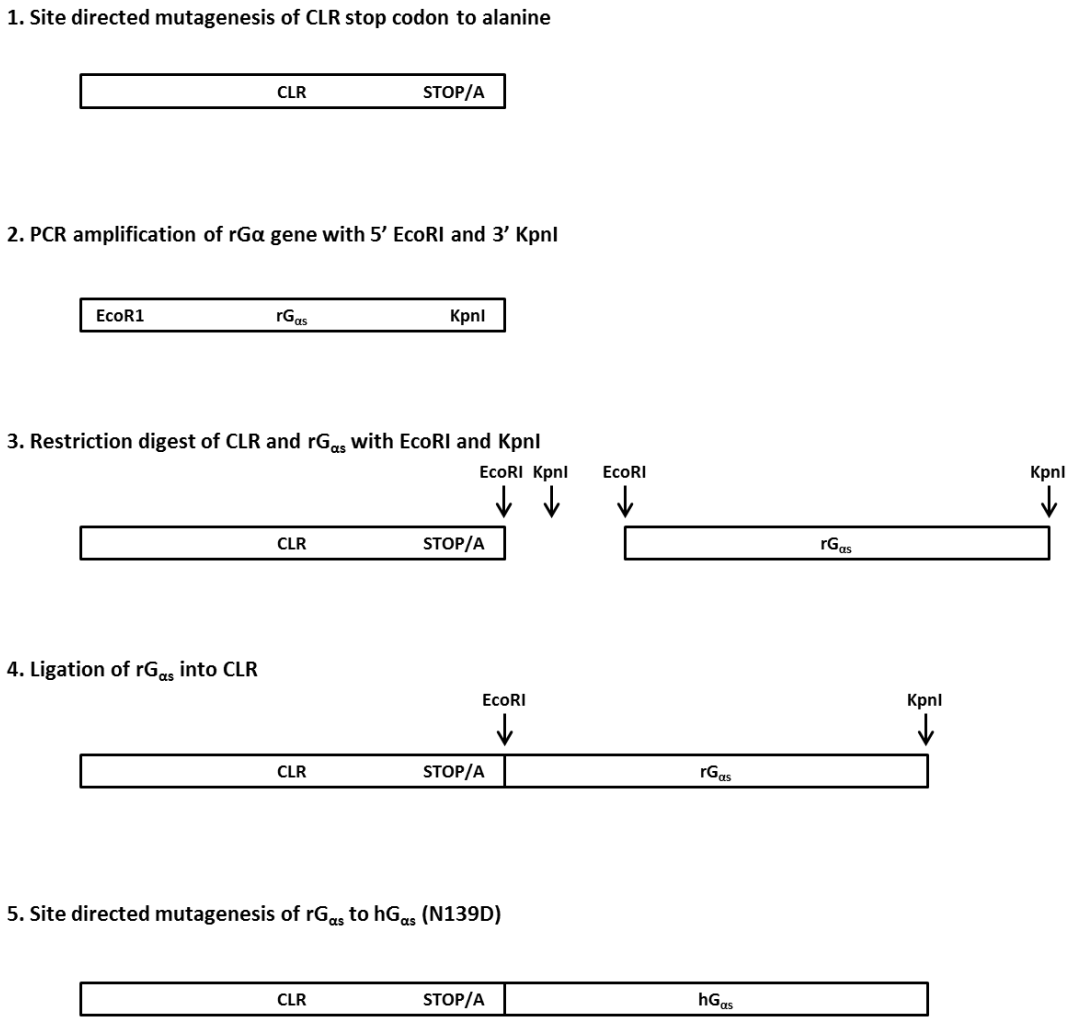

Figure 5.1. Creation of the CLR-$G_{\alpha s}$ fusion proteins.

A summary of the molecular biology approach used to synthesise the CLR-h$G_{\alpha s}$ fusion protein from the HA-CLR template in the pcDNA3.1- vector and the r$G_{\alpha s}$ gene. The protocol is described in detail in 5.2.3. Briefly, the CLR stop codon was mutated to alanine. The r$G_{\alpha s}$ gene was amplied with a 5'EcoRI site and 3' KpnI site using PCR. The CLR (STOP/A) and r$G_{\alpha s}$ PCR DNA were digested with EcoRI and KpnI and r$G_{\alpha s}$ was ligated into CLR (STOP/A). CLR-r$G_{\alpha s}$ was changed to CLR-h$G_{\alpha s}$ (N139D) using sited directed mutagenesis.

construct (in the mammalian expression vector pcDNA3.1-) was mutated to alanine using the primers described in Table 2.4, following the QuikChange site directed mutagenesis protocol (2.2.3) to create a CLR (stopA) construct. Following DpnI degradation of the template DNA, the product was transformed into chemically competent Top10 *E.coli* cells (2.2.10) and plasmid DNA was amplified and purified (2.2.11). The purified DNA was electrophoresed alongside a pre-DpnI treated sample (2.2.7) to confirm successful degradation of the template DNA and the purified DNA was sequenced (2.2.12) to confirm successful mutagenesis.

The $rG_{\alpha s}$ gene was PCR amplified with a 5' EcoRI and 3' KpnI site using primers described in Table 2.4 following protocol 2.2.4. Following amplification the PCR product was digested using restriction enzymes EcoRI and KpnI following protocol 2.2.6.

The CLR (stopA) construct was digested using restriction enzymes EcoRI and KpnI and the 5' phosphate groups were removed using calf intestinal phosphatase following protocol 2.2.6 to prevent self-ligation. The restriction digest products were separated through agarose gel electrophoresis following protocol 2.2.7. The required DNA band was excised and purified using a Qiagen gel extraction kit.

The $rG_{\alpha s}$ fragment was ligated into the CLR (Stop to A) vector following protocol 2.2.8. The ligation reaction was transformed into chemically competent Top10 *E.coli* cells (2.2.10) and plasmid DNA was amplified and purified (2.2.11).

The CLR-$rG_{\alpha s}$ fusion construct was mutated to CLR-$hG_{\alpha s}$ using primers described in Table 2.4 and an N-terminal HA tagged hCLR construct in the mammalian expression vector pcDNA3.1- as a template, following the QuikChange site directed mutagenesis (2.2.3). Following DpnI degradation of the template DNA, the PCR product was transformed into chemically competent Top10 E.coli cells (2.2.10) and plasmid DNA was amplified and purified (2.2.11). The purified DNA was electrophoresed alongside a pre-DpnI treated sample (2.2.7) to confirm successful degradation of the template DNA. The purified DNA was sequenced (2.2.12) to confirm successful mutagenesis.

5.3 Results

5.3.1 Effect of ICL1/ICL2/ICL3/H8/C-terminal co-expression on CGRP receptor signalling

The effect of the competition of the individual intracellular domains of CLR and WT CLR with the downstream signalling components was tested by measuring the effect of the co-expression of the CGRP receptor with each specific intracellular domain on cAMP signalling.

The results are summarised in Table 5.1. Rows highlighted in blue show a significant increase in pEC_{50}, basal or E_{max} levels. The cAMP signalling curve for each biological repeat of the tested WT CGRP receptor co-transfected with each intracellular domain is shown in Figure 5.2 to Figure 5.6.

There was no significant difference in cAMP pEC_{50} values for any of the intracellular domains co-transfected with the WT receptor. Co-expression of ICL2 and the C-terminus with the CGRP receptor had a significant increase in basal signalling (15.89 % and 22.31 % respectively). ICL1 did not have a significant difference in basal values. ICL3 and H8 had a significantly increased basal which was lost following Bonferroni correction. Co-expression of the C-terminus resulted in a significantly increased E_{max} (~117.7 %). There was no significant difference in the E_{max} values for the other intracellular domains.

5.3.2 CGRP receptor and G protein-coupling

The signalling capability of the CLR-$G_{\alpha s}$ fusion proteins was measured using a cAMP signalling assay. This was to confirm that the CLR unit of the fusion protein is able to initiate a cAMP signalling response following stimulation with CGRP.

The pEC_{50}, basal and E_{max} results for the CLR-h$G_{\alpha s}$ fusion protein are summarised in Table 5.2. The CLR-r$G_{\alpha s}$ construct did not produce a signalling response after multiple experimental repeats. Rows highlighted in blue show a significant increase in values and rows highlighted in red show a significant decrease. The CLR-h$G_{\alpha s}$ dose response curves are shown in Figure 5.7.

Intracellular	pEC_{50} (WT CLR + ICD)			pEC_{50} (WT CLR)			Statistical analysis		Basal (WT CLR + ICD)			Statistical analysis		E_{max} (WT CLR + ICD)			Statistical analysis	
domain (ICD)	Mean	SEM	N	Mean	SEM	N	t-test	Bonferroni	Mean	SEM	N	t-test	Bonferroni	Mean	SEM	N	t-test	Bonferroni
ICL1	-8.48	0.2	3	-8.48	0.1	3	0.9811	1	6.12	7.16	3	0.4827	1	105.3	8.99	3	0.6179	1
ICL2	-8.2	0.22	3	-8.48	0.1	3	0.4433	1	15.89	0.94	3	0.0035**	0.0105*	102.4	10.83	3	0.8476	1
ICL3	-8.33	0.13	3	-8.48	0.1	3	0.2344	0.7032	23.85	3.84	3	0.0249*	0.0747	112.5	8.97	3	0.2985	0.8955
H8	-8.45	0.09	3	-8.9	0.07	3	0.077	0.154	14.34	3.131	3	0.0445*	0.089	114.5	7.853	3	0.2061	0.4122
CT	-8.4	0.24	3	-8.9	0.07	3	0.1959	0.3918	22.31	2.031	3	0.0082**	0.0164*	117.7	2.727	3	0.023*	0.046*

Increased pEC_{50}/basal/E_{max} value

Table 5.1. Summary of the pEC_{50}, basal and E_{max} mean and SEM values for the CGRP receptor co-transfected with the CLR intracellular domains and the WT receptor paired in each experiment.

Cos7 cells transfected with WT and alanine substitution receptor were dose dependently stimulated with CGRP and levels of the cAMP second messenger were detected using a TR-FRET based cAMP assay. A sigmoidal dose response curve was fitted to the data using GraphPad Prism software. The intracellular domain co-expression was normalised to WT, taking the maximum and minimum values obtained from the WT dose response curve. The number of experimental repeats is denoted in the N column and the significance was obtained through paired t-test. *p < 0.05, ** p < 0.01, ***p <0.001.

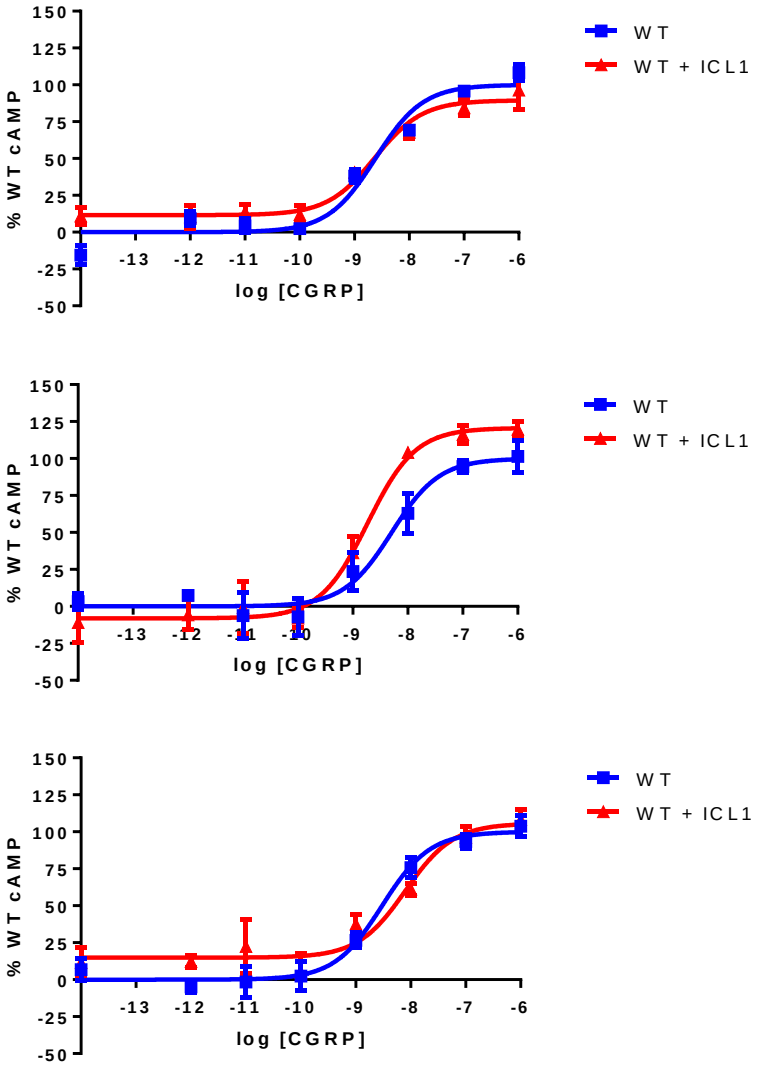

Figure 5.2. Dose response curves of cAMP signalling data produced for the CGRP mediated cAMP stimulation of the WT receptor co-expressed with the ICL1 domain.
Transfected Cos7 cells were dose dependently stimulated with CGRP and levels of the cAMP second messenger were detected using a TR-FRET based cAMP assay. A sigmoidal dose response curve was fitted to the data using GraphPad Prism software. The co-transfected ICL1 data were normalised to WT, taking the maximum and minimum values obtained from the WT dose response curve.

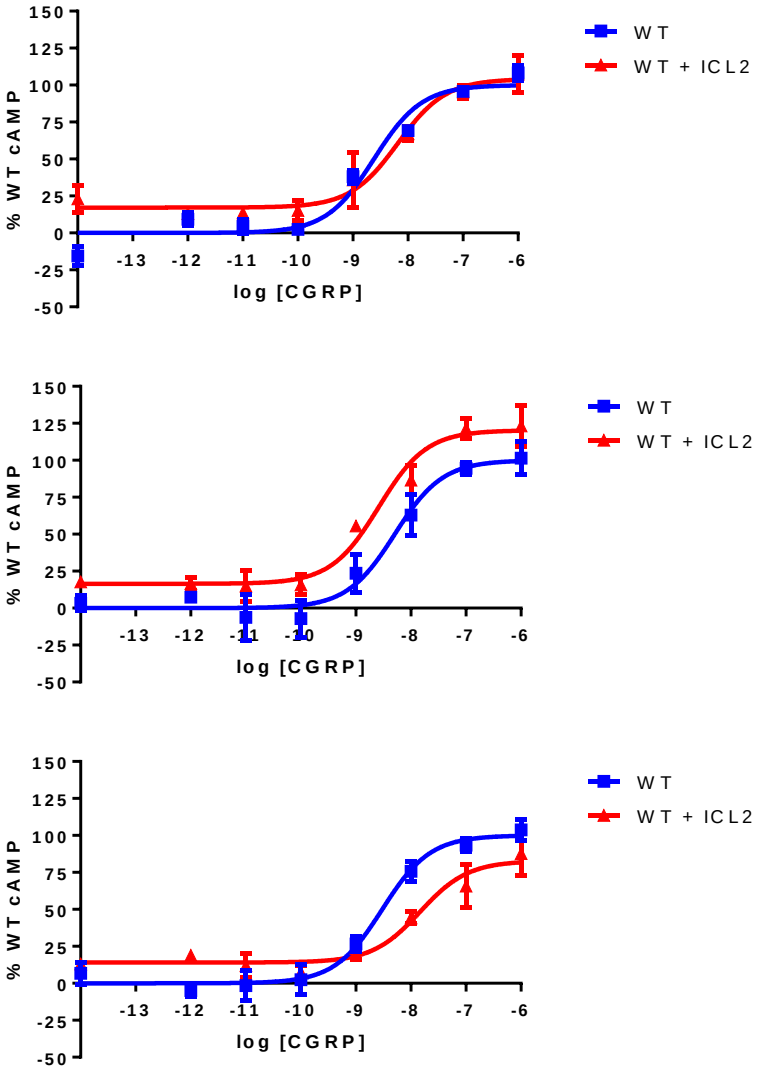

Figure 5.3. Dose response curves of cAMP signalling data produced for the CGRP mediated cAMP stimulation of the WT receptor co-expressed with the ICL2 domain.
Transfected Cos7 cells were dose dependently stimulated with CGRP and levels of the cAMP second messenger were detected using a TR-FRET based cAMP assay. A sigmoidal dose response curve was fitted to the data using GraphPad Prism software. The co-transfected ICL2 data were normalised to WT, taking the maximum and minimum values obtained from the WT dose response curve.

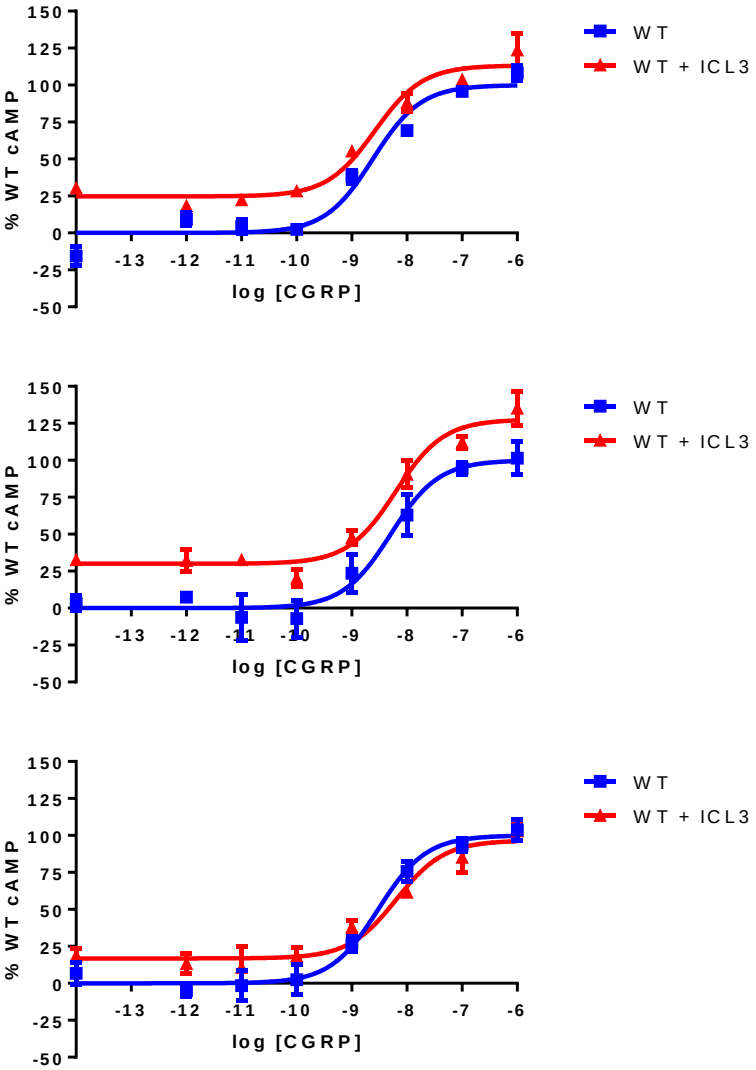

Figure 5.4. Dose response curves of cAMP signalling data produced for the CGRP mediated cAMP stimulation of the WT receptor co-expressed with the ICL3 domain.
Transfected Cos7 cells were dose dependently stimulated with CGRP and levels of the cAMP second messenger were detected using a TR-FRET based cAMP assay. A sigmoidal dose response curve was fitted to the data using GraphPad Prism software The co-transfected ICL3 data were normalised to WT, taking the maximum and minimum values obtained from the WT dose response curve.

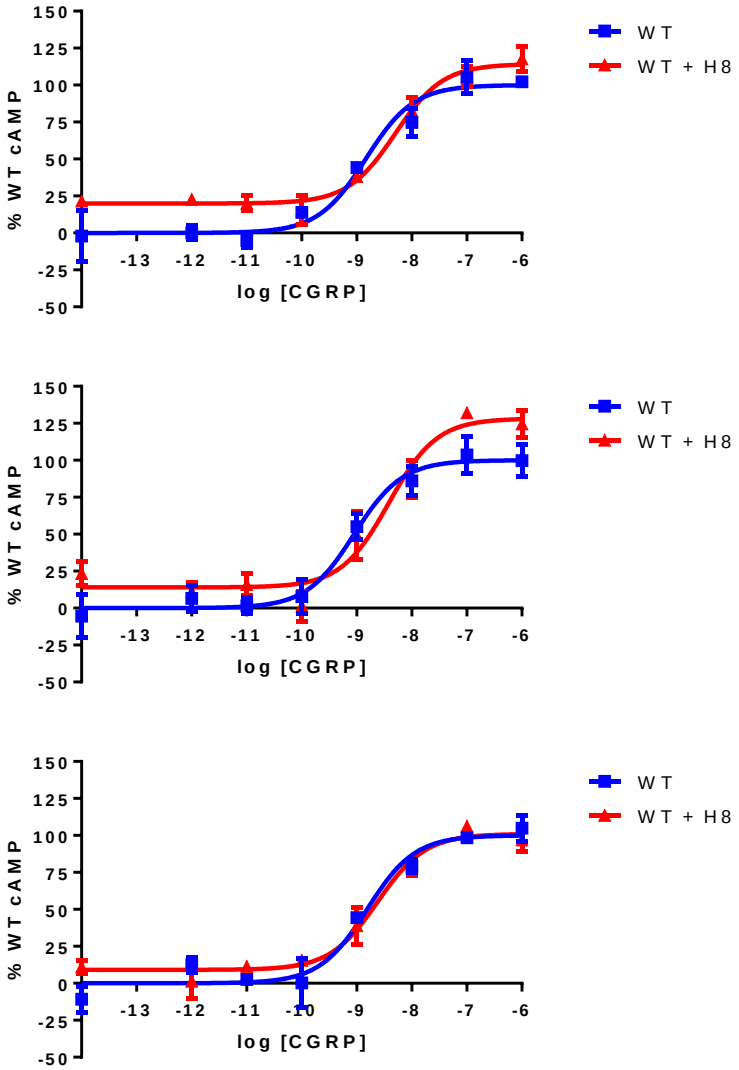

Figure 5.5. Dose response curves of cAMP signalling data produced for the CGRP mediated cAMP stimulation of the WT receptor co-expressed with the H8 domain.
Transfected Cos7 cells were dose dependently stimulated with CGRP and levels of the cAMP second messenger were detected using a TR-FRET based cAMP assay. A sigmoidal dose response curve was fitted to the data using GraphPad Prism software. The co-transfected helix 8 data were normalised to WT, taking the maximum and minimum values obtained from the WT dose response curve.

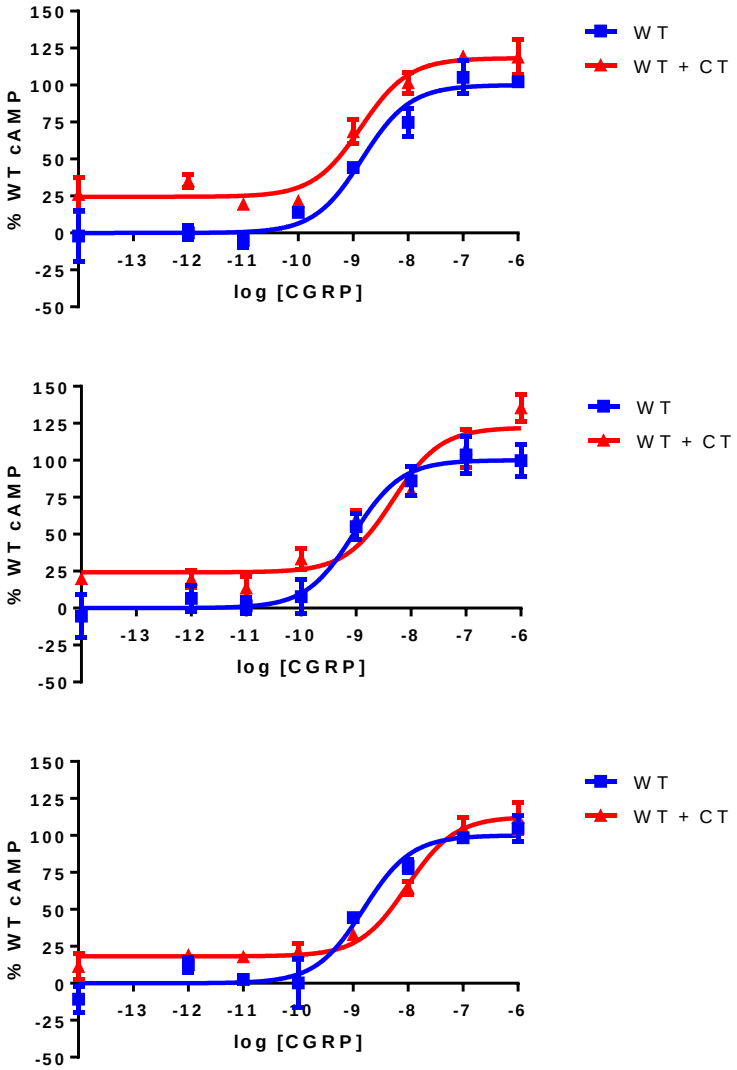

Figure 5.6. Dose response curves of cAMP signalling data produced for the CGRP mediated cAMP stimulation of the WT receptor co-expressed with the C-terminus domain.

Transfected Cos7 cells were dose dependently stimulated with CGRP and levels of the cAMP second messenger were detected using a TR-FRET based cAMP assay. A sigmoidal dose response curve was fitted to the data using GraphPad Prism software. The co-transfected C-terminus data were normalised to WT, taking the maximum and minimum values obtained from the WT dose response curve.

Receptor construct	pEC_{50} CLR-$hG_{\alpha s}$ Mean	SEM	N	pEC_{50} WT CLR Mean	SEM	N	pEC_{50} t-test	Basal CLR-$hG_{\alpha s}$ Mean	SEM	N	Basal t-test	E_{max} CLR-$hG_{\alpha s}$ Mean	SEM	N	E_{max} t-test
CLR-$hG_{\alpha s}$	-9.17	0.16	3	-10.42	0.23	3	0.0108*	18.30	1.14	3	0.0039**	62.12	3.07	3	0.0065**

Reduced pEC_{50}/basal/E_{max} value Increased pEC_{50}/basal/E_{max} value

Table 5.2. Summary of the EC_{50}, basal and E_{max} mean and SEM values for the CLR-$hG_{\alpha s}$ fusion and WT CLR receptor co-transfected with RAMP1.
Transfected Cos7 cells were dose dependently stimulated with CGRP and levels of the cAMP second messenger were detected using a TR-FRET based cAMP assay. A sigmoidal dose response curve was fitted to the data using GraphPad Prism software. The intracellular domain co-expression was normalised to WT, taking the maximum and minimum values obtained from the WT dose response curve. The number of experimental repeats is denoted in the N column and the significance was obtained through unpaired t-test. *$p < 0.05$, ** $p < 0.01$, ***$p < 0.001$.

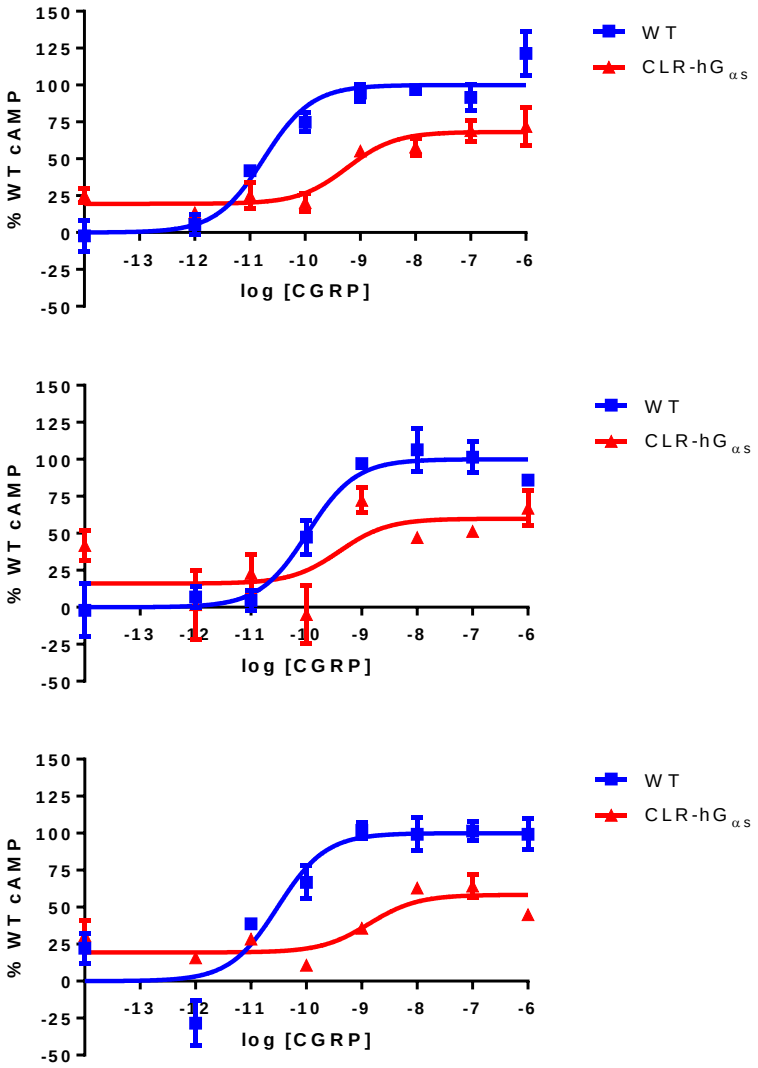

Figure 5.7. Dose response curves of cAMP signalling data of the CLR-hG$_{\alpha s}$ fusion and WT CLR co-transfected with RAMP1.

Transfected Cos7 cells were dose dependently stimulated with CGRP and levels of the cAMP second messenger were detected using a TR-FRET based cAMP assay. A sigmoidal dose response curve was fitted to the data using GraphPad Prism software. The CLR-hG$_{\alpha s}$ fusion receptor co-transfected with RAMP1 data were normalised to WT, taking the maximum and minimum values obtained from the WT dose response curve.

The CLR-h$G_{\alpha s}$ construct produced a cAMP signalling response, however with a significantly reduced pEC_{50} value (~20 fold reduction) and E_{max} (~62% of WT) and a significantly increased basal (~18% above WT).

5.4 Discussion

5.4.1 Data integrity

5.4.1.1 Co-expression of individual intracellular domains with WT CLR

The cAMP signalling data is shown in Table 5.1 and Figure 5.2 to Figure 5.6. The pEC_{50} values for the WT CLR control were lower than expected (8.48 to 8.9) compared with previously published values (9.5 to 10.5) (Barwell *et al.*, 2011). However these values were similar to pEC_{50} values observed in the alanine substitution study of chapter 3 and were consistent across experimental repeats. They were therefore considered acceptable to use. The basal and E_{max} signalling illustrated in Figure 5.2 to Figure 5.6 often showed higher levels when co-expressed with the intracellular domains. This was reflected in a higher mean for all the basal (6.12 % to 23.85 %) and Emax (102 % to 117 %) values however the only statistically significant differences were observed with ICL2 and C-terminus co-expression for basal and C-terminus for the E_{max}. It has been previously observed that higher basal and Emax signalling reflects variations in the assay set up (e.g. cell numbers) however it was unlikely that this occurred in each experimental repeat for each co-expression treatment. Further investigation would be required to ensure this is a biological effect.

5.4.1.2 Synthesis and functional analysis of the CLR-h$G_{\alpha s}$ fusion protein

The functional analysis of the CLR-h$G_{\alpha s}$ fusion protein was done through cAMP signalling. These results are shown in Table 5.2 and Figure 5.7. The pEC_{50} value for the WT CLR control was 10.42 which is consistent with published data (Barwell *et al.*, 2011). The signalling observed with the CLR-$G_{\alpha s}$ fusion protein had a consistently reduced pEC_{50} value, increased basal and reduced Emax. All these variations were statistically significant. However signalling was successful at a reduced pEC50 of ~ 20 fold and an Emax of 62.12 % WT CLR.

5.4.2 Co-expression of individual intracellular domains with WT CLR

The expression of individual GPCR ICL domains has been previously shown to inhibit receptor signalling. This was done through the expression the δ-OR ICL3 domain in

cells expressing a variety of GPCRs. The inhibition was common between receptors that shared similar G protein signalling pathways indicating inhibition through G protein interaction (Morou & Georgoussi, 2005). Co-expression of both the α1B-AR ICL3 and C-terminal domain was found to reduce the maximal IP_3 signalling of the α1B-AR, however when tested, basal and pEC_{50} values were not significantly different to WT (Hawes et al., 1994; Luttrell et al., 1993).

Work in this chapter investigated the effect on receptor signalling through co-expression of the intracellular domains of the CGRP receptor. These included ICL1, ICL2, ICL3, H8 and the C-terminus. Co-expression of these domains with the WT CGRP receptor did not result in a significant change in cAMP pEC_{50} values. Basal levels of CGRP receptor co-transfected with ICL2 and the C-terminus were significantly increased (15.89 % and 22.31 % respectively). ICL2 of the WT receptor is expected to interact with the G protein during the activation process. It is possible that the isolated loop is interacting with the G protein resulting in an increased signalling response. The CGRP receptor co-expressed with the C-terminal domain had a significantly increase E_{max}. The increased basal and E_{max} signalling observed with the co-expression of the C-terminus could be explained with this domain competing with the internalisation machinery that is known to bind to the C-terminus (Conner et al., 2008) preventing internalisation of the WT receptor and increasing the maximum signalling capacity. These results show that the co-expressed CLR intracellular domains do have an effect on receptor function however to be certain that this is as a result of successful expression and competition of the intracellular domains, further experiments are required.

The δ-OR ICL3 domain was cloned into a mammalian expression vector using a similar approach, except a ribosome consensus sequence was included at the 5' terminus. An N-terminal GST-tagged construct was also created. Expression of the δ-OR ICL3 domain was determined using RT-PCR and western blot analysis. Successful expression of the intracellular domains of the CGRP receptor was not tested; therefore the absence of significant signalling effect may be due to a lack of expression or degradation of expressed protein. The nature of the experimental design, by cloning only the intracellular domain DNA sequences without tags or

markers and the test for functional effect through the cAMP signalling assay was used as an initial screen due to limits in time. To continue this investigation further, the introduction of tags and fluorescent markers to the isolated intracellular fragments could be used to ensure successful expression. If successful expression of these isolated domains is occurring then it is also possible that they may interfere with the cell surface expression of the receptor or internalisation following CGRP-mediated activation. To measure this, the cell surface expression ELISA could be used.

5.4.3 Synthesis and functional analysis of a CLR-$G_{\alpha s}$ fusion protein

GPCR-$G_{\alpha s}$ fusion proteins have been shown to signal at levels similar or greater than co-expression of the individual subunits (Bertin *et al.*, 1994; Seifert *et al.*, 1998a; Seifert *et al.*, 1998b). This has provided a more consistent platform for the study of GPCR-G protein interactions in cell systems consisting of sub-units in 1:1 stoichiometry. Two CLR-$G_{\alpha s}$ fusion constructs were created as a proof of concept to use this technique to study interactions between these two components specifically for the CGRP receptor. The CLR-h$G_{\alpha s}$ produced a CGRP-mediated signalling response, however with a significantly reduced pEC_{50} value (~20 fold reduction), increased basal value (~18%) and reduced E_{max} (~62%). The increased basal activity could be explained due to the close proximity of the h$G_{\alpha s}$ subunit to the receptor. Given the fluid nature of the receptor to exist in multiple conformations and exhibit constitutive activity, a more closely associated G protein could be activated more frequently than an independently expressed subunit, resulting in an increase in signalling. However this close association could also explain the reduced E_{max}. A fused G protein is less able to dissociate and be recycled and also to allow other G proteins to be activated by the same receptor. Another factor to be considered is the endogenous G proteins of the Cos7 cell line. The CLR-r$G_{\alpha s}$ fusion protein did not produce a cAMP signalling response. This is unexpected as the primary sequence of these two proteins only differs by a single amino acid. More experiments are required to see if this is a real result or instead reflects an issue with the DNA construct or transfection process.

This is preliminary evidence to support a proof of concept that the fusion $G_{\alpha s}$ sub-unit is being used for signalling (at least in part) and that this construct might be useful for future work. As the observed cAMP response could be through the endogenous Cos7 $G_{\alpha s}$ proteins, signalling would need to be shown in cells that do not express the endogenous $G_{\alpha s}$ proteins. Mutagenesis of the $G_{\alpha s}$ subunit has been done that impaired GDP binding or increased GTPase activity, which reduced receptor-mediated activation (Warner & Weinstein, 1999; Warner *et al.*, 1998). Repeating this with the CLR-h$G_{\alpha s}$ construct would show if signalling is through the fused $G_{\alpha s}$ protein or the endogenous one. This was not done due to time limitations.

5.4.4 Conclusions

This chapter set out to provide evidence for proof of concept of two novel signalling investigation techniques for the CGRP receptor. These experiments were designed to see whether CGRP receptor signalling could be manipulated with the co-expression of its intracellular domains or studied through a functional CLR-h$G_{\alpha s}$ fusion protein. The first set of experiments created receptor fragments that had a functional effect on cAMP signalling when co-expressed with the WT receptor. The second set of experiments created a CLR-h$G_{\alpha s}$ fusion protein that produced a successful set of preliminary signalling results. A more comprehensive set of experiments are now required to confirm this however this could be a useful new construct for the study of receptor-G protein interactions.

6 Final Discussion

6.1 Introduction

This thesis has described studies that investigated various signalling aspects of the CGRP receptor. The main focus has been the ECL2 domain of CLR, the GPCR component of the receptor. This project has shown that ECL2 is the most important single, functional domain for ligand-based activation of the CGRP receptor, with evidence for the first time that a large number of residues are involved. These were initially identified through alanine substitution mutagenesis of each individual residue of ECL2, described in chapter 3. These results were used by collaborators to iteratively develop and refine a computer model of CLR bound to CGRP in the active state. An extensive program of mutagenesis targeting important residues of ECL2 has started to reveal the complex set of intra- and inter-molecular interactions that occur for both structural integrity and ligand-mediated receptor activation. These results are described in chapter 4. The final part of the study into CGRP receptor function looked at the intracellular interactions that occur during receptor signalling. The involvement of each intracellular domain of the CGRP receptor in signalling was studied and preliminary results for a new CLR-h$G_{\alpha s}$ fusion construct that could be used for receptor-G protein interaction research were described. These results are described in chapter 5.

6.2 Key aspects of the mutagenesis program

The work described in chapters 3 and 4 used substitution mutagenesis on each individual residue of ECL2, including the interface with TM4 and 5, to investigate the function of each amino acid of this loop in cell surface expression, ligand binding, receptor signalling and internalisation. 24 residues were substituted with alanine and of these, 14 were found to have a significantly reduced pEC_{50} compared with WT. The most dramatic reductions were R274A (~100 fold reduction), D280A (~80 fold reduction) and W283A (~300 fold reduction). These three residues have been highlighted on the highest scoring models for both the CGRP and AM receptor. The

equivalent three residues have also been highlighted on the CRHR1 and GCGR crystal structures (Hollenstein *et al.*, 2013; Siu *et al.*, 2013). These are shown in Figure 6.1. The amino acids selected were the conserved TM4/ECL2 basic residue and the conserved ECL2 tryptophan residue. The ECL2 acidic residue that is predicted to form a salt bridge with the TM4/ECL2 basic residue in the crystal structures was chosen however is located in a different position in the ECL2 primary sequence to D280.

Also notable were Y277A and Y278A (both ~10 fold reduction), I284A (~10 fold reduction) and T288A (~20 fold reduction). C282A had significantly reduced signalling (~10 fold) however the double alanine substitution C212AC282A recovered signalling indicating its function in disulphide bond formation.

Using this data, receptor modelling was undertaken by collaborators that indicated that R274 had a structural role, potentially bridging with the plasma membrane and D280 or the nearby tyrosine residues (Y277 or Y278). The precise length of the R274 side chain was important as substitution with the conservative R274K only partially recovered signalling compared with the alanine substitution. Signalling at positions Y277 and Y278 was recovered with an individual phenylalanine substitution (Y277F and Y278F), showing the importance of the aromatic part of the tyrosine side chain. However at position Y277, a leucine substitution (Y277L) also recovered signalling indicating that the functional effect at this position is due to hydrophobicity. This result also makes the predicted R274-Y277 interaction unlikely. The dramatic reduction in signalling of the alanine substitution at position D280 (D280A) was not recovered by a number of amino acid replacements, including the conservative glutamate substitution (D280E) indicating the required specificity of the charge and position of the aspartate side chain. Given the similar reduction in signalling potency of the R27A and D280A substitutions and the requirement of the WT residue for full functional effect at each position, the predicted R274-D280 interaction remains possible. The highest scoring CGRP model (Figure 6.1) does not position these two residues close enough to form a salt bridge however the highest scoring AM receptor model does.

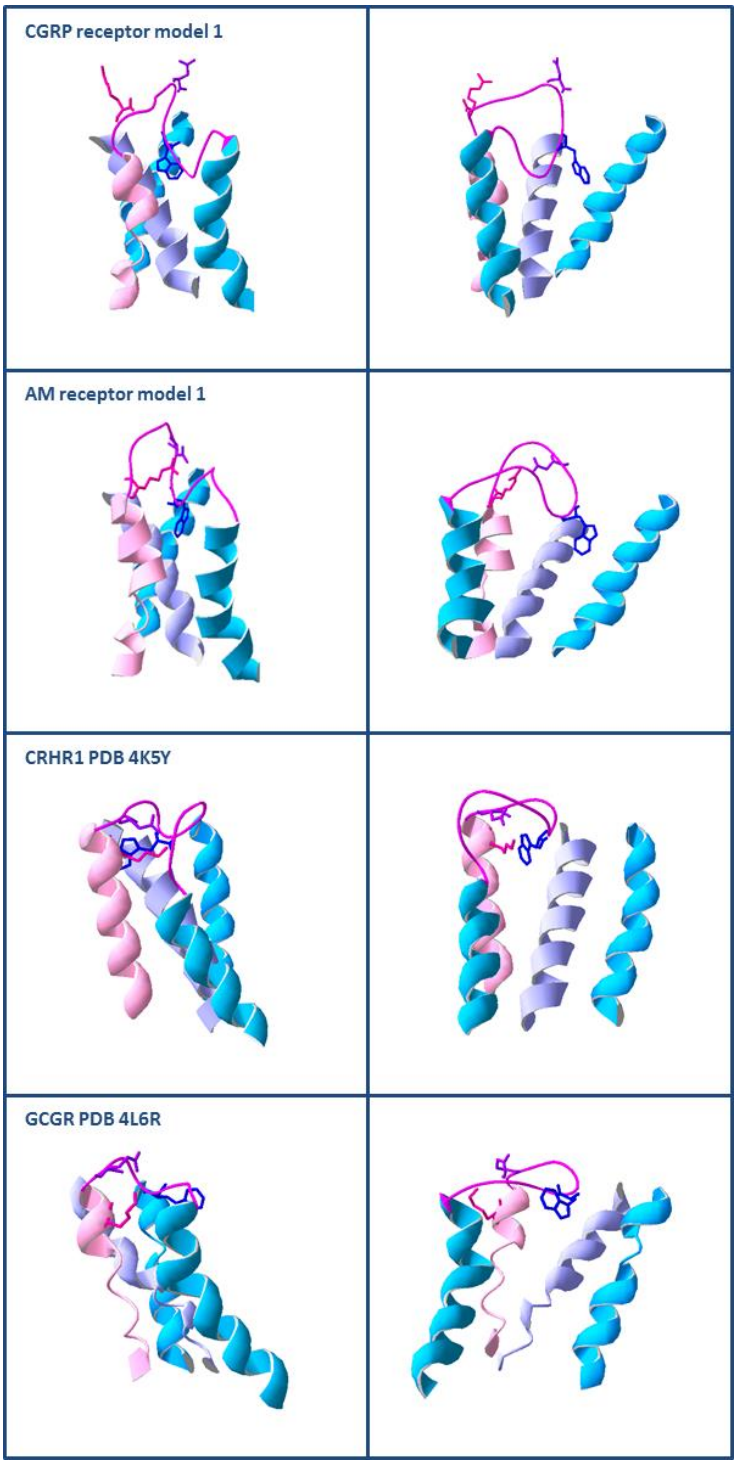

Figure 6.1. Key ECL2 residues highlighted in CGRP and AM receptors models and equivalent residues in CRHR1 and GCGR1 crystal structures.

CLR structures for the highest scoring CGRP and AM receptor models are shown. The CRHR1 crystal structure (PDB 4K5Y) and the GCGR crystal structure (PDB4L6R) are also shown. TM2 (light blue), TM3 (lilac), TM4 (salmon), TM5 (turquoise) and ECL2 (purple) are shown. R274 (pink), D280 (purple) and W283 (blue) are highlighted. The equivalent resides selected in the CRHR1 and GCGR1 are the TM4/ECL2 conserved basic residue, the ECL2 acidic residues predicted to form a salt bridge with the TM4/ECL2 basic residue and the conserved ECL2 tryptophan residue.

The mutagenesis of W283 produced some of the most interesting data. The ~300 fold reduction observed with the alanine substitution mutant was partially recovered with a phenylalanine substitution (W283F, ~100 fold) however was completely recovered with a histidine substitution (W283H). This brings our attention to the imidazole portion of the tryptophan side chain, through which computer modelling proposes can form hydrogen bonds with histidine residues in TM2 and 3. The orientation of W283 back towards the TM helices instead of into the centre of the TM bundle more closely resembles the CRHR1 structure compared with GCGR (Figure 6.1).

The middle and the C-terminus of the loop are predicted to be involved in both structural and ligand interactions. Important contact points with CGRP are thought to be through D280, D287 and T288, however this has not yet been empirically deduced. Residues D287 and T288 at the C-terminus of ECL2 are speculated to be CGRP binding sites. Conservative substitutions at each of these positions (D287E and T288S) recovered signalling. This suggests that although the electrostatic properties of the side chain are important for receptor function, the precise location at these positions is more flexible. Cell surface expression remained unaffected except for a cluster of four residues from C282 to S285 which all had significantly reduced expression levels (50-70% WT). This cluster may be a coincidental finding or could reflect a trafficking motif.

There is a hydrophobic cluster of residues at the ECL2/TM5 interface at which individual alanine substitutions result in a small reduction in cAMP signalling (3-10 fold reduction) however multiple alanine substitutions produce substantial effects (L290AL291AY292A, ~10,000 fold reduction; L290AL291A, ~300 fold reduction; L290Y292, ~30 fold reduction). This suggests that this cluster functions as a functional hydrophobic motif that is maintained during the removal of individual side chains of this cluster however is dramatically lost if two or more of these side chains are removed.

6.3 Signalling elements within the intracellular regions of CLR

Chapter 5 presents preliminary findings of new experimental techniques that can be used to study CGRP receptor signalling in further detail.

The first was the use of a co-expression system using individually expressed CLR domains together with the WT receptor to investigate the functional effect. More precisely, the intracellular domains were cloned into a mammalian expression vector, co-expressed with the WT CGRP receptor and the effect of ligand-mediated cAMP signalling was measured. This approach has successfully identified ICL3 and the C-terminus as G protein-binding partners in other GPCRs (Hawes *et al.*, 1994; Luttrell *et al.*, 1993). Co-expression of the intracellular domains resulted in some significant changes to cAMP signalling, most notable a significantly increased E_{max} (~115% of WT) with the co-expression of the C-terminal domain with the CGRP receptor.

The second was the creation of a functional receptor-$G_{\alpha s}$ protein fusion construct. Two fusion constructs were created. These were CLR-h$G_{\alpha s}$ and CLR-r$G_{\alpha s}$. CLR-h$G_{\alpha s}$ produced a CGRP-induced signalling response, however with a reduced pEC_{50}, an increased basal and a reduced E_{max}. CLR-r$G_{\alpha s}$ did not produce a cAMP signalling response. This is the first time a GPCR-G protein fusion approach has been used for family B GPCRs. Before this system can be used to study CLR-h$G_{\alpha s}$ interactions further work is required to verify that the observed signalling is through the fused $G_{\alpha s}$ protein, however this is a promising new strategy for the future of CGRP receptor signalling research.

6.4 Physiological relevance of structure and function understanding of the CGRP receptor

CGRP is a potent vasodilator, released from the central and peripheral nervous system, with a physiological role in migraine, neurogenic inflammation, hypertension and has been found to be cardioprotective (Doggrell, 2001). CGRP

receptor antagonists have been investigated as possible therapeutics in the treatment of migraine (Durham & Vause, 2010) and during myocardial ischemia, CGRP release stops the development of myocardial infarction (Franco-Cereceda & Liska, 2000). There is evidence that CGRP has a protective effect in hypertension (Smillie & Brain, 2011). Given the involvement of CGRP in a number of pathophysiological conditions, understanding the mechanism through which the ligand binds to and activates its receptor is of considerable interest and importance in the design and development of therapeutics to tackle these conditions. The data described in this work provide the platform for potential therapeutic design as it can be used to investigate the docking site of CGRP with its receptor.

6.5 Future work

The results described in chapters 3 and 4 show that the CLR ECL2 domain is very important for CGRP binding and activation. The key residues of this domain that are involved have been identified and some of the interactions through which these residues function have been determined. This information is now ready to be built on to understand the structure of the loop, the location of the ligand binding pocket and the mechanism through which receptor activation occurs. The combined work of the alanine substitution mutagenesis in chapter 3 and the computer modelling of CLR (Woolley et al., 2013) indicates that the N-terminal portion of the loop (between R274 and D280) is important for the structural integrity of this domain with the C-terminal portion of the loop likely to bind CGRP.

The computer modelling suggests that the structural scaffold of the N-terminal part of the loop could be conferred through interactions with either R274 and D280 or between R274 and either of the two tyrosines (Y277 or Y278). The further substitution mutagenesis of chapter 4 shows how important the exact positioning of the charge of the side chain is for both R274 and D280 and the requirement of the aromatic ring of either tyrosine of phenylalanine (Y or F) at position Y278, however do not confirm what each residue is interacting with. A further set of mutagenesis experiments, either creating reciprocal pairings of R274-D280 (R274D/D280R), R274-Y277 (R274Y/Y277R) and R274-Y278 (R274Y/Y278R) could

start to pinpoint the exact site of interactions. One of the higher scoring models predicted R274 to interact with D280 enabling binding to R11 of CGRP. To test this, a number of reciprocal mutants of both CLR and CGRP could be used together with a CGRP analogue at position 11, CGRP R11E. These include R274E/D280N(H)/R11, R274/D280N(H)/R11E and R274E/D280H(R/K)/R11E.

The speculated ligand binding section of ECL2 (N-terminus) allowed a greater flexibility in amino acid substitutions in chapter 4. Given that this is the expected location for CGRP binding it is experimentally more difficult to determine interactions site. It therefore appears to be more strategic to refine the loop structure through the N-terminus allowing for a more directed approach in studying the C-terminus.

There are a number of other experimental techniques that can be used to determine the positioning of individual amino acids and therefore deduce the topography of the domain. These include the scanning cysteine accessibility method (SCAM) which provides information of the exposure of the selected residue to the aqueous environment (Javitch et al., 2002) and Zn^{2+} cross linking of substituted histidine residues to measure the proximity of selected residues (Elling & Schwartz, 1996).

All of the signalling analysis on the CGRP receptor in this thesis has focused on the cAMP signalling pathway. This is the best characterised signalling pathway of this receptor (Walker et al., 2010) and therefore was the most appropriate tool to measure receptor function. However current understanding of GPCR signalling acknowledges that receptors signal through multiple pathways with ligands acting as agonists, antagonist or inverse agonists depending on the pathway (Kenakin, 2007). The CGRP receptor has been shown to signal through $G_{\alpha q}$ with intracellular increases in Ca^{2+} and through β-arrestin measured through ERK1/2 (Walker et al., 2010). To gain comprehensive understanding into the mechanism through which CGRP activates its receptor, the effect of the ECL2 substitution mutagenesis on these alternative pathways could be investigated.

The preliminary results introduced in chapter 5 could produce novel methods for CGRP receptor research to study the functional effect of individual domains and the

specific points of interaction between the receptor and coupled proteins. Currently more work is required to validate both methods as being robust and reliable screens for receptor function. With respect to the intracellular domain co-expression experiments, the successful expression of these domains needs to be shown more conclusively. Before the CLR-h$G_{\alpha s}$ fusion protein can be used to study coupling interactions, it needs to be verified that the observed signalling is through the fused h$G_{\alpha s}$ and not endogenous G proteins.

6.6 Final summary

The work described in this thesis has produced novel and unique information that contributed to both the specific knowledge and understanding of the CGRP receptor and to the field of GPCR research in general. The CLR ECL2 domain was shown to be fundamental with respect to CGRP binding and receptor activation. The individual residues that are involved in this process were identified and through a comprehensive set of substitution mutagenesis, the molecular interactions that produce this functional effect have started to be deduced. Further to this, two new approaches to CGRP receptor functional analysis have been tested and shown to be promising techniques for the future research of this receptor.

7 References

AbdAlla, S., Lother, H. & Quitterer, U. (2000) AT1-receptor heterodimers show enhanced G-protein activation and altered receptor sequestration. *Nature*, 407 (6800): 94-98.

Achour, L., Labbé-Jullié, C., Scott, M. G. & Marullo, S. (2008) An escort for GPCRs: implications for regulation of receptor density at the cell surface. *Trends Pharmacol Sci*, 29 (10): 528-535.

Adelhorst, K., Hedegaard, B. B., Knudsen, L. B. & Kirk, O. (1994) Structure-activity studies of glucagon-like peptide-1. *J Biol Chem*, 269 (9): 6275-6278.

Ahn, K. H., Bertalovitz, A. C., Mierke, D. F. & Kendall, D. A. (2009) Dual role of the second extracellular loop of the cannabinoid receptor 1: ligand binding and receptor localization. *Mol Pharmacol*, 76 (4): 833-842.

Ahuja, S., Hornak, V., Yan, E. C., Syrett, N., Goncalves, J. A., Hirshfeld, A., Ziliox, M., Sakmar, T. P., Sheves, M., Reeves, P. J., Smith, S. O. & Eilers, M. (2009) Helix movement is coupled to displacement of the second extracellular loop in rhodopsin activation. *Nat Struct Mol Biol*, 16 (2): 168-175.

Aittaleb, M., Boguth, C. A. & Tesmer, J. J. (2010) Structure and function of heterotrimeric G protein-regulated Rho guanine nucleotide exchange factors. *Mol Pharmacol*, 77 (2): 111-125.

Aiyar, N., Rand, K., Elshourbagy, N. A., Zeng, Z., Adamou, J. E., Bergsma, D. J. & Li, Y. (1996) A cDNA encoding the calcitonin gene-related peptide type 1 receptor. *J Biol Chem*, 271 (19): 11325-11329.

Al-Sabah, S. & Donnelly, D. (2003a) The positive charge at Lys-288 of the glucagon-like peptide-1 (GLP-1) receptor is important for binding the N-terminus of peptide agonists. *FEBS Lett*, 553 (3): 342-346.

Al-Sabah, S. & Donnelly, D. (2003b) A model for receptor-peptide binding at the glucagon-like peptide-1 (GLP-1) receptor through the analysis of truncated ligands and receptors. *Br J Pharmacol*, 140 (2): 339-346.

Aldecoa, A., Gujer, R., Fischer, J. A. & Born, W. (2000) Mammalian calcitonin receptor-like receptor/receptor activity modifying protein complexes define calcitonin gene-related peptide and adrenomedullin receptors in Drosophila Schneider 2 cells. *FEBS Lett*, 471 (2-3): 156-160.

Amara, S. G., Arriza, J. L., Leff, S. E., Swanson, L. W., Evans, R. M. & Rosenfeld, M. G. (1985) Expression in brain of a messenger RNA encoding a novel neuropeptide homologous to calcitonin gene-related peptide. *Science*, 229 (4718): 1094-1097.

Amara, S. G., Jonas, V., Rosenfeld, M. G., Ong, E. S. & Evans, R. M. (1982) Alternative RNA processing in calcitonin gene expression generates mRNAs encoding different polypeptide products. *Nature*, 298 (5871): 240-244.

André, N., Cherouati, N., Prual, C., Steffan, T., Zeder-Lutz, G., Magnin, T., Pattus, F., Michel, H., Wagner, R. & Reinhart, C. (2006) Enhancing functional production of G protein-coupled receptors in Pichia pastoris to levels required for structural studies via a single expression screen. *Protein Sci*, 15 (5): 1115-1126.

Angers, S., Salahpour, A., Joly, E., Hilairet, S., Chelsky, D., Dennis, M. & Bouvier, M. (2000) Detection of beta 2-adrenergic receptor dimerization in living cells using bioluminescence resonance energy transfer (BRET). *Proc Natl Acad Sci U S A*, 97 (7): 3684-3689.

Arunlakshana, O. & Schild, H. O. (1959) Some quantitative uses of drug antagonists. *Br J Pharmacol Chemother*, 14 (1): 48-58.

Assas, B. M., Pennock, J. I. & Miyan, J. A. (2014) Calcitonin gene-related peptide is a key neurotransmitter in the neuro-immune axis. *Front Neurosci*, 8 23.

Assil-Kishawi, I. & Abou-Samra, A. B. (2002) Sauvagine cross-links to the second extracellular loop of the corticotropin-releasing factor type 1 receptor. *J Biol Chem*, 277 (36): 32558-32561.

Attramadal, H., Arriza, J. L., Aoki, C., Dawson, T. M., Codina, J., Kwatra, M. M., Snyder, S. H., Caron, M. G. & Lefkowitz, R. J. (1992) Beta-arrestin2, a novel member of the arrestin/beta-arrestin gene family. *J Biol Chem*, 267 (25): 17882-17890.

Attwood, T. K. & Findlay, J. B. (1994) Fingerprinting G-protein-coupled receptors. *Protein Eng*, 7 (2): 195-203.

Avlani, V. A., Gregory, K. J., Morton, C. J., Parker, M. W., Sexton, P. M. & Christopoulos, A. (2007) Critical role for the second extracellular loop in the binding of both orthosteric and allosteric G protein-coupled receptor ligands. *J Biol Chem*, 282 (35): 25677-25686.

Azzi, M., Charest, P. G., Angers, S., Rousseau, G., Kohout, T., Bouvier, M. & Piñeyro, G. (2003) Beta-arrestin-mediated activation of MAPK by inverse agonists

reveals distinct active conformations for G protein-coupled receptors. *Proc Natl Acad Sci U S A*, 100 (20): 11406-11411.

Bailey, R. & Hay, D. (2007) Agonist-dependent consequences of proline to alanine substitution in the transmembrane helices of the calcitonin receptor. *Br J Pharmacol*, 151 (5): 678-687.

Baker, J. G., Hall, I. P. & Hill, S. J. (2003) Agonist and inverse agonist actions of beta-blockers at the human beta 2-adrenoceptor provide evidence for agonist-directed signaling. *Mol Pharmacol*, 64 (6): 1357-1369.

Baldwin, J. M. (1993) The probable arrangement of the helices in G protein-coupled receptors. *EMBO J*, 12 (4): 1693-1703.

Baldwin, J. M., Schertler, G. F. & Unger, V. M. (1997) An alpha-carbon template for the transmembrane helices in the rhodopsin family of G-protein-coupled receptors. *J Mol Biol*, 272 (1): 144-164.

Banerjee, S., Evanson, J., Harris, E., Lowe, S. L., Thomasson, K. A. & Porter, J. E. (2006) Identification of specific calcitonin-like receptor residues important for calcitonin gene-related peptide high affinity binding. *BMC Pharmacol*, 6 9.

Barnes, W. G., Reiter, E., Violin, J. D., Ren, X. R., Milligan, G. & Lefkowitz, R. J. (2005) beta-Arrestin 1 and Galphaq/11 coordinately activate RhoA and stress fiber formation following receptor stimulation. *J Biol Chem*, 280 (9): 8041-8050.

Barnett-Norris, J., Lynch, D. & Reggio, P. H. (2005) Lipids, lipid rafts and caveolae: their importance for GPCR signaling and their centrality to the endocannabinoid system. *Life Sci*, 77 (14): 1625-1639.

Bartlett, S. E., Enquist, J., Hopf, F. W., Lee, J. H., Gladher, F., Kharazia, V., Waldhoer, M., Mailliard, W. S., Armstrong, R., Bonci, A. & Whistler, J. L. (2005) Dopamine responsiveness is regulated by targeted sorting of D2 receptors. *Proc Natl Acad Sci U S A*, 102 (32): 11521-11526.

Barwell, J., Conner, A. & Poyner, D. R. (2011) Extracellular loops 1 and 3 and their associated transmembrane regions of the calcitonin receptor-like receptor are needed for CGRP receptor function. *Biochim Biophys Acta*, 1813 (10): 1906-1916.

Barwell, J., Miller, P. S., Donnelly, D. & Poyner, D. R. (2010) Mapping interaction sites within the N-terminus of the calcitonin gene-related peptide receptor; the role of residues 23-60 of the calcitonin receptor-like receptor. *Peptides*, 31 (1): 170-176.

Bayburt, T. H., Leitz, A. J., Xie, G., Oprian, D. D. & Sligar, S. G. (2007) Transducin activation by nanoscale lipid bilayers containing one and two rhodopsins. *J Biol Chem*, 282 (20): 14875-14881.

Beaulieu, J. M., Sotnikova, T. D., Marion, S., Lefkowitz, R. J., Gainetdinov, R. R. & Caron, M. G. (2005) An Akt/beta-arrestin 2/PP2A signaling complex mediates dopaminergic neurotransmission and behavior. *Cell*, 122 (2): 261-273.

Benovic, J. L., Kühn, H., Weyand, I., Codina, J., Caron, M. G. & Lefkowitz, R. J. (1987) Functional desensitization of the isolated beta-adrenergic receptor by the beta-adrenergic receptor kinase: potential role of an analog of the retinal protein arrestin (48-kDa protein). *Proc Natl Acad Sci U S A*, 84 (24): 8879-8882.

Benovic, J. L., Strasser, R. H., Caron, M. G. & Lefkowitz, R. J. (1986) Beta-adrenergic receptor kinase: identification of a novel protein kinase that phosphorylates the agonist-occupied form of the receptor. *Proc Natl Acad Sci U S A*, 83 (9): 2797-2801.

Bergwitz, C., Gardella, T., Flannery, M., Potts, J. J., Kronenberg, H., Goldring, S. & Jüppner, H. (1996) Full activation of chimeric receptors by hybrids between parathyroid hormone and calcitonin. Evidence for a common pattern of ligand-receptor interaction. *J Biol Chem*, 271 (43): 26469-26472.

Bertin, B., Freissmuth, M., Jockers, R., Strosberg, A. D. & Marullo, S. (1994) Cellular signaling by an agonist-activated receptor/Gs alpha fusion protein. *Proc Natl Acad Sci U S A*, 91 (19): 8827-8831.

Beyermann, M., Heinrich, N., Fechner, K., Furkert, J., Zhang, W., Kraetke, O., Bienert, M. & Berger, H. (2007) Achieving signalling selectivity of ligands for the corticotropin-releasing factor type 1 receptor by modifying the agonist's signalling domain. *Br J Pharmacol*, 151 (6): 851-859.

Binet, V., Duthey, B., Lecaillon, J., Vol, C., Quoyer, J., Labesse, G., Pin, J. P. & Prézeau, L. (2007) Common structural requirements for heptahelical domain function in class A and class C G protein-coupled receptors. *J Biol Chem*, 282 (16): 12154-12163.

Blin, N., Yun, J. & Wess, J. (1995) Mapping of single amino acid residues required for selective activation of Gq/11 by the m3 muscarinic acetylcholine receptor. *J Biol Chem*, 270 (30): 17741-17748.

Blumer, K. J. & Thorner, J. (1991) Receptor-G protein signaling in yeast. *Annu Rev Physiol*, 53 37-57.

Bockaert, J. & Pin, J. (1999) Molecular tinkering of G protein-coupled receptors: an evolutionary success. *EMBO J*, 18 (7): 1723-1729.

Boguth, C. A., Singh, P., Huang, C. C. & Tesmer, J. J. (2010) Molecular basis for activation of G protein-coupled receptor kinases. *EMBO J*, 29 (19): 3249-3259.

Bomberger, J. M., Parameswaran, N., Hall, C. S., Aiyar, N. & Spielman, W. S. (2005) Novel function for receptor activity-modifying proteins (RAMPs) in post-endocytic receptor trafficking. *J Biol Chem*, 280 (10): 9297-9307.

Bos, J. L., Rehmann, H. & Wittinghofer, A. (2007) GEFs and GAPs: critical elements in the control of small G proteins. *Cell*, 129 (5): 865-877.

Boulanger, Y., Khiat, A., Chen, Y., Senécal, L., Tu, Y., St-Pierre, S. & Fournier, A. (1995) Structure of human calcitonin gene-related peptide (hCGRP) and of its antagonist hCGRP 8-37 as determined by NMR and molecular modeling. *Pept Res*, 8 (4): 206-213.

Bownds, D., Dawes, J., Miller, J. & Stahlman, M. (1972) Phosphorylation of frog photoreceptor membranes induced by light. *Nat New Biol*, 237 (73): 125-127.

Brain, S. D. & Grant, A. D. (2004) Vascular actions of calcitonin gene-related peptide and adrenomedullin. *Physiol Rev*, 84 (3): 903-934.

Burstein, E. S., Spalding, T. A. & Brann, M. R. (1996) Amino acid side chains that define muscarinic receptor/G-protein coupling. Studies of the third intracellular loop. *J Biol Chem*, 271 (6): 2882-2885.

Burstein, E. S., Spalding, T. A. & Brann, M. R. (1998) The second intracellular loop of the m5 muscarinic receptor is the switch which enables G-protein coupling. *J Biol Chem*, 273 (38): 24322-24327.

Béjà, O., Aravind, L., Koonin, E. V., Suzuki, M. T., Hadd, A., Nguyen, L. P., Jovanovich, S. B., Gates, C. M., Feldman, R. A., Spudich, J. L., Spudich, E. N. & DeLong, E. F. (2000) Bacterial rhodopsin: evidence for a new type of phototrophy in the sea. *Science*, 289 (5486): 1902-1906.

Bühlmann, N., Aldecoa, A., Leuthäuser, K., Gujer, R., Muff, R., Fischer, J. A. & Born, W. (2000) Glycosylation of the calcitonin receptor-like receptor at Asn(60) or Asn(112) is important for cell surface expression. *FEBS Lett*, 486 (3): 320-324.

Caffrey, M. & Cherezov, V. (2009) Crystallizing membrane proteins using lipidic mesophases. *Nat Protoc*, 4 (5): 706-731.

Caffrey, M., Li, D. & Dukkipati, A. (2012) Membrane protein structure determination using crystallography and lipidic mesophases: recent advances and successes. *Biochemistry*, 51 (32): 6266-6288.

Camps, M., Carozzi, A., Schnabel, P., Scheer, A., Parker, P. J. & Gierschik, P. (1992) Isozyme-selective stimulation of phospholipase C-beta 2 by G protein beta gamma-subunits. *Nature*, 360 (6405): 684-686.

Cardoso, J., Pinto, V., Vieira, F., Clark, M. & Power, D. (2006) Evolution of secretin family GPCR members in the metazoa. *BMC Evol Biol*, 6 108.

Chai, W., Mehrotra, S., Jan Danser, A. H. & Schoemaker, R. G. (2006) The role of calcitonin gene-related peptide (CGRP) in ischemic preconditioning in isolated rat hearts. *Eur J Pharmacol*, 531 (1-3): 246-253.

Chamberlain, A. K., Lee, Y., Kim, S. & Bowie, J. U. (2004) Snorkeling preferences foster an amino acid composition bias in transmembrane helices. *J Mol Biol*, 339 (2): 471-479.

Chan, K., Pang, R. & Chow, B. (2001) Functional segregation of the highly conserved basic motifs within the third endoloop of the human secretin receptor. *Endocrinology*, 142 (9): 3926-3934.

Chandrashekar, J., Hoon, M. A., Ryba, N. J. & Zuker, C. S. (2006) The receptors and cells for mammalian taste. *Nature*, 444 (7117): 288-294.

Chen, Z., Gaudreau, R., Le Gouill, C., Rola-Pleszczynski, M. & Stanková, J. (2004) Agonist-induced internalization of leukotriene B(4) receptor 1 requires G-protein-coupled receptor kinase 2 but not arrestins. *Mol Pharmacol*, 66 (3): 377-386.

Cherezov, V., Rosenbaum, D., Hanson, M., Rasmussen, S., Thian, F., Kobilka, T., Choi, H., Kuhn, P., Weis, W., Kobilka, B. & Stevens, R. (2007) High-resolution crystal structure of an engineered human beta2-adrenergic G protein-coupled receptor. *Science*, 318 (5854): 1258-1265.

Chien, E. Y., Liu, W., Zhao, Q., Katritch, V., Han, G. W., Hanson, M. A., Shi, L., Newman, A. H., Javitch, J. A., Cherezov, V. & Stevens, R. C. (2010) Structure of the human dopamine D3 receptor in complex with a D2/D3 selective antagonist. *Science*, 330 (6007): 1091-1095.

Chini, B. & Parenti, M. (2009) G-protein-coupled receptors, cholesterol and palmitoylation: facts about fats. *J Mol Endocrinol*, 42 (5): 371-379.

Choe, H. W., Kim, Y. J., Park, J. H., Morizumi, T., Pai, E. F., Krauss, N., Hofmann, K. P., Scheerer, P. & Ernst, O. P. (2011) Crystal structure of metarhodopsin II. *Nature*, 471 (7340): 651-655.

Christopoulos, A., Christopoulos, G., Morfis, M., Udawela, M., Laburthe, M., Couvineau, A., Kuwasako, K., Tilakaratne, N. & Sexton, P. M. (2003) Novel receptor partners and function of receptor activity-modifying proteins. *J Biol Chem*, 278 (5): 3293-3297.

Christopoulos, G., Perry, K. J., Morfis, M., Tilakaratne, N., Gao, Y., Fraser, N. J., Main, M. J., Foord, S. M. & Sexton, P. M. (1999) Multiple amylin receptors arise from receptor activity-modifying protein interaction with the calcitonin receptor gene product. *Mol Pharmacol*, 56 (1): 235-242.

Chugunov, A. O., Simms, J., Poyner, D. R., Dehouck, Y., Rooman, M., Gilis, D. & Langer, I. (2010) Evidence that interaction between conserved residues in transmembrane helices 2, 3, and 7 are crucial for human VPAC1 receptor activation. *Mol Pharmacol*, 78 (3): 394-401.

Claing, A., Laporte, S. A., Caron, M. G. & Lefkowitz, R. J. (2002) Endocytosis of G protein-coupled receptors: roles of G protein-coupled receptor kinases and beta-arrestin proteins. *Prog Neurobiol*, 66 (2): 61-79.

Clark, A., Cooper, G. J., Lewis, C. E., Morris, J. F., Willis, A. C., Reid, K. B. & Turner, R. C. (1987) Islet amyloid formed from diabetes-associated peptide may be pathogenic in type-2 diabetes. *Lancet*, 2 (8553): 231-234.

Colson, A. O., Perlman, J. H., Smolyar, A., Gershengorn, M. C. & Osman, R. (1998) Static and dynamic roles of extracellular loops in G-protein-coupled receptors: a mechanism for sequential binding of thyrotropin-releasing hormone to its receptor. *Biophys J*, 74 (3): 1087-1100.

Conner, A., Hay, D., Simms, J., Howitt, S., Schindler, M., Smith, D., Wheatley, M. & Poyner, D. (2005) A key role for transmembrane prolines in calcitonin receptor-like receptor agonist binding and signalling: implications for family B G-protein-coupled receptors. *Mol Pharmacol*, 67 (1): 20-31.

Conner, A., Simms, J., Conner, M., Wootten, D., Wheatley, M. & Poyner, D. (2006a) Diverse functional motifs within the three intracellular loops of the CGRP1 receptor. *Biochemistry*, 45 (43): 12976-12985.

Conner, A., Simms, J., Howitt, S., Wheatley, M. & Poyner, D. (2006b) The second intracellular loop of the calcitonin gene-related peptide receptor provides molecular determinants for signal transduction and cell surface expression. *J Biol Chem*, 281 (3): 1644-1651.

Conner, A. C., Simms, J., Barwell, J., Wheatley, M. & Poyner, D. R. (2007a) Ligand binding and activation of the CGRP receptor. *Biochem Soc Trans*, 35 (Pt 4): 729-732.

Conner, M., Hawtin, S. R., Simms, J., Wootten, D., Lawson, Z., Conner, A. C., Parslow, R. A. & Wheatley, M. (2007b) Systematic analysis of the entire second extracellular loop of the V(1a) vasopressin receptor: key residues, conserved throughout a G-protein-coupled receptor family, identified. *J Biol Chem*, 282 (24): 17405-17412.

Conner, M., Hicks, M., Dafforn, T., Knowles, T., Ludwig, C., Staddon, S., Overduin, M., Günther, U., Thome, J., Wheatley, M., Poyner, D. & Conner, A. (2008) Functional and biophysical analysis of the C-terminus of the CGRP-receptor; a family B GPCR. *Biochemistry*, 47 (32): 8434-8444.

Copp, D. H. & Cheney, B. (1962) Calcitonin-a hormone from the parathyroid which lowers the calcium-level of the blood. *Nature*, 193 381-382.

Cornea, A., Janovick, J. A., Maya-Núñez, G. & Conn, P. M. (2001) Gonadotropin-releasing hormone receptor microaggregation. Rate monitored by fluorescence resonance energy transfer. *J Biol Chem*, 276 (3): 2153-2158.

Cottrell, G. S., Padilla, B., Pikios, S., Roosterman, D., Steinhoff, M., Grady, E. F. & Bunnett, N. W. (2007) Post-endocytic sorting of calcitonin receptor-like receptor and receptor activity-modifying protein 1. *J Biol Chem*, 282 (16): 12260-12271.

Craft, C. M., Whitmore, D. H. & Wiechmann, A. F. (1994) Cone arrestin identified by targeting expression of a functional family. *J Biol Chem*, 269 (6): 4613-4619.

Daaka, Y., Luttrell, L. M., Ahn, S., Della Rocca, G. J., Ferguson, S. S., Caron, M. G. & Lefkowitz, R. J. (1998) Essential role for G protein-coupled receptor endocytosis in the activation of mitogen-activated protein kinase. *J Biol Chem*, 273 (2): 685-688.

Daaka, Y., Luttrell, L. M. & Lefkowitz, R. J. (1997) Switching of the coupling of the beta2-adrenergic receptor to different G proteins by protein kinase A. *Nature*, 390 (6655): 88-91.

Dalman, H. M. & Neubig, R. R. (1991) Two peptides from the alpha 2A-adrenergic receptor alter receptor G protein coupling by distinct mechanisms. *J Biol Chem*, 266 (17): 11025-11029.

Davis, D., Liu, X. & Segaloff, D. L. (1995) Identification of the sites of N-linked glycosylation on the follicle-stimulating hormone (FSH) receptor and assessment of their role in FSH receptor function. *Mol Endocrinol*, 9 (2): 159-170.

Davis, N. S., DiSant'Agnese, P. A., Ewing, J. F. & Mooney, R. A. (1989) The neuroendocrine prostate: characterization and quantitation of calcitonin in the human gland. *J Urol*, 142 (3): 884-888.

De Lean, A., Stadel, J. M. & Lefkowitz, R. J. (1980) A ternary complex model explains the agonist-specific binding properties of the adenylate cyclase-coupled beta-adrenergic receptor. *J Biol Chem*, 255 (15): 7108-7117.

Defea, K. (2008) Beta-arrestins and heterotrimeric G-proteins: collaborators and competitors in signal transduction. *Br J Pharmacol*, 153 Suppl 1 S298-309.

Dehal, P. & Boore, J. L. (2005) Two rounds of whole genome duplication in the ancestral vertebrate. *PLoS Biol*, 3 (10): e314.

Deslauriers, B., Ponce, C., Lombard, C., Larguier, R., Bonnafous, J. C. & Marie, J. (1999) N-glycosylation requirements for the AT1a angiotensin II receptor delivery to the plasma membrane. *Biochem J*, 339 (Pt 2) 397-405.

Deupi, X., Edwards, P., Singhal, A., Nickle, B., Oprian, D., Schertler, G. & Standfuss, J. (2012) Stabilized G protein binding site in the structure of constitutively active metarhodopsin-II. *Proc Natl Acad Sci U S A*, 109 (1): 119-124.

Deupi, X. & Standfuss, J. (2011) Structural insights into agonist-induced activation of G-protein-coupled receptors. *Curr Opin Struct Biol*, 21 (4): 541-551.

DeWire, S. M., Ahn, S., Lefkowitz, R. J. & Shenoy, S. K. (2007) Beta-arrestins and cell signaling. *Annu Rev Physiol*, 69 483-510.

Doggrell, S. A. (2001) Migraine and beyond: cardiovascular therapeutic potential for CGRP modulators. *Expert Opin Investig Drugs*, 10 (6): 1131-1138.

Dong, M., Pinon, D., Asmann, Y. & Miller, L. (2006) Possible endogenous agonist mechanism for the activation of secretin family G protein-coupled receptors. *Mol Pharmacol*, 70 (1): 206-213.

Dong, M., Pinon, D. & Miller, L. (2005) Insights into the structure and molecular basis of ligand docking to the G protein-coupled secretin receptor using charge-modified amino-terminal agonist probes. *Mol Endocrinol*, 19 (7): 1821-1836.

Dong, M., Pinon, D. I., Cox, R. F. & Miller, L. J. (2004) Molecular approximation between a residue in the amino-terminal region of calcitonin and the third extracellular loop of the class B G protein-coupled calcitonin receptor. *J Biol Chem*, 279 (30): 31177-31182.

Dong, M., Xu, X., Ball, A. M., Makhoul, J. A., Lam, P. C., Pinon, D. I., Orry, A., Sexton, P. M., Abagyan, R. & Miller, L. J. (2012) Mapping spatial approximations between the amino terminus of secretin and each of the extracellular loops of its receptor using cysteine trapping. *FASEB J*, 26 (12): 5092-5105.

Donnelly, D. (1997) The arrangement of the transmembrane helices in the secretin receptor family of G-protein-coupled receptors. *FEBS Lett*, 409 (3): 431-436.

Doré, A. S., Robertson, N., Errey, J. C., Ng, I., Hollenstein, K., Tehan, B., Hurrell, E., Bennett, K., Congreve, M., Magnani, F., Tate, C. G., Weir, M. & Marshall, F. H. (2011) Structure of the adenosine A(2A) receptor in complex with ZM241385 and the xanthines XAC and caffeine. *Structure*, 19 (9): 1283-1293.

Downes, G. B. & Gautam, N. (1999) The G protein subunit gene families. *Genomics*, 62 (3): 544-552.

Drake, M. T., Shenoy, S. K. & Lefkowitz, R. J. (2006) Trafficking of G protein-coupled receptors. *Circ Res*, 99 (6): 570-582.

Durham, P. L. (2008) Inhibition of calcitonin gene-related peptide function: a promising strategy for treating migraine. *Headache*, 48 (8): 1269-1275.

Durham, P. L. & Vause, C. V. (2010) Calcitonin gene-related peptide (CGRP) receptor antagonists in the treatment of migraine. *CNS Drugs*, 24 (7): 539-548.

Duvernay, M. T., Filipeanu, C. M. & Wu, G. (2005) The regulatory mechanisms of export trafficking of G protein-coupled receptors. *Cell Signal*, 17 (12): 1457-1465.

Egea, S. C. & Dickerson, I. M. (2012) Direct interactions between calcitonin-like receptor (CLR) and CGRP-receptor component protein (RCP) regulate CGRP receptor signaling. *Endocrinology*, 153 (4): 1850-1860.

Egloff, P., Hillenbrand, M., Klenk, C., Batyuk, A., Heine, P., Balada, S., Schlinkmann, K. M., Scott, D. J., Schütz, M. & Plückthun, A. (2014) Structure of signaling-competent neurotensin receptor 1 obtained by directed evolution in Escherichia coli. *Proc Natl Acad Sci U S A*, 111 (6): E655-662.

Elling, C. E. & Schwartz, T. W. (1996) Connectivity and orientation of the seven helical bundle in the tachykinin NK-1 receptor probed by zinc site engineering. *EMBO J*, 15 (22): 6213-6219.

Evans, B. N., Rosenblatt, M. I., Mnayer, L. O., Oliver, K. R. & Dickerson, I. M. (2000) CGRP-RCP, a novel protein required for signal transduction at calcitonin gene-related peptide and adrenomedullin receptors. *J Biol Chem*, 275 (40): 31438-31443.

Fanciullacci, M., Alessandri, M., Figini, M., Geppetti, P. & Michelacci, S. (1995) Increase in plasma calcitonin gene-related peptide from the extracerebral circulation during nitroglycerin-induced cluster headache attack. *Pain*, 60 (2): 119-123.

Fischer, J. A., Tobler, P. H., Henke, H. & Tschopp, F. A. (1983) Salmon and human calcitonin-like peptides coexist in the human thyroid and brain. *J Clin Endocrinol Metab*, 57 (6): 1314-1316.

Fitzpatrick, V. D. & Vandlen, R. L. (1994) 6agonist selectivity determinants in somatostatin receptor subtypes I and II. *J Biol Chem*, 269 (40): 24621-24626.

Flahaut, M., Rossier, B. C. & Firsov, D. (2002) Respective roles of calcitonin receptor-like receptor (CRLR) and receptor activity-modifying proteins (RAMP) in cell surface expression of CRLR/RAMP heterodimeric receptors. *J Biol Chem*, 277 (17): 14731-14737.

Flühmann, B., Muff, R., Hunziker, W., Fischer, J. A. & Born, W. (1995) A human orphan calcitonin receptor-like structure. *Biochem Biophys Res Commun*, 206 (1): 341-347.

Foord, S. M., Bonner, T. I., Neubig, R. R., Rosser, E. M., Pin, J. P., Davenport, A. P., Spedding, M. & Harmar, A. J. (2005) International Union of Pharmacology. XLVI. G protein-coupled receptor list. *Pharmacol Rev*, 57 (2): 279-288.

Franco-Cereceda, A. & Liska, J. (2000) Potential of calcitonin gene-related peptide in coronary heart disease. *Pharmacology*, 60 (1): 1-8.

Fredriksson, R., Lagerström, M., Lundin, L. & Schiöth, H. (2003) The G-protein-coupled receptors in the human genome form five main families. Phylogenetic analysis, paralogon groups, and fingerprints. *Mol Pharmacol*, 63 (6): 1256-1272.

Friedman, J. & Raisz, L. G. (1965) Thyrocalcitonin: inhibitor of bone resorption in tissue culture. *Science*, 150 (3702): 1465-1467.

Frimurer, T. & Bywater, R. (1999) Structure of the integral membrane domain of the GLP1 receptor. *Proteins*, 35 (4): 375-386.

Fuhrman, J. A., Schwalbach, M. S. & Stingl, U. (2008) Proteorhodopsins: an array of physiological roles? *Nat Rev Microbiol*, 6 (6): 488-494.

Fukushima, Y., Oka, Y., Saitoh, T., Katagiri, H., Asano, T., Matsuhashi, N., Takata, K., van Breda, E., Yazaki, Y. & Sugano, K. (1995) Structural and functional analysis of the canine histamine H2 receptor by site-directed mutagenesis: N-glycosylation is not vital for its action. *Biochem J*, 310 (Pt 2) 553-558.

Gage, R. M., Kim, K. A., Cao, T. T. & von Zastrow, M. (2001) A transplantable sorting signal that is sufficient to mediate rapid recycling of G protein-coupled receptors. *J Biol Chem*, 276 (48): 44712-44720.

Gallai, V., Sarchielli, P., Floridi, A., Franceschini, M., Codini, M., Glioti, G., Trequattrini, A. & Palumbo, R. (1995) Vasoactive peptide levels in the plasma of young migraine patients with and without aura assessed both interictally and ictally. *Cephalalgia*, 15 (5): 384-390.

Gallwitz, B., Schmidt, W. E., Conlon, J. M. & Creutzfeldt, W. (1990) Glucagon-like peptide-1(7-36)amide: characterization of the domain responsible for binding to its receptor on rat insulinoma RINm5F cells. *J Mol Endocrinol*, 5 (1): 33-39.

Galvez, T., Urwyler, S., Prézeau, L., Mosbacher, J., Joly, C., Malitschek, B., Heid, J., Brabet, I., Froestl, W., Bettler, B., Kaupmann, K. & Pin, J. P. (2000) Ca(2+) requirement for high-affinity gamma-aminobutyric acid (GABA) binding at GABA(B) receptors: involvement of serine 269 of the GABA(B)R1 subunit. *Mol Pharmacol*, 57 (3): 419-426.

Galés, C., Van Durm, J. J., Schaak, S., Pontier, S., Percherancier, Y., Audet, M., Paris, H. & Bouvier, M. (2006) Probing the activation-promoted structural rearrangements in preassembled receptor-G protein complexes. *Nat Struct Mol Biol*, 13 (9): 778-786.

Gao, Z., Ni, Y., Szabo, G. & Linden, J. (1999) Palmitoylation of the recombinant human A1 adenosine receptor: enhanced proteolysis of palmitoylation-deficient mutant receptors. *Biochem J*, 342 (Pt 2) 387-395.

Gardella, T. & Jüppner, H. (2001) Molecular properties of the PTH/PTHrP receptor. *Trends Endocrinol Metab*, 12 (5): 210-217.

Gelling, R., Coy, D., Pederson, R., Wheeler, M., Hinke, S., Kwan, T. & McIntosh, C. (1997) GIP(6-30amide) contains the high affinity binding region of GIP and is a potent inhibitor of GIP1-42 action in vitro. *Regul Pept*, 69 (3): 151-154.

German, M. S., Moss, L. G., Wang, J. & Rutter, W. J. (1992) The insulin and islet amyloid polypeptide genes contain similar cell-specific promoter elements that bind identical beta-cell nuclear complexes. *Mol Cell Biol*, 12 (4): 1777-1788.

Gether, U. (2000) Uncovering molecular mechanisms involved in activation of G protein-coupled receptors. *Endocr Rev*, 21 (1): 90-113.

Gibson, N. J. & Brown, M. F. (1993) Lipid headgroup and acyl chain composition modulate the MI-MII equilibrium of rhodopsin in recombinant membranes. *Biochemistry*, 32 (9): 2438-2454.

Gilman, A. G. (1987) G proteins: transducers of receptor-generated signals. *Annu Rev Biochem*, 56 615-649.

Gkountelias, K., Tselios, T., Venihaki, M., Deraos, G., Lazaridis, I., Rassouli, O., Gravanis, A. & Liapakis, G. (2009) Alanine scanning mutagenesis of the second extracellular loop of type 1 corticotropin-releasing factor receptor revealed residues critical for peptide binding. *Mol Pharmacol*, 75 (4): 793-800.

Goadsby, P. J. & Edvinsson, L. (1993) The trigeminovascular system and migraine: studies characterizing cerebrovascular and neuropeptide changes seen in humans and cats. *Ann Neurol*, 33 (1): 48-56.

Goadsby, P. J., Edvinsson, L. & Ekman, R. (1988) Release of vasoactive peptides in the extracerebral circulation of humans and the cat during activation of the trigeminovascular system. *Ann Neurol*, 23 (2): 193-196.

Goadsby, P. J., Edvinsson, L. & Ekman, R. (1990) Vasoactive peptide release in the extracerebral circulation of humans during migraine headache. *Ann Neurol*, 28 (2): 183-187.

Goadsby, P. J., Lipton, R. B. & Ferrari, M. D. (2002) Migraine--current understanding and treatment. *N Engl J Med*, 346 (4): 257-270.

Gorn, A. H., Lin, H. Y., Yamin, M., Auron, P. E., Flannery, M. R., Tapp, D. R., Manning, C. A., Lodish, H. F., Krane, S. M. & Goldring, S. R. (1992) Cloning, characterization, and expression of a human calcitonin receptor from an ovarian carcinoma cell line. *J Clin Invest*, 90 (5): 1726-1735.

Grace, C., Perrin, M., DiGruccio, M., Miller, C., Rivier, J., Vale, W. & Riek, R. (2004) NMR structure and peptide hormone binding site of the first extracellular domain of a type B1 G protein-coupled receptor. *Proc Natl Acad Sci U S A*, 101 (35): 12836-12841.

Grace, C., Perrin, M., Gulyas, J., Digruccio, M., Cantle, J., Rivier, J., Vale, W. & Riek, R. (2007) Structure of the N-terminal domain of a type B1 G protein-coupled receptor in complex with a peptide ligand. *Proc Natl Acad Sci U S A*, 104 (12): 4858-4863.

Grace, C. R., Perrin, M. H., Gulyas, J., Rivier, J. E., Vale, W. W. & Riek, R. (2010) NMR structure of the first extracellular domain of corticotropin-releasing factor receptor 1 (ECD1-CRF-R1) complexed with a high affinity agonist. *J Biol Chem*, 285 (49): 38580-38589.

Grammatopoulos, D. K. (2012) Insights into mechanisms of corticotropin-releasing hormone receptor signal transduction. *Br J Pharmacol*, 166 (1): 85-97.

Grammatopoulos, D. K., Dai, Y., Randeva, H. S., Levine, M. A., Karteris, E., Easton, A. J. & Hillhouse, E. W. (1999) A novel spliced variant of the type 1 corticotropin-releasing hormone receptor with a deletion in the seventh transmembrane domain present in the human pregnant term myometrium and fetal membranes. *Mol Endocrinol*, 13 (12): 2189-2202.

Grammatopoulos, D. K., Randeva, H. S., Levine, M. A., Kanellopoulou, K. A. & Hillhouse, E. W. (2001) Rat cerebral cortex corticotropin-releasing hormone receptors: evidence for receptor coupling to multiple G-proteins. *J Neurochem*, 76 (2): 509-519.

Granier, S., Manglik, A., Kruse, A. C., Kobilka, T. S., Thian, F. S., Weis, W. I. & Kobilka, B. K. (2012) Structure of the δ-opioid receptor bound to naltrindole. *Nature*, 485 (7398): 400-404.

Gray, D. W. & Marshall, I. (1992) Nitric oxide synthesis inhibitors attenuate calcitonin gene-related peptide endothelium-dependent vasorelaxation in rat aorta. *Eur J Pharmacol*, 212 (1): 37-42.

Grishina, G. & Berlot, C. H. (1998) Mutations at the domain interface of GSalpha impair receptor-mediated activation by altering receptor and guanine nucleotide binding. *J Biol Chem*, 273 (24): 15053-15060.

Gullapalli, A., Wolfe, B. L., Griffin, C. T., Magnuson, T. & Trejo, J. (2006) An essential role for SNX1 in lysosomal sorting of protease-activated receptor-1: evidence for retromer-, Hrs-, and Tsg101-independent functions of sorting nexins. *Mol Biol Cell*, 17 (3): 1228-1238.

Gurevich, V. V. & Gurevich, E. V. (2006) The structural basis of arrestin-mediated regulation of G-protein-coupled receptors. *Pharmacol Ther*, 110 (3): 465-502.

Gurevich, V. V. & Gurevich, E. V. (2008) How and why do GPCRs dimerize? *Trends Pharmacol Sci*, 29 (5): 234-240.

Haga, K., Kruse, A. C., Asada, H., Yurugi-Kobayashi, T., Shiroishi, M., Zhang, C., Weis, W. I., Okada, T., Kobilka, B. K., Haga, T. & Kobayashi, T. (2012) Structure of the human M2 muscarinic acetylcholine receptor bound to an antagonist. *Nature*, 482 (7386): 547-551.

Hamm, H. E., Deretic, D., Hofmann, K. P., Schleicher, A. & Kohl, B. (1987) Mechanism of action of monoclonal antibodies that block the light activation of the guanyl nucleotide-binding protein, transducin. *J Biol Chem*, 262 (22): 10831-10838.

Han, M., Gurevich, V. V., Vishnivetskiy, S. A., Sigler, P. B. & Schubert, C. (2001) Crystal structure of beta-arrestin at 1.9 A: possible mechanism of receptor binding and membrane Translocation. *Structure*, 9 (9): 869-880.

Han, Y., Moreira, I. S., Urizar, E., Weinstein, H. & Javitch, J. A. (2009) Allosteric communication between protomers of dopamine class A GPCR dimers modulates activation. *Nat Chem Biol*, 5 (9): 688-695.

Hanson, M. A., Cherezov, V., Griffith, M. T., Roth, C. B., Jaakola, V. P., Chien, E. Y., Velasquez, J., Kuhn, P. & Stevens, R. C. (2008) A specific cholesterol binding site is established by the 2.8 A structure of the human beta2-adrenergic receptor. *Structure*, 16 (6): 897-905.

Hanson, M. A., Roth, C. B., Jo, E., Griffith, M. T., Scott, F. L., Reinhart, G., Desale, H., Clemons, B., Cahalan, S. M., Schuerer, S. C., Sanna, M. G., Han, G. W., Kuhn, P., Rosen, H. & Stevens, R. C. (2012) Crystal structure of a lipid G protein-coupled receptor. *Science*, 335 (6070): 851-855.

Hareter, A., Hoffmann, E., Bode, H. P., Göke, B. & Göke, R. (1997) The positive charge of the imidazole side chain of histidine7 is crucial for GLP-1 action. *Endocr J*, 44 (5): 701-705.

Harikumar, K. G., Simms, J., Christopoulos, G., Sexton, P. M. & Miller, L. J. (2009) Molecular basis of association of receptor activity-modifying protein 3 with the family B G protein-coupled secretin receptor. *Biochemistry*, 48 (49): 11773-11785.

Hauger, R., Risbrough, V., Brauns, O. & Dautzenberg, F. (2006) Corticotropin releasing factor (CRF) receptor signaling in the central nervous system: new molecular targets. *CNS Neurol Disord Drug Targets*, 5 (4): 453-479.

Hawes, B. E., Luttrell, L. M., Exum, S. T. & Lefkowitz, R. J. (1994) Inhibition of G protein-coupled receptor signaling by expression of cytoplasmic domains of the receptor. *J Biol Chem*, 269 (22): 15776-15785.

Hay, D. L., Christopoulos, G., Christopoulos, A. & Sexton, P. M. (2006) Determinants of 1-piperidinecarboxamide, N-[2-[[5-amino-l-[[4-(4-pyridinyl)-l-piperazinyl]carbonyl]pentyl]amino]-1-[(3,5-dibromo-4-hydroxyphenyl)methyl]-2-oxoethyl]-4-(1,4-dihydro-2-oxo-3(2H)-quinazolinyl) (BIBN4096BS) affinity for calcitonin gene-related peptide and amylin receptors--the role of receptor activity modifying protein 1. *Mol Pharmacol*, 70 (6): 1984-1991.

Hay, D. L., Harris, P. W., Kowalczyk, R., Brimble, M. A., Rathbone, D. L., Barwell, J., Conner, A. C. & Poyner, D. R. (2014) Structure-activity relationships of the N-terminus of calcitonin gene-related peptide: key roles of alanine-5 and threonine-6 in receptor activation. *Br J Pharmacol*, 171 (2): 415-426.

Hebert, T. E., Moffett, S., Morello, J. P., Loisel, T. P., Bichet, D. G., Barret, C. & Bouvier, M. (1996) A peptide derived from a beta2-adrenergic receptor transmembrane domain inhibits both receptor dimerization and activation. *J Biol Chem*, 271 (27): 16384-16392.

Heck, M. & Hofmann, K. P. (2001) Maximal rate and nucleotide dependence of rhodopsin-catalyzed transducin activation: initial rate analysis based on a double displacement mechanism. *J Biol Chem*, 276 (13): 10000-10009.

Hein, P. & Bünemann, M. (2009) Coupling mode of receptors and G proteins. *Naunyn Schmiedebergs Arch Pharmacol*, 379 (5): 435-443.

Henderson, R. & Unwin, P. N. (1975) Three-dimensional model of purple membrane obtained by electron microscopy. *Nature*, 257 (5521): 28-32.

Hepler, J. R. & Gilman, A. G. (1992) G proteins. *Trends Biochem Sci*, 17 (10): 383-387.

Hershey, J. C., Corcoran, H. A., Baskin, E. P., Salvatore, C. A., Mosser, S., Williams, T. M., Koblan, K. S., Hargreaves, R. J. & Kane, S. A. (2005) Investigation of the species selectivity of a nonpeptide CGRP receptor antagonist using a novel pharmacodynamic assay. *Regul Pept*, 127 (1-3): 71-77.

Hilairet, S., Bélanger, C., Bertrand, J., Laperrière, A., Foord, S. & Bouvier, M. (2001) Agonist-promoted internalization of a ternary complex between calcitonin receptor-like receptor, receptor activity-modifying protein 1 (RAMP1), and beta-arrestin. *J Biol Chem*, 276 (45): 42182-42190.

Hill, S. J. (2006) G-protein-coupled receptors: past, present and future. *Br J Pharmacol*, 147 Suppl 1 S27-37.

Hinke, S., Manhart, S., Pamir, N., Demuth, H., W Gelling, R., Pederson, R. & McIntosh, C. (2001) Identification of a bioactive domain in the amino-terminus of glucose-dependent insulinotropic polypeptide (GIP). *Biochim Biophys Acta*, 1547 (1): 143-155.

Hino, T., Arakawa, T., Iwanari, H., Yurugi-Kobayashi, T., Ikeda-Suno, C., Nakada-Nakura, Y., Kusano-Arai, O., Weyand, S., Shimamura, T., Nomura, N., Cameron, A. D., Kobayashi, T., Hamakubo, T., Iwata, S. & Murata, T. (2012) G-protein-coupled receptor inactivation by an allosteric inverse-agonist antibody. *Nature*, 482 (7384): 237-240.

Hirsch, P. F., Gauthier, G. F. & Munson, P. L. (1963) Thyroid hypocalcemic principle and recurrent laryngeal nerve injury as factors affecting the response to parathyroidectomy in rats. *Endocrinology*, 73 244-252.

Hjorth, S. A., Adelhorst, K., Pedersen, B. B., Kirk, O. & Schwartz, T. W. (1994) Glucagon and glucagon-like peptide 1: selective receptor recognition via distinct peptide epitopes. *J Biol Chem*, 269 (48): 30121-30124.

Hoare, S. (2005) Mechanisms of peptide and nonpeptide ligand binding to Class B G-protein-coupled receptors. *Drug Discov Today*, 10 (6): 417-427.

Hoare, S., Sullivan, S., Schwarz, D., Ling, N., Vale, W., Crowe, P. & Grigoriadis, D. (2004) Ligand affinity for amino-terminal and juxtamembrane domains of the corticotropin releasing factor type I receptor: regulation by G-protein and nonpeptide antagonists. *Biochemistry*, 43 (13): 3996-4011.

Hoare, S. & Usdin, T. (2001) Molecular mechanisms of ligand recognition by parathyroid hormone 1 (PTH1) and PTH2 receptors. *Curr Pharm Des*, 7 (8): 689-713.

Hoffmann, C., Moro, S., Nicholas, R. A., Harden, T. K. & Jacobson, K. A. (1999) The role of amino acids in extracellular loops of the human P2Y1 receptor in surface expression and activation processes. *J Biol Chem*, 274 (21): 14639-14647.

Hollenstein, K., de Graaf, C., Bortolato, A., Wang, M. W., Marshall, F. H. & Stevens, R. C. (2014) Insights into the structure of class B GPCRs. *Trends Pharmacol Sci*, 35 (1): 12-22.

Hollenstein, K., Kean, J., Bortolato, A., Cheng, R. K., Doré, A. S., Jazayeri, A., Cooke, R. M., Weir, M. & Marshall, F. H. (2013) Structure of class B GPCR corticotropin-releasing factor receptor 1. *Nature*, 499 (7459): 438-443.

Holst, B. & Schwartz, T. W. (2003) Molecular mechanism of agonism and inverse agonism in the melanocortin receptors: Zn(2+) as a structural and functional probe. *Ann N Y Acad Sci*, 994 1-11.

Hong, Y., Hay, D. L., Quirion, R. & Poyner, D. R. (2012) The pharmacology of adrenomedullin 2/intermedin. *Br J Pharmacol*, 166 (1): 110-120.

Horvat, R. D., Roess, D. A., Nelson, S. E., Barisas, B. G. & Clay, C. M. (2001) Binding of agonist but not antagonist leads to fluorescence resonance energy transfer between intrinsically fluorescent gonadotropin-releasing hormone receptors. *Mol Endocrinol*, 15 (5): 695-703.

Howitt, S. G., Kilk, K., Wang, Y., Smith, D. M., Langel, U. & Poyner, D. R. (2003) The role of the 8-18 helix of CGRP8-37 in mediating high affinity binding to CGRP receptors; coulombic and steric interactions. *Br J Pharmacol*, 138 (2): 325-332.

Hu, J., Wang, Y., Zhang, X., Lloyd, J. R., Li, J. H., Karpiak, J., Costanzi, S. & Wess, J. (2010) Structural basis of G protein-coupled receptor-G protein interactions. *Nat Chem Biol*, 6 (7): 541-548.

Huang, C. C. & Tesmer, J. J. (2011) Recognition in the face of diversity: interactions of heterotrimeric G proteins and G protein-coupled receptor (GPCR) kinases with activated GPCRs. *J Biol Chem*, 286 (10): 7715-7721.

Hulme, E. C. (2013) GPCR activation: a mutagenic spotlight on crystal structures. *Trends Pharmacol Sci*, 34 (1): 67-84.

Hällbrink, M., Holmqvist, T., Olsson, M., Ostenson, C. G., Efendic, S. & Langel, U. (2001) Different domains in the third intracellular loop of the GLP-1 receptor are responsible for Galpha(s) and Galpha(i)/Galpha(o) activation. *Biochim Biophys Acta*, 1546 (1): 79-86.

Inooka, H., Ohtaki, T., Kitahara, O., Ikegami, T., Endo, S., Kitada, C., Ogi, K., Onda, H., Fujino, M. & Shirakawa, M. (2001) Conformation of a peptide ligand bound to its G-protein coupled receptor. *Nat Struct Biol*, 8 (2): 161-165.

Ishimitsu, T., Ono, H., Minami, J. & Matsuoka, H. (2006) Pathophysiologic and therapeutic implications of adrenomedullin in cardiovascular disorders. *Pharmacol Ther*, 111 (3): 909-927.

Ittner, L. M., Luessi, F., Koller, D., Born, W., Fischer, J. A. & Muff, R. (2004) Aspartate(69) of the calcitonin-like receptor is required for its functional expression together with receptor-activity-modifying proteins 1 and -2. *Biochem Biophys Res Commun*, 319 (4): 1203-1209.

Jaakola, V., Griffith, M., Hanson, M., Cherezov, V., Chien, E., Lane, J., Ijzerman, A. & Stevens, R. (2008) The 2.6 angstrom crystal structure of a human A2A adenosine receptor bound to an antagonist. *Science*, 322 (5905): 1211-1217.

Jakubík, J., Janíčková, H., Randáková, A., El-Fakahany, E. E. & Doležal, V. (2011) Subtype differences in pre-coupling of muscarinic acetylcholine receptors. *PLoS One*, 6 (11): e27732.

Janz, J. M. & Farrens, D. L. (2004) Rhodopsin activation exposes a key hydrophobic binding site for the transducin alpha-subunit C terminus. *J Biol Chem*, 279 (28): 29767-29773.

Javitch, J. A., Shi, L. & Liapakis, G. (2002) Use of the substituted cysteine accessibility method to study the structure and function of G protein-coupled receptors. *Methods Enzymol*, 343 137-156.

Jones, K. A., Borowsky, B., Tamm, J. A., Craig, D. A., Durkin, M. M., Dai, M., Yao, W. J., Johnson, M., Gunwaldsen, C., Huang, L. Y., Tang, C., Shen, Q., Salon, J. A., Morse, K., Laz, T., Smith, K. E., Nagarathnam, D., Noble, S. A., Branchek, T. A. & Gerald, C. (1998) GABA(B) receptors function as a heteromeric assembly of the subunits GABA(B)R1 and GABA(B)R2. *Nature*, 396 (6712): 674-679.

Juhasz, G., Zsombok, T., Modos, E. A., Olajos, S., Jakab, B., Nemeth, J., Szolcsanyi, J., Vitrai, J. & Bagdy, G. (2003) NO-induced migraine attack: strong increase in plasma calcitonin gene-related peptide (CGRP) concentration and negative correlation with platelet serotonin release. *Pain*, 106 (3): 461-470.

Kamitani, S. & Sakata, T. (2001) Glycosylation of human CRLR at Asn123 is required for ligand binding and signaling. *Biochim Biophys Acta*, 1539 (1-2): 131-139.

Kannan, N., Haste, N., Taylor, S. S. & Neuwald, A. F. (2007) The hallmark of AGC kinase functional divergence is its C-terminal tail, a cis-acting regulatory module. *Proc Natl Acad Sci U S A*, 104 (4): 1272-1277.

Karnik, S. S., Ridge, K. D., Bhattacharya, S. & Khorana, H. G. (1993) Palmitoylation of bovine opsin and its cysteine mutants in COS cells. *Proc Natl Acad Sci U S A*, 90 (1): 40-44.

Katritch, V., Cherezov, V. & Stevens, R. C. (2013) Structure-function of the G protein-coupled receptor superfamily. *Annu Rev Pharmacol Toxicol*, 53 531-556.

Kaupmann, K., Malitschek, B., Schuler, V., Heid, J., Froestl, W., Beck, P., Mosbacher, J., Bischoff, S., Kulik, A., Shigemoto, R., Karschin, A. & Bettler, B.

(1998) GABA(B)-receptor subtypes assemble into functional heteromeric complexes. *Nature*, 396 (6712): 683-687.

Kenakin, T. (2007) Collateral efficacy in drug discovery: taking advantage of the good (allosteric) nature of 7TM receptors. *Trends Pharmacol Sci*, 28 (8): 407-415.

Kenakin, T. (2011) Functional selectivity and biased receptor signaling. *J Pharmacol Exp Ther*, 336 (2): 296-302.

Kenakin, T. & Miller, L. J. (2010) Seven transmembrane receptors as shapeshifting proteins: the impact of allosteric modulation and functional selectivity on new drug discovery. *Pharmacol Rev*, 62 (2): 265-304.

Kennedy, D. P., McRobb, F. M., Leonhardt, S. A., Purdy, M., Figler, H., Marshall, M. A., Chordia, M., Figler, R., Linden, J., Abagyan, R. & Yeager, M. (2014) The second extracellular loop of the adenosine A1 receptor mediates activity of allosteric enhancers. *Mol Pharmacol*, 85 (2): 301-309.

Kim, J., Jiang, Q., Glashofer, M., Yehle, S., Wess, J. & Jacobson, K. A. (1996) Glutamate residues in the second extracellular loop of the human A2a adenosine receptor are required for ligand recognition. *Mol Pharmacol*, 49 (4): 683-691.

Kim, Y. J., Hofmann, K. P., Ernst, O. P., Scheerer, P., Choe, H. W. & Sommer, M. E. (2013) Crystal structure of pre-activated arrestin p44. *Nature*, 497 (7447): 142-146.

Kitamura, K., Kangawa, K., Kawamoto, M., Ichiki, Y., Nakamura, S., Matsuo, H. & Eto, T. (1993) Adrenomedullin: a novel hypotensive peptide isolated from human pheochromocytoma. *Biochem Biophys Res Commun*, 192 (2): 553-560.

Klco, J. M., Wiegand, C. B., Narzinski, K. & Baranski, T. J. (2005) Essential role for the second extracellular loop in C5a receptor activation. *Nat Struct Mol Biol*, 12 (4): 320-326.

Kniazeff, J., Bessis, A. S., Maurel, D., Ansanay, H., Prézeau, L. & Pin, J. P. (2004) Closed state of both binding domains of homodimeric mGlu receptors is required for full activity. *Nat Struct Mol Biol*, 11 (8): 706-713.

Kniazeff, J., Galvez, T., Labesse, G. & Pin, J. P. (2002) No ligand binding in the GB2 subunit of the GABA(B) receptor is required for activation and allosteric interaction between the subunits. *J Neurosci*, 22 (17): 7352-7361.

Kniazeff, J., Prézeau, L., Rondard, P., Pin, J. P. & Goudet, C. (2011) Dimers and beyond: The functional puzzles of class C GPCRs. *Pharmacol Ther*, 130 (1): 9-25.

Kolakowski, L. J. (1994) GCRDb: a G-protein-coupled receptor database. *Receptors Channels*, 2 (1): 1-7.

Koole, C., Wootten, D., Simms, J., Miller, L. J., Christopoulos, A. & Sexton, P. M. (2012) Second extracellular loop of human glucagon-like peptide-1 receptor (GLP-1R) has a critical role in GLP-1 peptide binding and receptor activation. *J Biol Chem*, 287 (6): 3642-3658.

Koshland, D. E. (1958) Application of a Theory of Enzyme Specificity to Protein Synthesis. *Proc Natl Acad Sci U S A*, 44 (2): 98-104.

Kosugi, S., Kohn, L. D., Akamizu, T. & Mori, T. (1994) The middle portion in the second cytoplasmic loop of the thyrotropin receptor plays a crucial role in adenylate cyclase activation. *Mol Endocrinol*, 8 (4): 498-509.

Koth, C. M., Murray, J. M., Mukund, S., Madjidi, A., Minn, A., Clarke, H. J., Wong, T., Chiang, V., Luis, E., Estevez, A., Rondon, J., Zhang, Y., Hötzel, I. & Allan, B. B. (2012) Molecular basis for negative regulation of the glucagon receptor. *Proc Natl Acad Sci U S A*, 109 (36): 14393-14398.

Kozasa, T., Hajicek, N., Chow, C. R. & Suzuki, N. (2011) Signalling mechanisms of RhoGTPase regulation by the heterotrimeric G proteins G12 and G13. *J Biochem*, 150 (4): 357-369.

Kraetke, O., Holeran, B., Berger, H., Escher, E., Bienert, M. & Beyermann, M. (2005) Photoaffinity cross-linking of the corticotropin-releasing factor receptor type 1 with photoreactive urocortin analogues. *Biochemistry*, 44 (47): 15569-15577.

Krishnan, A., Almén, M. S., Fredriksson, R. & Schiöth, H. B. (2012) The origin of GPCRs: identification of mammalian like Rhodopsin, Adhesion, Glutamate and Frizzled GPCRs in fungi. *PLoS One*, 7 (1): e29817.

Kruse, A. C., Hu, J., Pan, A. C., Arlow, D. H., Rosenbaum, D. M., Rosemond, E., Green, H. F., Liu, T., Chae, P. S., Dror, R. O., Shaw, D. E., Weis, W. I., Wess, J. & Kobilka, B. K. (2012) Structure and dynamics of the M3 muscarinic acetylcholine receptor. *Nature*, 482 (7386): 552-556.

Kruse, A. C., Ring, A. M., Manglik, A., Hu, J., Hu, K., Eitel, K., Hübner, H., Pardon, E., Valant, C., Sexton, P. M., Christopoulos, A., Felder, C. C., Gmeiner, P., Steyaert, J., Weis, W. I., Garcia, K. C., Wess, J. & Kobilka, B. K. (2013) Activation and allosteric modulation of a muscarinic acetylcholine receptor. *Nature*, 504 (7478): 101-106.

Kuestner, R. E., Elrod, R. D., Grant, F. J., Hagen, F. S., Kuijper, J. L., Matthewes, S. L., O'Hara, P. J., Sheppard, P. O., Stroop, S. D. & Thompson, D. L. (1994) Cloning and characterization of an abundant subtype of the human calcitonin receptor. *Mol Pharmacol*, 46 (2): 246-255.

Kumar, S., Pioszak, A., Zhang, C., Swaminathan, K. & Xu, H. E. (2011) Crystal structure of the PAC1R extracellular domain unifies a consensus fold for hormone recognition by class B G-protein coupled receptors. *PLoS One*, 6 (5): e19682.

Kunishima, N., Shimada, Y., Tsuji, Y., Sato, T., Yamamoto, M., Kumasaka, T., Nakanishi, S., Jingami, H. & Morikawa, K. (2000) Structural basis of glutamate recognition by a dimeric metabotropic glutamate receptor. *Nature*, 407 (6807): 971-977.

Kusano, S., Kukimoto-Niino, M., Akasaka, R., Toyama, M., Terada, T., Shirouzu, M., Shindo, T. & Yokoyama, S. (2008) Crystal structure of the human receptor activity-modifying protein 1 extracellular domain. *Protein Sci*, 17 (11): 1907-1914.

Kusano, S., Kukimoto-Niino, M., Hino, N., Ohsawa, N., Okuda, K., Sakamoto, K., Shirouzu, M., Shindo, T. & Yokoyama, S. (2012) Structural basis for extracellular interactions between calcitonin receptor-like receptor and receptor activity-modifying protein 2 for adrenomedullin-specific binding. *Protein Sci*, 21 (2): 199-210.

Kuwasako, K., Hay, D. L., Nagata, S., Hikosaka, T., Kitamura, K. & Kato, J. (2012) The third extracellular loop of the human calcitonin receptor-like receptor is crucial for the activation of adrenomedullin signalling. *Br J Pharmacol*, 166 (1): 137-150.

Kuwasako, K., Kitamura, K., Nagata, S., Hikosaka, T., Takei, Y. & Kato, J. (2011) Shared and separate functions of the RAMP-based adrenomedullin receptors. *Peptides*, 32 (7): 1540-1550.

Kuwasako, K., Kitamura, K., Uemura, T., Nagoshi, Y., Kato, J. & Eto, T. (2003) The function of extracellular cysteines in the human adrenomedullin receptor. *Hypertens Res*, 26 Suppl S25-31.

Kuwasako, K., Shimekake, Y., Masuda, M., Nakahara, K., Yoshida, T., Kitaura, M., Kitamura, K., Eto, T. & Sakata, T. (2000) Visualization of the calcitonin receptor-like receptor and its receptor activity-modifying proteins during internalization and recycling. *J Biol Chem*, 275 (38): 29602-29609.

Kühn, H. & Dreyer, W. J. (1972) Light dependent phosphorylation of rhodopsin by ATP. *FEBS Lett*, 20 (1): 1-6.

Lambright, D. G., Sondek, J., Bohm, A., Skiba, N. P., Hamm, H. E. & Sigler, P. B. (1996) The 2.0 A crystal structure of a heterotrimeric G protein. *Nature*, 379 (6563): 311-319.

Lebon, G., Warne, T., Edwards, P. C., Bennett, K., Langmead, C. J., Leslie, A. G. & Tate, C. G. (2011) Agonist-bound adenosine A2A receptor structures reveal common features of GPCR activation. *Nature*, 474 (7352): 521-525.

Lefkowitz, R. J. & Shenoy, S. K. (2005) Transduction of receptor signals by beta-arrestins. *Science*, 308 (5721): 512-517.

Leitz, A. J., Bayburt, T. H., Barnakov, A. N., Springer, B. A. & Sligar, S. G. (2006) Functional reconstitution of Beta2-adrenergic receptors utilizing self-assembling Nanodisc technology. *Biotechniques*, 40 (5): 601-602, 604, 606, passim.

Lennerz, J. K., Rühle, V., Ceppa, E. P., Neuhuber, W. L., Bunnett, N. W., Grady, E. F. & Messlinger, K. (2008) Calcitonin receptor-like receptor (CLR), receptor activity-modifying protein 1 (RAMP1), and calcitonin gene-related peptide (CGRP) immunoreactivity in the rat trigeminovascular system: differences between peripheral and central CGRP receptor distribution. *J Comp Neurol*, 507 (3): 1277-1299.

Li, B., Nowak, N. M., Kim, S. K., Jacobson, K. A., Bagheri, A., Schmidt, C. & Wess, J. (2005) Random mutagenesis of the M3 muscarinic acetylcholine receptor expressed in yeast: identification of second-site mutations that restore function to a coupling-deficient mutant M3 receptor. *J Biol Chem*, 280 (7): 5664-5675.

Lin, H. Y., Harris, T. L., Flannery, M. S., Aruffo, A., Kaji, E. H., Gorn, A., Kolakowski, L. F., Lodish, H. F. & Goldring, S. R. (1991) Expression cloning of an adenylate cyclase-coupled calcitonin receptor. *Science*, 254 (5034): 1022-1024.

Liu, J., Maurel, D., Etzol, S., Brabet, I., Ansanay, H., Pin, J. P. & Rondard, P. (2004a) Molecular determinants involved in the allosteric control of agonist affinity in the GABAB receptor by the GABAB2 subunit. *J Biol Chem*, 279 (16): 15824-15830.

Liu, W., Chun, E., Thompson, A. A., Chubukov, P., Xu, F., Katritch, V., Han, G. W., Roth, C. B., Heitman, L. H., IJzerman, A. P., Cherezov, V. & Stevens, R. C. (2012) Structural basis for allosteric regulation of GPCRs by sodium ions. *Science*, 337 (6091): 232-236.

Liu, X., He, Q., Studholme, D. J., Wu, Q., Liang, S. & Yu, L. (2004b) NCD3G: a novel nine-cysteine domain in family 3 GPCRs. *Trends Biochem Sci*, 29 (9): 458-461.

Lodowski, D. T., Tesmer, V. M., Benovic, J. L. & Tesmer, J. J. (2006) The structure of G protein-coupled receptor kinase (GRK)-6 defines a second lineage of GRKs. *J Biol Chem*, 281 (24): 16785-16793.

Lohse, M. J., Benovic, J. L., Codina, J., Caron, M. G. & Lefkowitz, R. J. (1990) beta-Arrestin: a protein that regulates beta-adrenergic receptor function. *Science*, 248 (4962): 1547-1550.

Luttrell, L. M., Ferguson, S. S., Daaka, Y., Miller, W. E., Maudsley, S., Della Rocca, G. J., Lin, F., Kawakatsu, H., Owada, K., Luttrell, D. K., Caron, M. G. & Lefkowitz, R. J. (1999) Beta-arrestin-dependent formation of beta2 adrenergic receptor-Src protein kinase complexes. *Science*, 283 (5402): 655-661.

Luttrell, L. M., Ostrowski, J., Cotecchia, S., Kendall, H. & Lefkowitz, R. J. (1993) Antagonism of catecholamine receptor signaling by expression of cytoplasmic domains of the receptors. *Science*, 259 (5100): 1453-1457.

López de Maturana, R. & Donnelly, D. (2002) The glucagon-like peptide-1 receptor binding site for the N-terminus of GLP-1 requires polarity at Asp198 rather than negative charge. *FEBS Lett*, 530 (1-3): 244-248.

López de Maturana, R., Treece-Birch, J., Abidi, F., Findlay, J. B. & Donnelly, D. (2004) Met-204 and Tyr-205 are together important for binding GLP-1 receptor agonists but not their N-terminally truncated analogues. *Protein Pept Lett*, 11 (1): 15-22.

López de Maturana, R., Willshaw, A., Kuntzsch, A., Rudolph, R. & Donnelly, D. (2003) The isolated N-terminal domain of the glucagon-like peptide-1 (GLP-1) receptor binds exendin peptides with much higher affinity than GLP-1. *J Biol Chem*, 278 (12): 10195-10200.

MacKinnon, A. C., Tufail-Hanif, U., Wheatley, M., Rossi, A. G., Haslett, C., Seckl, M. & Sethi, T. (2009) Targeting V1A-vasopressin receptors with [Arg6, D-Trp7,9, NmePhe8]-substance P (6-11) identifies a strategy to develop novel anti-cancer therapies. *Br J Pharmacol*, 156 (1): 36-47.

Maguire, M. E., Van Arsdale, P. M. & Gilman, A. G. (1976) An agonist-specific effect of guanine nucleotides on binding to the beta adrenergic receptor. *Mol Pharmacol*, 12 (2): 335-339.

Mahon, M., Donowitz, M., Yun, C. & Segre, G. (2002) Na(+)/H(+) exchanger regulatory factor 2 directs parathyroid hormone 1 receptor signalling. *Nature*, 417 (6891): 858-861.

Mallee, J. J., Salvatore, C. A., LeBourdelles, B., Oliver, K. R., Longmore, J., Koblan, K. S. & Kane, S. A. (2002) Receptor activity-modifying protein 1 determines the species selectivity of non-peptide CGRP receptor antagonists. *J Biol Chem*, 277 (16): 14294-14298.

Manglik, A., Kruse, A. C., Kobilka, T. S., Thian, F. S., Mathiesen, J. M., Sunahara, R. K., Pardo, L., Weis, W. I., Kobilka, B. K. & Granier, S. (2012) Crystal structure of the μ-opioid receptor bound to a morphinan antagonist. *Nature*, 485 (7398): 321-326.

Mann, R. J., Al-Sabah, S., de Maturana, R. L., Sinfield, J. K. & Donnelly, D. (2010) Functional coupling of Cys-226 and Cys-296 in the glucagon-like peptide-1 (GLP-1) receptor indicates a disulfide bond that is close to the activation pocket. *Peptides*, 31 (12): 2289-2293.

Mapelli, C., Natarajan, S. I., Meyer, J. P., Bastos, M. M., Bernatowicz, M. S., Lee, V. G., Pluscec, J., Riexinger, D. J., Sieber-McMaster, E. S., Constantine, K. L., Smith-Monroy, C. A., Golla, R., Ma, Z., Longhi, D. A., Shi, D., Xin, L., Taylor, J. R., Koplowitz, B., Chi, C. L., Khanna, A., Robinson, G. W., Seethala, R., Antal-Zimanyi, I. A., Stoffel, R. H., Han, S., Whaley, J. M., Huang, C. S., Krupinski, J. & Ewing, W. R. (2009) Eleven amino acid glucagon-like peptide-1 receptor agonists with antidiabetic activity. *J Med Chem*, 52 (23): 7788-7799.

Margeta-Mitrovic, M., Jan, Y. N. & Jan, L. Y. (2001) Function of GB1 and GB2 subunits in G protein coupling of GABA(B) receptors. *Proc Natl Acad Sci U S A*, 98 (25): 14649-14654.

Markovic, D. & Grammatopoulos, D. K. (2009) Focus on the splicing of secretin GPCRs transmembrane-domain 7. *Trends Biochem Sci*, 34 (9): 443-452.

Mathi, S., Chan, Y., Li, X. & Wheeler, M. (1997) Scanning of the glucagon-like peptide-1 receptor localizes G protein-activating determinants primarily to the N terminus of the third intracellular loop. *Mol Endocrinol*, 11 (4): 424-432.

Mattera, R., Graziano, M. P., Yatani, A., Zhou, Z., Graf, R., Codina, J., Birnbaumer, L., Gilman, A. G. & Brown, A. M. (1989) Splice variants of the alpha subunit of the G protein Gs activate both adenylyl cyclase and calcium channels. *Science*, 243 (4892): 804-807.

May, D. C., Ross, E. M., Gilman, A. G. & Smigel, M. D. (1985) Reconstitution of catecholamine-stimulated adenylate cyclase activity using three purified proteins. *J Biol Chem*, 260 (29): 15829-15833.

Mazur, A. W., Wang, F., Tscheiner, M., Tcheiner, M., Donnelly, E. & Isfort, R. J. (2004) Determinants of corticotropin releasing factor. Receptor selectivity of corticotropin releasing factor related peptides. *J Med Chem*, 47 (13): 3450-3454.

McCudden, C. R., Hains, M. D., Kimple, R. J., Siderovski, D. P. & Willard, F. S. (2005) G-protein signaling: back to the future. *Cell Mol Life Sci*, 62 (5): 551-577.

McLatchie, L., Fraser, N., Main, M., Wise, A., Brown, J., Thompson, N., Solari, R., Lee, M. & Foord, S. (1998) RAMPs regulate the transport and ligand specificity of the calcitonin-receptor-like receptor. *Nature*, 393 (6683): 333-339.

McLaughlin, J. N., Shen, L., Holinstat, M., Brooks, J. D., Dibenedetto, E. & Hamm, H. E. (2005) Functional selectivity of G protein signaling by agonist peptides and thrombin for the protease-activated receptor-1. *J Biol Chem*, 280 (26): 25048-25059.

Mialet-Perez, J., Green, S. A., Miller, W. E. & Liggett, S. B. (2004) A primate-dominant third glycosylation site of the beta2-adrenergic receptor routes receptors to degradation during agonist regulation. *J Biol Chem*, 279 (37): 38603-38607.

Min, L., Galet, C. & Ascoli, M. (2002) The association of arrestin-3 with the human lutropin/choriogonadotropin receptor depends mostly on receptor activation rather than on receptor phosphorylation. *J Biol Chem*, 277 (1): 702-710.

Moench, S. J., Moreland, J., Stewart, D. H. & Dewey, T. G. (1994) Fluorescence studies of the location and membrane accessibility of the palmitoylation sites of rhodopsin. *Biochemistry*, 33 (19): 5791-5796.

Monaghan, P., Thomas, B. E., Woznica, I., Wittelsberger, A., Mierke, D. F. & Rosenblatt, M. (2008) Mapping peptide hormone-receptor interactions using a disulfide-trapping approach. *Biochemistry*, 47 (22): 5889-5895.

Monod, J., Wyman, J. & Changeux, J. P. (1965) On the nature of allosteric transitions: a plausible model. *J Mol Biol*, 12 88-118.

Monticelli, L., Mammi, S. & Mierke, D. (2002) Molecular characterization of a ligand-tethered parathyroid hormone receptor. *Biophys Chem*, 95 (2): 165-172.

Moore, E. L., Gingell, J. J., Kane, S. A., Hay, D. L. & Salvatore, C. A. (2010) Mapping the CGRP receptor ligand binding domain: tryptophan-84 of RAMP1 is critical for agonist and antagonist binding. *Biochem Biophys Res Commun*, 394 (1): 141-145.

Moreira, I. S. (2014) Structural features of the G-protein/GPCR interactions. *Biochim Biophys Acta*, 1840 (1): 16-33.

Morfis, M., Christopoulos, A. & Sexton, P. (2003) RAMPs: 5 years on, where to now? *Trends Pharmacol Sci*, 24 (11): 596-601.

Moro, O., Lameh, J., Högger, P. & Sadée, W. (1993) Hydrophobic amino acid in the i2 loop plays a key role in receptor-G protein coupling. *J Biol Chem*, 268 (30): 22273-22276.

Moro, S., Hoffmann, C. & Jacobson, K. A. (1999) Role of the extracellular loops of G protein-coupled receptors in ligand recognition: a molecular modeling study of the human P2Y1 receptor. *Biochemistry*, 38 (12): 3498-3507.

Morou, E. & Georgoussi, Z. (2005) Expression of the third intracellular loop of the delta-opioid receptor inhibits signaling by opioid receptors and other G protein-coupled receptors. *J Pharmacol Exp Ther*, 315 (3): 1368-1379.

Mosselman, S., Höppener, J. W., Zandberg, J., van Mansfeld, A. D., Geurts van Kessel, A. H., Lips, C. J. & Jansz, H. S. (1988) Islet amyloid polypeptide: identification and chromosomal localization of the human gene. *FEBS Lett*, 239 (2): 227-232.

Muff, R., Bühlmann, N., Fischer, J. A. & Born, W. (1999) An amylin receptor is revealed following co-transfection of a calcitonin receptor with receptor activity modifying proteins-1 or -3. *Endocrinology*, 140 (6): 2924-2927.

Mukund, S., Shang, Y., Clarke, H. J., Madjidi, A., Corn, J. E., Kates, L., Kolumam, G., Chiang, V., Luis, E., Murray, J., Zhang, Y., Hötzel, I., Koth, C. M. & Allan, B. B. (2013) Inhibitory mechanism of an allosteric antibody targeting the glucagon receptor. *J Biol Chem*, 288 (50): 36168-36178.

Mulderry, P. K., Ghatei, M. A., Spokes, R. A., Jones, P. M., Pierson, A. M., Hamid, Q. A., Kanse, S., Amara, S. G., Burrin, J. M. & Legon, S. (1988) Differential expression of alpha-CGRP and beta-CGRP by primary sensory neurons and enteric autonomic neurons of the rat. *Neuroscience*, 25 (1): 195-205.

Mushegian, A., Gurevich, V. V. & Gurevich, E. V. (2012) The origin and evolution of G protein-coupled receptor kinases. *PLoS One*, 7 (3): e33806.

Muto, T., Tsuchiya, D., Morikawa, K. & Jingami, H. (2007) Structures of the extracellular regions of the group II/III metabotropic glutamate receptors. *Proc Natl Acad Sci U S A*, 104 (10): 3759-3764.

Natochin, M., Moussaif, M. & Artemyev, N. O. (2001) Probing the mechanism of rhodopsin-catalyzed transducin activation. *J Neurochem*, 77 (1): 202-210.

Natochin, M., Muradov, K. G., McEntaffer, R. L. & Artemyev, N. O. (2000) Rhodopsin recognition by mutant G(s)alpha containing C-terminal residues of transducin. *J Biol Chem*, 275 (4): 2669-2675.

Neumann, J., Couvineau, A., Murail, S., Lacapère, J., Jamin, N. & Laburthe, M. (2008) Class-B GPCR activation: is ligand helix-capping the key? *Trends Biochem Sci*, 33 (7): 314-319.

Nicoletti, P., Trevisani, M., Manconi, M., Gatti, R., De Siena, G., Zagli, G., Benemei, S., Capone, J. A., Geppetti, P. & Pini, L. A. (2008) Ethanol causes neurogenic vasodilation by TRPV1 activation and CGRP release in the trigeminovascular system of the guinea pig. *Cephalalgia*, 28 (1): 9-17.

Nielsen, S. M., Nielsen, L. Z., Hjorth, S. A., Perrin, M. H. & Vale, W. W. (2000) Constitutive activation of tethered-peptide/corticotropin-releasing factor receptor chimeras. *Proc Natl Acad Sci U S A*, 97 (18): 10277-10281.

Niu, S. L., Mitchell, D. C., Lim, S. Y., Wen, Z. M., Kim, H. Y., Salem, N. & Litman, B. J. (2004) Reduced G protein-coupled signaling efficiency in retinal rod outer segments in response to n-3 fatty acid deficiency. *J Biol Chem*, 279 (30): 31098-31104.

Njuki, F., Nicholl, C. G., Howard, A., Mak, J. C., Barnes, P. J., Girgis, S. I. & Legon, S. (1993) A new calcitonin-receptor-like sequence in rat pulmonary blood vessels. *Clin Sci (Lond)*, 85 (4): 385-388.

Noel, J. P., Hamm, H. E. & Sigler, P. B. (1993) The 2.2 A crystal structure of transducin-alpha complexed with GTP gamma S. *Nature*, 366 (6456): 654-663.

Nordström, K. J., Lagerström, M. C., Wallér, L. M., Fredriksson, R. & Schiöth, H. B. (2009) The Secretin GPCRs descended from the family of Adhesion GPCRs. *Mol Biol Evol*, 26 (1): 71-84.

Nordström, K. J., Sällman Almén, M., Edstam, M. M., Fredriksson, R. & Schiöth, H. B. (2011) Independent HHsearch, Needleman--Wunsch-based, and motif analyses reveal the overall hierarchy for most of the G protein-coupled receptor families. *Mol Biol Evol*, 28 (9): 2471-2480.

Nutt, R., Caulfield, M., Levy, J., Gibbons, S., Rosenblatt, M. & McKee, R. (1990) Removal of partial agonism from parathyroid hormone (PTH)-related protein-(7-34)NH2 by substitution of PTH amino acids at positions 10 and 11. *Endocrinology*, 127 (1): 491-493.

O'Brien, P. J. & Zatz, M. (1984) Acylation of bovine rhodopsin by [3H]palmitic acid. *J Biol Chem*, 259 (8): 5054-5057.

O'Connell, J. P., Kelly, S. M., Raleigh, D. P., Hubbard, J. A., Price, N. C., Dobson, C. M. & Smith, B. J. (1993) On the role of the C-terminus of alpha-calcitonin-gene-related peptide (alpha CGRP). The structure of des-phenylalaninamide37-alpha CGRP and its interaction with the CGRP receptor. *Biochem J*, 291 (Pt 1) 205-210.

O'Dowd, B. F., Hnatowich, M., Caron, M. G., Lefkowitz, R. J. & Bouvier, M. (1989) Palmitoylation of the human beta 2-adrenergic receptor. Mutation of Cys341 in the carboxyl tail leads to an uncoupled nonpalmitoylated form of the receptor. *J Biol Chem*, 264 (13): 7564-7569.

O'Hara, P. J., Sheppard, P. O., Thøgersen, H., Venezia, D., Haldeman, B. A., McGrane, V., Houamed, K. M., Thomsen, C., Gilbert, T. L. & Mulvihill, E. R. (1993) The ligand-binding domain in metabotropic glutamate receptors is related to bacterial periplasmic binding proteins. *Neuron*, 11 (1): 41-52.

Oakley, R. H., Laporte, S. A., Holt, J. A., Barak, L. S. & Caron, M. G. (2001) Molecular determinants underlying the formation of stable intracellular G protein-coupled receptor-beta-arrestin complexes after receptor endocytosis*. *J Biol Chem*, 276 (22): 19452-19460.

Oakley, R. H., Laporte, S. A., Holt, J. A., Caron, M. G. & Barak, L. S. (2000) Differential affinities of visual arrestin, beta arrestin1, and beta arrestin2 for G protein-coupled receptors delineate two major classes of receptors. *J Biol Chem*, 275 (22): 17201-17210.

Oakley, R. H., Olivares-Reyes, J. A., Hudson, C. C., Flores-Vega, F., Dautzenberg, F. M. & Hauger, R. L. (2007) Carboxyl-terminal and intracellular loop sites for CRF1 receptor phosphorylation and beta-arrestin-2 recruitment: a mechanism regulating stress and anxiety responses. *Am J Physiol Regul Integr Comp Physiol*, 293 (1): R209-222.

Oesterhelt, D. (1998) The structure and mechanism of the family of retinal proteins from halophilic archaea. *Curr Opin Struct Biol*, 8 (4): 489-500.

Ohguro, H., Palczewski, K., Ericsson, L. H., Walsh, K. A. & Johnson, R. S. (1993) Sequential phosphorylation of rhodopsin at multiple sites. *Biochemistry*, 32 (21): 5718-5724.

Okazaki, K. & Takada, S. (2008) Dynamic energy landscape view of coupled binding and protein conformational change: induced-fit versus population-shift mechanisms. *Proc Natl Acad Sci U S A*, 105 (32): 11182-11187.

Olah, M. E., Jacobson, K. A. & Stiles, G. L. (1994) Role of the second extracellular loop of adenosine receptors in agonist and antagonist binding. Analysis of chimeric A1/A3 adenosine receptors. *J Biol Chem*, 269 (40): 24692-24698.

Oldham, W. M. & Hamm, H. E. (2008) Heterotrimeric G protein activation by G-protein-coupled receptors. *Nat Rev Mol Cell Biol*, 9 (1): 60-71.

Olivella, M., Caltabiano, G. & Cordomí, A. (2013) The role of Cysteine 6.47 in class A GPCRs. *BMC Struct Biol*, 13 3.

Omary, M. B. & Trowbridge, I. S. (1981) Covalent binding of fatty acid to the transferrin receptor in cultured human cells. *J Biol Chem*, 256 (10): 4715-4718.

Onaran, H. O. & Costa, T. (1997) Agonist efficacy and allosteric models of receptor action. *Ann N Y Acad Sci*, 812 98-115.

Opekarová, M. & Tanner, W. (2003) Specific lipid requirements of membrane proteins--a putative bottleneck in heterologous expression. *Biochim Biophys Acta*, 1610 (1): 11-22.

Ostrom, R. S. & Insel, P. A. (2004) The evolving role of lipid rafts and caveolae in G protein-coupled receptor signaling: implications for molecular pharmacology. *Br J Pharmacol*, 143 (2): 235-245.

Padilla, B. E., Cottrell, G. S., Roosterman, D., Pikios, S., Muller, L., Steinhoff, M. & Bunnett, N. W. (2007) Endothelin-converting enzyme-1 regulates endosomal sorting of calcitonin receptor-like receptor and beta-arrestins. *J Cell Biol*, 179 (5): 981-997.

Paing, M. M., Temple, B. R. & Trejo, J. (2004) A tyrosine-based sorting signal regulates intracellular trafficking of protease-activated receptor-1: multiple regulatory mechanisms for agonist-induced G protein-coupled receptor internalization. *J Biol Chem*, 279 (21): 21938-21947.

Pal, K., Melcher, K. & Xu, H. E. (2012) Structure and mechanism for recognition of peptide hormones by Class B G-protein-coupled receptors. *Acta Pharmacol Sin*, 33 (3): 300-311.

Pal, K., Swaminathan, K., Xu, H. E. & Pioszak, A. A. (2010) Structural basis for hormone recognition by the Human CRFR2{alpha} G protein-coupled receptor. *J Biol Chem*, 285 (51): 40351-40361.

Palczewski, K., Buczyłko, J., Lebioda, L., Crabb, J. W. & Polans, A. S. (1993) Identification of the N-terminal region in rhodopsin kinase involved in its interaction with rhodopsin. *J Biol Chem*, 268 (8): 6004-6013.

Palczewski, K., Kumasaka, T., Hori, T., Behnke, C., Motoshima, H., Fox, B., Le Trong, I., Teller, D., Okada, T., Stenkamp, R., Yamamoto, M. & Miyano, M. (2000) Crystal structure of rhodopsin: A G protein-coupled receptor. *Science*, 289 (5480): 739-745.

Papadopoulou, N., Chen, J., Randeva, H. S., Levine, M. A., Hillhouse, E. W. & Grammatopoulos, D. K. (2004) Protein kinase A-induced negative regulation of the corticotropin-releasing hormone R1alpha receptor-extracellularly regulated kinase signal transduction pathway: the critical role of Ser301 for signaling switch and selectivity. *Mol Endocrinol*, 18 (3): 624-639.

Pardo, L., Ballesteros, J. A., Osman, R. & Weinstein, H. (1992) On the use of the transmembrane domain of bacteriorhodopsin as a template for modeling the three-dimensional structure of guanine nucleotide-binding regulatory protein-coupled receptors. *Proc Natl Acad Sci U S A*, 89 (9): 4009-4012.

Park, S. H., Das, B. B., Casagrande, F., Tian, Y., Nothnagel, H. J., Chu, M., Kiefer, H., Maier, K., De Angelis, A. A., Marassi, F. M. & Opella, S. J. (2012) Structure of the chemokine receptor CXCR1 in phospholipid bilayers. *Nature*, 491 (7426): 779-783.

Parmentier, M. L., Prézeau, L., Bockaert, J. & Pin, J. P. (2002) A model for the functioning of family 3 GPCRs. *Trends Pharmacol Sci*, 23 (6): 268-274.

Parthier, C., Kleinschmidt, M., Neumann, P., Rudolph, R., Manhart, S., Schlenzig, D., Fanghänel, J., Rahfeld, J., Demuth, H. & Stubbs, M. (2007) Crystal structure of the incretin-bound extracellular domain of a G protein-coupled receptor. *Proc Natl Acad Sci U S A*, 104 (35): 13942-13947.

Parthier, C., Reedtz-Runge, S., Rudolph, R. & Stubbs, M. (2009) Passing the baton in class B GPCRs: peptide hormone activation via helix induction? *Trends Biochem Sci*, 34 (6): 303-310.

Peeters, M. C., van Westen, G. J., Guo, D., Wisse, L. E., Müller, C. E., Beukers, M. W. & Ijzerman, A. P. (2011) GPCR structure and activation: an essential role for the first extracellular loop in activating the adenosine A2B receptor. *FASEB J*, 25 (2): 632-643.

Peeters, M. C., Wisse, L. E., Dinaj, A., Vroling, B., Vriend, G. & Ijzerman, A. P. (2012) The role of the second and third extracellular loops of the adenosine A1 receptor in activation and allosteric modulation. *Biochem Pharmacol*, 84 (1): 76-87.

Perlman, J. H., Colson, A. O., Jain, R., Czyzewski, B., Cohen, L. A., Osman, R. & Gershengorn, M. C. (1997) Role of the extracellular loops of the thyrotropin-releasing hormone receptor: evidence for an initial interaction with thyrotropin-releasing hormone. *Biochemistry*, 36 (50): 15670-15676.

Perrin, M., DiGruccio, M., Koerber, S., Rivier, J., Kunitake, K., Bain, D., Fischer, W. & Vale, W. (2003) A soluble form of the first extracellular domain of mouse type 2beta corticotropin-releasing factor receptor reveals differential ligand specificity. *J Biol Chem*, 278 (18): 15595-15600.

Perrin, M., Grace, C., Digruccio, M., Fischer, W., Maji, S., Cantle, J., Smith, S., Manning, G., Vale, W. & Riek, R. (2007) Distinct structural and functional roles of conserved residues in the first extracellular domain of receptors for corticotropin-releasing factor and related G-protein-coupled receptors. *J Biol Chem*, 282 (52): 37529-37536.

Perry, S. J., Baillie, G. S., Kohout, T. A., McPhee, I., Magiera, M. M., Ang, K. L., Miller, W. E., McLean, A. J., Conti, M., Houslay, M. D. & Lefkowitz, R. J. (2002) Targeting of cyclic AMP degradation to beta 2-adrenergic receptors by beta-arrestins. *Science*, 298 (5594): 834-836.

Petermann, J. B., Born, W., Chang, J. Y. & Fischer, J. A. (1987) Identification in the human central nervous system, pituitary, and thyroid of a novel calcitonin gene-related peptide, and partial amino acid sequence in the spinal cord. *J Biol Chem*, 262 (2): 542-545.

Pfeuffer, T., Gaugler, B. & Metzger, H. (1983) Isolation of homologous and heterologous complexes between catalytic and regulatory components of adenylate cyclase by forskolin-Sepharose. *FEBS Lett*, 164 (1): 154-160.

Pioszak, A., Parker, N., Suino-Powell, K. & Xu, H. (2008) Molecular recognition of corticotropin-releasing factor by its G-protein-coupled receptor CRFR1. *J Biol Chem*, 283 (47): 32900-32912.

Pioszak, A. & Xu, H. (2008) Molecular recognition of parathyroid hormone by its G protein-coupled receptor. *Proc Natl Acad Sci U S A*, 105 (13): 5034-5039.

Pioszak, A. A., Harikumar, K. G., Parker, N. R., Miller, L. J. & Xu, H. E. (2010) Dimeric arrangement of the parathyroid hormone receptor and a structural mechanism for ligand-induced dissociation. *J Biol Chem*, 285 (16): 12435-12444.

Pioszak, A. A., Parker, N. R., Gardella, T. J. & Xu, H. E. (2009) Structural basis for parathyroid hormone-related protein binding to the parathyroid hormone receptor and design of conformation-selective peptides. *J Biol Chem*, 284 (41): 28382-28391.

Piserchio, A., Zelesky, V., Yu, J., Taylor, L., Polgar, P. & Mierke, D. (2005) Bradykinin B2 receptor signaling: structural and functional characterization of the C-terminus. *Biopolymers*, 80 (2-3): 367-373.

Pitcher, J. A., Fredericks, Z. L., Stone, W. C., Premont, R. T., Stoffel, R. H., Koch, W. J. & Lefkowitz, R. J. (1996) Phosphatidylinositol 4,5-bisphosphate (PIP2)-enhanced G protein-coupled receptor kinase (GRK) activity. Location, structure, and regulation of the PIP2 binding site distinguishes the GRK subfamilies. *J Biol Chem*, 271 (40): 24907-24913.

Pitcher, J. A., Freedman, N. J. & Lefkowitz, R. J. (1998) G protein-coupled receptor kinases. *Annu Rev Biochem*, 67 653-692.

Poyner, D. R., Andrew, D. P., Brown, D., Bose, C. & Hanley, M. R. (1992) Pharmacological characterization of a receptor for calcitonin gene-related peptide on rat, L6 myocytes. *Br J Pharmacol*, 105 (2): 441-447.

Poyner, D. R., Sexton, P. M., Marshall, I., Smith, D. M., Quirion, R., Born, W., Muff, R., Fischer, J. A. & Foord, S. M. (2002) International Union of Pharmacology. XXXII. The mammalian calcitonin gene-related peptides, adrenomedullin, amylin, and calcitonin receptors. *Pharmacol Rev*, 54 (2): 233-246.

Poyner, D. R., Soomets, U., Howitt, S. G. & Langel, U. (1998) Structural determinants for binding to CGRP receptors expressed by human SK-N-MC and Col 29 cells: studies with chimeric and other peptides. *Br J Pharmacol*, 124 (8): 1659-1666.

Prado, G. N., Mierke, D. F., Pellegrini, M., Taylor, L. & Polgar, P. (1998) Motif mutation of bradykinin B2 receptor second intracellular loop and proximal C terminus is critical for signal transduction, internalization, and resensitization. *J Biol Chem*, 273 (50): 33548-33555.

Prado, M. A., Evans-Bain, B., Oliver, K. R. & Dickerson, I. M. (2001) The role of the CGRP-receptor component protein (RCP) in adrenomedullin receptor signal transduction. *Peptides*, 22 (11): 1773-1781.

Qanbar, R. & Bouvier, M. (2003) Role of palmitoylation/depalmitoylation reactions in G-protein-coupled receptor function. *Pharmacol Ther*, 97 (1): 1-33.

Qi, T., Ly, K., Poyner, D. R., Christopoulos, G., Sexton, P. M. & Hay, D. L. (2011) Structure-function analysis of amino acid 74 of human RAMP1 and RAMP3 and its role in peptide interactions with adrenomedullin and calcitonin gene-related peptide receptors. *Peptides*, 32 (5): 1060-1067.

Raddino, R., Pelà, G., Manca, C., Barbagallo, M., D'Aloia, A., Passeri, M. & Visioli, O. (1997) Mechanism of action of human calcitonin gene-related peptide in rabbit heart and in human mammary arteries. *J Cardiovasc Pharmacol*, 29 (4): 463-470.

Rajagopal, S., Bassoni, D. L., Campbell, J. J., Gerard, N. P., Gerard, C. & Wehrman, T. S. (2013) Biased agonism as a mechanism for differential signaling by chemokine receptors. *J Biol Chem*, 288 (49): 35039-35048.

Rasmussen, S., Choi, H., Rosenbaum, D., Kobilka, T., Thian, F., Edwards, P., Burghammer, M., Ratnala, V., Sanishvili, R., Fischetti, R., Schertler, G., Weis, W. & Kobilka, B. (2007) Crystal structure of the human beta2 adrenergic G-protein-coupled receptor. *Nature*, 450 (7168): 383-387.

Rasmussen, S. G., Choi, H. J., Fung, J. J., Pardon, E., Casarosa, P., Chae, P. S., Devree, B. T., Rosenbaum, D. M., Thian, F. S., Kobilka, T. S., Schnapp, A., Konetzki, I., Sunahara, R. K., Gellman, S. H., Pautsch, A., Steyaert, J., Weis, W. I. & Kobilka, B. K. (2011a) Structure of a nanobody-stabilized active state of the β(2) adrenoceptor. *Nature*, 469 (7329): 175-180.

Rasmussen, S. G., DeVree, B. T., Zou, Y., Kruse, A. C., Chung, K. Y., Kobilka, T. S., Thian, F. S., Chae, P. S., Pardon, E., Calinski, D., Mathiesen, J. M., Shah, S. T., Lyons, J. A., Caffrey, M., Gellman, S. H., Steyaert, J., Skiniotis, G., Weis, W. I., Sunahara, R. K. & Kobilka, B. K. (2011b) Crystal structure of the β2 adrenergic receptor-Gs protein complex. *Nature*, 477 (7366): 549-555.

Ray, K. & Hauschild, B. C. (2000) Cys-140 is critical for metabotropic glutamate receptor-1 dimerization. *J Biol Chem*, 275 (44): 34245-34251.

Reiter, E. & Lefkowitz, R. J. (2006) GRKs and beta-arrestins: roles in receptor silencing, trafficking and signaling. *Trends Endocrinol Metab*, 17 (4): 159-165.

Rivier, J., Rivier, C. & Vale, W. (1984) Synthetic competitive antagonists of corticotropin-releasing factor: effect on ACTH secretion in the rat. *Science*, 224 (4651): 889-891.

Robinson, S. D., Aitken, J. F., Bailey, R. J., Poyner, D. R. & Hay, D. L. (2009) Novel peptide antagonists of adrenomedullin and calcitonin gene-related peptide receptors: identification, pharmacological characterization, and interactions with position 74 in receptor activity-modifying protein 1/3. *J Pharmacol Exp Ther*, 331 (2): 513-521.

Roh, J., Chang, C. L., Bhalla, A., Klein, C. & Hsu, S. Y. (2004) Intermedin is a calcitonin/calcitonin gene-related peptide family peptide acting through the calcitonin receptor-like receptor/receptor activity-modifying protein receptor complexes. *J Biol Chem*, 279 (8): 7264-7274.

Romano, C., Miller, J. K., Hyrc, K., Dikranian, S., Mennerick, S., Takeuchi, Y., Goldberg, M. P. & O'Malley, K. L. (2001) Covalent and noncovalent interactions mediate metabotropic glutamate receptor mGlu5 dimerization. *Mol Pharmacol*, 59 (1): 46-53.

Rondard, P., Huang, S., Monnier, C., Tu, H., Blanchard, B., Oueslati, N., Malhaire, F., Li, Y., Trinquet, E., Labesse, G., Pin, J. P. & Liu, J. (2008) Functioning of the dimeric GABA(B) receptor extracellular domain revealed by glycan wedge scanning. *EMBO J*, 27 (9): 1321-1332.

Rosenbaum, D., Cherezov, V., Hanson, M., Rasmussen, S., Thian, F., Kobilka, T., Choi, H., Yao, X., Weis, W., Stevens, R. & Kobilka, B. (2007) GPCR engineering yields high-resolution structural insights into beta2-adrenergic receptor function. *Science*, 318 (5854): 1266-1273.

Rosenbaum, D. M., Zhang, C., Lyons, J. A., Holl, R., Aragao, D., Arlow, D. H., Rasmussen, S. G., Choi, H. J., Devree, B. T., Sunahara, R. K., Chae, P. S., Gellman, S. H., Dror, R. O., Shaw, D. E., Weis, W. I., Caffrey, M., Gmeiner, P. & Kobilka, B. K. (2011) Structure and function of an irreversible agonist-β(2) adrenoceptor complex. *Nature*, 469 (7329): 236-240.

Rosenfeld, M. G., Amara, S. G. & Evans, R. M. (1984) Alternative RNA processing: determining neuronal phenotype. *Science*, 225 (4668): 1315-1320.

Ruiz-González, M. X. & Marín, I. (2004) New insights into the evolutionary history of type 1 rhodopsins. *J Mol Evol*, 58 (3): 348-358.

Runge, S., Thøgersen, H., Madsen, K., Lau, J. & Rudolph, R. (2008) Crystal structure of the ligand-bound glucagon-like peptide-1 receptor extracellular domain. *J Biol Chem*, 283 (17): 11340-11347.

Runge, S., Wulff, B. S., Madsen, K., Bräuner-Osborne, H. & Knudsen, L. B. (2003) Different domains of the glucagon and glucagon-like peptide-1 receptors

provide the critical determinants of ligand selectivity. *Br J Pharmacol*, 138 (5): 787-794.

Sagoo, J. K., Bose, C., Beeley, N. R. & Tendler, S. J. (1991) Structural studies on the [Bu(t)-Cys18](19-37)-fragment of human beta-calcitonin-gene-related peptide. *Biochem J*, 280 (Pt 1) 147-150.

Salon, J. A., Lodowski, D. T. & Palczewski, K. (2011) The significance of G protein-coupled receptor crystallography for drug discovery. *Pharmacol Rev*, 63 (4): 901-937.

Salvatore, C. A., Hershey, J. C., Corcoran, H. A., Fay, J. F., Johnston, V. K., Moore, E. L., Mosser, S. D., Burgey, C. S., Paone, D. V., Shaw, A. W., Graham, S. L., Vacca, J. P., Williams, T. M., Koblan, K. S. & Kane, S. A. (2008) Pharmacological characterization of MK-0974 [N-[(3R,6S)-6-(2,3-difluorophenyl)-2-oxo-1-(2,2,2-trifluoroethyl)azepan-3-yl]-4-(2-oxo-2,3-dihydro-1H-imidazo[4,5-b]pyridin-1-yl)piperidine-1-carboxamide], a potent and orally active calcitonin gene-related peptide receptor antagonist for the treatment of migraine. *J Pharmacol Exp Ther*, 324 (2): 416-421.

Sansuk, K., Deupi, X., Torrecillas, I. R., Jongejan, A., Nijmeijer, S., Bakker, R. A., Pardo, L. & Leurs, R. (2011) A structural insight into the reorientation of transmembrane domains 3 and 5 during family A G protein-coupled receptor activation. *Mol Pharmacol*, 79 (2): 262-269.

Scheerer, P., Park, J., Hildebrand, P., Kim, Y., Krauss, N., Choe, H., Hofmann, K. & Ernst, O. (2008) Crystal structure of opsin in its G-protein-interacting conformation. *Nature*, 455 (7212): 497-502.

Schertler, G. F., Villa, C. & Henderson, R. (1993) Projection structure of rhodopsin. *Nature*, 362 (6422): 770-772.

Schmidt, C., Li, B., Bloodworth, L., Erlenbach, I., Zeng, F. Y. & Wess, J. (2003) Random mutagenesis of the M3 muscarinic acetylcholine receptor expressed in yeast. Identification of point mutations that "silence" a constitutively active mutant M3 receptor and greatly impair receptor/G protein coupling. *J Biol Chem*, 278 (32): 30248-30260.

Schmidt, C. J., Thomas, T. C., Levine, M. A. & Neer, E. J. (1992) Specificity of G protein beta and gamma subunit interactions. *J Biol Chem*, 267 (20): 13807-13810.

Schubert, B., VanDongen, A. M., Kirsch, G. E. & Brown, A. M. (1989) Beta-adrenergic inhibition of cardiac sodium channels by dual G-protein pathways. *Science*, 245 (4917): 516-519.

Schwartz, T., Frimurer, T., Holst, B., Rosenkilde, M. & Elling, C. (2006) Molecular mechanism of 7TM receptor activation--a global toggle switch model. *Annu Rev Pharmacol Toxicol*, 46 481-519.

Seifert, R., Lee, T. W., Lam, V. T. & Kobilka, B. K. (1998a) Reconstitution of beta2-adrenoceptor-GTP-binding-protein interaction in Sf9 cells--high coupling efficiency in a beta2-adrenoceptor-G(s alpha) fusion protein. *Eur J Biochem*, 255 (2): 369-382.

Seifert, R., Wenzel-Seifert, K. & Kobilka, B. K. (1999) GPCR-Galpha fusion proteins: molecular analysis of receptor-G-protein coupling. *Trends Pharmacol Sci*, 20 (9): 383-389.

Seifert, R., Wenzel-Seifert, K., Lee, T. W., Gether, U., Sanders-Bush, E. & Kobilka, B. K. (1998b) Different effects of Gsalpha splice variants on beta2-adrenoreceptor-mediated signaling. The Beta2-adrenoreceptor coupled to the long splice variant of Gsalpha has properties of a constitutively active receptor. *J Biol Chem*, 273 (18): 5109-5116.

Semyonov, J., Park, J. I., Chang, C. L. & Hsu, S. Y. (2008) GPCR genes are preferentially retained after whole genome duplication. *PLoS One*, 3 (4): e1903.

Serrano-Vega, M., Magnani, F., Shibata, Y. & Tate, C. (2008) Conformational thermostabilization of the beta1-adrenergic receptor in a detergent-resistant form. *Proc Natl Acad Sci U S A*, 105 (3): 877-882.

Sexton, P. M., Albiston, A., Morfis, M. & Tilakaratne, N. (2001) Receptor activity modifying proteins. *Cell Signal*, 13 (2): 73-83.

Sharma, A. K., Spudich, J. L. & Doolittle, W. F. (2006) Microbial rhodopsins: functional versatility and genetic mobility. *Trends Microbiol*, 14 (11): 463-469.

Sheikh, S., Vilardarga, J., Baranski, T., Lichtarge, O., Iiri, T., Meng, E., Nissenson, R. & Bourne, H. (1999) Similar structures and shared switch mechanisms of the beta2-adrenoceptor and the parathyroid hormone receptor. Zn(II) bridges between helices III and VI block activation. *J Biol Chem*, 274 (24): 17033-17041.

Sheikh, S. P., Zvyaga, T. A., Lichtarge, O., Sakmar, T. P. & Bourne, H. R. (1996) Rhodopsin activation blocked by metal-ion-binding sites linking transmembrane helices C and F. *Nature*, 383 (6598): 347-350.

Shenoy, S. K., Drake, M. T., Nelson, C. D., Houtz, D. A., Xiao, K., Madabushi, S., Reiter, E., Premont, R. T., Lichtarge, O. & Lefkowitz, R. J. (2006) beta-arrestin-

dependent, G protein-independent ERK1/2 activation by the beta2 adrenergic receptor. *J Biol Chem*, 281 (2): 1261-1273.

Shenoy, S. K. & Lefkowitz, R. J. (2003a) Multifaceted roles of beta-arrestins in the regulation of seven-membrane-spanning receptor trafficking and signalling. *Biochem J*, 375 (Pt 3): 503-515.

Shenoy, S. K. & Lefkowitz, R. J. (2003b) Trafficking patterns of beta-arrestin and G protein-coupled receptors determined by the kinetics of beta-arrestin deubiquitination. *J Biol Chem*, 278 (16): 14498-14506.

Shenoy, S. K., McDonald, P. H., Kohout, T. A. & Lefkowitz, R. J. (2001) Regulation of receptor fate by ubiquitination of activated beta 2-adrenergic receptor and beta-arrestin. *Science*, 294 (5545): 1307-1313.

Shimamura, T., Shiroishi, M., Weyand, S., Tsujimoto, H., Winter, G., Katritch, V., Abagyan, R., Cherezov, V., Liu, W., Han, G. W., Kobayashi, T., Stevens, R. C. & Iwata, S. (2011) Structure of the human histamine H1 receptor complex with doxepin. *Nature*, 475 (7354): 65-70.

Shimizu, N., Guo, J. & Gardella, T. (2001) Parathyroid hormone (PTH)-(1-14) and -(1-11) analogs conformationally constrained by alpha-aminoisobutyric acid mediate full agonist responses via the juxtamembrane region of the PTH-1 receptor. *J Biol Chem*, 276 (52): 49003-49012.

Shukla, A. K., Manglik, A., Kruse, A. C., Xiao, K., Reis, R. I., Tseng, W. C., Staus, D. P., Hilger, D., Uysal, S., Huang, L. Y., Paduch, M., Tripathi-Shukla, P., Koide, A., Koide, S., Weis, W. I., Kossiakoff, A. A., Kobilka, B. K. & Lefkowitz, R. J. (2013) Structure of active β-arrestin-1 bound to a G-protein-coupled receptor phosphopeptide. *Nature*, 497 (7447): 137-141.

Sibley, D. R., Strasser, R. H., Caron, M. G. & Lefkowitz, R. J. (1985) Homologous desensitization of adenylate cyclase is associated with phosphorylation of the beta-adrenergic receptor. *J Biol Chem*, 260 (7): 3883-3886.

Simms, J., Hay, D. L., Bailey, R. J., Konycheva, G., Bailey, G., Wheatley, M. & Poyner, D. R. (2009) Structure-function analysis of RAMP1 by alanine mutagenesis. *Biochemistry*, 48 (1): 198-205.

Simon, M. I., Strathmann, M. P. & Gautam, N. (1991) Diversity of G proteins in signal transduction. *Science*, 252 (5007): 802-808.

Simonin, F., Karcher, P., Boeuf, J. J., Matifas, A. & Kieffer, B. L. (2004) Identification of a novel family of G protein-coupled receptor associated sorting proteins. *J Neurochem*, 89 (3): 766-775.

Simons, K. & Vaz, W. L. (2004) Model systems, lipid rafts, and cell membranes. *Annu Rev Biophys Biomol Struct*, 33 269-295.

Singer, S. J. & Nicolson, G. L. (1972) The fluid mosaic model of the structure of cell membranes. *Science*, 175 (4023): 720-731.

Singh, S., Hedley, D., Kara, E., Gras, A., Iwata, S., Ruprecht, J., Strange, P. G. & Byrne, B. (2010) A purified C-terminally truncated human adenosine A(2A) receptor construct is functionally stable and degradation resistant. *Protein Expr Purif*, 74 (1): 80-87.

Siu, F. Y., He, M., de Graaf, C., Han, G. W., Yang, D., Zhang, Z., Zhou, C., Xu, Q., Wacker, D., Joseph, J. S., Liu, W., Lau, J., Cherezov, V., Katritch, V., Wang, M. W. & Stevens, R. C. (2013) Structure of the human glucagon class B G-protein-coupled receptor. *Nature*, 499 (7459): 444-449.

Smillie, S. J. & Brain, S. D. (2011) Calcitonin gene-related peptide (CGRP) and its role in hypertension. *Neuropeptides*, 45 (2): 93-104.

Spudich, J. L. & Luecke, H. (2002) Sensory rhodopsin II: functional insights from structure. *Curr Opin Struct Biol*, 12 (4): 540-546.

Stadel, J. M., Nambi, P., Shorr, R. G., Sawyer, D. F., Caron, M. G. & Lefkowitz, R. J. (1983) Catecholamine-induced desensitization of turkey erythrocyte adenylate cyclase is associated with phosphorylation of the beta-adrenergic receptor. *Proc Natl Acad Sci U S A*, 80 (11): 3173-3177.

Standfuss, J., Edwards, P. C., D'Antona, A., Fransen, M., Xie, G., Oprian, D. D. & Schertler, G. F. (2011) The structural basis of agonist-induced activation in constitutively active rhodopsin. *Nature*, 471 (7340): 656-660.

Standfuss, J., Xie, G., Edwards, P. C., Burghammer, M., Oprian, D. D. & Schertler, G. F. (2007) Crystal structure of a thermally stable rhodopsin mutant. *J Mol Biol*, 372 (5): 1179-1188.

Steenbergh, P. H., Höppener, J. W., Zandberg, J., Lips, C. J. & Jansz, H. S. (1985) A second human calcitonin/CGRP gene. *FEBS Lett*, 183 (2): 403-407.

Steinberg, S. F. (2008) Structural basis of protein kinase C isoform function. *Physiol Rev*, 88 (4): 1341-1378.

Steiner, S., Born, W., Fischer, J. A. & Muff, R. (2003) The function of conserved cysteine residues in the extracellular domain of human receptor-activity-modifying protein. *FEBS Lett*, 555 (2): 285-290.

Steiner, S., Muff, R., Gujer, R., Fischer, J. A. & Born, W. (2002) The transmembrane domain of receptor-activity-modifying protein 1 is essential for the functional expression of a calcitonin gene-related peptide receptor. *Biochemistry*, 41 (38): 11398-11404.

Stevens, R. C., Cherezov, V., Katritch, V., Abagyan, R., Kuhn, P., Rosen, H. & Wüthrich, K. (2013) The GPCR Network: a large-scale collaboration to determine human GPCR structure and function. *Nat Rev Drug Discov*, 12 (1): 25-34.

Strathmann, M. P. & Simon, M. I. (1991) G alpha 12 and G alpha 13 subunits define a fourth class of G protein alpha subunits. *Proc Natl Acad Sci U S A*, 88 (13): 5582-5586.

Sugo, S., Minamino, N., Kangawa, K., Miyamoto, K., Kitamura, K., Sakata, J., Eto, T. & Matsuo, H. (1994a) Endothelial cells actively synthesize and secrete adrenomedullin. *Biochem Biophys Res Commun*, 201 (3): 1160-1166.

Sugo, S., Minamino, N., Shoji, H., Kangawa, K., Kitamura, K., Eto, T. & Matsuo, H. (1994b) Production and secretion of adrenomedullin from vascular smooth muscle cells: augmented production by tumor necrosis factor-alpha. *Biochem Biophys Res Commun*, 203 (1): 719-726.

Sugo, S., Minamino, N., Shoji, H., Kangawa, K., Kitamura, K., Eto, T. & Matsuo, H. (1995) Interleukin-1, tumor necrosis factor and lipopolysaccharide additively stimulate production of adrenomedullin in vascular smooth muscle cells. *Biochem Biophys Res Commun*, 207 (1): 25-32.

Sun, C., Song, D., Davis-Taber, R., Barrett, L., Scott, V., Richardson, P., Pereda-Lopez, A., Uchic, M., Solomon, L., Lake, M., Walter, K., Hajduk, P. & Olejniczak, E. (2007) Solution structure and mutational analysis of pituitary adenylate cyclase-activating polypeptide binding to the extracellular domain of PAC1-RS. *Proc Natl Acad Sci U S A*, 104 (19): 7875-7880.

Sunahara, R. K., Tesmer, J. J., Gilman, A. G. & Sprang, S. R. (1997) Crystal structure of the adenylyl cyclase activator Gsalpha. *Science*, 278 (5345): 1943-1947.

Takei, Y., Hyodo, S., Katafuchi, T. & Minamino, N. (2004) Novel fish-derived adrenomedullin in mammals: structure and possible function. *Peptides*, 25 (10): 1643-1656.

Takhar, S., Gyomorey, S., Su, R. C., Mathi, S. K., Li, X. & Wheeler, M. B. (1996) The third cytoplasmic domain of the GLP-1[7-36 amide] receptor is required for coupling to the adenylyl cyclase system. *Endocrinology*, 137 (5): 2175-2178.

Tams, J. W., Knudsen, S. M. & Fahrenkrug, J. (2001) Characterization of a G protein coupling "YL" motif of the human VPAC1 receptor, equivalent to the first two amino acids in the "DRY" motif of the rhodopsin family. *J Mol Neurosci*, 17 (3): 325-330.

Tan, C. M., Brady, A. E., Nickols, H. H., Wang, Q. & Limbird, L. E. (2004) Membrane trafficking of G protein-coupled receptors. *Annu Rev Pharmacol Toxicol*, 44 559-609.

Tang, W. J. & Gilman, A. G. (1991) Type-specific regulation of adenylyl cyclase by G protein beta gamma subunits. *Science*, 254 (5037): 1500-1503.

Tateyama, M., Abe, H., Nakata, H., Saito, O. & Kubo, Y. (2004) Ligand-induced rearrangement of the dimeric metabotropic glutamate receptor 1alpha. *Nat Struct Mol Biol*, 11 (7): 637-642.

Taussig, R., Iñiguez-Lluhi, J. A. & Gilman, A. G. (1993) Inhibition of adenylyl cyclase by Gi alpha. *Science*, 261 (5118): 218-221.

Taylor, E. W. & Agarwal, A. (1993) Sequence homology between bacteriorhodopsin and G-protein coupled receptors: exon shuffling or evolution by duplication? *FEBS Lett*, 325 (3): 161-166.

Taylor, S. S., Yang, J., Wu, J., Haste, N. M., Radzio-Andzelm, E. & Anand, G. (2004) PKA: a portrait of protein kinase dynamics. *Biochim Biophys Acta*, 1697 (1-2): 259-269.

Teli, T., Markovic, D., Levine, M. A., Hillhouse, E. W. & Grammatopoulos, D. K. (2005) Regulation of corticotropin-releasing hormone receptor type 1alpha signaling: structural determinants for G protein-coupled receptor kinase-mediated phosphorylation and agonist-mediated desensitization. *Mol Endocrinol*, 19 (2): 474-490.

ter Haar, E., Koth, C. M., Abdul-Manan, N., Swenson, L., Coll, J. T., Lippke, J. A., Lepre, C. A., Garcia-Guzman, M. & Moore, J. M. (2010) Crystal structure of the ectodomain complex of the CGRP receptor, a class-B GPCR, reveals the site of drug antagonism. *Structure*, 18 (9): 1083-1093.

Thompson, A. A., Liu, W., Chun, E., Katritch, V., Wu, H., Vardy, E., Huang, X. P., Trapella, C., Guerrini, R., Calo, G., Roth, B. L., Cherezov, V. & Stevens, R. C. (2012)

Structure of the nociceptin/orphanin FQ receptor in complex with a peptide mimetic. *Nature*, 485 (7398): 395-399.

Thorens, B., Porret, A., Bühler, L., Deng, S., Morel, P. & Widmann, C. (1993) Cloning and functional expression of the human islet GLP-1 receptor. Demonstration that exendin-4 is an agonist and exendin-(9-39) an antagonist of the receptor. *Diabetes*, 42 (11): 1678-1682.

Tilakaratne, N., Christopoulos, G., Zumpe, E. T., Foord, S. M. & Sexton, P. M. (2000) Amylin receptor phenotypes derived from human calcitonin receptor/RAMP coexpression exhibit pharmacological differences dependent on receptor isoform and host cell environment. *J Pharmacol Exp Ther*, 294 (1): 61-72.

Tobin, A. B. (2008) G-protein-coupled receptor phosphorylation: where, when and by whom. *Br J Pharmacol*, 153 Suppl 1 S167-176.

Tolkovsky, A. M. & Levitzki, A. (1978) Mode of coupling between the beta-adrenergic receptor and adenylate cyclase in turkey erythrocytes. *Biochemistry*, 17 (18): 3795.

Tsuchiya, D., Kunishima, N., Kamiya, N., Jingami, H. & Morikawa, K. (2002) Structural views of the ligand-binding cores of a metabotropic glutamate receptor complexed with an antagonist and both glutamate and Gd3+. *Proc Natl Acad Sci U S A*, 99 (5): 2660-2665.

Tsuji, Y., Shimada, Y., Takeshita, T., Kajimura, N., Nomura, S., Sekiyama, N., Otomo, J., Usukura, J., Nakanishi, S. & Jingami, H. (2000) Cryptic dimer interface and domain organization of the extracellular region of metabotropic glutamate receptor subtype 1. *J Biol Chem*, 275 (36): 28144-28151.

Tucker, J. & Grisshammer, R. (1996) Purification of a rat neurotensin receptor expressed in Escherichia coli. *Biochem J*, 317 (Pt 3) 891-899.

Unal, H., Jagannathan, R., Bhat, M. B. & Karnik, S. S. (2010) Ligand-specific conformation of extracellular loop-2 in the angiotensin II type 1 receptor. *J Biol Chem*, 285 (21): 16341-16350.

Underwood, C. R., Garibay, P., Knudsen, L. B., Hastrup, S., Peters, G. H., Rudolph, R. & Reedtz-Runge, S. (2010) Crystal structure of glucagon-like peptide-1 in complex with the extracellular domain of the glucagon-like peptide-1 receptor. *J Biol Chem*, 285 (1): 723-730.

Urano, D. & Jones, A. M. (2013) "Round up the usual suspects": a comment on nonexistent plant G protein-coupled receptors. *Plant Physiol*, 161 (3): 1097-1102.

Valiquette, M., Parent, S., Loisel, T. P. & Bouvier, M. (1995) Mutation of tyrosine-141 inhibits insulin-promoted tyrosine phosphorylation and increased responsiveness of the human beta 2-adrenergic receptor. *EMBO J*, 14 (22): 5542-5549.

van Koppen, C. J. & Nathanson, N. M. (1990) Site-directed mutagenesis of the m2 muscarinic acetylcholine receptor. Analysis of the role of N-glycosylation in receptor expression and function. *J Biol Chem*, 265 (34): 20887-20892.

van Rossum, D., Hanisch, U. K. & Quirion, R. (1997) Neuroanatomical localization, pharmacological characterization and functions of CGRP, related peptides and their receptors. *Neurosci Biobehav Rev*, 21 (5): 649-678.

Venkatakrishnan, A. J., Deupi, X., Lebon, G., Tate, C. G., Schertler, G. F. & Babu, M. M. (2013) Molecular signatures of G-protein-coupled receptors. *Nature*, 494 (7436): 185-194.

Vohra, S., Taddese, B., Conner, A. C., Poyner, D. R., Hay, D. L., Barwell, J., Reeves, P. J., Upton, G. J. & Reynolds, C. A. (2013) Similarity between class A and class B G-protein-coupled receptors exemplified through calcitonin gene-related peptide receptor modelling and mutagenesis studies. *J R Soc Interface*, 10 (79): 20120846.

Wade, S. M., Scribner, M. K., Dalman, H. M., Taylor, J. M. & Neubig, R. R. (1996) Structural requirements for G(o) activation by receptor-derived peptides: activation and modulation domains of the alpha 2-adrenergic receptor i3c region. *Mol Pharmacol*, 50 (2): 351-358.

Walker, C. S., Conner, A. C., Poyner, D. R. & Hay, D. L. (2010) Regulation of signal transduction by calcitonin gene-related peptide receptors. *Trends Pharmacol Sci*, 31 (10): 476-483.

Walker, P., Munoz, M., Martinez, R. & Peitsch, M. C. (1994) Acidic residues in extracellular loops of the human Y1 neuropeptide Y receptor are essential for ligand binding. *J Biol Chem*, 269 (4): 2863-2869.

Wang, Y., Zhou, Y., Szabo, K., Haft, C. R. & Trejo, J. (2002) Down-regulation of protease-activated receptor-1 is regulated by sorting nexin 1. *Mol Biol Cell*, 13 (6): 1965-1976.

Warne, T., Chirnside, J. & Schertler, G. F. (2003) Expression and purification of truncated, non-glycosylated turkey beta-adrenergic receptors for crystallization. *Biochim Biophys Acta*, 1610 (1): 133-140.

Warne, T., Serrano-Vega, M., Baker, J., Moukhametzianov, R., Edwards, P., Henderson, R., Leslie, A., Tate, C. & Schertler, G. (2008) Structure of a beta1-adrenergic G-protein-coupled receptor. *Nature*, 454 (7203): 486-491.

Warner, D. R. & Weinstein, L. S. (1999) A mutation in the heterotrimeric stimulatory guanine nucleotide binding protein alpha-subunit with impaired receptor-mediated activation because of elevated GTPase activity. *Proc Natl Acad Sci U S A*, 96 (8): 4268-4272.

Warner, D. R., Weng, G., Yu, S., Matalon, R. & Weinstein, L. S. (1998) A novel mutation in the switch 3 region of Gsalpha in a patient with Albright hereditary osteodystrophy impairs GDP binding and receptor activation. *J Biol Chem*, 273 (37): 23976-23983.

Warshawsky, H., Goltzman, D., Rouleau, M. F. & Bergeron, J. J. (1980) Direct in vivo demonstration by radioautography of specific binding sites for calcitonin in skeletal and renal tissues of the rat. *J Cell Biol*, 85 (3): 682-694.

Watkins, H. A., Au, M. & Hay, D. L. (2012) The structure of secretin family GPCR peptide ligands: implications for receptor pharmacology and drug development. *Drug Discov Today*, 17 (17-18): 1006-1014.

Wei, H., Ahn, S., Shenoy, S. K., Karnik, S. S., Hunyady, L., Luttrell, L. M. & Lefkowitz, R. J. (2003) Independent beta-arrestin 2 and G protein-mediated pathways for angiotensin II activation of extracellular signal-regulated kinases 1 and 2. *Proc Natl Acad Sci U S A*, 100 (19): 10782-10787.

Weller, M., Virmaux, N. & Mandel, P. (1975) Light-stimulated phosphorylation of rhodopsin in the retina: the presence of a protein kinase that is specific for photobleached rhodopsin. *Proc Natl Acad Sci U S A*, 72 (1): 381-385.

Westermark, P., Andersson, A. & Westermark, G. T. (2011) Islet amyloid polypeptide, islet amyloid, and diabetes mellitus. *Physiol Rev*, 91 (3): 795-826.

Wheatley, M. & Hawtin, S. R. (1999) Glycosylation of G-protein-coupled receptors for hormones central to normal reproductive functioning: its occurrence and role. *Hum Reprod Update*, 5 (4): 356-364.

Wheatley, M., Wootten, D., Conner, M. T., Simms, J., Kendrick, R., Logan, R. T., Poyner, D. R. & Barwell, J. (2012) Lifting the lid on GPCRs: the role of extracellular loops. *Br J Pharmacol*, 165 (6): 1688-1703.

Whistler, J. L., Enquist, J., Marley, A., Fong, J., Gladher, F., Tsuruda, P., Murray, S. R. & Von Zastrow, M. (2002) Modulation of postendocytic sorting of G protein-coupled receptors. *Science*, 297 (5581): 615-620.

White, J. F., Grodnitzky, J., Louis, J. M., Trinh, L. B., Shiloach, J., Gutierrez, J., Northup, J. K. & Grisshammer, R. (2007) Dimerization of the class A G protein-coupled neurotensin receptor NTS1 alters G protein interaction. *Proc Natl Acad Sci U S A*, 104 (29): 12199-12204.

White, J. H., Wise, A., Main, M. J., Green, A., Fraser, N. J., Disney, G. H., Barnes, A. A., Emson, P., Foord, S. M. & Marshall, F. H. (1998) Heterodimerization is required for the formation of a functional GABA(B) receptor. *Nature*, 396 (6712): 679-682.

Whorton, M. R., Bokoch, M. P., Rasmussen, S. G., Huang, B., Zare, R. N., Kobilka, B. & Sunahara, R. K. (2007) A monomeric G protein-coupled receptor isolated in a high-density lipoprotein particle efficiently activates its G protein. *Proc Natl Acad Sci U S A*, 104 (18): 7682-7687.

Widmann, C., Dolci, W. & Thorens, B. (1996) Heterologous desensitization of the glucagon-like peptide-1 receptor by phorbol esters requires phosphorylation of the cytoplasmic tail at four different sites. *J Biol Chem*, 271 (33): 19957-19963.

Wilden, U., Hall, S. W. & Kühn, H. (1986) Phosphodiesterase activation by photoexcited rhodopsin is quenched when rhodopsin is phosphorylated and binds the intrinsic 48-kDa protein of rod outer segments. *Proc Natl Acad Sci U S A*, 83 (5): 1174-1178.

Williams, L. T. & Lefkowitz, R. J. (1977) Slowly reversible binding of catecholamine to a nucleotide-sensitive state of the beta-adrenergic receptor. *J Biol Chem*, 252 (20): 7207-7213.

Woolley, M. J. & Conner, A. C. (2013) Comparing the molecular pharmacology of CGRP and adrenomedullin. *Curr Protein Pept Sci*, 14 (5): 358-374.

Woolley, M. J., Watkins, H. A., Taddese, B., Karakullukcu, Z. G., Barwell, J., Smith, K. J., Hay, D. L., Poyner, D. R., Reynolds, C. A. & Conner, A. C. (2013) The role of ECL2 in CGRP receptor activation: a combined modelling and experimental approach. *J R Soc Interface*, 10 (88): 20130589.

Wootten, D., Lindmark, H., Kadmiel, M., Willcockson, H., Caron, K. M., Barwell, J., Drmota, T. & Poyner, D. R. (2012) Receptor Activity Modifying Proteins (RAMPs) Interact with the VPAC(2) Receptor and CRF(1) Receptors and modulate their function. *Br J Pharmacol*,

Wootten, D., Simms, J., Miller, L. J., Christopoulos, A. & Sexton, P. M. (2013) Polar transmembrane interactions drive formation of ligand-specific and signal pathway-biased family B G protein-coupled receptor conformations. *Proc Natl Acad Sci U S A*, 110 (13): 5211-5216.

Wu, B., Chien, E. Y., Mol, C. D., Fenalti, G., Liu, W., Katritch, V., Abagyan, R., Brooun, A., Wells, P., Bi, F. C., Hamel, D. J., Kuhn, P., Handel, T. M., Cherezov, V. & Stevens, R. C. (2010) Structures of the CXCR4 chemokine GPCR with small-molecule and cyclic peptide antagonists. *Science*, 330 (6007): 1066-1071.

Wu, H., Wacker, D., Mileni, M., Katritch, V., Han, G. W., Vardy, E., Liu, W., Thompson, A. A., Huang, X. P., Carroll, F. I., Mascarella, S. W., Westkaemper, R. B., Mosier, P. D., Roth, B. L., Cherezov, V. & Stevens, R. C. (2012) Structure of the human κ-opioid receptor in complex with JDTic. *Nature*, 485 (7398): 327-332.

Xu, F., Wu, H., Katritch, V., Han, G. W., Jacobson, K. A., Gao, Z. G., Cherezov, V. & Stevens, R. C. (2011) Structure of an agonist-bound human A2A adenosine receptor. *Science*, 332 (6027): 322-327.

8 Appendix

JOURNAL OF THE ROYAL SOCIETY Interface

rsif.royalsocietypublishing.org

Research

Cite this article: Woolley MJ, Watkins HA, Taddese B, Karakullukcu ZG, Barwell J, Smith KJ, Hay DL, Poyner DR, Reynolds CA, Conner AC. 2013 The role of ECL2 in CGRP receptor activation: a combined modelling and experimental approach. J R Soc Interface 10: 20130589.
http://dx.doi.org/10.1098/rsif.2013.0589

Received: 3 July 2013
Accepted: 29 August 2013

Subject Areas:
computational biology, biochemistry

Keywords:
calcitonin gene-related peptide, class B G-protein-coupled receptor, loop modelling, site-directed mutagenesis, calcitonin receptor-like receptor

Authors for correspondence:
David R. Poyner
e-mail: d.r.poyner@aston.ac.uk
Christopher A. Reynolds
e-mail: reync@essex.ac.uk
Alex C. Conner
e-mail: a.c.conner@bham.ac.uk

Electronic supplementary material is available at http://dx.doi.org/10.1098/rsif.2013.0589 or via http://rsif.royalsocietypublishing.org.

Royal Society Publishing
Informing the science of the future

The role of ECL2 in CGRP receptor activation: a combined modelling and experimental approach

Michael. J. Woolley[1], Harriet A. Watkins[2], Bruck Taddese[3], Z. Gamze Karakullukcu[3], James Barwell[4], Kevin J. Smith[3], Debbie L. Hay[2], David R. Poyner[4], Christopher A. Reynolds[3] and Alex C. Conner[1]

[1]Warwick Medical School, University of Warwick, Coventry CV4 7AL, UK
[2]School of Biological Sciences, University of Auckland, 3 Symonds Street, Private Bag 92 019, New Zealand
[3]School of Biological Sciences, University of Essex, Wivenhoe Park, Colchester CO4 3SQ, UK
[4]School of Life and Health Sciences, Aston University, Aston Triangle, Birmingham B4 7ET, UK

The calcitonin gene-related peptide (CGRP) receptor is a complex of a calcitonin receptor-like receptor (CLR), which is a family B G-protein-coupled receptor (GPCR) and receptor activity modifying protein 1. The role of the second extracellular loop (ECL2) of CLR in binding CGRP and coupling to Gs was investigated using a combination of mutagenesis and modelling. An alanine scan of residues 271–294 of CLR showed that the ability of CGRP to produce cAMP was impaired by point mutations at 13 residues; most of these also impaired the response to adrenomedullin (AM). These data were used to select probable ECL2-modelled conformations that are involved in agonist binding, allowing the identification of the likely contacts between the peptide and receptor. The implications of the most likely structures for receptor activation are discussed.

1. Introduction

The extracellular loops of G protein-coupled receptors (GPCRs) are important for receptor function. They contribute to protein folding, provide structure to the extracellular region and mediate movement of the transmembrane (TM) helices on activation. The second extracellular loop (ECL2) is of significance for ligand binding and receptor activation [1–3]. In family B (or secretin-like) GPCRs, it is the most conserved and often the longest of all the ECLs, and so is in a good position to interact with the endogenous peptide agonists for these receptors and is in a prominent central position to mediate conformational changes [1]. The peptide ligands typically contain 30–50 amino acids. The family B receptors are characterized by a large N-terminal domain (approx. 100 amino acids), which interacts with the C-termini of their cognate peptide ligands [4]. The N-termini of these peptides interact with the ECLs and the TM region of the receptors resulting in activation [4,5]. ECL2 has been implicated in agonist binding at the GLP-1, secretin and CRF1 receptors [6–10]. For the GLP-1 receptor, ECL2 plays an important role in directing coupling towards stimulation of ERK1/2 activation versus Gs and activation of adenylate cyclase [7]. However, the molecular basis for this observation remains obscure.

Several distinct conformations have been recognized for ECL2 in family A GPCRs, ranging from the 'lid' seen in rhodopsin, which encloses the bound retinal ligand, to the extended sheet seen for most of the peptide GPCRs [11–13]. Movement of ECL2 seems to be important in the activation of family A GPCRs; this is linked to agonist-induced changes in TM5 and helps propagate these changes to other parts of the GPCR [11,14].

There is currently no crystal structure showing how a peptide agonist binds to the ECLs or TM domain of a family B GPCR. A number of models have been proposed based on cross-linking and mutagenesis data [8,15,16] but it has proved extremely

difficult to accurately predict the ECL conformations by this approach or by simulation [17]. Given the variety in family B peptide sequences [5,17], it seems likely that there is no single mode of peptide binding to the ECLs of family B GPCRs [18].

We have previously used a combination of mutagenesis and computation to produce a model indicating how the TM domain of the calcitonin receptor-like receptor (CLR) can interact with Gs [19]. CLR is the GPCR component of the calcitonin gene-related peptide (CGRP) receptor. CGRP is part of a peptide family that also includes adrenomedullin (AM), calcitonin and amylin and is involved in heart disease and migraine [20]. CLR interacts with a single TM protein, receptor activity-modifying protein 1 (RAMP1), in order to bind CGRP and also AM [21], though AM interacts with CLR more strongly in the presence of RAMP2. Using an independent modelling approach, Wootten *et al*. [22] have produced a broadly similar model for the GLP-1 receptor, which indicates how agonists can activate the receptor by interacting with different TM residues. Using both mutagenesis and computation is a powerful strategy for studying the activation of GPCRs [12], especially given that structural techniques for instance crystallography give static pictures of what is fundamentally a dynamic process.

In previous work, we have examined the role of the first and third ECLs (ECL1/3) of the CGRP receptor. However, only a small number of residues within ECLs 1 and 3 were implicated in CGRP binding [18]. Consequently, we have now addressed the role of ECL2 in this receptor. In an extension of the strategy used to examine the TM residues of CLR, we have experimentally identified CLR residues that reside within the last turn of TM4, ECL2 and the first turn of the turn of TM5 and that are key for CGRP and AM interactions with the CGRP receptor. We have then used all of our data for each ECL and the TM domain, in combination with heuristic loop modelling, molecular dynamics, docking and sequence analysis to model the interaction between the N-terminus of the CGRP peptide and CLR, based on a model of the Gs-coupled state of the CGRP receptor.

2. Material and methods

2.1. Preparation of mutants, transfection, receptor expression and radioligand binding

The preparation of mutants and molecular biology was as described earlier [23]. An HA-tagged CLR construct was used to allow measurement of cell surface receptor expression by ELISA [20,23]. Mutants were transfected into Cos 7 cells using PEI [20,23]. Radioligand binding was carried out on cell membranes using [^{125}I] iodohistidyl-human alpha CGRP (Perkin Elmer) [20,23].

2.2. Measurement of cAMP

For the investigation of CGRP-mediated activation of the receptor, cAMP was measured using a FRET-based PerkinElmer LANCE cAMP 384 kit according to manufacturer's instructions. Briefly, transfected cells were removed from the plate with trypsin EDTA, washed with phosphate-buffered saline and resuspended in assay stimulation buffer (SB; phosphate-buffered saline + 0.1% (w/v) bovine serum albumin + 0.5 mM isobutylmethylxanthine). Cells were counted with a haemocytometer and the appropriate cell number resuspended in SB + 1/100 AlexaFluor 647-anti cAMP antibody at an assay concentration of 2000 cells/10 µl. A total of 2000 cells/well were loaded onto a 96-well white Optiplate (PerkinElmer) and were concentration-dependently stimulated in triplicate with a logarithmic increase of CGRP diluted in SB from 10^{-6} to 10^{-12} M with SB as a basal point. The plate was incubated in the absence of light for 30 min at room temperature before 20 µl/well of detection mix was added. The plate was incubated in the absence of light for a further 60 min. FRET was recorded by excitation at 320 nm and emission at 665 nm. The experimental pEC_{50} values for wild-type (WT) receptor in the electronic supplementary materials, table S1 show some variation, reflecting differences in coupling efficiencies between cells as the data were collected in excess of a year. Such drift has been observed previously with CGRP receptors [24,25]. To control for this, a paired design-test was used so that each mutant was compared in the same experiment against a corresponding WT control. For the investigation of AM-mediated stimulation of the CGRP receptor, cAMP was measured with alphascreen, as described previously [26]. Data were normalized against the maximum fitted response for CGRP or AM; basal cAMP was taken as the fitted minimum.

2.3. Data analysis

Curve fitting was done with GraphPad Prism 5 or 6 (GraphPad Software Inc., San Diego, CA, USA). Both this and statistical analysis were as described previously [20].

2.4. CLR models

The starting point for the models indicating the interaction between CGRP and ECL2 was a recent model of the active state [19]. The most appropriate X-ray crystal structure model for a fully active GPCR is that of the β_2-adrenergic receptor (β_2-AR) coupled to Gs [27], which is similar to the β_2-AR nanobody stabilized [28] and the rhodopsin active structures stabilized by a C-terminal peptide from transducin [29,30]; these active structures are characterized by the outward tilt of the intracellular end of TM6 that is necessary for G protein binding. In the absence of G protein or G protein-derived peptides, X-ray crystal structures of agonists bound to GPCRs stabilize substates that are not too different to the inactive form [31], i.e. they lack the outward tilt of TM6; in such agonist-bound structures, the conformation of $Y^{5.58}$ is taken to be indicative of the state because in the inactive form, it usually interacts with $L^{1.63}$ and $L^{8.50}$, whereas in the active substate, it stabilizes the active conformation of $R^{3.50}$. Our active structures are stabilized by the Gs C-terminal peptide (R373-L394), and hence included the outward tilt of TM6 [27]. Nevertheless, the conformation of $Y^{5.58}$ (and the tilt of TM6) was monitored to check that active state character was maintained as fully as possible and that the simulations could be terminated should the active structure begin to acquire inactive character. The underlying alignment was based on a novel approach to the class A–class B alignment, aided by a GCR1/class E alignment that was used as a bridge between the class A and class B sequences. This has been repeated using improved methodology but the alignment remains unaltered [32]. The status of GCR1, GCR2 and other putative plant GPCRs has been questioned [33–35], but GCR1 has all the features expected for a GPCR fold [32], while GCR2 was predicted [36] and later shown to be a lanbiotic cyclase [37]. The simulations that underlie the CLR modelling [19] were extended to 100 ns (see the electronic supplementary material).

To model the peptide binding, disulfide-bonded cyclic $CGRP_{1-7}$ was constructed in Maestro and docked to the active CLR model (after 80 ns, i.e. just before the first signs of the onset of inactive character; [19]) using Glide SP [38,39], as described in the electronic supplementary material. The best-scoring pose was verified by sequence analysis, as described below. The CGRP extension (up to residue 32) was modelled onto $CGRP_{1-7}$ using the NMR solution structure of salmon calcitonin (PDB code 2glh) [40], using the alignment of Watkins *et al*. [5].

In the molecular dynamics simulations, the active structure begins to acquire some inactive character after 80 ns (i.e. $F^{7.53}$ switched towards the inactive conformation; see the electronic

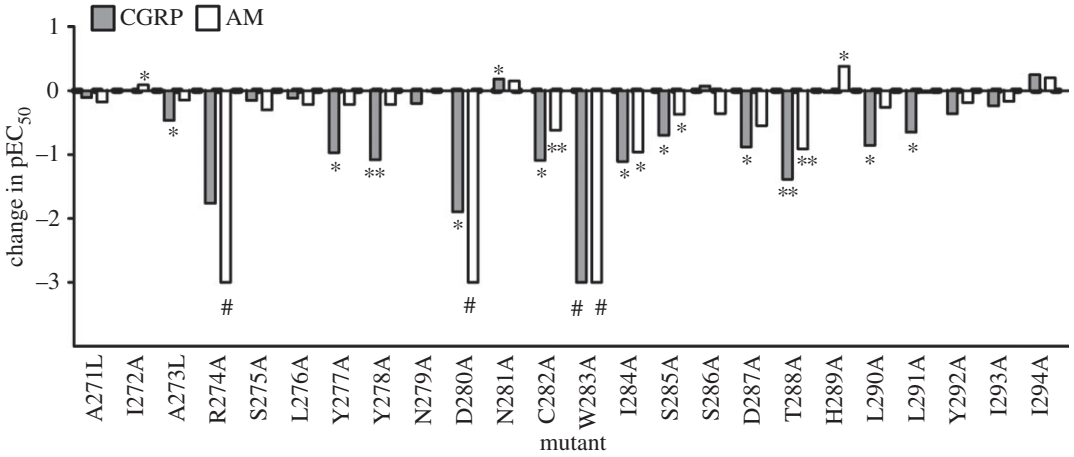

Figure 1. Effect of mutations on the pEC_{50} for AM (white bars) and CGRP (grey bars) at cAMP production. The difference in mean pEC_{50} between the mutant and WT receptor is shown, hence a negative value shows a decrease in potency. Where there was no detectable stimulation of the mutant by peptide (#), an arbitrary value of −3 has been shown in the figure. Data are shown in the electronic supplementary material, table S1. *$p < 0.05$, **$p < 0.01$, pEC_{50} of mutant significantly different from that of WT by paired Student's *t*-test or repeated measures ANOVA followed by Dunnett's test as appropriate.

supplementary material, figure S1). This is well before it would be possible to fully sample the loop conformations, despite high principle components for ECL2 residues; see the electronic supplementary material, figure S1D. Thus, given that the MODELLER scoring functions are approximate, we have taken a heuristic approach to determining the ECL2 conformation. We have therefore generated and refined 100 independent loop conformations; suitable conformations were selected if key loop residues identified by the mutagenesis interacted with CGRP or AM to within a cut-off of 5.5 Å. There are many assumptions inherent in this approach, as discussed below in §3.2.5; this is apparent because it was impossible to generate conformations where each significant ECL2 residue interacted with CGRP. Thus, multiple conformations of ECL1 (residues 202–212), ECL2 (residues 274–293) and ECL3 (residues 353–363) were simultaneously generated in the presence of $CGRP_{1-32}$ using MODELLER [41–43]. Each conformation is characterized by its DOPE score; a lower score corresponds to a more likely conformation. AM binding to CLR was similarly modelled by simultaneously mutating CGRP to AM and generating the loop conformations within MODELLER.

2.5. Sequence analysis

The sequences of CGRP and amylin (which binds to the calcitonin receptor (CTR)) from several species were aligned [5,44]. The sequences of amylin and CGRP and the sequences of CTR and CLR were analysed in parallel to identify mutations that are correlated between the CTR–amylin and CLR–CGRP systems, with a view to identifying contact points.

2.6. Residue numbering

For amino acids within the proposed ECLs of CLR, only the residue numbers are shown. For residues that are within the TM helices of CLR, a superscript denotes their position using an adaption of the Ballasteros–Weinstein numbering proposed elsewhere [19]. The peptide residue numbers are given as superscripts.

3. Results and discussion

3.1. Experimental analysis of the CGRP receptor

In this section, the results of an alanine scan of the CGRP receptor will be presented. The implications of these data will be discussed alongside the modelling in §3.2.

3.1.1. Effects of alanine substitution on CGRP-mediated cAMP production

Twenty-four individual residues of CLR ECL2 from A271 to I294 were mutated to alanine (alanine residues were mutated to leucine) and their ability to respond to CGRP and stimulate cAMP production was investigated when co-expressed with human RAMP1. These residues were selected as they are most likely to incorporate the whole of ECL2 and approximately one turn of helices 4 and 5 immediately adjacent to the loop, based on our previous analysis [19]. Figures 1 and 2 and the electronic supplementary materials, table S1 and figure S2 show that the pEC_{50} values of 14 of the 24 mutants were significantly different to WT, indicating that ECL2 is particularly important for CGRP receptor function. Seven mutants resulted in significant cAMP reduction of more than 10-fold. These are R274A, Y278A, D280A, C282A, W283A, I284A and T288A. Of the remaining seven mutations, N281A showed a small increase in potency and six mutants had small but significant reductions in pEC_{50}. Y292A and I294A showed significant but small increases in maximal cAMP response (E_{max}) (see the electronic supplementary material, table S2).

3.1.2. Cell surface expression of receptors and CGRP binding

Owing to the likelihood of attenuated binding of CGRP, radioligand binding could not be reliably used to provide an estimate of receptor expression for these constructs. Accordingly, an ELISA to measure receptors at the cell surface was used (see the electronic supplementary materials, table S3). All of the mutants were expressed at the cell surface to within approximately 60% of WT levels. Reductions to this level of expression has been previously shown to have little effect on the potency of CGRP-mediated cAMP signalling for this or CTR expressed in Cos 7 cells [45,46] and in this study, there was only a very low correlation between expression and pEC_{50} ($r^2 = 0.23$). Mutated receptors that had large impairments of cAMP production were examined for their ability to bind CGRP using a radioligand-binding assay (see the electronic supplementary materials, table S4). All of the mutants examined, except Y277A had reduced affinity for the radioligand.

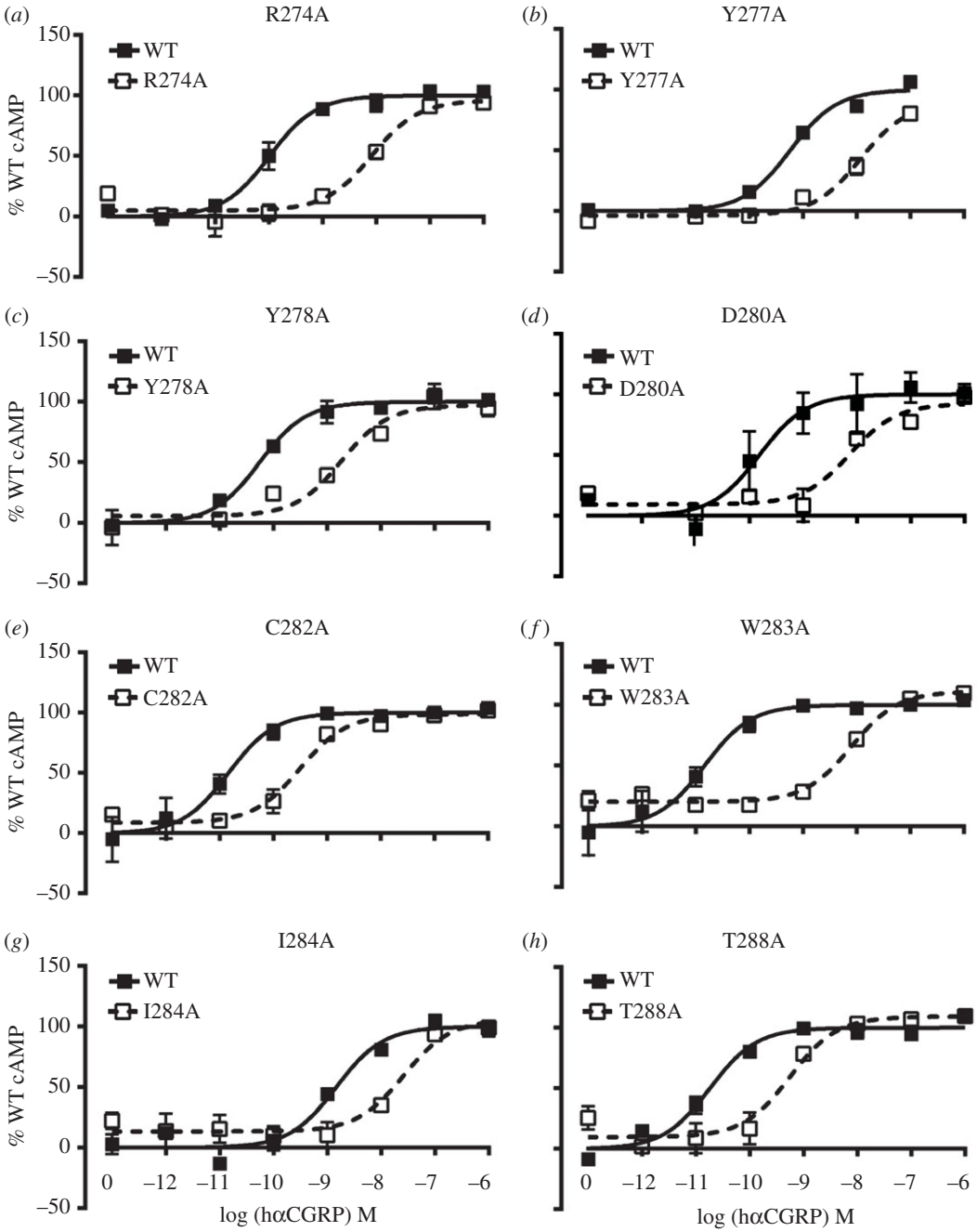

Figure 2. (*a–h*) Concentration–response curves of mutants showing changes in pEC_{50} in response to CGRP. Representative curves are shown from experiments repeated at least three times. The curves are normalized to the fitted E_{max} for CGRP on the WT receptor, which is defined as 100%.

3.1.3. Effects of alanine substitution on AM-mediated cAMP production

The CGRP receptor also acts as a functional AM receptor with an affinity of approximately 10-folds less than that for CGRP [47]. To explore the effects of the above mutants further, their ability to respond to AM through cAMP production was subsequently investigated. The majority of the effects were in line with those seen with CGRP (figure 1 and the electronic supplementary material, table S2), the most notable differences being the lack of effects of AM at Y277 and Y278 and for some mutants, it was impossible to measure any activation of the receptor (figure 3). In the case of R274A, W283A and D280A, the response was so low that an E_{max} could not be reliably determined. There was especially good agreement between the two agonists for the central area of functional importance ranging from D280 to T288. As with CGRP, many of these alanine substitutions reduced AM potency. The effect of mutations at the N- and C-termini of ECL2 was more variable between the two peptides. At the N-terminus, the CGRP-affecting mutants Y277A or Y278A did not show AM-mediated effects on pEC_{50}. However, there were approximately 25% reductions in the maximal cAMP response. At the C-terminus of ECL2, the two leucine mutants (L290A and L291A), which showed a reduction in potency with CGRP, were not significantly affected when stimulated with AM.

3.1.4. Basal activity

In the investigation of CGRP (with Cos 7 cells from a UK source and measuring cAMP with a LANCE assay), N281A and I294A showed a significant increase in basal cAMP signalling (i.e. constitutive ligand-independent signalling activity; see the electronic supplementary material, table S2). These values increased by $9.9 \pm 0.9\%$ and $21.8 \pm 2.9\%$ above WT, respectively. When the cells were investigated

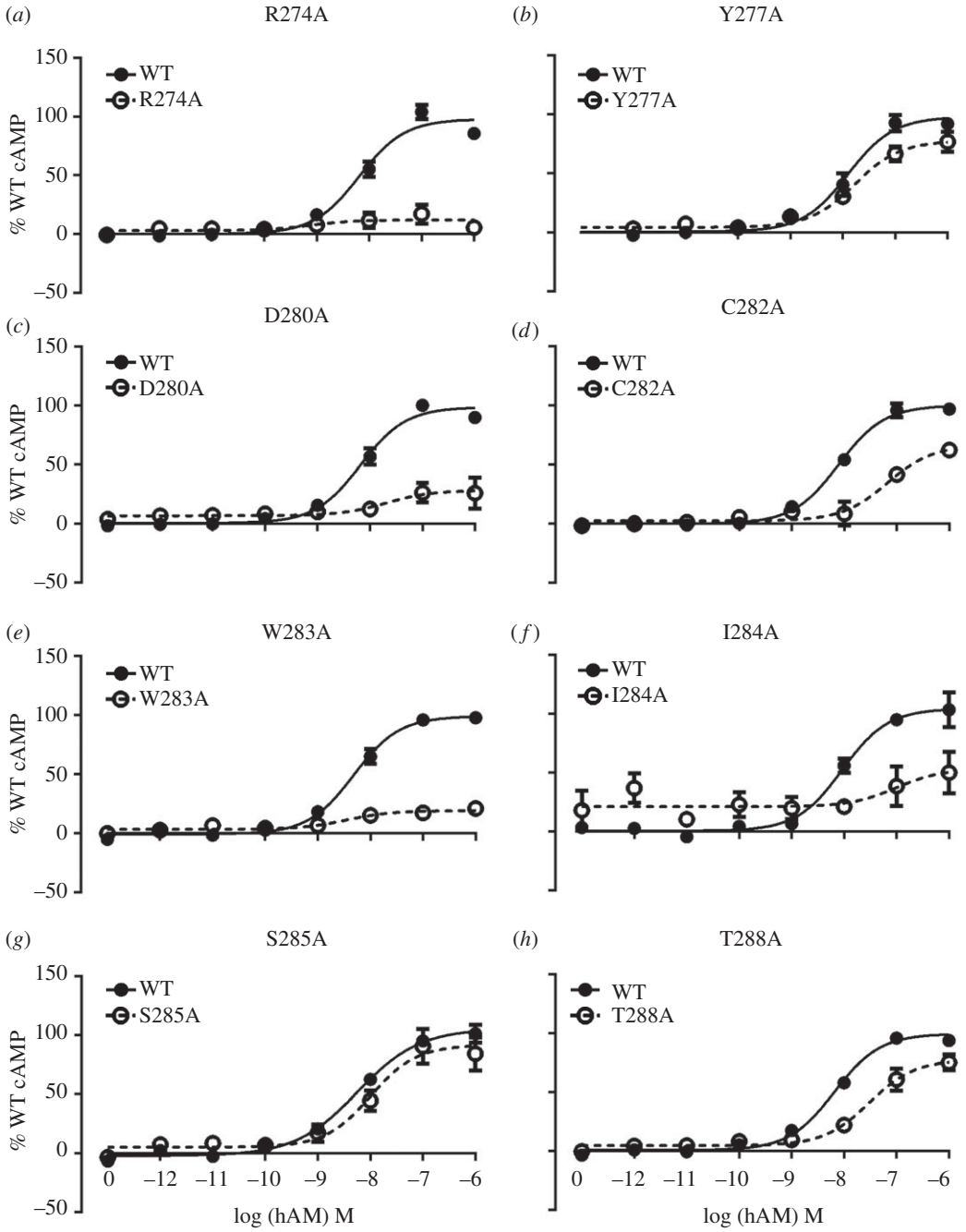

Figure 3. (*a–h*) Concentration–response curves of mutants showing changes in cAMP in response to AM. Data are mean ± s.e.m. of combined normalized data from at least three independent experiments. The curves are normalized to the fitted E_{max} for AM on the WT receptor, which is defined as 100%.

for AM responsiveness (using Cos 7 cells from a New Zealand source and Alphascreen), small but statistically significant elevations were noted for A273L, Y277A and I284A but not N281A and I294A. Thus, the increase in basal cAMP depended on experimental conditions and was always small. In the course of analysing over 200 mutants of CLR [19,20,48], we have observed very few that showed elevated activity, possibly indicating that there are multiple locks in place to keep the receptor in an inactive form; it is possible that the RAMPs might contribute to this.

3.1.5. The importance of the ECL2–TM3 disulfide linkage

As C282 is predicted to form a disulfide bond with $C212^{3.25}$ [19], further mutagenesis was used to explore this, using CGRP as the agonist. The mutant C212A impaired cAMP production in much the same way as C282A (pEC_{50} values: WT 9.62 ± 0.76, C212A 8.10 ± 0.43, $n = 3$, $p < 0.05$, Student's *t*-test); however, the double mutant C212AC282A showed a WT response (pEC_{50} values: WT 9.49 ± 0.11 $n = 3$, C212AC282A 9.41 ± 0.09, $n = 3$), thus implying that the disulfide bond itself is not crucial for CGRP binding or signalling.

3.1.6. The importance of the ECL2/TM5 junction

As noted above, L290A and L291A both showed small but significant reductions in CGRP potency. As movements at the top of TM5 have been implicated in the early stages of activation of the β_2-AR and rhodopsin [11], the role of residues in this region was probed by further mutagenesis. The individual reduction in EC_{50} values for L290A (approx. eightfold) and L291A (approx. fourfold) was highly exacerbated by an L290AL291A double mutant that reduced the EC_{50} by approximately 500-fold compared with WT (WT

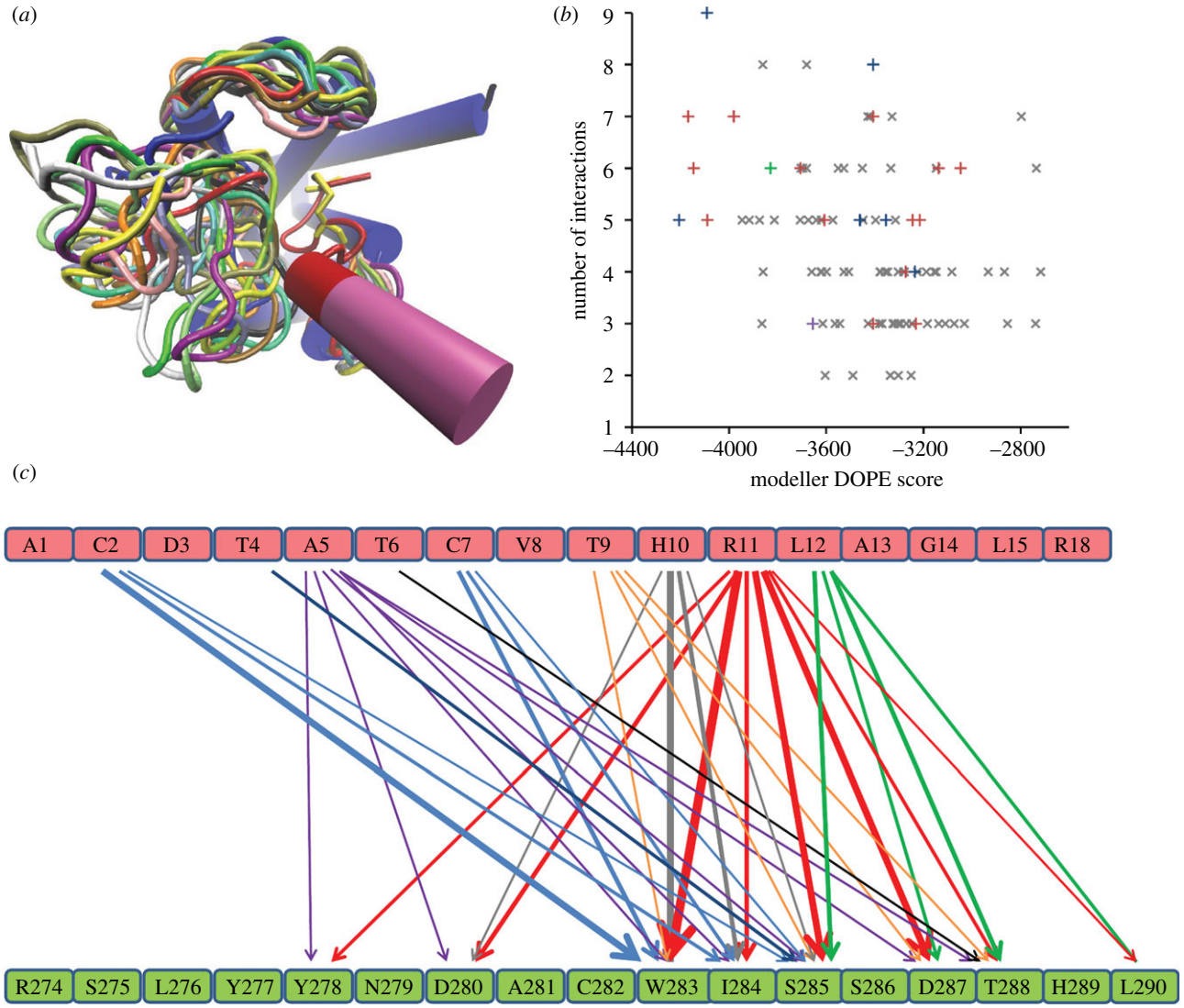

Figure 4. (*a*) A sample (20/100) of ECL1, ECL2 and ECL3 conformations generated by Modeller for the CLR : CGRP complex; each of the 20 loops is shown in a different colour. CLR is shown in blue, helices are shown as cylinders, $CGCR_{1-12}$ is shown in red and $CGRP_{12-18}$, which has relatively few interactions to ECL2, is shown in mauve. The C^2-C^7 disulfide bond is shown in yellow. (*b*) A plot of the number of residue–residue interactions between ECL2 and CGRP against the Modeller DOPE score for the CLR conformation; the lower the score, the more probable the loop conformation. Conformations that interact with T^6 via T288, D287, D280 or both D287 and T288 are shown as red, blue green and purple crosses (+), respectively. Conformation were these residues do not interact with T^6 are shown as grey crosses (×). (*c*) The interactions between ECL2 residues and CGRP residues as observed over the full set of 100 ECL2 conformations; the thickness of the line is broadly in line with the frequency of the interactions. For clarity interactions observed in fewer than 10 structures are omitted (but see the electronic supplementary materials, figure S3 for the full set of interactions). The coloured lines indicate interactions of specific CGRP residues: D^3 (brown), A^5 (purple), T^6 (black), T^9 (orange), H^{10} (grey), R^{11}, R^{18} (red) and L^{12}, L^{15} (green).

pEC_{50} 10.6 ± 0.11, L290AL291A pEC_{50} 7.93 ± 0.13, $n = 3$, $p < 0.01$, Student's *t*-test).

3.2. Modelling of ECL2 and interactions with CGRP and AM

3.2.1. Analysis of the Modeller-generated ECL2 conformations

The loop conformations spanned a large proportion of the space available to ECL2 (figure 4*a*). The analysis of the full set of interactions for all loop conformations is given in figure 4*b*,*c*. Although this analysis includes high-energy conformations, it is interesting as it highlights general interaction preferences of several amino acids in CGRP and ECL2. ECL2 forms an extended loop; this conformation is often seen as two antiparallel beta-strands in all peptide GPCRs for which structures are available, creating a large interface for peptide–receptor contacts [12]. Here, we re-interpret several previously reported experimental observations that were made in the absence of a modelled structure [44] and that are consistent with our models. D^3 of CGRP in our model is not in a constrained pocket, hence it makes few interactions with ECL2; indeed this position can accommodate a photoaffinity probe [44]. The fact that it can be readily replaced by arginine in the AM model provides further justification for our model. By contrast, A^5 of CGRP is sterically constrained and indeed makes a relatively large number of interactions (figure 4*c*), showing that it has many close neighbours. T^6 is discussed in more detail below; here, the preferred interactions are to T288. In several loop conformations, T^9 of CGRP interacts with polar residues such as D280, D287 and T288. There is some indirect evidence that H^{10} may also be part of this network that responds to negative charges [44]. L^{15} of CGRP can be replaced by a large benzoyl-phenylalanine moiety with

Table 1. Data used to select loop conformations.

CLR residues	CGRP effect	AM effect
A273	√	√
R274	√	√
Y277	√	
Y278	√	
D280	√	√
C282	√	
W283	√	√
I284	√	√
S285	√	√
D287	√	
T288	√	√
L290	√	
L291	√	

only small changes in affinity (it makes few interactions to ECL2); however, replacement of L^{12} of CGRP causes around a 10-fold decrease (it makes more interactions with ECL2) [44]. Replacement of R^{18} of CGRP by alanine has virtually no effect, and indeed it makes few interactions, but the double alanine mutant $R^{11}AR^{18}A$ shows 100-fold reduction in affinity [44]. Replacing either of these arginine residues with glutamate caused over a 10-fold reduction in affinity; but replacement with glutamine led to retention of high affinity binding [24,25,49], presumably because glutamine can still donate hydrogen bonds. Indeed, we see that both D280 and D287 are able to interact with R^{11}, but as D287 is less significant for AM (where K substitutes for R^{11}), it is more likely that D280 is the preferred partner to R^{11}, even though D287 makes more interactions. CGRP residues 1, 4, 8, 13 and beyond are predicted to make few, if any contacts with ECL2; this is consistent with the known structure activity relationships for CGRP where they seem to be of only minor importance [44]; this observation justifies the orientation of the helical extension to $CGRP_{1-7}$.

W283 and I284, which reside in the centre of ECL2, make the most interactions; these are either to the region around R^{11} or to the N-terminal region (see below).

Having analysed the pattern of interactions over all loop conformations, we see that this pattern is consistent with known experimental data on the CGRP peptide [44] and so we can now seek to identify preferred conformations and interactions from the mutagenesis data given in table 1, which indicates the most important residues for CGRP or AM binding.

The residue that is the equivalent to position 6 in CGRP is conserved as threonine in all members of the CGRP/CT/AM/amylin family of peptides and is essential for CGRP agonist activity [44,50]. Sequence analysis shows that the most likely candidates that are (i) conserved in CLR and CTR and (ii) able to donate or accept an H-bond are in ECL2 where D280, D287 and T288 are the best candidates. As D280 makes few interactions to T^6 (see above) and D287 is not significant in AM binding (figure 1) and is of moderate importance in CGRP activation, it would seem that T288 is the most promising candidate.

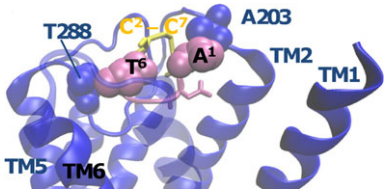

Figure 5. The highest scoring docked pose of $CGRP_{1-7}$ (mauve). Resides A^1 and T^6 reside close to Ala203 and Thr288, respectively (blue). The CGRP disulfide bond is shown in yellow. The loop conformation shown here for ECL2 was a high scoring (i.e. favoured) conformation. TM7 is shown as transparent.

Figure 5 shows that the best-scoring docked conformation of $CGRP_{1-7}$ satisfies the T^6 criteria (by interacting with D280/D287/T288) in the presence of a sample ECL2 conformation (figure 4), and that D^3 is not in a sterically crowded region (see also figure 4*c*). This indicates that the docked $CGRP_{1-7}$ has provided a suitable template for modelling the full CGRP peptide and hence modelling the conformations of ECL2. In the docked conformation, A^1 of CGRP is not only close to A203 of ECL1 of CGRP, but also able to accommodate N-terminal extensions. As discussed in the electronic supplementary material, this is consistent with mutagenesis and bioinformatic analysis of CGRP and AM binding.

3.2.2. Filtering the ECL2 conformations

The number of interactions made by key ECL2 residues (table 1) to CGRP for each of the 100 loop conformations are displayed in figure 4*b* (*y*-axis). The ideal loop conformation should make an interaction between T^6 of CGRP and D280, D287 or T288, have a large negative DOPE score, make a high number of key interactions and ideally have W283 in a vertical orientation (see below). The majority of conformations, denoted by a grey cross in figure 4*b*, do not make an appropriate interaction with T^6 and are discarded. Several conformations make 6–9 interactions, including those to T^6 via D280, D287 or T288. Because interactions to D280, D287 or T288 are observed in the top 15% of the most energetically preferred conformations and because the DOPE score is an empirical rather than a rigorously accurate score, it is not advisable to use energy (i.e. the DOPE score) as the sole criteria to identify the preferred binding mode, hence the importance of filtering the loop conformations using the mutagenesis data. Only one conformation (conformation 34, top left of figure 4*b*) records a direct interaction with $R274^{4.64}$, for either CGRP or AM, but this interaction is to R^{11} of CGRP and the distance is long; closer inspection shows that D280 bridges between $R274^{4.64}$ and R^{11} of CGRP. Several other conformations of $R274^{4.64}$ act in this way, and could help to orientate a D280-R^{11} interaction. Thus, a direct interaction between CGRP and $R274^{4.64}$ is probably an unrealistic selection criterion. $R274^{4.64}$ is highly conserved as arginine or lysine across the class B GPCRs; mutation in the GLP-1 and secretin receptors also impairs function [6,7,51]. It is possible that the positively charged head group may also interact with the phospholipid bilayer [52].

Based on the data in figure 4*b* (and similarly for AM interactions with the CGRP receptor which altered pEC_{50}), we selected six conformations for CGRP and seven for AM (see the electronic supplementary material, figure S4). Apart from one CLR/CGRP structure (conformation 34), these all have a similar conformation for ECL2. However, despite a similar

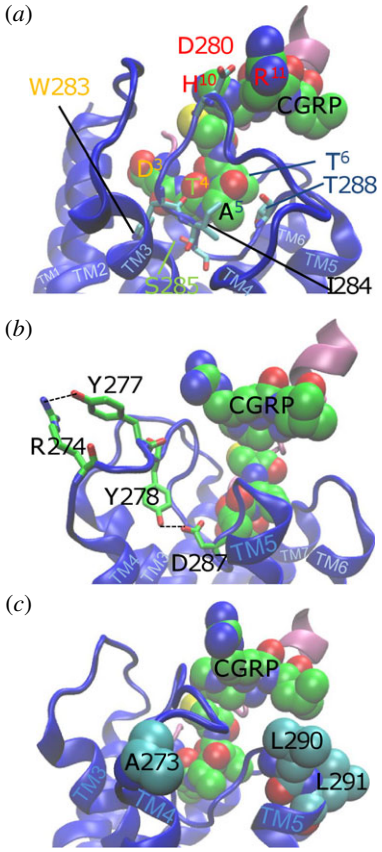

Figure 6. The interactions in the high scoring models for CGRP model. The interactions include D280 with H^{10} and R^{11}, T288 with T^6 (and A^5), S285 with A^5 and D287 with A^5 (shown in (*b*); the ECL2 hydrophobic residue interactions include W283 with D^3 and T^4 as well as residues on TM2 and TM3, and I284 with A^5. (*b*) Hydrogen bonds between significant ECL2 residues include R274 interacting with Y277 and D287 (close to A5) interacting with Y278, which seem to stabilize the ECL2 fold. (*c*) The remaining significant ECL2 residues, namely A273, L290 and L291; A273 and L291 do not interact with CGRP, L290 interacts with L^{12} in some ECL2 conformations while L291 points towards TM7, but could also affect the RAMP interaction; it is notable that most of these non-interacting residues plus Y277 and Y278 are not significant in the binding of AM and so it is likely that in CLR they are important in RAMP1-directed indirect effects on the binding. These structures have not been refined by molecular dynamics simulations for reasons discussed above and so the molecular information should not be overinterpreted.

ECL2 conformation, there are differences in the orientations of the W283 side chain, and only one high scoring CGRP and one high scoring AM conformation have W283 in a vertical orientation (a range of W283 interactions is shown in the electronic supplementary material, figures S4 and S5). The preferred CGRP structure (figure 6) satisfies 6/13 of the mutagenesis results given in table 1, whereas the AM model (see the electronic supplementary material, figure S6) satisfies 4/7.

3.2.3. The orientation of W283

The loop generation alone does not help to address the orientation of W283 as it interacts with CGRP in most conformations of ECL2. However, the docking raises an interesting question with regard to the site-directed mutagenesis data on TM2 and TM3, as shown in the electronic supplementary material, figure S7. A number of residues on TM2 and TM3 (namely $T191^{2.57}$, $L195^{2.61}$, $V198^{2.64}$, $A199^{2.65}$ and $H219^{3.32}$) show reduced cAMP production on mutation [19]. In our model, CGRP can interact with $L195^{2.61}$, $V198^{2.64}$, $A199^{2.65}$ but not $T191^{2.57}$ and $H219^{3.32}$ because they lie too deeply within the helical bundle. If CGRP were positioned to interact with these residues, it would then most likely not satisfy the interactions of A^1 and T^6. The alanine-substitution effect at $T191^{2.57}$ and $H219^{3.32}$ may instead result from interactions with W283 of ECL2 as suggested by analysis of inactive CLR simulations and selected high scoring loop conformations (figure 6; see the electronic supplementary material, figures S5–S7). The hydrophobic patch of $L195^{2.61}$, $V198^{2.64}$ and $A199^{2.65}$ on TM2 is important in CLR for CGRP-mediated activation of cAMP production [20] but while this region is more polar in some GPCRs, alternative hydrophobic regions reside nearby in other family B GPCRs where W283 could bind. Consequently, we prefer the vertical conformation of W283 as no other conformation satisfies the mutation data on $T191^{2.57}$ and $H219^{3.32}$.

3.2.4. AM binding

Our models can also explain the mutagenesis data for AM-mediated activation of the same receptor. It is proposed that AM sits in a very similar orientation to CGRP in the presumed binding pocket (see the supplementary material) but accesses a slightly different subset of ECL conformations. There are no direct interactions with $R274^{4.64}$, Y277 and Y278, but in the case of CGRP, the model suggests that there are also few, if any, direct interactions with these residues and instead they work primarily to stabilize productive conformations of ECL2. In the case of CGRP, we suggest that the consequence of this is to strengthen the interactions between the contact points between the peptide and ECL2 and so enhance potency. AM probably makes fewer contacts with ECL2; RAMP2 may be required to generate a full complement of interactions with this loop.

3.2.5. Implications for receptor activation

The binding of an agonist has to stabilize an active conformation of the receptor, increasing the activity of effector proteins. For the CGRP receptor, the best characterized interaction is with Gs, leading to the production of cAMP and, based on homology with the active crystal structures of rhodopsin and the β_2-AR and extensive mutagenesis, we produced a model of how this can take place [19]. Based on the current data, it is possible to make some broad points in regard to possible agonist activation mechanisms in CLR. A change in the C-terminal region of ECL2 could easily be propagated to TM5 and changes in this helix that are linked to movement of TM6 have been identified as one of the earliest steps leading to receptor activation in family A GPCRs [11,53]. It may be significant that T^6 of CGRP, important for agonist activity in both CGRP and AM [44,50], is in close proximity to the C-terminal region of ECL2 where D287 or preferably T288 are its most likely interaction partners. Further support for an important role of TM5 in receptor activation comes from the disrupting effect of the double mutant of L220/L221A. A shift in TM5 in CLR could subsequently allow movement of TM6. In family B GPCRs, there is a conserved proline residue in TM6, which is likely to produce a kink [23] analogous to the situation found in family A GPCRs, so displacement of TM6 will lead to the opening of a G protein-binding pocket between it and TM3 [11].

The conserved N-terminal part of ECL2 [1] links ECL2 not only with TM4 but is also likely to influence ECL1 and hence TM2 and 3. While ECL1 is of only minor importance in the binding of CGRP, residues just below it in TM2 and H219$^{3.32}$ of TM3 are of considerable significance for receptor activation [20]. Similar clusters are not obvious in the upper regions of the other TMs [19], although systematic mutagenesis is needed to test this. These residues at the tops of TM2 and 3 may be in a position to make contacts with residues at the base of ECL2, such as W283 and I284 as proposed in this study (see the electronic supplementary material, figure S7). Thus, CGRP has the potential to influence TM2 and 3 both directly and indirectly via ECL2. In family A GPCRs, TM3 is of particular importance for receptor activation partly owing to its angle of tilt across the TM bundle linking different parts of the bundle together. TM3 also constrains the C-terminal end of TM6 in at least some receptors via an ionic or polar lock [11,54]. In family B GPCRs, the equivalent of the ionic lock is probably a set of polar interactions involving residues at the C-terminal ends of TMs 2, 3 and 6 [19,22,55]; there are further interactions involving a polar network in the mid-regions of TMs 2, 3 and 7 [19,22,56]. Any interaction with TMs 2 and 3 is likely to play a key role in the activation of a family B GPCR.

The model developed for CGRP binding is therefore consistent with what is known about how CGRP activates its receptor, although it is speculative. It is also important to note that we have interpreted the effects of the mutations directly on the conformation of ECL2 itself. We cannot rule out that some of the effects may be on the TM bundle or extracellular domains of CLR or even of the RAMP. The data can be used to address these issues more fully once a crystal structure of the active CLR/RAMP1 complex becomes available.

4. Conclusion

We have evaluated the role of ECL2 in the binding of both CGRP and AM to the CGRP receptor and have interpreted the results by means of molecular modelling. The study indicates that ECL2 is particularly important for the interaction of CGRP with its receptor involving 13 ECL2 residues in the loop out of 24 residues studied. By contrast, only two residues in ECL1 and one in ECL3 influence the interaction of CGRP with its receptor [19,20]. Within ECL2, R274, W283, D280, D287 and T288 are of particular importance. We have suggested mechanisms where binding to this loop causes changes to the extracellular ends of TMs 2, 3 and 5, which in turn can be linked to movements of the cytoplasmic ends of TMs 3, 6 and 7, to allow G protein binding and activation.

While ECL2 appears to be involved in the binding of many peptide agonists to family B GPCRs, its precise role is probably receptor and ligand dependent. Models have been produced based on either mutagenesis or cross-linking data for the binding of secretin, GLP-1, VIP and PTH to their receptors [8,15,16,57,58]. While there are of course limitations to any modelling study, it is striking that there is no agreement as to the mode of binding. In the case of some models developed for GLP-1, secretin and VIP, their N-termini penetrate more deeply to interact with TM2, providing a more direct method of altering the conformation of both this helix and probably the adjacent TM3 during the process of receptor activation. While GLP-1 may not bind in the same way as CGRP (where the disulfide bond makes the N-terminus more bulky), a study of this receptor has provided the clearest evidence yet that ECL2 is an important determinant of signalling specificity [6,7]. Even in possession of crystal structures, the flexible nature of ECLs requires studies such as this to shed more light on how GPCRs respond to peptide agonists. Our approach used to model the interaction between either CGRP or AM and the receptor may be applicable to other GPCRs. The full set of structures is available from ftp.essex.ac.uk/pub/oyster/CLR_ECL2_2013/CLR_ECL2_structures.tar.gz (see also the electronic supplementary material); these structures compare favourably to the recent class B X-ray structures of glucagon and the corticotropin-releasing factor-1 receptors as described in the electronic supplementary material.

Funding statement. This work was supported by grants from the Wellcome Trust to D.R.P. (091496), the New Zealand Heart Foundation to H.A.W., the MRC to C.A.R. (G1001812) and a grant of computer time at Montpellier under the HPC Europa^2 programme (B.T.).

References

1. Wheatley M, Wootten D, Conner MT, Simms J, Kendrick R, Logan RT, Poyner DR, Barwell J. 2012 Lifting the lid on GPCRs: the role of extracellular loops. *Br. J. Pharmacol.* **165**, 1688–1703. (doi:10.1111/j.1476-5381.2011.01629.x)
2. Peeters MC, van Westen GJ, Li Q, Ijzerman AP. 2011 Importance of the extracellular loops in G protein-coupled receptors for ligand recognition and receptor activation. *Trends Pharmacol. Sci.* **32**, 35–42. (doi:10.1016/j.tips.2010.10.001)
3. Conner M, Hawtin SR, Simms J, Wootten D, Lawson Z, Conner AC, Parslow RA, Wheatley M. 2007 Systematic analysis of the entire second extracellular loop of the V_{1a} vasopressin receptor: key residues, conserved throughout a G-protein-coupled receptor family, identified. *J. Biol. Chem.* **282**, 17 405–17 412. (doi:10.1074/jbc.M702151200)
4. Hoare SR. 2005 Mechanisms of peptide and nonpeptide ligand binding to Class B G-protein-coupled receptors. *Drug Discov. Today* **10**, 417–427. (doi:10.1016/S1359-6446(05)03370-2)
5. Watkins HA, Au M, Hay DL. 2012 The structure of secretin family GPCR peptide ligands: implications for receptor pharmacology and drug development. *Drug Discov. Today* **17**, 1006–1014. (doi:10.1016/j.drudis.2012.05.005)
6. Koole C, Wootten D, Simms J, Savage EE, Miller LJ, Christopoulos A, Sexton PM. 2012 Second extracellular loop of human glucagon-like peptide-1 receptor (GLP-1R) differentially regulates orthosteric but not allosteric agonist binding and function. *J. Biol. Chem.* **287**, 3659–3673. (doi:10.1074/jbc.M111.309369)
7. Koole C, Wootten D, Simms J, Miller LJ, Christopoulos A, Sexton PM. 2012 Second extracellular loop of human glucagon-like peptide-1 receptor (GLP-1R) has a critical role in GLP-1 peptide binding and receptor activation. *J. Biol. Chem.* **287**, 3642–3658. (doi:10.1074/jbc.M111.309328)
8. Dong M *et al*. 2012 Mapping spatial approximations between the amino terminus of secretin and each of the extracellular loops of its receptor using cysteine trapping. *FASEB J.* **26**, 5092–5105. (doi:10.1096/fj.12-212399)
9. Assil-Kishawi I, Abou-Samra AB. 2002 Sauvagine cross-links to the second extracellular loop of the corticotropin-releasing factor type 1 receptor. *J. Biol. Chem.* **277**, 32 558–32 561. (doi:10.1074/jbc.M204964200)
10. Gkountelias K, Tselios T, Venihaki M, Deraos G, Lazaridis I, Rassouli O, Gravanis A, Liapakis G. 2009 Alanine scanning mutagenesis of the second

extracellular loop of type 1 corticotropin-releasing factor receptor revealed residues critical for peptide binding. *Mol. Pharmacol.* **75**, 793–800. (doi:10.1124/mol.108.052423)

11. Hulme EC. 2013 GPCR activation: a mutagenic spotlight on crystal structures. *Trends Pharmacol. Sci.* **34**, 67–84. (doi:10.1016/j.tips.2012.11.002)
12. Zhang C *et al*. 2012 High-resolution crystal structure of human protease-activated receptor 1. *Nature* **492**, 387–392. (doi:10.1038/nature11701)
13. Palczewski K *et al*. 2000 Crystal structure of rhodopsin: a G protein-coupled receptor. *Science* **289**, 739–745. (doi:10.1126/science.289.5480.739)
14. Ahuja S *et al*. 2009 Helix movement is coupled to displacement of the second extracellular loop in rhodopsin activation. *Nat. Struct. Mol. Biol.* **16**, 168–175. (doi:10.1038/nsmb.1549)
15. Coopman K, Wallis R, Robb G, Brown AJ, Wilkinson GF, Timms D, Willars GB. 2011 Residues within the transmembrane domain of the glucagon-like peptide-1 receptor involved in ligand binding and receptor activation: modelling the ligand-bound receptor. *Mol. Endocrinol.* **25**, 1804–1818. (doi:10.1210/me.2011-1160)
16. Monaghan P, Thomas BE, Woznica I, Wittelsberger A, Mierke DF, Rosenblatt M. 2008 Mapping peptide hormone–receptor interactions using a disulfide-trapping approach. *Biochemistry* **47**, 5889–5895. (doi:10.1021/bi800122f)
17. Goldfeld DA, Zhu K, Beuming T, Friesner RA. 2011 Successful prediction of the intra- and extracellular loops of four G-protein-coupled receptors. *Proc. Natl Acad. Sci. USA* **108**, 8275–8280. (doi:10.1073/pnas.1016951108)
18. Barwell J, Gingell JJ, Watkins HA, Archbold JK, Poyner DR, Hay DL. 2012 Calcitonin and calcitonin receptor-like receptors: common themes with family B GPCRs? *Br. J. Pharmacol.* **166**, 51–65. (doi:10.1111/j.1476-5381.2011.01525.x)
19. Vohra S, Taddese B, Conner AC, Poyner DR, Hay DL, Barwell J, Reeves PJ, Upton GJ, Reynolds CA. 2013 Similarity between class A and class B G-protein-coupled receptors exemplified through calcitonin gene-related peptide receptor modelling and mutagenesis studies. *J. R. Soc. Interface* **10**, 20120846. (doi:10.1098/rsif.2012.0846)
20. Barwell J, Conner A, Poyner DR. 2011 Extracellular loops 1 and 3 and their associated transmembrane regions of the calcitonin receptor-like receptor are needed for CGRP receptor function. *Biochim. Biophys. Acta* **1813**, 1906–1916. (doi:10.1016/j.bbamcr.2011.06.005)
21. McLatchie LM, Fraser NJ, Main MJ, Wise A, Brown J, Thompson N, Solari R, Lee MG, Foord SM. 1998 RAMPs regulate the transport and ligand specificity of the calcitonin-receptor-like receptor. *Nature* **393**, 333–339. (doi:10.1038/30666)
22. Wootten D, Simms J, Miller LJ, Christopoulos A, Sexton PM. 2013 Polar transmembrane interactions drive formation of ligand-specific and signal pathway-biased family B G protein-coupled receptor conformations. *Proc. Natl Acad. Sci. USA* **110**, 5211–5216. (doi:10.1073/pnas.1221585110)
23. Conner AC, Hay DL, Simms J, Howitt SG, Schindler M, Smith DM, Wheatley M, Poyner DR. 2005 A key role for transmembrane prolines in calcitonin receptor-like receptor agonist binding and signalling: implications for family B G-protein-coupled receptors. *Mol. Pharmacol.* **67**, 20–31. (doi:10.1124/mol.67.1.)
24. Poyner DR, Soomets U, Howitt SG, Langel U. 1998 Structural determinants for binding to CGRP receptors expressed by human SK-N-MC and Col 29 cells: studies with chimeric and other peptides. *Br. J. Pharmacol.* **124**, 1659–1666. (doi:10.1038/sj.bjp.0702032)
25. Howitt SG, Kilk K, Wang Y, Smith DM, Langel U, Poyner DR. 2003 The role of the 8–18 helix of CGRP8–37 in mediating high affinity binding to CGRP receptors; coulombic and steric interactions. *Br. J. Pharmacol.* **138**, 325–332. (doi:10.1038/sj.bjp.0705040)
26. Gingell JJ, Qi T, Bailey RJ, Hay DL. 2010 A key role for tryptophan 84 in receptor activity-modifying protein 1 in the amylin 1 receptor. *Peptides* **31**, 1400–1404. (doi:10.1016/j.peptides.2010.03.027)
27. Rasmussen SG *et al*. 2011 Crystal structure of the beta2 adrenergic receptor-Gs protein complex. *Nature* **477**, 549–555. (doi:10.1038/nature10361)
28. Rasmussen SG *et al*. 2011 Structure of a nanobody-stabilized active state of the beta(2) adrenoceptor. *Nature* **469**, 175–180. (doi:10.1038/nature09648)
29. Standfuss J, Edwards PC, D'Antona A, Fransen M, Xie G, Oprian DD, Schertler GF. 2011 The structural basis of agonist-induced activation in constitutively active rhodopsin. *Nature* **471**, 656–660. (doi:10.1038/nature09795)
30. Choe HW, Kim YJ, Park JH, Morizumi T, Pai EF, Krauss N, Hofmann KP, Scheerer P, Ernst OP. 2011 Crystal structure of metarhodopsin II. *Nature* **471**, 651–655. (doi:10.1038/nature09789)
31. Katritch V, Cherezov V, Stevens RC. 2013 Structure-function of the G protein-coupled receptor superfamily. *Annu. Rev. Pharmacol. Toxicol.* **53**, 531–556. (doi:10.1146/annurev-pharmtox-032112-135923)
32. Taddese B, Upton GJ, Bailey G, Reeves PJ, Reynolds CA. Submitted. Structure and functional motifs of GCR1, the only plant protein with a GPCR fold?
33. Urano D, Jones AM. 2013 'Round up the usual suspects': a comment on nonexistent plant G protein-coupled receptors. *Plant Physiol.* **161**, 1097–1102. (doi:10.1104/pp.112.212324)
34. Urano D, Chen JG, Botella JR, Jones AM. 2013 Heterotrimeric G protein signalling in the plant kingdom. *Open Biol.* **3**, 120186. (doi:10.1098/rsob.120186)
35. Bradford W, Buckholz A, Morton J, Price C, Jones AM, Urano D. 2013 Eukaryotic G protein signaling evolved to require G protein-coupled receptors for activation. *Sci. Signal.* **6**, ra37. (doi:10.1126/scisignal.2003768)
36. Illingworth CJ, Parkes KE, Snell CR, Mullineaux PM, Reynolds CA. 2008 Criteria for confirming sequence periodicity identified by Fourier transform analysis: application to GCR2, a candidate plant GPCR? *Biophys. Chem.* **133**, 28–35. (doi:10.1016/j.bpc.2007.11.004)
37. Chen J-H, Guo J, Chen J-G, Nair SK. 2013 Crystal structure of *Arabidopsis* GCR2 identifies a novel clade of lantibiotic cyclase-like proteins. See http://www.rcsb.org, pdb code 3T33.
38. Halgren TA, Murphy RB, Friesner RA, Beard HS, Frye LL, Pollard WT, Banks JL. 2004 Glide: a new approach for rapid, accurate docking and scoring. 2. Enrichment factors in database screening. *J. Med. Chem.* **47**, 1750–1759. (doi:10.1021/jm030644s)
39. Friesner RA *et al*. 2004 Glide: a new approach for rapid, accurate docking and scoring. 1. Method and assessment of docking accuracy. *J. Med. Chem.* **47**, 1739–1749. (doi:10.1021/jm0306430)
40. Andreotti G, Mendez BL, Amodeo P, Morelli MA, Nakamuta H, Motta A. 2006 Structural determinants of salmon calcitonin bioactivity: the role of the Leu-based amphipathic α-helix. *J. Biol. Chem.* **281**, 24 193–24 203. (doi:10.1074/jbc.M603528200)
41. Eswar N, Webb B, Marti-Renom MA, Madhusudhan MS, Eramian D, Shen MY, Pieper U, Sali A. 2006 Comparative protein structure modeling using Modeller. *Curr. Protoc. Bioinformatics* (editoral board, Andreas D Baxevanis *et al*.) Chapter 5, Unit 5.6, pp. 5.6.1–5.6.30. (doi:10.1002/0471250953.bi0506s15)
42. Shen MY, Sali A. 2006 Statistical potential for assessment and prediction of protein structures. *Protein Sci.* **15**, 2507–2524. (doi:10.1110/ps.062416606)
43. Sali A, Blundell TL. 1993 Comparative protein modelling by satisfaction of spatial restraints. *J. Mol. Biol.* **234**, 779–815. (doi:10.1006/jmbi.1993.1626)
44. Watkins HA, Rathbone DL, Barwell J, Hay DL, Poyner DR. 2012 Structure–activity relationships for alpha calcitonin gene-related peptide. *Br. J. Pharmacol.* (doi:10.1111/bph.12072)
45. Conner AC, Simms J, Conner MT, Wootten DL, Wheatley M, Poyner DR. 2006 Diverse functional motifs within the three intracellular loops of the CGRP1 receptor. *Biochemistry* **45**, 12 976–12 985. (doi:10.1021/bi0615801)
46. Bailey RJ, Hay DL. 2007 Agonist-dependent consequences of proline to alanine substitution in the transmembrane helices of the calcitonin receptor. *Br. J. Pharmacol.* **151**, 678–687. (doi:10.1038/sj.bjp.0707246)
47. Bailey RJ, Hay DL. 2006 Pharmacology of the human CGRP1 receptor in Cos 7 cells. *Peptides* **27**, 1367–1375. (doi:10.1016/j.peptides.2005.11.014)
48. Barwell J, Miller PS, Donnelly D, Poyner DR. 2010 Mapping interaction sites within the N-terminus of the calcitonin gene-related peptide receptor; the role of residues 23–60 of the calcitonin receptor-like receptor. *Peptides* **31**, 170–176. (doi:10.1016/j.peptides.2009.10.021)
49. Miranda LP *et al*. 2008 Identification of potent, selective, and metabolically stable peptide antagonists to the calcitonin gene-related peptide (CGRP) receptor. *J. Med. Chem.* **51**, 7889–7897. (doi:10.1021/jm8009298)
50. Barwell J, Conner AC, Poyner DR. 2010 A cysteine-scan of the N-terminus of calcitonin gene-related peptide.

Proc. Br. Pharmacol. Soc. See http://wwwpA2onlineorg/abstracts/Vol8Issue1abst115Ppdf.

51. Di Paolo E, Vilardaga JP, Petry H, Moguilevsky N, Bollen A, Robberecht P, Waelbroeck M. 1999 Role of charged amino acids conserved in the vasoactive intestinal polypeptide/secretin family of receptors on the secretin receptor functionality. *Peptides* **20**, 1187–1193. (doi:10.1016/S0196-9781(99)00122-9)
52. Hawtin SR, Simms J, Conner M, Lawson Z, Parslow RA, Trim J, Sheppard A, Wheatley M. 2006 Charged extracellular residues, conserved throughout a G-protein-coupled receptor family, are required for ligand binding, receptor activation, and cell-surface expression. *J. Biol. Chem.* **281**, 38 478–38 488. (doi:10.1074/jbc.M607639200)
53. Warne T, Tate CG. 2013 The importance of interactions with helix 5 in determining the efficacy of beta-adrenoceptor ligands. *Biochem. Soc. Trans.* **41**, 159–165. (doi:10.1042/BST20120228)
54. Katritch V, Cherezov V, Stevens RC. 2012 Diversity and modularity of G protein-coupled receptor structures. *Trends Pharmacol. Sci.* **33**, 17–27. (doi:10.1016/j.tips.2011.09.003)
55. Frimurer TM, Bywater RP. 1999 Structure of the integral membrane domain of the GLP1 receptor. *Proteins* **35**, 375–386. (doi:10.1002/(SICI)1097-0134(19990601)35:4<375::AID-PROT1>3.0.CO;2-2)
56. Chugunov AO, Simms J, Poyner DR, Dehouck Y, Rooman M, Gilis D, Langer I. 2010 Evidence that interaction between conserved residues in transmembrane helices 2, 3, and 7 are crucial for human VPAC1 receptor activation. *Mol. Pharmacol.* **78**, 394–401. (doi:10.1124/mol.110.063578)
57. Miller LJ, Chen Q, Lam PC, Pinon DI, Sexton PM, Abagyan R, Dong M. 2011 Refinement of glucagon-like peptide 1 docking to its intact receptor using mid-region photolabile probes and molecular modeling. *J. Biol. Chem.* **286**, 15 895–15 907. (doi:10.1074/jbc.M110.217901)
58. Ceraudo E *et al*. 2012 Spatial proximity between the VPAC1 receptor and the amino terminus of agonist and antagonist peptides reveals distinct sites of interaction. *FASEB J.* **26**, 2060–2071. (doi:10.1096/fj.11-196444)